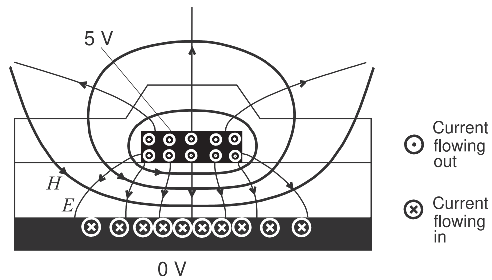

Figure 3-2: Cross-sectional view of a microstrip line showing electric and magnetic field lines and current flow. The electric and magnetic fields are in two mediums—the dielectric and air. If the line is homogeneous (the same dielectric everywhere) the electric and magnetic fields are only in the transverse plane, a field configuration known as the transverse electromagnetic mode (TEM).

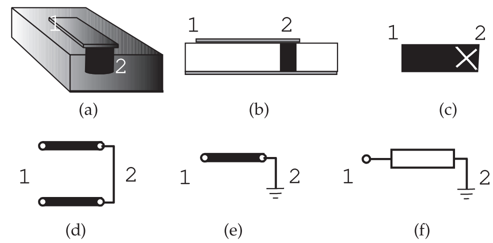

Figure 3-3: Representations of a shorted microstrip line with a short (or via) at port 2: (a) three-dimensional (3D) view indicating via; (b) side view; (c) top view with via indicated by X; (d) schematic representation of transmission line; (e) alternative schematic representation; and (f) representation as a circuit element.

In the microstrip line, electric field lines start on one of the conductors and finish on the other and are located almost entirely in the plane transverse to the long length of the line. The magnetic field is also mostly confined to the transverse plane, and so this line is referred to as a **transverse electromagnetic** (**TEM**) line. Integrating the electric field along a path gives the voltage. Since the voltage between the top and bottom conductors is more or less the same everywhere, longer E field lines correspond to lower levels of E field. The strength of the E field is also indicated by the density of the E field lines. This is a drawing convention for both electric and magnetic fields. A further comment is warranted for this line. This line is more accurately called a **quasi-TEM** line, as the longitudinal fields, particularly in the air region, are not negligible. The relative level of the longitudinal fields increases with frequency, but below about 10 GHz and for typical dimensions used, the line is still essentially TEM. In Figure 3-2 current flows in the strip and a return current flows in what is normally regarded as the ground conductor. Both the signal and return currents induce a magnetic field and the closed path integral of the magnetic field is equal to the current enclosed by the path.

Various schematic representations of a microstrip line are used. Consider the representations in Figure 3-3 of a length of microstrip line shorted by a via at the end denoted by "2" (specifically the "2" refers to Port 2). The views in Figure 3-3(a and b) provide perspectives. The representations shown in Figure 3-3(d–f) are symbols used in circuit diagrams with the one used depending on the number of microstrip lines in a circuit diagram. If a circuit diagram has many transmission line elements, then the simple representation of Figure 3-3(f) is most common. If there are few transmission line elements, then the representation of Figure 3-3(d) is most common.

3.2 Substrates

Planar transmission line design involves choosing both the transmission line structure to use and the substrate. In this section the electrical properties of materials will be discussed and then substrates commonly used with planar interconnects will be considered.

3.2.1 Dielectric Effect

The presence of material between the conductors alters the electrical characteristics of the interconnect. With a dielectric, the application of an electric field moves the centers of positive and negative charge at the atomic and molecular level. Moving the charge centers changes the amount of energy stored in the electric field—a process akin to storing energy in a stretched spring. The extra energy storage property is described by the **relative permittivity**, ε_r, which is the ratio of the permittivity of the material to that of free space:

$$\varepsilon_r = \varepsilon/\varepsilon_0. \tag{3.1}$$

The relative permittivities of materials commonly used with interconnects range from 2.08 for Teflon™, used in high-performance PCBs and coaxial cables, to 11.9 for silicon (Si), to 3.8–4.2 for silicon dioxide (SiO_2), and 12.4 for gallium arsenide (GaAs).

When the fields are in more than one medium (a **nonhomogeneous transmission line**), as for the microstrip line, the effective relative permittivity, $\varepsilon_{r,e}$ (or usually just $\varepsilon_e = \varepsilon_{r,e}$), is used. The characteristics of the nonhomogeneous line are then more or less the same as for the same structure with a uniform dielectric of permittivity, $\varepsilon_{\text{eff}} = \varepsilon_e\varepsilon_0$. The ε_{eff} changes with frequency as the proportion of energy stored in the different regions changes. This effect is called **dispersion** and causes a pulse to spread out as the different frequency components of the pulse want to travel at different speeds.

3.2.2 Dielectric Loss Tangent, $\tan\delta$

Loss in a dielectric comes from two sources: (a) **dielectric damping** (also called **dielectric relaxation**) and (b) conduction losses in the dielectric. Dielectric damping originates from the movement of charge centers resulting in mechanical distortion of the dielectric lattice. An alternating electric field results in vibrational (or phonon) energy in the dielectric, thus energy is lost from the electric field. It is easy to see that this loss increases linearly with frequency and is zero at DC. Because of this, in the frequency domain loss is described by incorporating an imaginary term in the **permittivity**. So now the permittivity of a dielectric becomes

$$\varepsilon = \varepsilon_r\varepsilon_0 = \varepsilon' - \jmath\varepsilon'' = \varepsilon_0\left(\varepsilon_r' - \jmath\varepsilon_r''\right). \tag{3.2}$$

If there is no dielectric damping loss, $\varepsilon'' = 0$. The other type of loss that occurs in the dielectric is due to the movement of charge carriers in the dielectric. The ability to move charges is described by the conductivity, σ, and the loss due to current conduction is independent of frequency. So the energy lost in the dielectric is proportional to $\omega\varepsilon'' + \sigma$ and the energy stored in the electric field is proportional to $\omega\varepsilon'$. Thus a loss tangent is introduced:

$$\tan\delta = \frac{\omega\varepsilon'' + \sigma}{\omega\varepsilon'}. \tag{3.3}$$

Also the relative permittivity can be redefined as

$$\varepsilon_r = \varepsilon_r' - \jmath \left(\varepsilon_r'' + \frac{\sigma}{\omega \varepsilon_0} \right). \tag{3.4}$$

With the exception of silicon, the loss tangent is very small for dielectrics that are useful at RF and microwave frequencies and so most of the time

$$|\varepsilon_r| \approx \varepsilon_r', \tag{3.5}$$

and this is what is quoted as the permittivity of a material. Thus

$$\varepsilon_r = \varepsilon_r' - \jmath \left(\varepsilon_r'' + \sigma/(\omega \varepsilon_0) \right) \approx \varepsilon_r' \left(1 - \jmath \tan \delta \right). \tag{3.6}$$

3.2.3 Magnetic Material Effect

A similar effect on energy storage in the magnetic field occurs for a few materials. The magnetic properties of materials are due to the magnetic dipole moments that result from alignment of electron spins—an intrinsic property of electrons. In most materials the electron spins occur in pairs with opposite signs, with the result that there is no net **magnetic moment**. However, in magnetic materials, some of the electron spins are not canceled and there is a net magnetic moment. This net magnetic moment aligns itself with an applied H field and so provides a mechanism for additional storage of **magnetic energy**. The relative permeability, μ_r, describes this effect and

$$\mu = \mu_r \mu_0. \tag{3.7}$$

Most materials have $\mu_r = 1$. One notable exception is nickel, which has a high permeability, is a very convenient processing material, and is often used in electronic packaging for its desirable processing properties.

As with dielectrics, the effect of loss in a magnetic material can be described by its complex permeability:

$$\mu = \mu' - \jmath \mu''. \tag{3.8}$$

Lossy magnetic effects are due to the movement of magnetic dipoles, which creates vibrations in a material and hence loss.

3.2.4 Substrates for Planar Transmission Lines

The properties of a number of common substrate materials are given in Table 3-1; more are given in Appendix 2.A. Crystal substrates such as sapphire, quartz, and semiconductors (Si, GaAs, and InP) have very good dimensional tolerances and uniformity of electrical properties. Many other substrates have high surface roughness and electrical properties that can vary. For example, FR4 is the most common type of printed circuit board substrate and is a weave of fiberglass embedded in resin. So the material is not uniform and in the assembly of a multilayer circuit board layers of FR4 are pressed together and the resin flows so that there is an unpredictable localized variation in the proportion of resin and glass. High-performance FR4 for microwave applications has a fine weave.

Material	$10^4 \tan\delta$ (at 10 GHz)	ε_r
Air (dry)	≈ 0	1
Alumina, 99.5%	1–2	10.1
Sapphire	0.4–0.7	9.4, 11.6
Glass, typical	20	5
Polyimide	50	3.2
Quartz (fused)	1	3.8
FR4 circuit board	100	4.3–4.5
RT-duroid 5880	5–15	2.16–2.24
RT-duroid 6010	10–60	10.2–10.7
AT-1000	20	10.0–13.0
Si (high resistivity)	10–100	11.9
GaAs	6	12.85
InP	10	12.4
SiO_2 (on-chip)	—	4.0–4.2
LTCC (typical, green tape(TM) 951)	15	7.8

Table 3-1: Properties of common substrate materials. The dielectric loss tangent is scaled. For example, for glass, $\tan\delta$ is typically 0.002.

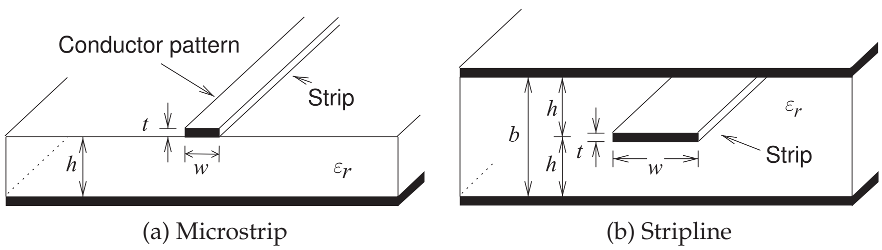

Figure 3-4: Planar transmission lines.

3.3 Planar Transmission Line Structures

Planar transmission lines are the most common transmission lines for high-speed digital, RF, and microwave circuits. Two planar transmission line structures are shown in Figure 3-4. The reason these are so popular is that they can be mass produced. For the microstrip line in Figure 3-4(a) the fabrication process begins with a dielectric sheet with solid metal layers on the top and bottom. One of these is covered with a photosensitive material, called a photoresist, exposed to a prepared pattern that defines the interconnect line network, then the photoresist is developed and the unexposed (or exposed, depending on whether the photoresist is positive or negative) metal on one side is etched away. The stripline in Figure 3-4(b) is fabricated similarly to microstrip but followed by one more step in which a dielectric sheet with a ground plane only is bonded on top.

There are two major categories of planar transmission lines that can be sorted according to the uniformity of the medium surrounding the transmission line conductors. When the embedding medium is uniform the transmission line structures are referred to as homogeneous. If there are two or more regions with different permittivity the transmission line is called inhomogeneous. The most important planar transmission line structures are shown in Figure 3-5. With the homogeneous lines virtually all of the fields are in the plane transverse to the direction of propagation (i.e., the longitudinal direction). Transmission lines where the longitudinal fields are

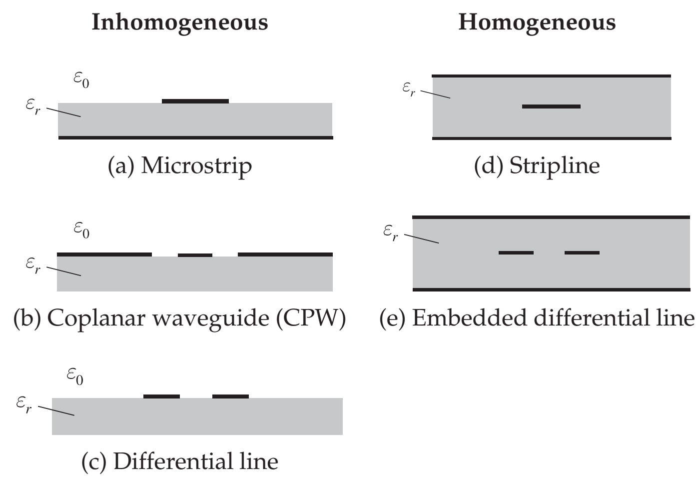

Figure 3-5: Cross sections of several homogeneous and inhomogeneous planar transmission line structures.

almost insignificant are referred to as supporting a TEM mode, and they are called TEM lines.

The most important inhomogeneous lines are shown in Figure 3-5(a–c). The main difference between the two sets of configurations (homogeneous and inhomogeneous) is the frequency-dependent variation of the EM field distributions with inhomogeneous lines. With inhomogeneous lines, the EM fields are not confined entirely to the transverse plane even if the conductors are perfect. However, they are largely confined to the transverse plane and so these lines are called **quasi-TEM lines**. The inhomogeneous lines are simpler to make. Each transmission line structure comprises a combination of metal (shown as dense black) and dielectric (indicated by the shaded region and having permittivity ε). It is common not to separately designate the permeability, μ, of the materials because, except for magnetic materials, $\mu = \mu_0$. The region with permittivity ε_0 is air. In most cases the dielectric principally supports the metal pattern, acting as a substrate, and clearly influences the wave propagation. The actual choice of structure depends on several factors, including operating frequency and the type of substrate and metallization system available.

3.3.1 Microstrip

Microwave circuits on compound semiconductor substrates (e.g. GaAs) are called **monolithic microwave integrated circuits** (**MMICs**). Microwave circuits on silicon (Si) semiconductor substrates are called **radio frequency integrated circuits** (**RFICs**) Microwave integrated circuits (MICs) are also called hybrid MICs.

Microstrip (Figure 3-5(a)) is the simplest structure to fabricate beginning with a thin dielectric substrate with metal on both sides. One metal sheet is kept as the electrical ground plane while the other is patterned using photolithography. The metal is chemically etched to form a microstrip transmission network. Although microstrip has a very simple geometric structure, the EM fields involved are complex and cannot be determined analytically. However, simple approaches to the field calculations combined with frequency-dependent expressions yield quite accurate designs. **Microwave integrated circuits** (**MICs**) using microstrip can be designed for frequencies up to several tens of gigahertz. At higher frequencies, particularly into the millimeter wavelength ranges (above 30 GHz), losses (including radiation) increase significantly, the transmission line characteristics vary greatly with frequency (called frequency dispersion), the field directions cannot be confined to the transverse plane, and fabrication tolerances become exceedingly difficult to meet as the required substrate thickness becomes very thin. With monolithic ICs, fabrication tolerances are much finer than with hybrid MICs and the options available for both microstrip and other transmission structures are extended.

3.3.2 Coplanar Waveguide

Coplanar waveguide (**CPW**) (Figure 3-5(b)) [1] supports a quasi-TEM mode of propagation with the active metallization and the ground planes on the same side of the substrate. Each "side-plane" conductor is grounded and the center strip carries the signal, thus much less field enters the substrate when compared with microstrip. In conventional CPW the ground planes extend indefinitely, but in **finite ground CPW** (**FGCPW**), the extent of the grounds is limited. It is important to connect the ground strips every tenth of a wavelength or so. This is done using wire bonds, via structures, or in integrated circuit form using air bridges. CPW does a good job of suppressing radiation, it has low frequency dispersion, and is preferred to microstrip for large spatially distributed circuits at frequencies above 20 GHz or so. It does have drawbacks, including the increased area required (compared with microstrip) and the need to use ground straps.

3.3.3 Coplanar Strip and Differential Line

This simple transmission structure (Figure 3-5(c)) is formed by two conductors in the same plane. As with the embedded differential line, the possible existence of ground planes is incidental and ideally these should not influence the field pattern. In one realization, one of the conductors is grounded, and this form is called coplanar stripline or **coplanar strip** (**CPS**) [2–12]. In this configuration, CPS is used as an area-efficient variation of CPW. When neither of the conductors is grounded and the line is driven differentially, the interconnect is called a differential line. A differential line is used extensively with RFICs and in critical nets in high-speed digital ICs. The two forms have essentially identical electrical characteristics, with differences resulting from interaction with other metallic structures such as ground planes.

Silicon-based RFICs generally use differential signaling for analog signals to overcome the problem of field coupling in high-density circuits and problems due to the finite conductivity of the silicon substrate that results in high levels of circuit noise in the substrate. The currents on each of the differential signal paths balance each other and thus each provides the signal return path for the other. This design practice effectively eliminates RF currents that would occur on ground conductors.

3.3.4 Stripline

Stripline (Figure 3-5(d)) is a symmetrical structure somewhat like a coaxial line completely flattened out so that the center conductor is a rectangular metal strip and the outer grounded metal is an extended rectangular box. The entire structure is 100% filled with dielectric, and therefore transmission is TEM and completely dependent upon the relative permittivity, ε_r. Therefore the wavelength is simply the free-space value divided by the square root of ε_r. Stripline is fabricated similarly to microstrip, but now a substrate with a ground plane backing is placed on top.

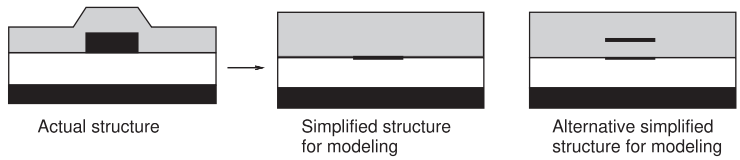

Figure 3-6: A microstrip line modeled as a zero-thickness microstrip line. Also shown is a more accurate alternative simplified structure.

3.3.5 Embedded Differential Line

This simple transmission structure (Figure 3-5(e)) is formed by having just two conductors embedded in a substrate with no specific ground plane. In this structure the possible existence of ground planes is incidental, and ideally these should not influence the field pattern. Essentially the substrate acts as a mechanical supporting element and a quasi-TEM mode forms the main propagating field distribution.

3.4 Modeling of Transmission Lines

Describing the signal on a line in terms of E and H requires a description of the E and H fields in the transverse plane. This can be quite difficult. It is fortunate that current and voltage descriptions can be successfully used to describe the state of a transmission line at a particular position along the line. This is an approximation and the designer needs to be aware of situations where this breaks down. Such extraordinary effects are left to the next chapter. Once the transmission line descriptions have been simplified to current and voltage, R, L, G, and C models of the line can be developed. A range of models are used for transmission lines depending on the accuracy required and the frequency of operation.

Uniform interconnects (with regular cross section) can most accurately be modeled using EM modeling software. Most commonly a specialized type of software called $2\frac{1}{2}$D EM is used, which only considers current flowing in the horizontal plane or in the vertical direction. A consequence is that planar interconnects are modeled as having zero thickness, as shown in Figure 3-6. This is reasonable for microwave interconnects, as the thickness of a planar strip is usually much less than the width of the interconnect. Many analytic formulas have also been derived for the characteristics of uniform interconnects. These formulas are important in arriving at synthesis formulas that can be used in design (i.e., arriving at the physical dimensions of an interconnect structure from its required electrical specifications). Just as importantly, the formulas provide insight into the effects of materials and geometry.

Simplification of the geometry of the type illustrated in Figure 3-6 for microstrip can lead to appreciable errors in some situations. More elaborate computer programs that capture the true geometry must still simplify the real situation. An example is that it is not possible to account for density variations of the dielectric. Consequently characterization of many RF and microwave structures requires measurements to "calibrate" simulations. Unfortunately it is also difficult to make measurements at microwave frequencies. Thus one of the paradigms in RF circuit engineering is requiring intuition, measurements, and simulations to develop self-consistent models of transmission lines and distributed elements.

3.5 Microstrip Transmission Lines

Transmission lines with conductors embedded in an inhomogeneous dielectric medium cannot support a pure TEM mode. This is the case even if the conductors are lossless. The most important member of this class is the microstrip transmission line (Figure 3-5(c)). Part of the field is in the air and part in the dielectric between the strip conductor and the ground. In most practical cases, the dielectric substrate is electrically thin, that is, $h \ll \lambda$. Then the transverse field is dominant and the fields are called quasi-TEM.

The original analysis of microstrip was based on the unfolding of a coaxial line [13].

3.5.1 Microstrip Line in the Quasi-TEM Approximation

In this section a number of relations are developed based on the principle that the phase velocity of an EM wave in an air-only homogeneous transmission with a TEM field line is just c. It is also shown that the static solutions for the transverse electric field alone can be used to calculate the characteristics of a transmission line. The procedure described is used in many EM computer programs to calculate the characteristics of transmission lines.

As a first step, the potential of the conductor strip is set to V_0 and Laplace's equation is solved using an EM simulator for the electrostatic potential everywhere in the dielectric. Then the per unit length (p.u.l.) electric charge, Q, on the conductor is determined. Using this in the following relation gives the line capacitance:

$$C = \frac{Q}{V_0}.$$

In the next step, the process is repeated with $\varepsilon_r = 1$ to determine $C_{\rm air}$ (the capacitance of the line without a dielectric).

If the microstrip line is now an air-filled lossless TEM structure,

$$v_{p,\rm air} = c = \frac{1}{LC_{\rm air}} \quad (3.9) \qquad \text{and so} \quad L = \frac{1}{c^2 C_{\rm air}}. \quad (3.10)$$

L is not affected by the dielectric properties of the medium.[1] L calculated above is the desired p.u.l. inductance of the line with the dielectric as well as in free space. Once L and C have been found, the characteristic impedance can be found using

$$Z_0 = \sqrt{\frac{L}{C}}, \quad (3.11) \qquad \text{rewritten as} \quad Z_0 = \frac{1}{c}\frac{1}{\sqrt{C\,C_{\rm air}}}, \quad (3.12)$$

and the phase velocity is

$$v_p = \frac{1}{\sqrt{LC}} = c\sqrt{\frac{C_{\rm air}}{C}}. \quad (3.13)$$

Now the field is distributed in the inhomogeneous medium and in free space, as shown in Figure 3-7(a). So the effective relative permittivity, ε_e, of the equivalent homogeneous microstrip line (see Figure 3-7(b)) is defined by

$$\sqrt{\varepsilon_e} = \frac{c}{v_p}. \quad (3.14)$$

[1] The assumption that L is not affected by the dielectric is a good approximation. However, there is a small discrepancy as a change in the electric field orientation affects the magnetic field, but there is little additional magnetic energy storage.

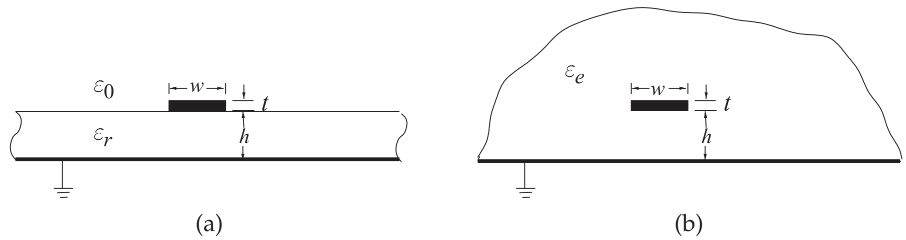

Figure 3-7: Microstrip /ink.sh micr (a) cross section; and (b) approximate equivalent structure where the strip is embedded in a dielectric of semi-infinite extent with effective relative permittivity ε_e.

Combining Equations (3.13) and (3.14), the effective relative permittivity (usually just the term effective permittivity is used) is obtained:

$$\varepsilon_e = \frac{C}{C_{\text{air}}}. \tag{3.15}$$

The effective permittivity can be interpreted as the permittivity of a homogeneous medium that replaces the air and the dielectric regions of the microstrip, as shown in Figure 3-7. Since some of the field is in the dielectric and some is in air, the effective relative permittivity must satisfy

$$1 < \varepsilon_e < \varepsilon_r. \tag{3.16}$$

However, the minimum ε_e will be greater than 1 as electrical energy will be distributed in air and dielectric. The wavelength on a transmission line, the guide wavelength λ_g, is related to the free space wavelength by $\lambda_g = \lambda_0/\sqrt{\varepsilon_e}$.

EXAMPLE 3.1 Microstrip Calculations

A microstrip line has a characteristic impedance Z_0 of 50 Ω derived from reflection coefficient measurements and an effective permittivity, ε_e, of 7 derived from measurement of phase velocity. What is the line's per-unit-length inductance, L, and capacitance, C?

Solution: The key equations are $Z_0 = \sqrt{L/C}$, $\varepsilon_e = C/C_{\text{air}}$, and for the air-filled microstrip line (with a TEM mode) $v_p = 1/\sqrt{LC_{\text{air}}} = c$. Also assume that $\mu_r = 1$ which is the default if not specified otherwise and also that L does not change if only the dielectric is changed. Thus

$$C_{\text{air}} = \frac{C}{\varepsilon_e} \quad \text{and then} \quad L = \frac{\varepsilon_e}{c^2 C} \quad \text{so that} \quad Z_0 = \sqrt{\frac{L}{C}} = \frac{\sqrt{\varepsilon_e}}{cC}, \quad \text{that is} \quad C = \frac{\sqrt{\varepsilon_e}}{cZ_0}.$$

So $C = \sqrt{7}/(2.998 \cdot 10^8 \times 50) = 1.765 \cdot 10^{-10} = 176.5\text{pF/m}$ and $L = Z_0^2 C = 441.3$ nH/m.

3.5.2 Input Impedance of a Shorted Microstrip Line Modeled using a Field Solver

In this example a shorted microstrip line is examined with the aid of a microwave computer-aided design tool. The specific tool used here is National Instruments AWR Design Environment (AWRDE), but most microwave analysis tools will provide the same insight. The project file for the AWR Design Environment is RFDesign_Shorted_Microstrip_Line.emp.

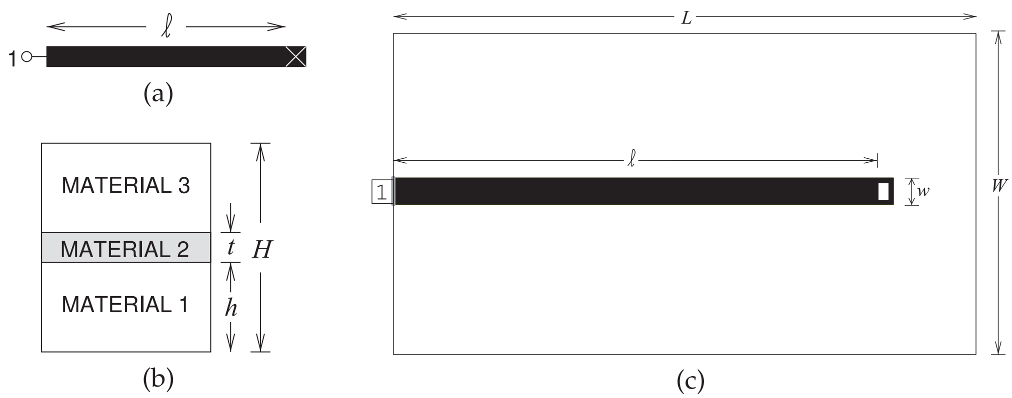

Figure 3-8: Microstrip line layout: (a) microstrip schematic; (b) stack-up of materials with material 1 being the substrate, material 2 being the metal of the strip, and Material 3 being vacuum; and (c) simulation layout. Dimensions are w = 500 μm, ℓ = 1 cm. The metal is $t = 6$ μm thick gold (conductivity $\sigma = 42.6 \times 10^6$ S/m) and the alumina substrate height is $h = 600$ μm with relative permittivity ε_r = 9.8 and loss tangent 0.001. The size of the simulation box is defined by W = 6 mm, L = 12 mm, and box height H = 2.61 mm.

The schematic of the microstrip line is shown in Figure 3-8(a). This is what the microstrip looks like from above, with the black region indicating metal and the white cross indicating a via that connects the strip to the ground plane. The distance from the start of the line to the wall of the via is ℓ. The via has a finite length and it is important to take the length of the line up to the wall that terminates the propagating electric and magnetic fields of the microstrip line and not to the center point of the via. While vias are typically cylinders, and so there is not an electric wall across the microstrip, the part of the wall of the via that first encounters the EM fields guided by the microstrip line is a good approximation.

To perform an EM analysis of this line it is necessary to define an enclosure with the cross section shown in Figure 3-8(b) and the top view shown in Figure 3-8(c). The enclosure sets up the walls that terminate the EM field lines. Here the enclosure is a metal box length $L = 12$ mm and width $W = 6$ mm. The height of the enclosure depends on the thicknesses assigned to the three materials that comprise the microstrip environment (see Figure 3-8(b)). The enclosure here is a metal box, but options are usually provided to define walls as electric or magnetic walls, and in addition the top walls of the box can be defined as absorbing walls. An absorbing or free-space wall presents an approximation to the free-space conditions. In this example six electric walls are used, with the side walls and top wall spaced a good distance from the line so that the fields are not perturbed by the presence of the side walls.

There are two main types of frequency-domain EM solvers used in microwave engineering. One type uses the finite element method (FEM), which solves for the fields at every grid point in a three-dimensional volume. This can provide a wealth of information and handle a broad range of microwave structures. However, it is very slow and runs into memory problems for all but the simplest structures. The other type of solver is called

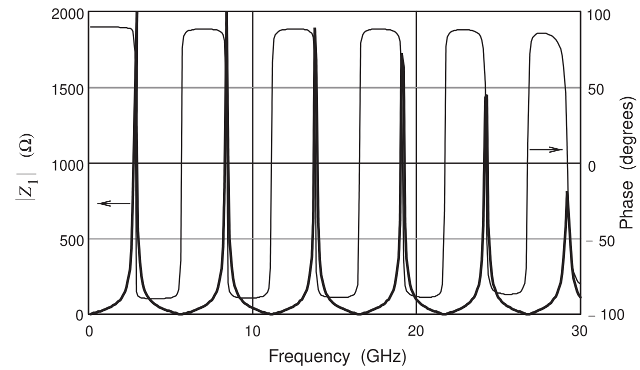

Figure 3-9: Magnitude and phase of the input impedance, Z_1, of the microstrip line in Figure 3-8.

a two-and-a-half dimensional (or $2\frac{1}{2}$D) field solver. This type of solver uses what is called the method of moments to solve for the charges on the surfaces of metals. Fields are not found at every point in space and so a $2\frac{1}{2}$D field solver is much faster than a 3D solver. The type of solver that will be used here is a $2\frac{1}{2}$D field solver available in the AWRDE environment and also used in the Sonnet simulations used elsewhere in this book. The restriction that comes with using a $2\frac{1}{2}$D field solver is that the conductors and dielectrics must be arranged in layers, as shown in Figure 3-8(b). Metals are treated as infinitely thin and, in some tools, dielectrics can be arranged as blocks, but still following the layering protocol.

The layout in the horizontal x-y plane in Figure 3-8(c) is very close to the schematic view shown in Figure 3-8(a). Port 1 (the only port) of the microstrip line is shown on the left in Figure 3-8(a) and in Figure 3-8(c) it is embedded in the left electric wall. As was mentioned, a $2\frac{1}{2}$D field solver finds the charges on the metal. A grid of cells is established and most often the grid is a regular rectangular mesh and curves and oblique angles can only be approximated. Even when more sophisticated meshes are used, a curved shape is approximated by straight lines. In Figure 3-8(c) the via is inserted as a rectangular cuboid. Another restriction of $2\frac{1}{2}$D field solvers is that currents must flow either in the x-y plane or in the vertical (z) direction. So as long as the via has a small (relative to a wavelength) dimension in the z direction and the x-y dimensions of the via are small, this is a small restriction in exchange for a simulation that can be thousands of times faster than full 3D methods.

The dimensions of the microstrip were chosen for a characteristic impedance of $50\ \Omega$ yielding w = 500 μm for the alumina dielectric with relative permittivity ε_r = 9.8 and height $h = 600$ μm. Also ℓ = 1 cm. Often it is necessary to include realistic loss for the materials to obtain physically meaningful results. Here the metal of the line and of the bottom wall is gold with conductivity $\sigma = 42.6 \times 10^6$ S/m and the loss tangent of the alumina is 0.001. The strip has a thickness $t = 6$ μm. The metal strip is simulated as though it was infinitely thin, but the thickness is used in calculating the resistance of the strip. The dielectric above the strip is free space with permittivity ε_0 and with a thickness of 2 mm. So the height of the box $H = h + t + 2$ mm = 2.610 mm.

The input impedance, $Z_{\rm in}$, of the shorted microstrip line is shown in Figure 3-9. The plots show the magnitude and phase of the input impedance. The phase is mostly $+90°$ or $-90°$, indicating that $Z_{\rm in}$ is mostly reactive. At low frequencies near 0 GHz, the input impedance is inductive since

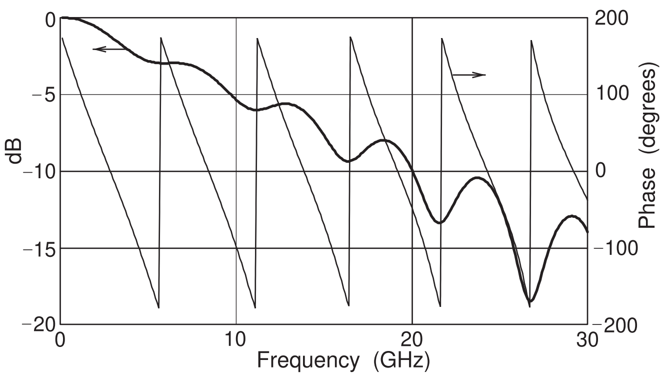

Figure 3-10: Magnitude and phase of the input reflection coefficient, Γ, of the microstrip line in Figure 3-8 but now with a high loss substrate with $\tan\delta = 0.1$.

the phase is approximately $+90°$. Z_{in} increases as would be expected from the approximate model of a shorted line. At 3 GHz, Z_{in} changes from inductive to capacitive going through a near-open circuit. The transition is not instantaneous, as the line is lossy. Z_{in} continues to cycle as the excitation frequency increases.

It is interesting to view what happens when the loss is greatly increased. Here this is done by increasing the loss tangent of the dielectric, $\tan\delta$, to 0.1. This is much higher than that of any useful substrate. The reflection coefficient of the high loss line is shown in Figure 3-10. At very low frequencies $|\Gamma| \approx 0$ dB, i.e., $|\Gamma| \approx 1$. The phase of $\Gamma \approx 180°$ so that $\Gamma \approx -1$ (i.e., a short circuit). As frequency increases $|\Gamma|$ decreases because of increasing dielectric loss and the phase of Γ monotonically decreases as the line becomes electrically longer.

3.5.3 Effective Permittivity and Characteristic Impedance

This section presents formulas for the effective permittivity and characteristic impedance of a microstrip line. These formulas are fits to the results of detailed EM simulations. Also, the form of the equations is based on good physical understanding. First, assume that the thickness, t, is zero. This is not a bad approximation, as $t \ll w, h$ for most microwave circuits.

Hammerstad and others provide well-accepted formulas for calculating the effective permittivity and characteristic impedance of microstrip lines [14–16]. Given ε_r, w, and h, the effective relative permittivity is

Mostly the term "**effective permittivity**" is used to mean effective relative permittivity (check the magnitude).

$$\varepsilon_e = \frac{\varepsilon_r + 1}{2} + \frac{\varepsilon_r - 1}{2}\left(1 + \frac{10h}{w}\right)^{-a\cdot b}, \tag{3.17}$$

where $$a(u)|_{u=w/h} = 1 + \frac{1}{49}\ln\left[\frac{u^4 + \{u/52\}^2}{u^4 + 0.432}\right] + \frac{1}{18.7}\ln\left[1 + \left(\frac{u}{18.1}\right)^3\right] \tag{3.18}$$

and $$b(\varepsilon_r) = 0.564\left[\frac{\varepsilon_r - 0.9}{\varepsilon_r + 3}\right]^{0.053}. \tag{3.19}$$

Take some time to interpret Equation (3.17), the formula for **effective relative permittivity**. If $\varepsilon_r = 1$, then $\varepsilon_e = (1+1)/2 + 0 = 1$, as expected. If ε_r is not that of air, then ε_e will be between 1 and ε_r, dependent on the geometry of the line, or more specifically, the ratio w/h. For a very wide line, $w/h \gg 1$, $\varepsilon_e = (\varepsilon_r + 1)/2 + (\varepsilon_r - 1)/2 = \varepsilon_r$, corresponding to the EM energy being confined to the dielectric. For a thin line $w/h \ll 1$, $\varepsilon_e = (\varepsilon_r + 1)/2$, the average of the dielectric and air permittivities.

The characteristic impedance is given by

$$Z_0 = \frac{Z_{01}}{\sqrt{\varepsilon_e}}, \tag{3.20}$$

where the characteristic impedance of the microstrip line in free space is

$$Z_{01} = Z_0|_{(\varepsilon_r=1)} = 60\ln\left[\frac{F_1 h}{w} + \sqrt{1+\left(\frac{2h}{w}\right)^2}\right] \tag{3.21}$$

and $$F_1 = 6 + (2\pi - 6)\exp\left\{-\left(30.666h/w\right)^{0.7528}\right\}. \tag{3.22}$$

The accuracy of Equation (3.17) is better than 0.2% for $0.01 \le w/h \le 100$ and $1 \le \varepsilon_r \le 128$. Also, the accuracy of Equation (3.21) is better than 0.1% for $w/h < 1000$. Note that Z_0 has a maximum value when w is small.

Now consider the special case where w is vanishingly small. Then ε_e has its minimum value:

$$\varepsilon_e = \tfrac{1}{2}(\varepsilon_r + 1). \tag{3.23}$$

This leads to an approximate (and convenient) form of Equation (3.17):

$$\varepsilon_e = \frac{(\varepsilon_r + 1)}{2} + \frac{(\varepsilon_r - 1)}{2}\frac{1}{\sqrt{1 + 12h/w}}. \tag{3.24}$$

This approximation has its greatest error of 1% for low and high ε_r and narrow lines, $w/h \ll 1$. Again, Equation (3.20) is used to calculate the characteristic impedance. A comparison of the line characteristics using the more precise formula for ε_e (Equation (3.17)) and the slightly less accurate fit (Equation (3.24)) is given in Table 3-2.

The more exact analysis, represented by Equation (3.17), was used to develop Table 3-3, which can be used in the design of microstrip on a silicon dioxide (SiO_2) substrate and on an FR4 printed circuit board that both have a relative permittivity of 4, on alumina with a permittivity of 10, on a silicon (Si) substrate with a relative permittivity of 11.9, and on a gallium arsenide (GaAs) substrate with a relative permittivity of 12.85.

EXAMPLE 3.2 Microstrip Calculations

The strip of a microstrip line has a width of 600 μm and is fabricated on a lossless substrate that is 635 μm thick and has a relative permittivity of 4.1.

(a) What is the effective relative permittivity?
(b) What is the characteristic impedance?
(c) What is the propagation constant at 5 GHz ignoring any losses?

Solution:

Use the formulas for effective permittivity, characteristic impedance, and attenuation constant from Section 3.5.3 with $w = 600$ μm ; $h = 635$ μm ; $\varepsilon_r = 4.1$; $w/h = 600/635 = 0.945$.

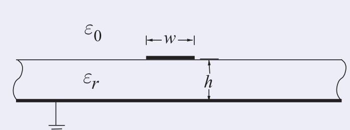

ε_r	w/h	ε_e Eq. (3.17), 0.2%	Z_0 Eq. (3.17), 0.2%	ε_e Eq. (3.24), 1%	Z_0 Eq. (3.24), 1%
1	0.01	1	401.1	1	401.1
1	0.1	1	262.9	1	262.9
1	1	1	126.5	1	126.5
1	10	1	29.04	1	29.04
1	100	1	3.61	1	3.61
2	0.01	1.525	322.5	1.514	325.9
2	0.1	1.565	210.0	1.545	211.5
2	1	1.645	98.64	1.639	98.83
2	10	1.848	21.36	1.837	21.43
2	100	1.969	2.58	1.972	2.58
10	0.01	5.683	165.8	5.630	169.0
10	0.1	6.016	107.0	5.909	108.2
10	1	6.705	48.86	6.748	48.70
10	10	8.556	9.93	8.534	9.94
10	100	9.707	1.16	9.752	1.16
20	0.01	10.88	119.6	10.77	122.2
20	0.1	11.57	77.14	11.36	78.00
20	1	13.01	35.07	13.13	34.91
20	10	16.93	7.06	16.91	7.06
20	100	19.38	0.821	19.48	0.819
128	0.01	66.90	48.15	66.30	49.25
128	0.1	71.51	31.02	70.27	31.37
128	1	81.12	14.05	82.11	13.96
128	10	71.51	2.80	70.27	2.80
128	100	123.8	0.325	124.5	0.324

Table 3-2: Comparison of two fitted equations for the effective relative permittivity and characteristic impedance of a microstrip line. Equation (3.17) has an accuracy of better than 0.2% and Equation (3.24) has an accuracy of better than 1%.

(a)
$$\varepsilon_e = \frac{\varepsilon_r + 1}{2} + \frac{\varepsilon_r - 1}{2}\left(1 + \frac{10h}{w}\right)^{-a\cdot b}$$

From Equations (3.18) and (3.19),

$$a = 1 + \frac{1}{49}\ln\left[\frac{(w/h)^4 + \{w/(52h)\}^2}{(w/h)^4 + 0.432}\right] + \frac{1}{18.7}\ln\left[1 + \left(\frac{w}{18.1h}\right)^3\right] = 0.991,$$

$$b = 0.564\left[\frac{\varepsilon_r - 0.9}{\varepsilon_r + 3}\right]^{0.053} = 0.541.$$

From Equation (3.17), $\varepsilon_e = 2.967$.

(b) In free space,
$$Z_0|_{\text{air}} = 60\ln\left[\frac{F_1 \cdot h}{w} + \sqrt{1 + \left(\frac{2h}{w}\right)^2}\right],$$

where $F_1 = 6 + (2\pi - 6)\exp\left\{-(30.666h/\omega)^{0.7528}\right\}$, $\quad Z_0 = Z_0|_{\text{air}}/\sqrt{\varepsilon_e}$

$$Z_0|_{\text{air}} = 129.7\,\Omega \quad \text{and} \quad Z_0 = Z_0|_{\text{air}}/\sqrt{\varepsilon_e} = 75.3\,\Omega.$$

(c) $f = 5$ GHz, $\omega = 2\pi f$, $\gamma = \jmath\omega\sqrt{\mu_0\varepsilon_0\varepsilon_e} = \jmath 180.5/$ m.

Table 3-3: Microstrip line normalized width u $(= w/h)$ and effective permittivity, ε_e, for specified characteristic impedance Z_0. Data derived from the analysis in Section 3.5.3.

Z_0	$\varepsilon_r = 4$ (SiO_2, FR4)		$\varepsilon_r = 10$ (Alumina)		$\varepsilon_r = 11.9$ (Si)	
(Ω)	u	ε_e	u	ε_e	u	ε_e
140	0.171	2.718	0.028	5.914	0.017	6.907
139	0.176	2.720	0.029	5.917	0.018	6.910
138	0.181	2.722	0.030	5.919	0.019	6.914
137	0.185	2.723	0.031	5.922	0.020	6.919
136	0.190	2.725	0.032	5.924	0.021	6.923
135	0.195	2.727	0.033	5.927	0.022	6.925
134	0.201	2.729	0.035	5.931	0.022	6.927
133	0.206	2.731	0.036	5.933	0.023	6.930
132	0.212	2.733	0.037	5.936	0.024	6.934
131	0.217	2.734	0.038	5.939	0.025	6.937
130	0.223	2.736	0.040	5.942	0.026	6.941
129	0.229	2.738	0.043	5.949	0.028	6.948
128	0.235	2.740	0.044	5.951	0.029	6.951
127	0.241	2.742	0.046	5.955	0.030	6.954
126	0.248	2.744	0.048	5.958	0.031	6.957
125	0.254	2.746	0.050	5.962	0.033	6.963
124	0.261	2.748	0.052	5.966	0.034	6.966
123	0.268	2.750	0.054	5.970	0.035	6.969
122	0.275	2.752	0.056	5.973	0.038	6.977
121	0.283	2.755	0.058	5.977	0.039	6.980
120	0.290	2.757	0.061	5.982	0.041	6.985
119	0.298	2.759	0.063	5.985	0.043	6.990
118	0.306	2.761	0.066	5.990	0.045	6.995
117	0.314	2.763	0.068	5.993	0.047	6.999
116	0.323	2.766	0.071	5.998	0.049	7.004
115	0.331	2.768	0.074	6.003	0.051	7.008
114	0.340	2.771	0.077	6.007	0.053	7.013
113	0.349	2.773	0.080	6.012	0.055	7.017
112	0.359	2.776	0.083	6.016	0.057	7.022
111	0.368	2.778	0.086	6.021	0.060	7.028
110	0.378	2.781	0.089	6.025	0.062	7.032
109	0.389	2.783	0.093	6.031	0.065	7.038
108	0.399	2.786	0.097	6.036	0.068	7.044
107	0.410	2.789	0.100	6.040	0.071	7.050
106	0.421	2.791	0.104	6.046	0.074	7.055
105	0.432	2.794	0.109	6.052	0.077	7.061
104	0.444	2.797	0.113	6.057	0.080	7.066
103	0.456	2.800	0.117	6.062	0.084	7.073
102	0.468	2.803	0.122	6.069	0.087	7.079
101	0.481	2.806	0.127	6.075	0.091	7.085
100	0.494	2.809	0.132	6.081	0.095	7.092
99	0.507	2.812	0.137	6.087	0.099	7.099
98	0.521	2.815	0.143	6.094	0.103	7.105
97	0.535	2.819	0.148	6.100	0.108	7.113
96	0.550	2.822	0.154	6.106	0.112	7.120
95	0.565	2.825	0.160	6.113	0.117	7.127
94	0.580	2.829	0.167	6.121	0.122	7.135
93	0.596	2.832	0.173	6.127	0.128	7.144
92	0.612	2.836	0.180	6.134	0.133	7.151
91	0.629	2.839	0.187	6.142	0.139	7.159
90	0.646	2.843	0.195	6.150	0.145	7.168
89	0.664	2.847	0.202	6.157	0.151	7.176
87	0.701	2.855	0.219	6.173	0.164	7.193
86	0.721	2.859	0.228	6.182	0.171	7.203
85	0.740	2.863	0.237	6.190	0.179	7.213
84	0.761	2.867	0.246	6.198	0.187	7.223
83	0.782	2.872	0.256	6.208	0.195	7.233
82	0.804	2.876	0.266	6.216	0.203	7.242
81	0.826	2.881	0.277	6.226	0.212	7.253
80	0.849	2.885	0.288	6.235	0.221	7.263

Table 3-3 continued.

Z_0 (Ω)	$\varepsilon_r = 4$ (SiO_2, FR4) u	ε_e	$\varepsilon_r = 10$ (Alumina) u	ε_e	$\varepsilon_r = 11.9$ (Si) u	ε_e
79	0.873	2.890	0.299	6.245	0.230	7.274
78	0.898	2.895	0.311	6.255	0.240	7.285
77	0.923	2.900	0.324	6.265	0.251	7.297
76	0.949	2.905	0.337	6.276	0.262	7.309
75	0.976	2.910	0.350	6.286	0.273	7.321
74	1.003	2.915	0.364	6.297	0.285	7.333
73	1.032	2.921	0.379	6.309	0.297	7.345
72	1.062	2.926	0.394	6.320	0.310	7.359
71	1.092	2.932	0.410	6.332	0.323	7.371
70	1.123	2.937	0.426	6.344	0.338	7.386
69	1.156	2.943	0.444	6.357	0.352	7.399
68	1.190	2.949	0.462	6.369	0.368	7.414
67	1.224	2.955	0.480	6.382	0.384	7.429
66	1.260	2.961	0.500	6.396	0.400	7.444
65	1.298	2.968	0.520	6.410	0.418	7.460
64	1.336	2.974	0.541	6.424	0.436	7.476
63	1.376	2.980	0.563	6.439	0.455	7.492
62	1.417	2.987	0.586	6.454	0.475	7.509
61	1.460	2.994	0.610	6.470	0.496	7.527
60	1.504	3.001	0.635	6.486	0.518	7.545
59	1.551	3.008	0.661	6.502	0.541	7.564
58	1.598	3.015	0.688	6.519	0.564	7.583
57	1.648	3.022	0.717	6.538	0.589	7.603
56	1.700	3.030	0.746	6.556	0.616	7.624
55	1.753	3.037	0.777	6.575	0.643	7.645
54	1.809	3.045	0.809	6.594	0.672	7.667
53	1.867	3.053	0.843	6.614	0.702	7.690
52	1.927	3.061	0.878	6.635	0.733	7.713
51	1.991	3.069	0.915	6.657	0.766	7.738
50	2.056	3.077	0.954	6.679	0.800	7.763
49	2.125	3.086	0.995	6.702	0.837	7.790
48	2.197	3.094	1.037	6.726	0.875	7.817
47	2.272	3.103	1.081	6.750	0.914	7.845
46	2.350	3.112	1.128	6.775	0.956	7.874
45	2.432	3.121	1.177	6.801	1.000	7.904
44	2.518	3.131	1.229	6.828	1.047	7.936
43	2.609	3.140	1.283	6.856	1.096	7.968
42	2.703	3.150	1.340	6.884	1.147	8.002
41	2.803	3.160	1.400	6.913	1.201	8.036
40	2.908	3.171	1.464	6.944	1.259	8.072
39	3.019	3.181	1.531	6.974	1.319	8.108
38	3.136	3.192	1.602	7.006	1.384	8.147
37	3.259	3.203	1.677	7.039	1.452	8.186
36	3.390	3.214	1.757	7.073	1.524	8.226
35	3.528	3.226	1.841	7.108	1.600	8.268
34	3.675	3.237	1.931	7.143	1.682	8.311
33	3.831	3.250	2.027	7.180	1.769	8.355
32	3.997	3.262	2.129	7.218	1.862	8.402
31	4.174	3.275	2.238	7.258	1.961	8.449
30	4.364	3.288	2.355	7.298	2.067	8.498
29	4.567	3.301	2.480	7.340	2.181	8.549
28	4.785	3.315	2.615	7.384	2.304	8.601
27	5.020	3.329	2.760	7.428	2.436	8.655
26	5.273	3.344	2.917	7.475	2.579	8.712
25	5.547	3.359	3.087	7.523	2.734	8.770
24	5.845	3.374	3.272	7.573	2.902	8.831
23	6.169	3.390	3.474	7.625	3.086	8.894
22	6.523	3.407	3.694	7.679	3.287	8.960
21	6.912	3.424	3.936	7.734	3.508	9.028
20	7.341	3.441	4.203	7.793	3.752	9.100
19	7.815	3.459	4.499	7.854	4.022	9.174
18	8.344	3.478	4.829	7.917	4.323	9.252
17	8.936	3.497	5.199	7.983	4.661	9.334
16	9.603	3.517	5.616	8.053	5.043	9.419
15	10.361	3.538	6.090	8.126	5.476	9.509
14	11.229	3.559	6.633	8.202	5.972	9.604
13	12.233	3.581	7.262	8.282	6.547	9.704
12	13.407	3.604	7.997	8.367	7.219	9.809
11	14.798	3.628	8.868	8.456	8.016	9.920
10	16.471	3.652	9.916	8.550	8.975	10.038

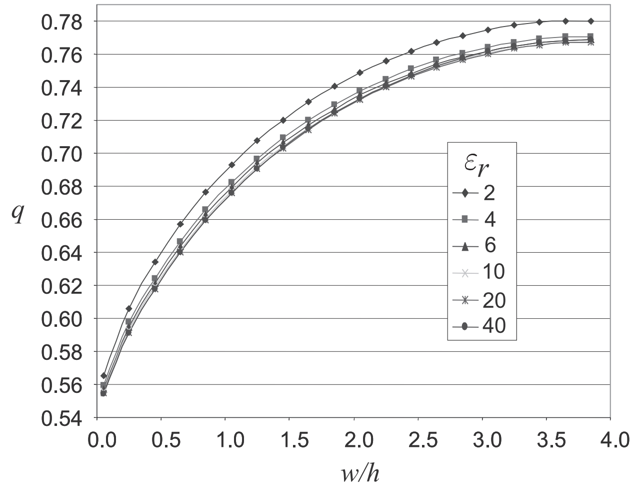

Figure 3-11: Dependence of the q factor of a microstrip line at 1 GHz for various permittivities and aspect (w/h) ratios. (Data obtained from EM field simulations using Sonnet.)

3.5.4 Filling Factor

Defining a filling factor, q, provides useful insight into the distribution of energy in an inhomogeneous transmission line. The effective microstrip permittivity is[2]

$$\varepsilon_e = 1 + q(\varepsilon_r - 1), \tag{3.25}$$

where for a microstrip line q has the bounds

$$\tfrac{1}{2} \leq q \leq 1. \tag{3.26}$$

The useful aspect of q is that it is almost independent of ε_r. A q factor of 1 would indicate that all of the fields are in the dielectric region. The dependence of the q of a microstrip line at 1 GHz for various permittivities and aspect (w/h) ratios is shown in Figure 3-11. The properties of a microstrip line, and uniform transmission lines in general, can be described very well by considering the geometric filling factor, q, and the dielectric permittivity separately. Fitting of the microstrip data yields a formula for q in terms of the geometry parameters [19]:

$$q = \tfrac{1}{2}\left(1 + \frac{1}{\sqrt{1 + 12h/w}}\right). \tag{3.27}$$

3.5.5 Microstrip Resistance

R for a microstrip line is the sum of the resistance of the strip and the resistance of the ground plane:

$$R = R_{\text{strip}} + R_{\text{ground}} \tag{3.28}$$

(with SI units of Ω/m). At low frequencies the current is uniformly distributed in the strip and so

$$R_{\text{strip}} = \frac{\rho}{wt} = \frac{R_s}{w}, \tag{3.29}$$

[2] The effective permittivity in Equation (3.25) is the upper bound on the permittivity of mixtures [17] and is known as the Maxwell Garnett mixing rule [18].

where ρ (with units of Ωm) is the resistivity of the strip metal, $R_s = \rho/t$ (with units of Ω but referred to as Ω/sq, ohms per square) is the **sheet resistance** (also called the **surface resistance**) of the strip, t is the thickness of the strip, and w is the width of the strip. The sheet resistance is used to indicate the resistance of a sheet of conductor without needing to factor in the thickness t in calculations.

At DC the current is distributed in the ground plane over the full width of the ground. At quite low frequencies this transitions so that the current is not uniformly distributed in the ground plane and the resistance of the ground plane is approximated as [19]

$$R_{\text{ground}} = \frac{R_{sg}}{w} \frac{w/h}{w/h + 5.8 + 0.03h/w}, \text{ for } 0.1 \leq w/h \leq 10, \tag{3.30}$$

where the sheet resistance of the ground plane is R_{sg}. The transition frequency from DC to the low-frequency approximation above has been found to be 1.3 MHz for a microstrip with $w = 200\ \mu\text{m}$, $h = 100\ \mu\text{m}$, $\varepsilon_r = 4$, and a ground plane width of 2 mm (i.e., a very wide ground) [20]. So at RF and microwave frequencies Equation (3.30) should be used as the low-frequency value of R_{ground}. Both R_{strip} and R_{ground} will increase at higher frequencies as then the charges rearrange at much higher frequencies. This will be considered in the next chapter.

Finally, the attenuation due to the conductor loss, α_c, from Equation (2.149), is $R/2Z_0$ and so

$$\alpha_c = \frac{R_{\text{strip}} + R_{\text{ground}}}{2Z_0}. \tag{3.31}$$

EXAMPLE 3.3 **Microstrip Attenuation**

If the strip in Example 3.2 has a resistance of 1 Ω/cm and the ground plane resistance can be ignored, what is the attenuation constant at 5 GHz?

Solution:

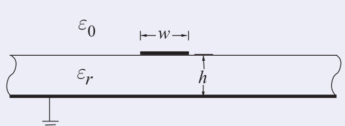

For a low-loss line, $\alpha = R/(2Z_0)$ (since there is no dielectric loss), $R = 1\ \Omega/\text{cm}$, $Z_0 = 75.3\ \Omega$, and so, using Equation (2.149),

$$\alpha = 0.664\ \text{Np/m}.$$

3.5.6 Microstrip Conductance

For a microstrip line, an estimate of G is [19]

$$G = \frac{\varepsilon_e - 1}{\varepsilon_r - 1} \omega (\tan\delta) \varepsilon_r C_{\text{air}}, \tag{3.32}$$

where $\tan\delta$ is the loss tangent of the microstrip substrate and ω is the radian frequency. So from Equations (2.148), (3.12), and (3.32),

$$\alpha_d = \frac{GZ_0}{2} = \frac{1}{2} \frac{\varepsilon_e - 1}{\varepsilon_r - 1} \omega (\tan\delta)\, \varepsilon_r C_{\text{air}} \frac{1}{c\sqrt{CC_{\text{air}}}}. \tag{3.33}$$

Or, using Equation (3.15), this can be written as

$$\alpha_d = \frac{\omega}{c}(\tan\delta)\,\frac{\varepsilon_r(\varepsilon_e - 1)}{2\sqrt{\varepsilon_e}(\varepsilon_r - 1)}\ \text{Np/m}. \tag{3.34}$$

This formula can be used with any TEM transmission line, that is, any transmission line in which the fields are perpendicular to the direction of propagation.

EXAMPLE 3.4 Microstrip "Rule-Of-Thumb"

A rule of thumb is a guideline that is not intended to be accurate but can be easily applied. The accurate formulas for the characteristic impedance and effective permittivity of a microstrip line, Equations (3.20)–(3.24), indicate an underlying trend. The very approximate 'rule of thumb,' for characteristic impedance of a microstrip line is

$$Z_{0,\mathrm{ROT}} = \frac{k}{\sqrt{\epsilon_r}}\sqrt{\frac{h}{w}}. \tag{3.35}$$

where k is a constant which is established for a reference line. Taking the reference as $\varepsilon_r = 10$ and $w/h = 0.954$ then from Tables 3-2 and 3-3, $Z_{0,\mathrm{REF}} = 50\ \Omega$. For this reference $k = 154.4\ \Omega$. The following table indicates the accuracy of this rule of thumb.

ε_r	w/h	actual Z_0 (Ω)	approximate $Z_{0,\mathrm{ROT}}$ (Ω)	error	ε_r	w/h	actual Z_0 (Ω)	approximate $Z_{0,\mathrm{ROT}}$ (Ω)	error
10	1	48.86	48.8	1%	4	2.056	50	53.8	8%
2	1	98.64	109	11%	10	0.954	50	50.0	0%
20	1	35.07	34.5	2%	11.9	0.800	50	50.0	0%
4	0.849	80	83.8	5%	4	4.364	30	37.0	23%
10	0.288	80	91.0	14%	10	2.355	30	31.8	6%
11.9	0.221	80	95.2	19%	11.9	2.067	30	31.1	4%

Thus the trends are correctly described. Even the worst case ($\varepsilon = 4, w/h = 4.364$) has an error of 23% for a factor of 11 parameter change from the reference ($\varepsilon = 10, w/h = 0.954$).

3.6 Microstrip Design Formulas

The formulas developed in Section 3.5.3 enable the electrical characteristics to be determined given the material properties and the physical dimensions of a microstrip line. In design, the physical dimensions must be determined given the desired electrical properties. Several people have developed procedures that can be used to synthesize microstrip lines [15, 21–24]. This subject is considered in much more depth in [19], and here just one approach is reported. The formulas are useful outside the range indicated, but with reduced accuracy. Again, these formulas are the result of curve fits, but starting with physically based equation forms.

3.6.1 High Impedance

For narrow strips, that is, when $Z_0 > (44 - 2\varepsilon_r)\ \Omega$,

$$\frac{w}{h} = \left(\frac{\exp H'}{8} - \frac{1}{4\exp H'}\right)^{-1}, \tag{3.36}$$

$$\text{where}\quad H' = \frac{Z_0\sqrt{2(\varepsilon_r + 1)}}{119.9} + \frac{1}{2}\left(\frac{\varepsilon_r - 1}{\varepsilon_r + 1}\right)\left(\ln\frac{\pi}{2} + \frac{1}{\varepsilon_r}\ln\frac{4}{\pi}\right). \tag{3.37}$$

For $Z_0 > (63 - 2\varepsilon_r)\ \Omega$, [24]

$$\varepsilon_e = \frac{\varepsilon_r + 1}{2}\left[1 + \frac{29.98}{Z_0}\left(\frac{2}{\varepsilon_r + 1}\right)^{1/2}\left(\frac{\varepsilon_r - 1}{\varepsilon_r + 1}\right)\left(\ln\frac{\pi}{2} + \frac{1}{\varepsilon_r}\ln\frac{4}{\pi}\right)\right]^2. \tag{3.38}$$

The formula for ε_e is accurate to better than 1% for $Z_0 > (44 - 2\varepsilon_r)\ \Omega$ (i.e $w/h < 1.3$) for $8 < \varepsilon_r < 12$ [24]. Overall the synthesis of w/h has an accuracy of better than 1%.

3.6.2 Low Impedance

Strips with low Z_0 are relatively wide and the formulas below can be used when $Z_0 < (44 - 2\varepsilon_r)\ \Omega$. The cross-sectional geometry is given by

$$\frac{w}{h} = \frac{2}{\pi}\left[(d_{\varepsilon_r} - 1) - \ln(2d_{\varepsilon_r} - 1)\right] + \frac{(\varepsilon_r - 1)}{\pi\varepsilon_r}\left[\ln(d_{\varepsilon_r} - 1) + 0.293 - \frac{0.517}{\varepsilon_r}\right], \tag{3.39}$$

where $$d_{\varepsilon_r} = \frac{59.95\pi^2}{Z_0\sqrt{\varepsilon_r}}. \tag{3.40}$$

For $Z_0 < (63 - 2\varepsilon_r)\ \Omega$ [24]

$$\varepsilon_e = \frac{\varepsilon_r}{0.96 + \varepsilon_r(0.109 - 0.004\varepsilon_r)[\log(10 + Z_0) - 1]}. \tag{3.41}$$

The expression for ε_e is accurate to better than 1% [24] for $8 < \varepsilon_r < 12$ and $8 \le Z_0 \le (63 - 2\varepsilon_r)\ \ \Omega$.

EXAMPLE 3.5 Microstrip Design

Design a microstrip line to have a characteristic impedance of 75 Ω at 10 GHz. The microstrip a substrate that is 500 µm thick with a relative permittivity of 5.6. (a) What is the width of the line? (b) What is the effective permittivity of the line?

Solution:

(a) The high-impedance (or narrow-strip) formula (Equation (3.36)) is to be used for $Z_0 > (44 - \varepsilon_r)\ [= (44 - 5.6) = 38.4]\ \Omega$.
With $\varepsilon_r = 5.6$ and $Z_0 = 75\ \Omega$, Equation (3.37) yields $H' = 2.445$. From Equation (3.36), $w/h = 0.704$, thus $w = w/h \times h = 0.704 \times 500\ \mu\text{m} = 352\ \mu\text{m}$.

(b) The effective permittivity formula is Equation (3.38), and so $\varepsilon_e = 3.82$.

3.7 Stripline

A symmetrical stripline is shown in Figure 3-12(a). A stripline resembles a microstrip line and comprises a center conductor pattern symmetrically embedded completely within a dielectric, the top and bottom layers of which are conducting ground planes. The strip of width w is considered to have a thickness t that is very small so that the strip is a distance h from each of the ground planes and the ground planes are separated by $b = 2h$. The strip is completely surrounded by the dielectric and so this is a homogeneous medium and there is no need to introduce an effective permittivity.

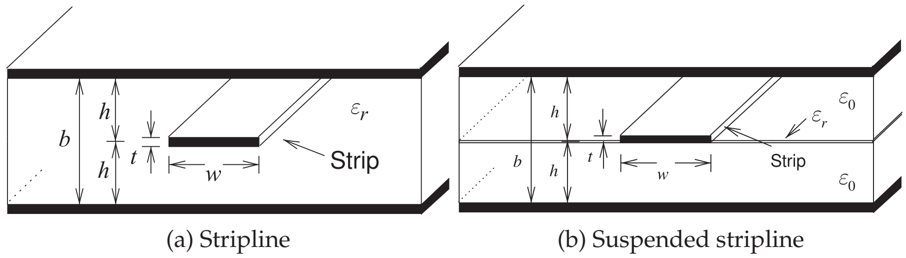

Figure 3-12: Stripline transmission lines. In the suspended stripline the strip is supported by a membrane.

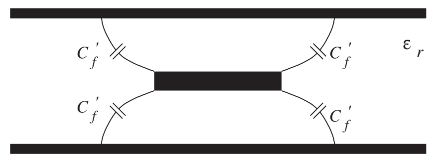

Figure 3-13: Fringe capacitance at the corners of the strip in a stripline transmission lines.

3.7.1 Characteristic Impedance of a Stripline

Finite Thickness

The characteristic impedance of a stripline is [25, 26]

$$Z_0 = \left[\frac{30\pi}{\sqrt{\varepsilon_r}}\right] \frac{(1 - t/b)}{(w_{\text{eff}}/b) + C_f}, \tag{3.42}$$

where the effective width of the strip, w_{eff}, is obtained from

$$\frac{w_{\text{eff}}}{b} = \begin{cases} \dfrac{w}{b} - \left[\dfrac{(0.35 - w/b)^2}{(1 + 12t/b)}\right] & \dfrac{w}{b} < 0.35 \\ \dfrac{w}{b} & \dfrac{w}{b} \geq 0.35 \end{cases} \tag{3.43}$$

$$\text{and} \quad C_f = \frac{2}{\pi} \ln\left[\frac{1}{1 - (t/b)} + 1\right] - \frac{t}{\pi b} \ln\left\{\frac{1}{[1 - (t/b)]^2} - 1\right\}. \tag{3.44}$$

C_f accounts for the fringing capacitance at the edges of the strip and incorporates the effect of the strip thickness for $t \ll b$. The fringing capacitance per unit length (e.g., F/m) at each corner of the strip is

$$C_f' = \frac{\epsilon_0 \varepsilon_r C_f}{1 - t/b} \tag{3.45}$$

and is shown in Figure 3-13. The accuracy of these formulas is better than 1% for $W/(b - t) > 0.05$ and $t/b < 0.025$.

Zero Thickness

If the strip has zero thickness, the characteristic impedance of stripline is

$$Z_0 = \left[\frac{30\pi}{\sqrt{\varepsilon_r}}\right] \frac{1}{(w_{\text{eff}}/b) + 2\ln 2/\pi} = \frac{94.25}{\sqrt{\varepsilon_r}} \frac{1}{(w_{\text{eff}}/b) + 0.441}, \tag{3.46}$$

where the effective width of the strip, w_{eff}, is obtained from

$$\frac{w_{\text{eff}}}{b} = \begin{cases} \dfrac{w}{b} - \left(0.35 - \dfrac{w}{b}\right)^2 & \dfrac{w}{b} < 0.35 \\ \dfrac{w}{b} & \dfrac{w}{b} \geq 0.35 \end{cases}. \tag{3.47}$$

The fringing capacitance per unit length at each corner of the strip is

$$C_f' = \frac{\epsilon_0 \varepsilon_r 2 \ln 2}{\pi} = 0.441 \epsilon_0 \varepsilon_r. \tag{3.48}$$

A stripline supports a purely TEM mode and there is no dielectric dispersion due to an effective permittivity change with frequency. Losses in a stripline are due to dielectric, conductor, and radiative losses. Radiative losses are confined to energy lost to excitation of the parallel plate waveguide mode, but this can be suppressed by shorting the ground planes together at regular intervals (say every tenth of a wavelength).

Formulas have also been developed for the characteristic impedance of asymmetrical stripline, that is, when the strip is not centered between the ground planes [27].

EXAMPLE 3.6 Stripline

A thin strip of a symmetrical stripline has a width of 0.5 mm, is embedded in a dielectric of relative permittivity 5.6, and is between ground planes separated by 1 mm. What is the characteristic impedance of the stripline?

Solution:

The structure is shown in Figure 3-12(a) with $w = 0.5$ mm and $b = 1$ mm. Since the strip is thin, consider that $t = 0$. So from Equations (3.43) and (3.44)

$$\frac{w_{\text{eff}}}{b} = 0.5 \quad \text{and} \quad C_f = 0.441, \tag{3.49}$$

and so

$$Z_0 = \frac{94.25}{\sqrt{5.6}} \frac{1}{(0.5 + 0.441)} = 42.77\ \Omega. \tag{3.50}$$

3.7.2 Attenuation on a Stripline

For a low-loss stripline with radiation loss suppressed by vias between the ground planes, the attenuation, α, comprises two parts, the conductive attenuation, α_c, and the dielectric attenuation, α_d, so that $\alpha = \alpha_c + \alpha_d$. From Equation (2.149)

$$\alpha_c = \frac{R}{2Z_0}, \tag{3.51}$$

where R is the resistance per unit length of the line. R is the sum of the strip and ground resistances. At low frequencies the resistance of the strip is

$$R_{\text{strip}} = R_s / w, \tag{3.52}$$

where R_s is the sheet resistance of the strip and w is the width of the strip. The treatment for the ground resistance is similar to that described in Section 3.5.5 for microstrip. At low microwave frequencies

$$R_{\text{ground}} = \frac{1}{2} \frac{R_{\text{sg}}}{w} \frac{w/h}{w/h + 5.8 + 0.03h/w}, \quad \text{for } 0.1 \leq w/h \leq 10, \tag{3.53}$$

where the sheet resistance of the ground plane is R_{sg}. The factor of one-half arises because there are two grounds and the resistance from each is in parallel. The effect of the ground on the line resistance is small. Both R_{strip} and R_{ground} will increase at higher frequencies as the charges rearrange at much higher frequencies. This will be considered in the next chapter.

The formula for the dielectric attenuation comes from Equation (3.34). The general formula for the attenuation constant due to dielectric loss is, for a low-loss TEM line,

$$\alpha_d = \frac{\omega}{c}\,(\tan\delta)\,\frac{\varepsilon_r(\varepsilon_e - 1)}{2\sqrt{\varepsilon_e}(\varepsilon_r - 1)}\ \text{Np/m}. \tag{3.54}$$

Since the effective permittivity of a stripline is just the relative permittivity of the substrate, $\varepsilon_e = \varepsilon_r$, then Equation (3.54) reduces to

$$\alpha_d = \frac{\omega}{2c}(\tan\delta)\sqrt{\varepsilon_r}\ \text{Np/m} = \tfrac{1}{2}\omega\sqrt{\mu_0\varepsilon_0\varepsilon_r}(\tan\delta)\ \text{Np/m}. \tag{3.55}$$

(Note that here ω is the radian frequency and not the width w.)

The suspended stripline structure shown in Figure 3-12(b) has minimal dielectric and hence minimal dielectric loss. Resonators built using a suspended stripline have a high Q and this structure can be used to realize high-performance filters.

EXAMPLE 3.7 Stripline Attenuation

What is the attenuation of a symmetrical stripline at 1 GHz with $w = h = 0.5$ mm, a $t = 4$ µm-thick strip, silver metallization, and an FR-4 substrate. The ground planes are 4 µm thick. Assume that high frequency effects on line resistance can be ignored.

Solution:

The strip is very thin and the results of Example 3.6 can be used so $Z_0 = 42.77\ \Omega$. The resistivity of silver is $\rho_{\text{Ag}} = 14.87\ \text{n}\Omega\cdot\text{m}$ and so the sheet resistivity of the strip, $R_s = \rho_{\text{Ag}}/t = (14.87\ \text{n}\Omega\cdot\text{m})/(4\ \mu\text{m}) = 3.968\ \text{m}\Omega$. From Equation (3.52) the resistance of the strip is $R_{\text{strip}} = R_s/w = (3.968\ \text{m}\Omega)/(1\ \text{mm}) = 3.968\ \Omega/\text{m}$. The sheet resistance of the grounds is the same as the strip so $R_{sg} = 3.968\ \text{m}\Omega$. From Equation (3.53) the resistance of the grounds is

$$\begin{aligned} R_{\text{ground}} &= \tfrac{1}{2}\frac{R_{\text{sg}}}{w}\,\frac{w/h}{w/h + 5.8 + 0.03h/w} \\ &= \tfrac{1}{2}\frac{(3.968\ \text{m}\Omega)}{(1\ \text{mm})}\,\frac{1}{1 + 5.8 + 0.03} = \frac{3.968\ \Omega/\text{m}}{6.83} = 0.581\ \Omega/\text{m} \end{aligned} \tag{3.56}$$

so that the total line resistance $R = R_{\text{strip}} + R_{\text{ground}} = 4.549\ \Omega/\text{m}$. Thus the attenuation due to conductor loss is $\alpha_c = R/(2Z_0) = 0.1064$ Np/m = 0.924 dB/m.

FR-4 has negligible conductivity and loss in the dielectric is due to dielectric relaxation. FR-4 has a loss tangent at 1 GHz of 0.01 and a relative dielectric constant of 4.3. From Equation (3.55)

$$\alpha_d = \tfrac{1}{2}\omega\sqrt{\mu_0\varepsilon_0\varepsilon_r}(\tan\delta)\ \text{Np/m.} = 0.2172\ \text{Np/m} = 1.886\ \text{dB/m}. \tag{3.57}$$

The total attenuation $\alpha = \alpha_c + \alpha_d = (0.924 + 1.886)\ \text{dB/m} = 2.810\ \text{dB/m}$.

3.7.3 Design Formulas for a Stripline

The synthesis of a symmetrical stripline with a substrate having a relative permittivity ε_r and thickness b requires determination of the width of the strip for a particular characteristic impedance [25]. The width w is obtained from

$$\frac{w}{b} = \begin{cases} x & \text{for } Z_0 \leq 120/\sqrt{\varepsilon_r}\,\Omega \\ 0.85 - \sqrt{0.6 - x} & \text{for } Z_0 > 120/\sqrt{\varepsilon_r}\,\Omega, \end{cases} \tag{3.58}$$

where $$x = \frac{30\pi}{\sqrt{\varepsilon_r} Z_0} - \frac{2\ln 2}{\pi} = \frac{94.25}{\sqrt{\varepsilon_r} Z_0} - 0.441. \tag{3.59}$$

3.8 Coplanar Waveguide

Microstrip is the most popular medium for circuit design at frequencies ranging from several hundred megahertz to tens of gigahertz. However, the electrical characteristics of a microstrip line are sensitive to variations of substrate thickness, and radiation from a microstrip line increases when the substrate is thick. The substrate thickness is not well controlled and can vary by 1%–5% in many substrate technologies. As a result, the characteristic impedance will change by about the same amount. This is not acceptable in many designs where it is desirable that microstrip synthesis be accurate to 1% or so. The lateral dimensions, however, are well controlled being photolithographically defined and then etched.

A solution to the problems of microstrip is coplanar waveguide (CPW) shown in Figure 3-14(a). CPW consists of a central strip flanked by two metal half-planes that carry the return current. The outer conductors can be regarded as ground, but they do not need to be explicitly connected to ground. Provided that the substrate is sufficiently thick, in practice this means that the substrate thickness is two or three times greater than both the strip width w and the metal separation s, the electrical characteristics of CPW are entirely determined by the lateral dimensions, since all of the metallization is on one layer.

Of course, the infinite half-grounds of CPW cannot be produced so a more realistic implementation of CPW is **finite ground CPW** (**FGCPW**), shown in Figure 3-14(b), where the signal return conductors are of finite width. For both the CPW and FGCPW lines, the vitalization and currents

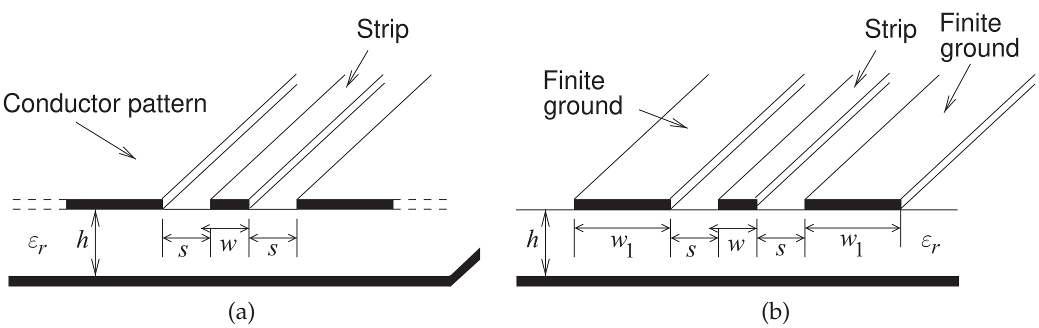

Figure 3-14: Coplanar waveguide (CPW): (a) conventional; and (b) finite ground CPW (FGCPW).

are confined to a single layer. However, the following discussion focuses on the idealized CPW structure in Figure 3-14(a) as this has been studied extensively. However, the characteristics of FGCPW are very close to those of CPW if $w_1 \geq 3w$ (see Figure 3-14(b)).

3.8.1 Effective Permittivity and Characteristic Impedance of CPW

The fields in CPW, and thus the EM energy, are almost equally divided between air and dielectric, especially when the gap is small relative to the thickness of the dielectric. The effective relative permittivity of CPW is [28]

$$\begin{aligned}\varepsilon_e = \varepsilon_{r,e} = & 0.5(\varepsilon_r + 1)\left\{\tanh[1.785\log(h/s) + 1.75]\right. \\ & \left. + (ks/h)[0.04 - 0.7k + 0.01(1 - 0.1\varepsilon_r)(0.25 + k)]\right\},\end{aligned} \tag{3.60}$$

which is accurate to 1.5% for $h/s \geq 1$. In Equation (3.60)

$$k = \frac{w}{w + 2s}. \tag{3.61}$$

Simply taking the effective permittivity as $(\varepsilon_r + 1)/2$ is a good starting point in analysis and design.

The characteristic impedance of CPW is [29]

$$Z_0 = \frac{30\pi}{\sqrt{\varepsilon_e}} \frac{K'(k)}{K(k)}, \tag{3.62}$$

where $$k' = \sqrt{(1 - k^2)} \quad \text{and} \quad K'(k) = K(k'). \tag{3.63}$$

$K(k)$ and $K(k')$ are elliptic integrals, but the ratio, which is all that is required, is much simpler [30]:

$$\begin{array}{lll} \dfrac{K(k)}{K'(k)} \approx \dfrac{1}{\pi}\ln\left(2\dfrac{1+\sqrt{k}}{1-\sqrt{k}}\right) & & 0 \leq k \leq 0.707 \\ \dfrac{K'(k)}{K(k)} \approx \dfrac{1}{\pi}\ln\left(2\dfrac{1+\sqrt{k'}}{1-\sqrt{k'}}\right) & & 0.707 < k \leq 1 \end{array}. \tag{3.64}$$

Note that with CPW, Z_0 is determined by the ratio of the center strip width w to the gap width s. This makes the design of a CPW line with a particular Z_0 non unique because an infinite range of w and s values will result in a specific Z_0 requirement. This provides additional design flexibility.

EXAMPLE 3.8 CPW

A CPW line is fabricated on a 500 μm thick GaAs substrate, has a strip with a width of 200 μm, and a gap of 200 μm between the strip and the ground planes. The relative permittivity of the substrate is 12.85 and the strip is 10 μm thick. What is the effective permittivity and characteristic impedance of the CPW line?

Solution:

The structure is that shown in Figure 3-14(a) with $w = 500$ μm, $s = 200$ μm, $h = 500$ μm, and $t = 10$ μm. From Equation (3.61),

$$k = \frac{w}{w + 2s} = \frac{500}{500 + 400} = 0.556. \tag{3.65}$$

From Equation (3.60),

$$\begin{aligned}\varepsilon_e &= 0.5(12.85+1)\,\{\tanh[1.785\log(500/200)+1.75]\\ &\quad +(0.556\cdot 200/500)[0.04-0.7\cdot 0.556+0.01(1-0.1\cdot 12.85)(0.25+0.556)]\}\\ &= 6.28.\end{aligned} \tag{3.66}$$

This compares to $\varepsilon_e = 6.925$ if the permittivities of air and the substrate are averaged. Several quantities need to be calculated before calculating Z_0. Since $0 \le k \le 0.707$,

$$\frac{K(k)}{K'(k)} = \frac{1}{\pi}\ln\left(2\frac{1+\sqrt{k}}{1-\sqrt{k}}\right) = 0.833. \tag{3.67}$$

Thus from Equation (3.62),

$$Z_0 = \frac{30\pi}{\sqrt{\varepsilon_e}}\frac{K'(k)}{K(k)} = 45.1\ \Omega. \tag{3.68}$$

3.8.2 Loss of CPW lines

Loss of a CPW line is primarily due to dielectric, radiative, and conductor losses. Dielectric loss is lower in a CPW line than in a microstrip line as the electric field lines are evenly divided between the air and dielectric, whereas with a microstrip line most of the field is concentrated in the dielectric. Also, radiation loss with CPW is much lower than with microstrip as the fields lines with a CPW line are much more tightly confined. In practice, when s/h is near to or greater than 1 the structure partially turns into a microstrip transmission line and it is of no use as a CPW line. This transfer of energy into the microstrip mode is another form of loss but can be avoided.

At low frequencies the strip resistance is

$$R_{\text{strip}} = R_s/w, \tag{3.69}$$

where R_s is the sheet resistance of the strip and w is the width of the central strip. The ground resistance can be ignored as the ground current spreads out considerably and the resistances of each ground are in parallel, thus further reducing the ground resistance.

Approximately, the dielectric and conductive components of the attenuation are (if ω, μ_0, and ε_0 have SI units) [19]

$$\alpha_D = \tfrac{1}{2}\omega\sqrt{\mu_0\varepsilon_0\varepsilon_r}\tan\delta\ \text{Np/m} \quad \text{and} \quad \alpha_C = \frac{R_{\text{strip}}}{2Z_0}\ \text{Np/m}, \tag{3.70}$$

respectively. So α_D is almost entirely due to the choice of substrate material.

In summary, it is necessary to calculate the loss of CPW lines using EM simulation software to obtain the required accuracy. This is due to the more tightly confined fields and the greater variation of current densities compared to microstrip and stripline. A key attribute of CPW is the relative frequency independence of the effective permittivity, as this leads to almost dispersion-free transmission of signals. Also, devices can be connected along the signal path without using vias.

3.8.3 CPW Structures

The various CPW structures shown in Figure 3-15 are used to realize transmission line elements. The CPW-to-microstrip transition shown in

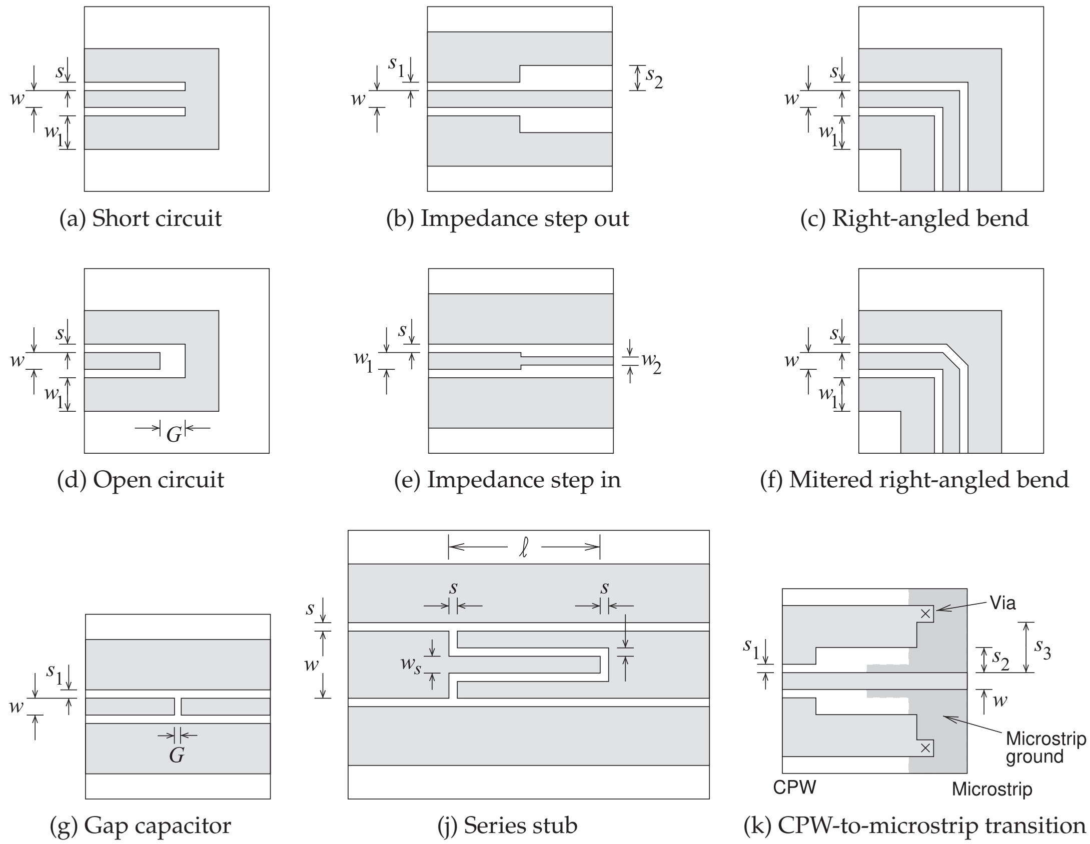

Figure 3-15: CPW structures.

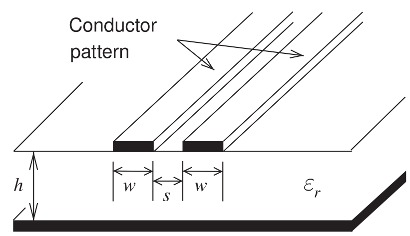

Figure 3-16: Differential line or coplanar strips (CPS).

Figure 3-15(k) requires vias to transfer the ground plane from the same surface as the strip in the CPW line to the second metal plane that forms the ground of microstrip.

3.8.4 Differential Line and Coplanar Strip

A coplanar strip (**CPS**) line is shown in Figure 3-16. CPS has only two conductors separated by a narrow longitudinal slot. It is a balanced line structure and is occasionally implemented in applications including radiating elements and transitions. CPS has become important for on-chip implementations, especially for RFICs and high-speed digital signal transmission, where it is usually referred to as differential line.

CPS is closely related to CPW, as the signal return path is well defined and the electrical characteristics are independent of substrate thickness. CPS is a good structure to use instead of CPW when space is at a premium. Differential line is commonly used with RFICs, as the signal path on the IC is almost always differential since differential circuits on-chip remove many of the distortion and noise-coupling concerns. CPS suffers from relatively high radiation losses when realized on low-permittivity substrates. The radiation also results in substantial interaction and cross talk between adjacent circuits, although this is lower than with a microstrip line.

3.8.5 Summary

Coplanar waveguide is the transmission medium of choice above 20 GHz or so, although the threshold for the switch from microstrip to CPW is higher for on-chip lines. CPW confines the EM fields in a more localized manner than does microstrip, thus reducing spurious coupling, radiation, and dispersion. The electrical characteristics of CPW are defined by the lateral dimensions that can be accurately defined photolithographically. This is a significant advantage when the thickness of a substrate cannot be accurately controlled. CPW provides a precisely defined signal return path and this reduces capacitive coupling of signal lines. CPS lines are also used as digital interconnect mediums where the desirable attribute is the differential signaling. Differential lines, having the same structure as CPS, are commonly used as off-chip transmission lines connecting RFICs.

3.9 Summary

This chapter considered the most important planar transmission lines: microstrip, CPW and stripline. These lines can be produced using printed circuit board techniques. At frequencies below 1 GHz, economics require that standard FR4 circuit boards be used. The weave of a conventional FR4 circuit board can be a significant fraction of critical transmission line dimensions and so affect electrical performance. Nonwoven substrates and sometimes hard substrates such as alumina ceramic, sapphire, or silicon crystal wafers are often required. These also provide higher-dimensional tolerance than can be achieved using conventional woven FR4 substrates. In general, once a design has been optimized in fabrication so that the desired electrical characteristics are obtained, microwave circuits using planar transmission lines can be cheaply and repeatably manufactured in volume. This is true even with ceramic substrates that shrink when they are fired in a process performed after the transmission lines have been patterned. Microstrip and CPW are ideal transmission lines enabling surface modification in design optimization. Buried transmission line mediums such as stripline are difficult to rework, but of course allow more compact designs and thus lower unit costs. However, the rework difficulty results in higher design cost. Stripline does have an advantage over microstrip. Microstrip radiates, but with the fields confined between ground planes, stripline does not. Also stripline design enables multilayer circuit boards to be used, and thus results in smaller overall circuit size, at the price of higher design cost since design on-the-bench optimization are much more difficult.

3.10 References

[1] C. Wen, "Coplanar waveguide: A surface strip transmission line suitable for nonreciprocal gyromagnetic device applications," *IEEE Trans. on Microwave Theory and Techniques*, vol. 17, no. 12, pp. 1087–1090, Dec. 1969.

[2] R. Simons, N. Dib, and L. Katehi, "Modeling of coplanar stripline discontinuities," *IEEE Trans. on Microwave Theory and Techniques*, vol. 44, no. 5, pp. 711–716, May 1996.

[3] D. Prieto, J. Cayrout, J. Cazaux, T. Parra, and J. Graffeuil, "Cps structure potentialities for mmics: a cps/cpw transition and a bias network," in *1998 IEEE MTT-S Int. Microwave Symp. Dig.*, Jun. 1998, pp. 111–114.

[4] K. Goverdhanam, R. Simons, and L. Katehi, "Micro-coplanar striplines-new transmission media for microwave applications," in *1998 IEEE MTT-S Int. Microwave Symp. Dig.*, Jun. 1998, pp. 1035–1038.

[5] ——, "Coplanar stripline components for high-frequency applications," *IEEE Trans. on Microwave Theory and Techniques*, vol. 45, no. 10, pp. 1725–1729, Oct. 1997.

[6] J. Knorr and K. Kuchler, "Analysis of coupled slots and coplanar strips on dielectric substrate," *IEEE Trans. on Microwave Theory and Techniques*, vol. 23, no. 7, pp. 541–548, Jul. 1975.

[7] S. Pintzos, "Full-wave spectral-domain analysis of coplanar strips," *IEEE Trans. on Microwave Theory and Techniques*, vol. 39, no. 2, pp. 239–246, Feb. 1991.

[8] M. Gunston, *Microwave Transmission-line Impedance Data*. Van Nostrand Reinhold Company, 1973.

[9] P. Holder, "X-band microwave integrated circuits using slotline and coplanar waveguide," *The Radio and Electronic Engineer*, vol. 48, no. 1/2, pp. 38–43, Jan./Feb. 1978.

[10] K. Gupta, R. Garg, and I. Bahl, *Microstrip Lines and Slotlines*, 2nd ed. Artech House, 1996.

[11] B. Spielman, "Computer-aided analysis of dissipation losses in isolated and coupled transmission lines for microwave and millimetre-wave applications," *NRL Formal Report*, no. 8009, 1976.

[12] A. Ganguly and B. Spielman, "Dispersion characteristics for arbitrarily configured transmission media," *IEEE Trans. on Microwave Theory and Techniques*, vol. 25, no. 12, pp. 1138–1141, Dec. 1977.

[13] R. Barrett, "Microwave printed circuits—a historical survey," *IRE Trans. on Microwave Theory and Techniques*, vol. 3, no. 2, pp. 1–9, Mar. 1955.

[14] E. Hammerstad and O. Jensen, "Accurate models for microstrip computer-aided design," in *1980 IEEE MTT-S Int. Microwave Symp. Digest*, May 1980, pp. 407–409.

[15] E. Hammerstad and F. Bekkadal, "A microstrip handbook, ELAB Report STF44 A74169," University of Trondheim, Norway, Tech. Rep., Feb. 1975.

[16] E. O. Hammerstad, "Equations for microstrip circuit design," in *5th European Microwave Conf.*, Sep. 1975, pp. 268–272.

[17] K. Karkkainen, A. Sihvola, and K. Nikoskinen, "Effective permittivity of mixtures: numerical validation by the fdtd method," *IEEE Trans. on Geoscience and Remote Sensing*, vol. 38, no. 3, pp. 1303–1308, May 2000.

[18] J. Garnett, "Colors in metal glasses and metal films," *Trans. Royal Society*, vol. 53, pp. 385–420, 1904.

[19] T. Edwards and M. Steer, *Foundations for Microstrip Circuit Design*. John Wiley & Sons, 2016.

[20] A. Djordjevic and T. Sarkar, "Closed-form formulas for frequency-dependent resistance and inductance per unit length of microstrip and strip transmission lines," *IEEE Trans. on Microwave Theory and Techniques,*, vol. 42, no. 2, pp. 241–248, Feb. 1994.

[21] H. Wheeler, "Transmission-line properties of parallel wide strips by a conformal-mapping approximation," *IEEE Trans. on Microwave Theory and Techniques*, vol. 12, no. 3, pp. 280–289, May 1964.

[22] ——, "Transmission-line properties of parallel strips separated by a dielectric sheet," *IEEE Trans. on Microwave Theory and Techniques*, vol. 13, no. 2, pp. 172–185, Feb. 1965.

[23] L. W. Cahill, "Approximate formulae for microstrip transmission lines," *Proc. Institute of Radio and Electrical Engineers*, vol. 35, pp. 317–321, Oct. 1974.

[24] R. Owens, "Accurate analytical determination of quasi-static microstrip line parameters," *Radio and Electronic Engineer*, vol. 46, no. 7, pp. 360–364, Jul. 1976.

[25] I. Bahl and R. Garg, "A designer's guide to stripline circuits," *Microwaves*, pp. 90–96, 1978.

[26] S. Cohn, "Problems in strip transmission lines," *IRE Trans. on Microwave Theory and Techniques*, vol. 3, no. 2, pp. 119–126, Mar. 1955.

[27] H. Howe, *Stripline Circuit Design*. Artech House, 1974.

[28] W. Hilberg, "From approximations to ex-

act relations for characteristic impedances," *IEEE Trans. on Microwave Theory and Techniques*, vol. 17, no. 5, pp. 259–265, May 1969.

[29] C. Wen, "Coplanar waveguide: A surface strip transmission line suitable for nonreciprocal gyromagnetic device applications," *IEEE Trans. on Microwave Theory and Techniques*, vol. 17, no. 12, pp. 1087–1090, Dec. 1969.

[30] M. Houdart, "Coplanar lines : Application to broadband microwave integrated circuits," in *6th European Microwave Conf.*, Sep. 1976, pp. 49–53.

3.11 Exercises

1. At low frequencies a microstrip line has a capacitance of 1 nF/m and when the dielectric is replaced by air its capacitance is 0.5 nF/m. What is the phase velocity of signals on the line with the dielectric substrate in place? Consider that the relative magnetic permeability is 1.
2. A non-magnetic microstrip line has a capacitance of 100 pF/m and when the dielectric is replaced by air it has a capacitance of 25 pF/m. What is the phase velocity of signals on the line with the dielectric?
3. At low frequencies a non-magnetic microstrip transmission line has a capacitance of 10 nF/m and when the dielectric is replaced by air it has a capacitance of 2.55 nF/m. What is the effective permittivity of the microstrip line of signals on the line with the dielectric substrate in place?
4. A microstrip line on 250 μm thick GaAs has a minimum and maximum strip widths of 50 μm and 250 μm respectively. What is the range of characteristic impedances that can be used in design?
5. A microstrip line with a substrate having a relative permittivity of 10 has an effective permittivity of 8. What is the wavelength of a 10 GHz signal propagating on the microstrip?
6. A microstrip line has a width of 500 μm and a substrate that is 635 μm thick with a relative permittivity of 20. What is the effective permittivity of the line?
7. The strip of a microstrip has a width of 250 μm and is fabricated on a lossless substrate that is 500 μm thick and has a relative permittivity of 2.3. [Parallels Example 3.2]
   (a) What is the effective relative permittivity of the line?
   (b) What is the characteristic impedance of the line?
   (c) What is the propagation constant at 3 GHz ignoring any losses?
   (d) If the strip has a resistance of 0.5 Ω/cm and the ground plane resistance can be ignored, what is the attenuation constant of the line at 3 GHz?
8. A microstrip line on a 250 μm-thick silicon substrate has a width of 200 μm. Use Table 3-3.
   (a) What is line's effective permittivity.
   (b) What is its characteristic impedance?
9. A 600 μm-wide microstrip line on a 500 μm-thick alumina substrate. Use Table 3-3.
   (a) What is line's effective permittivity.
   (b) What is its characteristic impedance?
10. A microstrip line on a 1 mm-thick FR4 substrate has a width of 0.497 mm. Use Table 3-3.
    (a) What is line's effective permittivity.
    (b) What is its characteristic impedance?
11. Consider a microstrip line on a substrate with a relative permittivity of 12 and thickness of 1 mm.
    (a) What is the minimum effective permittivity of the microstrip line if there is no limit on the minimum or maximum width of the strip?
    (b) What is the maximum effective permittivity of the microstrip line if there is no limit on the minimum or maximum width of the strip?
12. A microstrip line has a width of 1 mm and a substrate that is 1 mm thick with a relative permittivity of 20. What is the geometric filling factor of the line?
13. The substrate of a microstrip line has a relative permittivity of 16 but the calculated effective permittivity is 12. What is the filling factor?
14. A microstrip line has a strip width of 250 μm and a substrate with a relative permittivity of 10 and a thickness of 125 μm. What is the filling factor?
15. A microstrip line has a strip width of 250 μm and a substrate with a relative permittivity of 4 and thickness of 250 μm. Determine the filling factor and thus the effective relative permittivity of the line?
16. A microstrip line has a strip with a width of 100 μm and the substrate which is 250 μm thick and a relative permittivity of 8.
    (a) What is the filling factor, q, of the line?

(b) What is the line's effective relative permittivity?
(c) What is the characteristic impedance of the line?

17. An inhomogeneous transmission line is fabricated using a medium with a relative permittivity of 10 and has an effective permittivity of 7. What is the fill factor q?

18. A microstrip technology uses a substrate with a relative permittivity of 10 and thickness of 400 μm. The minimum strip width is 20 μm. What is the highest characteristic impedance that can be achieved?

19. A microstrip transmission line has a characteristic impedance of 75 Ω, a strip resistance of 5 Ω/m, and a ground plane resistance of 5 Ω/m. The dielectric of the line is lossless.
(a) What is the total resistance of the line in Ω/m?
(b) What is the attenuation constant in Np/m?
(c) What is the attenuation constant in dB/cm?

20. A microstrip line has a characteristic impedance of 50 Ω, a strip resistance of 10 Ω/m, and a ground plane resistance of 3 Ω/m.
(a) What is the total resistance of the line in Ω/m?
(b) What is the attenuation constant in Np/m?
(c) What is the attenuation constant in dB/cm?

21. A microstrip line has 10 μm-thick gold metallization for both the strip and ground plane. The strip has a width of 125 μm and the substrate is 125 μm thick.
(a) What is the low frequency resistance (in Ω/m) of the strip?
(b) What is the low frequency resistance of the ground plane?
(c) What is the total low frequency resistance of the microstrip line?

22. A 50 Ω microstrip line has 10 μm-thick gold metallization for both the strip and ground plane. The strip has a width of 250 μm and the lossless substrate is 250 μm thick.
(a) What is the low frequency resistance (in Ω/m) of the strip?
(b) What is the low frequency resistance of the ground plane?
(c) What is the total low frequency resistance of the microstrip line?
(c) What is the attenuation in dB/m of the line at low frequencies?

23. A 50 Ω microstrip line with a lossless substrate has a 0.5 mm-wide strip with a sheet resistance of 1.5 mΩ and the ground plane resistance can be ignored. What is the attenuation constant at 1 GHz? [Parallels Example 3.3]

24. A microstrip line operating at 10 GHz has a substrate with a relative permittivity of 10 and a loss tangent of 0.005. It has a characteristic impedance of 50 Ω and an effective permittivity of 7.
(a) What is the conductance of the line in S/m?
(b) What is the attenuation constant in Np/m?
(c) What is the attenuation constant in dB/cm?

25. A microstrip line has the per unit length parameters L = 2 nH/m and C = 1 pF/m, also at 10 GHz the substrate has a conductance G of 0.001 S/m. The substrate loss is solely due to dielectric relaxation loss and there is no substrate conductive loss. The resistances of the ground and strip are zero.
(a) What is G at 1 GHz?
(b) What is the magnitude of the characteristic impedance at 1 GHz?
(c) What is the dielectric attenuation constant of the line at 1 GHz in dB/m?

26. A microstrip line has the per unit length parameters L = 1 nH/m and C = 1 pF/m, also at 1 GHz the substrate has a conductance G of 0.001 S/m. The substrate loss is solely due to dielectric relaxation loss and there is no substrate conductive loss. The resistance of the strip is 0.5 Ω/m and the resistance of the ground plane is 0.1 Ω/m.
(a) What is the per unit length resistance of the microstrip line at 1 GHz?
(b) What is the magnitude of the characteristic impedance at 1 GHz?
(c) What is the conductive attenuation constant in Np/m?
(d) What is the dielectric attenuation constant of the line at 1 GHz in dB/m?

27. A microstrip line operating at 2 GHz has perfect metallization for both the strip and ground plane. The strip has a width of 250 μm and the substrate is 250 μm thick with a relative permittivity of 10 and a loss tangent of 0.001.
(a) What is the filling factor, q, of the line?
(b) What is the line's effective relative permittivity?
(c) What is the line's attenuation in Np/m?
(d) What is the line's attenuation in dB/m?

28. A 50 Ω microstrip line operating at 1 GHz has perfect metallization for both the strip and ground plane. The substrate has a relative permittivity of 10 and a loss tangent of 0.001. Without the dielectric the line has a capacitance of 100 pF/m.

(a) What is the line conductance in S/m?
(b) What is the line's attenuation in Np/m?
(c) What is the line's attenuation in dB/m?

29. Design a microstrip line having a 50 Ω characteristic impedance. The substrate has a permittivity of 2.3 and is 250 μm thick. The operating frequency is 18 GHz. You need to determine the width of the microstrip line.

30. A load has an impedance $Z = 75 + \jmath 15\ \Omega$.
(a) What is the load reflection coefficient, Γ_L, with reference impedance of 75 Ω?
(b) Design an open-circuited stub at the load that will make the impedance of the load plus the stub, call this Z_1, be purely real. Choose a stub characteristic impedance of 75 Ω. At this stage do an electrical design only. (This requires complete electrical information such as the electrical length of the stub.)
(c) Following on from (b), now design a quarter-wave transformer between the source and the stub that will present 50 Ω at the input. (The design must include the characteristic impedance of the transmission line and its electrical length. Thus the structure is a $\lambda/4$ transformer, a stub, and the load.)
(d) Now convert the electrical specifications of the design into a physical design at 1 GHz using microstrip technology with substrate thickness $h = 0.5$ mm and relative permittivity $\varepsilon_r = 10$. You must design the widths and lengths of the stub and the quarter-wave transformer.

31. Design a microstrip line to have a characteristic impedance of 65 Ω at 5 GHz. The substrate is 635 μm thick with a relative permittivity of 9.8. Ignore the thickness of the strip. [Parallels Example 3.5]
(a) What is the width of the line?
(b) What is the effective permittivity of the line?

32. Design a microstrip shorted stub at 10 GHz with the following characteristics:

- Characteristic impedance of 60 Ω.
- A substrate with a relative permittivity of 9.6 and thickness of 500 μm.
- Input impedance of $\jmath 60\ \Omega$.

(a) What is the width of the microstrip line?
(b) What is the length of the line in centimeters?
(c) What is the effective permittivity of the line?
(d) If the line is one-quarter wavelength longer than that calculated in (b), what will the input reactance be?
(e) Regardless of your calculations above, what is the input admittance of a one-quarter wavelength long shorted stub?

33. Design a microstrip line to have a characteristic impedance of 20 Ω. The microstrip is to be constructed on a substrate that is 1 mm thick with a relative permittivity of 12. [Parallels Example 3.5]
(a) What is the width of the line? Ignore the thickness of the strip and frequency-dependent effects.
(b) What is the effective permittivity of the line?

34. A load has an impedance $Z = 75 + \jmath 15\ \Omega$.
(a) What is the load reflection coefficient, Γ_L, if the system reference impedance is 75 Ω?
(b) Design a shorted stub at the load that will make the impedance of the load plus the stub, call this Z_1, be purely real; that is, the reflection coefficient of the effective load, Γ_1, has zero phase. Choose a stub characteristic impedance of 75 Ω. At this stage do an electrical design only. (This require complete electrical information , e.g. the electrical length of the stub.)
(c) Following on from (b), now design a quarter-wave transformer between the source and the stub that will present 50 Ω at the input. (The design must include the characteristic impedance of the transmission line and its electrical length. Thus the structure is a $\lambda/4$ transformer, a stub, and the load.)
(d) Now convert the electrical design into a physical design at 1 GHz using microstrip technology with substrate thickness $h = 0.5$ mm and relative permittivity $\varepsilon_r = 10$. You must design the widths and lengths of the stub and the quarter-wave transformer.

35. The strip of a symmetrical stripline has a width of 1 mm and the ground planes of the stripline are separated by 2 mm. The dielectric has a relative permittivity of 4.2. The strip has negligible thickness.
(a) What is the effective permittivity of the stripline?
(b) What is the characteristic impedance of the stripline at 1 GHz?

36. The strip of a symmetrical stripline has a width of 500 μm and the ground planes of the stripline are separated by 1 mm. The dielectric has a relative permittivity of 10. The strip has a thickness of 0.1 mm.
(a) What is the effective permittivity of the stripline?

(b) What is the characteristic impedance of the stripline?
(c) What is the total fringing capacitance in pF/m?

37. The strip of a symmetrical stripline has a width of 200 μm and the ground planes of the stripline are separated by 1 mm. The dielectric has a relative permittivity of 4. The strip has a thickness of 0.1 mm.
(a) What is the effective permittivity of the stripline?
(b) What is the characteristic impedance of the stripline?
(c) What is the total fringing capacitance in pF/m?

38. The strip of a symmetrical stripline has a width of 50 µm and the ground planes of the stripline are separated by 300 µm. The dielectric has a relative permittivity of 10. The strip has a thickness of 10 µm. What is the characteristic impedance of the stripline?

39. The strip of a symmetrical stripline has a width of 0.25 mm and the ground planes of the stripline are separated by 1 mm. The dielectric has a relative permittivity of 80. What is the effective width of the strip?

40. The strip of a symmetrical stripline has a width of 100 µm and is embedded in a lossless medium that is 400 µm thick and has a relative permittivity of 13, thus the separation, h, from the strip to each of the ground planes is 200 µm.
(a) Draw the effective waveguide model of a stripline with magnetic walls and an effective strip width, w_{eff}.
(b) What is the effective relative permittivity of the stripline waveguide model?
(c) What is w_{eff}?

41. A symmetrical stripline has a thin strip with a width of 200 µm, is embedded in a dielectric of relative permittivity 12, and is between ground planes separated by 500 µm. What is Z_0 of the line? [Parallels Example 3.6]

42. At 1 GHz a 60 Ω stripline has the per unit parameters $R = 2\ \Omega/\text{m}$ and $G = 1$ mS/m. What is the attenuation of the line in dB/m?

43. A 50 Ω symmetrical stripline has a 0.5 mm-wide strip and the ground planes are separated by 1.2 mm. The strip has a sheet resistance of 1.5 mΩ and each ground plane has a sheet resistance of 1 mΩ. (Ignore high frequency effects on resistance.) The substrate has a loss tangent of 0.005 and a relative permittivity of 6. [Parallels Example 3.7]
(a) What is the line's effective permittivity?
(b) What is its characteristic impedance?
(c) What is the attenuation constant of the line in dB/m at 2 GHz?

44. The strip of a CPW line has a width $w = 400$ µm and separations from the in-plane grounds of $s = 250$ µm. The substrate is $h = 1000$ µm thick and the thickness of the metal is $t = 5$ µm. What is the effective permittivity and characteristic impedance of the CPW line.

45. A CPW line with a 250 µm thick GaAs substrate, has a width of 125 µm and thickness of 3 µm, and a gap of 125 µm between the strip and ground planes. [Parallels Example 3.8]
(a) What is the line's effective permittivity?
(b) is the Z_0 of the line?

3.11.1 Exercises by Section

†challenging, ‡very challenging

§3.2	$1, 2, 3$
§3.5	$4, 5, 6^\dagger, 7^\dagger, 8, 9, 10, 11, 12, 13, 14, 15, 16, 17, 18, 19, 20, 21, 22, 23, 24, 25^\dagger, 26^\dagger, 27, 28$
§3.6	$29^\dagger, 30^\dagger, 31^\dagger, 32^\ddagger, 33^\dagger$
§3.7	$34^\ddagger, 35^\dagger, 36^\dagger, 37^\dagger, 38^\dagger, 39^\dagger, 40^\ddagger, 41^\dagger, 42, 43$
§3.8	$44, 45^\dagger$

3.11.2 Answers to Selected Exercises

6	12.75
7(c)	$\jmath 84.1\ \text{m}^{-1}$
19(c)	0.579 dB/m
20(a)	13 Ω/m
25(b)	44.72 Ω
31(a)	340 µm
34(b)	100.9° for open stub, 10.89° for shorted stub
33(b)	9.17
39	245.5 µm
40(c)	969 µm

CHAPTER 4

Extraordinary Transmission Line Effects

4.1 Introduction

Previous chapters discussed the low-frequency operation of transmission lines. This chapter describes the origins of, particularly of planar lines. Figure 4-1 shows the typical frequency dependence of a line's $RLGC$ parameters. The variations of R, L, and C are of most interest, and, except with some semiconductor substrates, G is usually negligible.

The major limitation on the dimensions and maximum operating frequency of a transmission line is determined by the origination of higher-order modes (i.e., orientations of the fields). Different modes on a transmission line travel at different velocities. Thus the problem is that if a signal on a line is split between two modes, then the information sent from one end of the line will reach the other end in two packets arriving at different times. The two modes have random partitioning of the signal

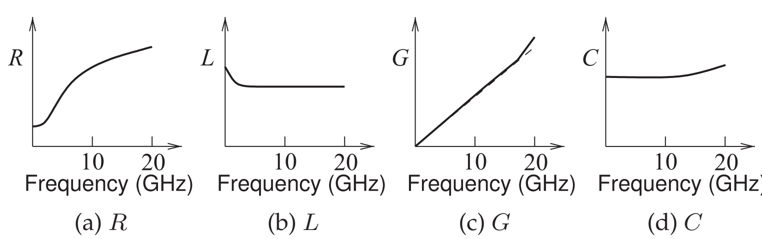

Figure 4-1: Frequency dependence of transmission line parameters.

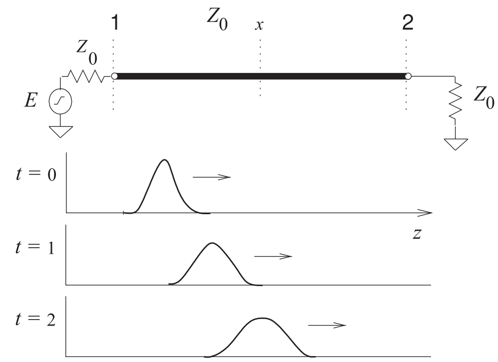

Figure 4-2: Dispersion of a pulse along a line.

energy and it is the combination that will be detected, and in general the information will be lost as the two modes combine in an incoherent manner. Multimoding must always be avoided.

4.2 Frequency-Dependent Characteristics

All interconnects have frequency-dependent behavior. In this section the origins of the frequency-dependent behavior of a microstrip line are examined because microstrip has the most significant frequency dependence among interconnects of general interest. Frequency-dependent behavior other than multimoding often results in dispersion. The effect can be seen in Figure 4-2 for a pulse traveling along a line. The pulse spreads out as the different frequency components travel at different speeds. For a long line, successive pulses will start merging and the signal will become unintelligible.

The most important frequency-dependent effects are

- changes of material properties (permittivity, permeability, and conductivity) with frequency (Section 4.2.1),
- current bunching (discussed in Section 4.2.3),
- skin effect (Sections 4.2.4 and 4.2.5),
- internal conductor inductance variation (Section 4.2.4),
- dielectric dispersion (Section 4.2.6), and
- multimoding (Section 4.4).

While the discussion focuses on microstrip lines, the effects occur with other planar and nonplanar transmission lines.

4.2.1 Material Dependency

Changes of permittivity, permeability, and conductivity with frequency are properties of the materials used. Fortunately the materials of interest in microwave technology have characteristics that are almost independent of frequency, at least up to 300 GHz or so.

4.2.2 Frequency-Dependent Charge Distribution

Skin effect, current bunching, and internal conductor inductance are all due to the necessary delay in transferring EM information from one location to another. This information cannot travel faster than the speed of light in the medium. In a dielectric material the speed of an EM wave will be slower

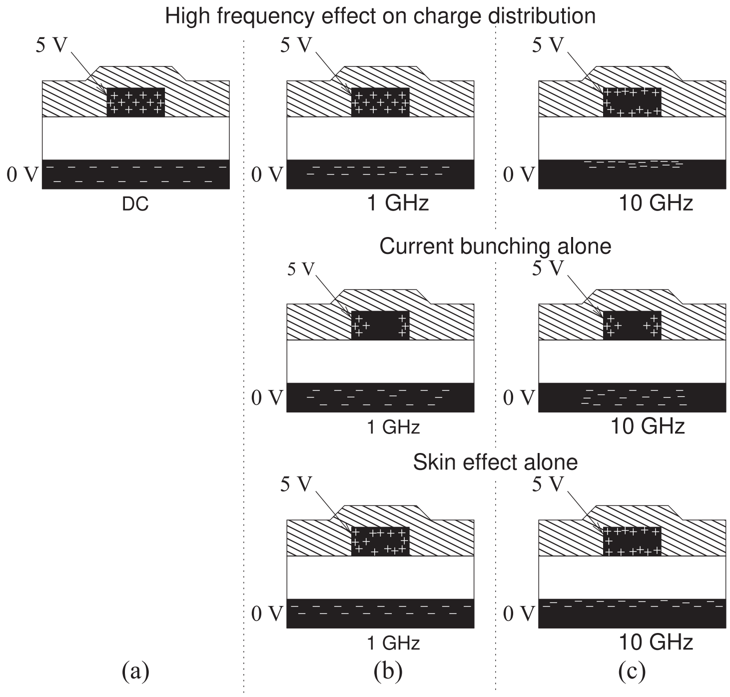

Figure 4-3: Cross-sectional view of the charge distribution on an interconnect at different frequencies. The + and − indicate charge concentrations of different polarity and corresponding current densities. There is no current bunching or skin effect at DC.

than that in free space by a factor of $\sqrt{\varepsilon_r}$, where ε_r is the relative permittivity of the material. Thus the speed of an EM wave in microwave dielectrics is reduced typically by a factor ranging from just over 1 to 300. However, the velocity in a conductor is extremely low because of high conductivity. In brief, current bunching is due to changes related to the finite velocity of information transfer through the dielectric, and skin effect and variations of internal conductor inductance are due to the very slow speed of information transfer inside a conductor. As frequency increases, only limited information to rearrange charges can be sent before the polarity of the signal reverses and information is sent to reverse the changes. The skin and charge-bunching effects on a microstrip line are illustrated in cross section in Figure 4-3.

4.2.3 Current Bunching

Consider the charge distribution for a microstrip line shown in the cross-sectional views in Figure 4-3. The microstrip cross sections shown here are typical of an interconnect on a printed circuit board or a monolithically integrated circuit where the top dielectric is a **passivation** layer. The thickness of the microstrip is often a significant fraction of its width, although this is exaggerated in Figure 4-3.

The charge distribution shown in Figure 4-3(a) applies when there is a positive DC voltage on the strip (the top conductor). In this case there are positive charges on the top conductor arranged with a fairly uniform distribution. The individual positive charges (caused by the absence of balancing electrons exposing positively charged ions) tend to repel each other, but this has little effect on the charge distribution for practical conductors with finite conductivity. (If the conductor had zero resistance then these net charges would be confined to the surface of the conductor.) The bottom conductor is known as the ground plane and there are balancing

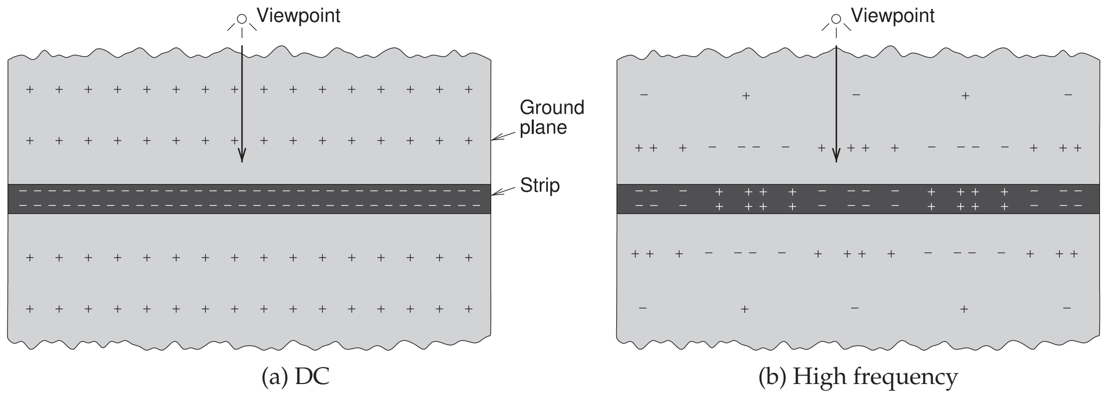

Figure 4-4: Current bunching effect in time. Positive and negative charges are shown on the strip and on the ground plane. The viewpoint is on the ground plane.

negative charges, or a surplus of electrons, so that electric field lines begin on the positive charges and terminate on the negative charges. The negative charges on the ground plane are uniformly distributed across the whole of the ground plane. An important point is that where there are unbalanced charges there can be current flow. So the charge distribution at DC, shown in Figure 4-3(a), indicates that for the top conductor, current would flow uniformly inside the conductors and the return current in the ground plane would be distributed over the whole of the ground plane.

The charge distribution becomes less uniform as frequency increases and eventually the signal changes so quickly that information to rearrange charges on the ground plane is soon (half a period latter) countered by reverse instructions. Thus the charge distribution depends on how fast the signal changes. Another way of looking at this effect is to view the charges on the strip of the microstrip line at one time. This is shown in Figure 4-4 for a DC signal on the line and for a high-frequency signal. The DC situation is shown in Figure 4-4(a) where there is a uniform distribution of negative charges on the strip. This uniform distribution (in this case of negative charges) is seen from the viewpoint shown. The field then induces uniformly distributed positive charges on the ground plane. At a high frequency the charges on the strip alternate between negative and positive charges, as shown in Figure 4-4(b). Now the effective charge on the strip that is "seen" depends on how far the viewpoint is from the strip. When the viewpoint is at a large distance, it will seem as though the positive and negative charges cancel each other out. Thus on the ground plane at a large distance from the strip there will effectively be very little net charge on the strip. Consequently, at distance, there will be few matching charges on the ground plane that match the charges on the strip. Closer into the strip the ground will "see" a more concentrated charge on the strip and the charges on the ground plane will correspond more closely to the DC situation.

The electric field lines, which must originate and terminate on charges, will concentrate in the substrate more closely under the strip as frequency increases. There will be fewer electric field lines in the air that go out to the fewer distant charges in the ground plane. The two major effects are that the effective permittivity of the microstrip line increases with frequency, and resistive loss increases as the average current density in the ground, which corresponds to the net charge density, increases. Thus the line resistance and capacitance increase with frequency (see Figure 4-1(a) and 4-1(d), respectively). For the majority of substrates G is due to dielectric relaxation rather than conduction in the dielectric. As such, G increases linearly with frequency with a superlinear increase at very high frequencies when the electric field is more concentrated in the dielectric (see Figure 4-1(c)).

In the frequency domain the current bunching effects are seen in the higher-frequency views shown in Figures 4-3(b and c). (The concentration of charges near the surface of the metal is a separate effect known as the skin effect.) The longitudinal impact of current or charge bunching alone is illustrated in Figures 4-5, 4-6, and 4-7. These figures present amplitudes of the current and charge phasors at various frequencies and were calculated using the **Sonnet** EM simulator. In interpreting these figures, take into account the magnitudes of the current and charge distributions as identified in the captions, as the scales are normalized. An alternative view (or time-domain view) is the instantaneous snapshot of current and charge shown in Figure 4-8.

This situation is not just confined to the transverse plane, and regions further along the interconnect also send instructions. The net effect is bunching of charges and hence of current on both the ground plane and the strip.

4.2.4 Skin Effect and Internal Conductor Inductance

At low frequencies, currents are distributed uniformly throughout a conductor. Thus there are magnetic fields inside the conductor and hence magnetic energy storage. As a result, there is internal conductor inductance. Transferring charge to the interior of conductors is particularly slow, and as the frequency of the signal increases, charges are confined closer to the surface of the metal. This effect is seen in Figure 4-9 where the current density inside the strip of a microstrip line is plotted at various frequencies. Thus time-varying EM fields are not able to penetrate the conductors as much as frequency increases. This phenomenon is known as the skin effect. With lower internal currents, the internal conductor inductance reduces and the total inductance of the line drops [1–4]. Thus the redistribution of the current results in a change of the inductance with frequency (see Figure 4-1(b)). Only above a few gigahertz or so can the line inductance be approximated as a constant for the transverse interconnect dimensions of a micron to several hundred microns.

The skin effect is characterized by the skin depth, δ_s, which is the distance at which the electric field, or equivalently the charge density, reduces to $1/\mathrm{e}$ of its value at the surface. The skin depth is determined to be

$$\delta_s = 1/\sqrt{\pi f \mu_0 \sigma_2}. \tag{4.1}$$

Here f is frequency and σ_2 is the conductivity of the conductor. The conductivity is a measured quantity that is determined by the same physical phenomenon.[1] The permittivity and permeability of metals typically used

[1] This phenomenon is described by M. Born and E. Wolf [5]. In a conductor an electric field

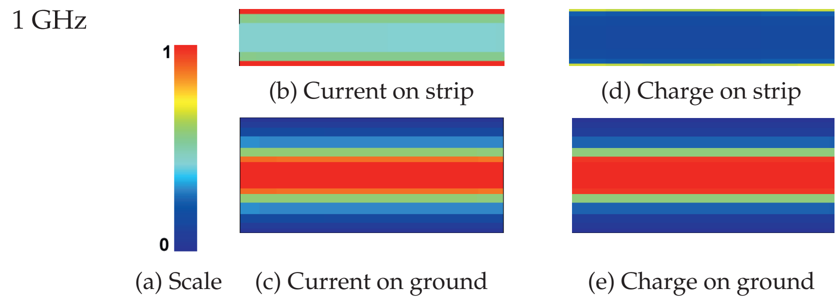

Figure 4-5: Normalized current and charge magnitudes on an alumina microstrip line at 1 GHz ($\varepsilon_r = 10.0$): (a) scale; (b) longitudinal current, i_z, on the strip (10–26 A/m); (c) on the ground plane (0–3.2 A/m); (d) charge on the strip (80–400 nC/m^2); and (e) on the ground (0–33 nC/m^2). See inside the back cover for a color image.

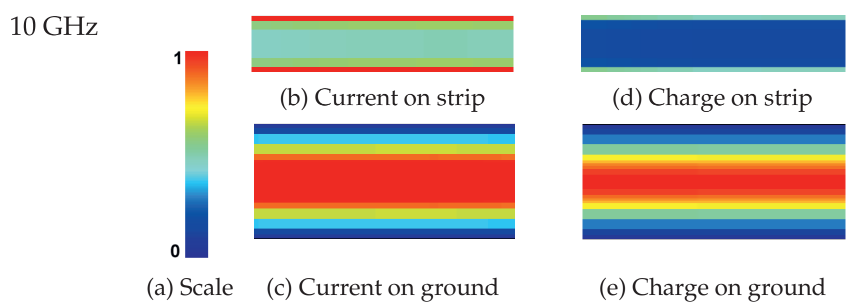

Figure 4-6: Normalized current and charge magnitudes on an alumina microstrip line at 10 GHz: (a) scale; (b) longitudinal current, i_z, on the strip (10–28 A/m); (c) on the ground plane (0–4.1 A/m); (d) charge on the strip (114–512 nC/m^2); and (e) on the ground (0–39 nC/m^2). See inside the back cover for a color image.

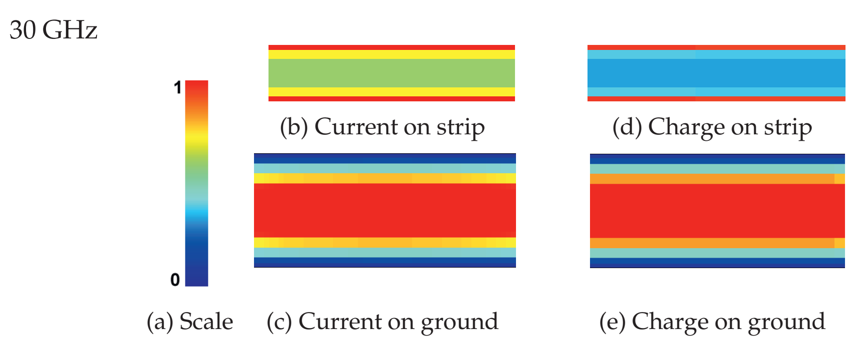

Figure 4-7: Normalized magnitudes of current and charge on an alumina microstrip line at 30 GHz: (a) scale; (b) longitudinal current, i_z, on the strip (10–31 A/m); (c) on the ground plane (0–6 A/m); (d) the charge on the strip (200–575 nC/m^2); and (e) on the ground (0–68 nC/m^2). See inside the back cover for a color image.

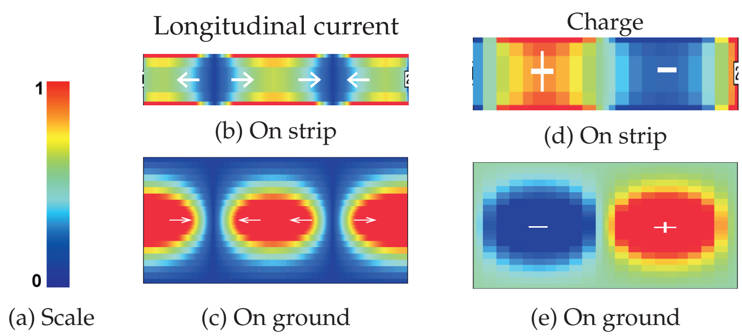

Figure 4-8: Normalized instantaneous current and charge on an alumina microstrip line at 30 GHz. Lighter regions have higher current density in (b) and (c), and more positive charge in (d) and (e).

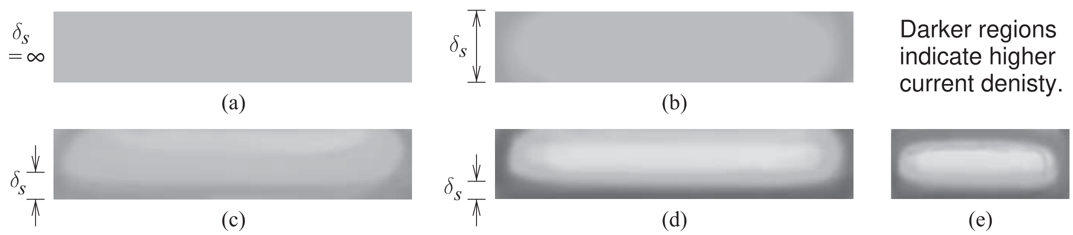

Figure 4-9: Cross sections of the strip of a microstrip line showing the impact of skin effect and current bunching on current density: (a) at dc (uniform current density); (b) the strip thickness, t, is equal to the skin depth, δ_s (i.e. at a low microwave frequency); (c) $t = 3\delta_s$; (d) $t = 5\delta_s$ (i.e. at a high microwave frequency); and (e) $t = 5\delta_s$ for a narrow strip. The plots are the result of 3D simulations of a microstrip line using internal conductor gridding.

for interconnects (e.g., gold, silver, copper, and aluminum) are that of free space, ε_0 and μ_0, respectively, as there is no mechanism to store electric energy (there is no separation of charge centers) and, except for magnetic materials, no mechanism to store magnetic energy (no unbalanced magnetic moments).

4.2.5 Skin Effect and Line Resistance

The skin effect is illustrated in Figure 4-3(b) at 1 GHz. The situation is more extreme as the frequency continues to increase (e.g., to 10 GHz) as in Figure 4-3(c). There are several important consequences of this. On the top conductor, as frequency increases, current flow is mostly concentrated near the surface of the conductors and the effective cross-sectional area of the conductor, as far as the current is concerned, is less. Thus the resistance of the top conductor increases. A more dramatic situation exists for the charge distribution in the ground plane. From the previous discussion of current bunching it was noted that charge is not uniformly distributed over the whole of the ground plane, but instead becomes more concentrated under

accelerates free electrons that in turn radiate around the direction of motion. This process is repeated as the field penetrates the conductor. While the leading edge of the electric field propagates quickly through the conductor it rapidly diminishes in amplitude. The average field penetrates very slowly due to the large number of free electrons and multiple scattering of the field. A rough guide is that the effective velocity at microwave frequencies for transfer of the bulk of the energy is about $c/1000$. It is not possible to determine an accurate number.

the strip as frequency increases. In addition to this, charges and current are confined to the skin of the ground conductor so that the frequency-dependent relative change of ground plane resistance with increasing frequency is greater than that of the strip. On the strip, current bunching results in charges being concentrated on the edges of the strip. This effect is more pronounced the higher the permittivity of the substrate.

The skin effect and current bunching result in frequency dependence of the line resistance, R, with

$$R(f) = \begin{cases} R(0) & f \text{ such that } t \le 3\delta_s \\ \\ R(0) + R_{\text{skin}}(f) & f \text{ such that } t > 3\delta_s, \end{cases} \tag{4.2}$$

where $R(0) = R_{\text{strip}}(0) + R_{\text{ground}}(0)$ is the resistance of the line at low frequencies (see Equation (3.28)). $R(f)$ describes the frequency-dependent line resistance that is due to both the skin effect and current bunching. Approximately,

$$R_{\text{skin}}(f) = R(0)k\sqrt{f}. \tag{4.3}$$

Here k is a constant, and while Equation (4.3) indicates proportionality to $\sqrt{f}$, this is an approximation, but $R(f)$ always increases more slowly than frequency [4, 6–8]. The dominant breakpoint is indicated in Equation (4.2).

The increased resistance of the strip at high frequencies results from both current bunching, increasing the current density at the edges of the strip and reducing it in the middle with respect to the width of the strip, and skin effect, increasing the current density on the top and bottom surfaces of the strip and reducing it in the middle with respect to the thickness of the strip (this is of concern at frequencies where $t > 3\delta_s$ [4, 7]). At low frequencies the contribution of the ground to the resistance of the line is small, but because of current bunching the resistance of the ground becomes significant [8] at higher frequencies. The resistance of the ground further increases because of the skin effect and at high microwave frequencies the resistance of the ground can be comparable to that of the strip. Surface roughness of the metal also affects line resistance [9]. This is easy to imagine if the roughness is comparable to the skin depth as the current path is increased by the roughness. Roughness of the metal surface primarily reflects the roughness of the substrate for hard substrates. With soft substrates the underside of the metal is intentionally roughened so that the rough needle-like metal surface penetrates into and anchors to the dielectric when the metal and dielectric are pressed together. For these reasons it is not possible to develop a simple and accurate expression for the frequency-dependent resistance of a microstrip line, and EM simulation is also necessary, but even then roughness cannot be accounted for. EM simulation is necessary in any case to determine attenuation due to radiation. It is essential to incorporate measurements into the design cycle of circuits at high microwave frequencies to account for effects that cannot be modeled [10, 11]. One observation on the frequency dependence of resistance is that it is pointless to make the thickness of the strip or of the ground thicker than three times the skin depth.

EXAMPLE 4.1 Skin Depth

Determine the skin depth for copper (Cu), silver (Ag), aluminum (Al), gold (Au), and titanium (Ti) at 100 MHz, 1 GHz, 10 GHz, and 100 GHz.

Solution:

The skin depth is calculated using Equation (4.1) and the conductivity from Appendix 2.A.

Metal	Resistivity ($n\Omega \cdot m$)	Conductivity (MS/m)	Skin depth, δ_s (μm) 100 MHz	1 GHz	10 GHz	100 GHz
Copper (Cu)	16.78	59.60	6.52	2.06	0.652	0.206
Silver (Ag)	15.87	63.01	6.34	2.01	0.634	0.201
Aluminum (Al)	26.50	37.74	8.19	2.59	0.819	0.259
Gold (Ag)	22.14	45.17	7.489	2.37	0.749	0.237
Titanium (Ti)	4200	0.2381	103.1	32.6	10.3	3.26

4.2.6 Dielectric Dispersion

Dispersion is principally the result of the propagation velocity of a sinusoidal signal being dependent on frequency. For a pulse on the line, dispersion manifests as the various frequency components of a signal traveling with different velocities.

The electric field lines shift as a result of the different distributions of charge, with more of the electric energy being in the dielectric as frequency increases. Thus the effective permittivity of a microstrip line increases with increasing frequency. At high frequencies, the fundamental result of the field rearrangement is that the capacitance of the line increases, but this change can be quite small—typically less than 10% over the range of DC to 100 GHz. (This effect is described by the frequency dependence of the effective permittivity of the transmission line.) To a lesser extent, dispersion is also the result of other transmission line parameters changing with frequency, such as an interconnect's resistance. For an IC where the interconnects can have very small transverse dimensions (e.g., microns) on digital ICs, the line resistance is the most significant source of dispersion. The qualitative effect of dispersion is the same whether it is related to the resistance (resistance-induced dispersion) or change in the effective permittivity (dielectric-inhomogeneity-induced dispersion).

Different interconnect technologies have different dispersion characteristics. For example, with a microstrip line the effective permittivity changes with frequency as the proportion of the EM energy in the air region to that in the dielectric region changes. Dispersion is reduced if the fields are localized and cannot change orientation with frequency. This is the case with coplanar interconnects—in particular, coplanar waveguide (CPW) and coplanar strip (CPS) lines. The stripline of Figure 3-5(k) also has low dispersion, as the fields are confined in one medium and the effective permittivity is just the permittivity of the medium. Thus interconnect choices can have a significant effect on the integrity of a signal being transmitted.

As discussed earlier, as the frequency is increased, the fields on a microstrip line become more concentrated in the region beneath the strip. Thus there is a frequency-dependent effective microstrip permittivity, $\varepsilon_e(f)$. This quantity increases with frequency and the wave is progressively slowed down. The effective microstrip permittivity is now

$$\varepsilon_e(f) = \{c/[v_p(f)]\}^2 . \tag{4.4}$$

Fundamentally, characterizing the dispersion problem then consists of solving the transmission line fields for the frequency-dependent phase velocity, $v_p(f)$. The limits of $\varepsilon_e(f)$ are readily established; at the low-frequency extreme it reduces to the static TEM value ε_e (or $\varepsilon_e(0)$), while as frequency is increased indefinitely, $\varepsilon_e(f)$ approaches the substrate permittivity itself, ε_r. That is,

$$\varepsilon_e(f) \to \begin{cases} \varepsilon_e(0) & \text{as } f \to 0 \\ \varepsilon_r & \text{as } f \to \infty. \end{cases} \tag{4.5}$$

Between these limits $\varepsilon_e(f)$ changes smoothly.

4.2.7 Summary

Various transmission line technologies have different frequency dispersion characteristics. The two most important technologies for microwave circuits are coaxial lines and microstrip. With both the variation of resistance with frequency due principally to the skin effect are significant. However this has little effect on characteristic impedance and effective permittivity with the dominate effect being increased loss at higher frequencies. With microstrip, but not with a coaxial line, variations due to changing orientation of the EM fields is the most significant effect. With increasing frequency the proportion of signal energy in the air region reduces and the proportion in the dielectric increases. The overall trend with microstrip is for the fields to be more concentrated in the dielectric as frequency increases and this increases a microstrip line's effective relative permittivity and hence slows down propagation. The variation of characteristic impedance of microstrip with frequency is more complex as the increasingly tight transverse rotation, i.e. curl, of the fields tends to increase characteristic impedance but the increasing effective permittivity tends to decrease characteristic impedance. Thus following the initial design of a microstrip circuit, it is important to use EM simulations to adjust designs to account for dispersion.

4.3 High-Frequency Properties of Microstrip Lines

Here the high-frequency properties of microstrip lines are discussed and formulas incorporating frequency dependence are presented for effective permittivity, characteristic impedance, and attenuation loss. The effective permittivity at DC (as calculated in the previous chapter) is denoted $\varepsilon_e(0)$ and the characteristic impedance at DC is $Z_0(0)$. These are also called the quasi-static effective permittivity and quasi-static characteristic impedance. Detailed analysis [12] yields the following formula for the **frequency-dependent effective permittivity** of a microstrip line:

$$\varepsilon_e(f) = \varepsilon_r - \frac{\varepsilon_r - \varepsilon_e(0)}{1 + (f/f_a)^m}, \tag{4.6}$$

where

$$f_a = \frac{f_b}{0.75 + \left(0.75 - 0.332\, \varepsilon_r^{-1.73}\right)(w/h)} \tag{4.7}$$

$$f_b = \frac{47.746 \times 10^6}{h\sqrt{\varepsilon_r - \varepsilon_e(0)}} \tan^{-1}\left\{\varepsilon_r \sqrt{\frac{\varepsilon_e(0) - 1}{\varepsilon_r - \varepsilon_e(0)}}\right\} \tag{4.8}$$

$$m = \begin{cases} m_0 m_c & m_0 m_c \le 2.32 \\ 2.32 & m_0 m_c > 2.32 \end{cases} \tag{4.9}$$

$$m_0 = 1 + \frac{1}{1 + \sqrt{w/h}} + 0.32\left(1 + \sqrt{w/h}\right)^{-3} \tag{4.10}$$

$$m_c = \begin{cases} 1 + \dfrac{1.4}{1 + w/h}\left\{0.15 - 0.235 e^{-0.45 f/f_a}\right\}, & \text{for } w/h \le 0.7 \\ 1, & \text{for } w/h > 0.7. \end{cases} \tag{4.11}$$

SI units are used in these equations. The accuracy of the equations is better than 0.6% for $0.1 \le w/h \le 10,\ 1 \le \varepsilon_r \le 128$, and for any value of h/λ provided that $h < \lambda/10$.

The **frequency-dependent characteristic impedance** is, with reference to Equations (3.21) and (3.20),

$$Z_0(f) = \frac{Z_{01}}{\sqrt{\varepsilon_e(f)}} = Z_0(0)\frac{\sqrt{\varepsilon_e(0)}}{\sqrt{\varepsilon_e(f)}}. \tag{4.12}$$

The free-space wavelength is λ_0, the wavelength in the medium is λ, and the guide wavelength (the wavelength on the line) is λ_g.

4.3.1 Frequency-Dependent Loss

The effect of loss on signal transmission is captured by the attenuation constant, α. There are two primary sources of loss: that resulting from the dielectric, captured by the dielectric attenuation constant, α_d, and that from the conductor loss, captured by the conductor attenuation constant, α_c. Thus

$$\alpha|_{\text{dB}} = \alpha_d|_{\text{dB}} + \alpha_c|_{\text{dB}}\,. \tag{4.13}$$

When dielectric loss is significant (e.g., the substrate is silicon which has appreciable conductivity), the previous formula for α_d (Equation (3.34)) provides a good estimate for the attenuation when ε_e is replaced by the frequency-dependent effective relative permittivity, $\varepsilon_e(f)$.

Frequency-dependent conductor loss, described by the conductor attenuation α_c, results from the concentration of current as frequency increases:

$$\alpha_c(f) = \frac{R(f)}{2\, Z_0}, \tag{4.14}$$

where $R(f)$ is the frequency-dependent line resistance described in Section 4.2.5.

A third source of loss is radiation loss, leading to an attenuation factor, α_r. At the frequencies at which a transmission line is generally used, it is usually smaller than dielectric and conductor losses. So, in full,

$$\alpha(f) = \alpha_d(f) \cdot \alpha_c(f) \cdot \alpha_r(f), \tag{4.15}$$

and in decibels

$$\alpha(f)|_{dB} = \alpha_d(f)|_{dB} + \alpha_c(f)|_{dB} + \alpha_r(f)|_{dB}\,. \tag{4.16}$$

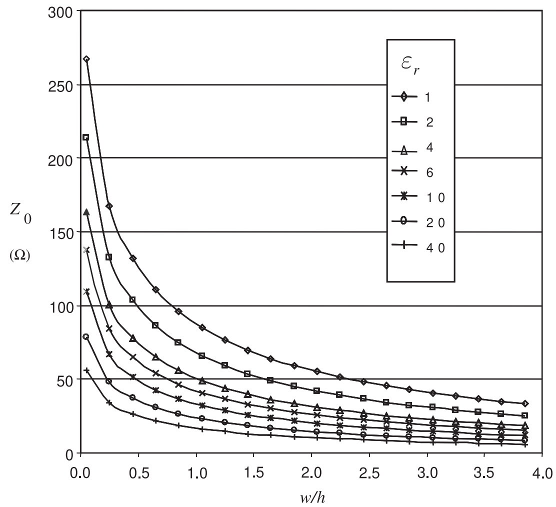

Figure 4-10: Dependence of Z_0 of a microstrip line at 1 GHz for various permittivities and aspect (w/h) ratios.

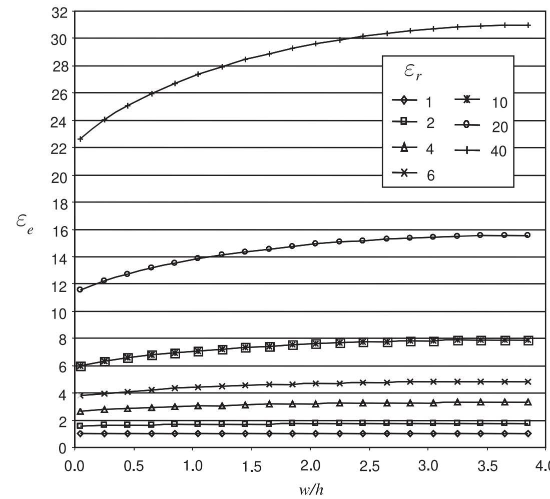

Figure 4-11: Dependence of effective relative permittivity, ε_e, of a microstrip line at 1 GHz for various permittivities and aspect ratios (w/h).

4.3.2 Field Simulations

In this section, results are presented for EM simulations of microstrip lines with a variety of parameters. These simulations were performed using the Sonnet EM simulator. Figure 4-10 presents calculations of Z_0 for various aspect ratios (w/h) and substrate permittivities (ε_r) when there is no loss. The key information here is that narrow strips and low-permittivity substrates have high Z_0. Conversely, wide strips and high-permittivity substrates have low Z_0. The dependence of permittivity on aspect ratio is shown in Figure 4-11, where it can be seen that the effective permittivity, ε_e, increases for wide strips. This is because more of the EM field is in the substrate.

When loss is incorporated, ε_e becomes complex and the imaginary components indicate loss mostly due to conductor loss. Figure 4-12 presents the frequency dependence of three microstrip lines with different substrates and aspect ratios. These simulations took into account finite loss in the conductors and in the dielectric. In Figure 4-12(a) it can be seen that the effective permittivity, ε_e, increases with frequency as the fields become confined more to the substrate. Also, the real part of the characteristic impedance is plotted with respect to frequency. Up to 20 GHz a drop-off in Z_0 is observed as frequency increases. This is due to both reduction of internal strip and ground inductances as charges move to the skin of the conductor and also to greater confinement of the EM fields in the dielectric as frequency increases. It is not long before the characteristic impedance increases. This effect is not due to the skin effect and current bunching that were previously described. Rather it is due to other EM effects that are only captured in EM simulation. It is a result of spatial variations being developed in the fields (related to the fact that not all parts of the fields are in instantaneous contact).

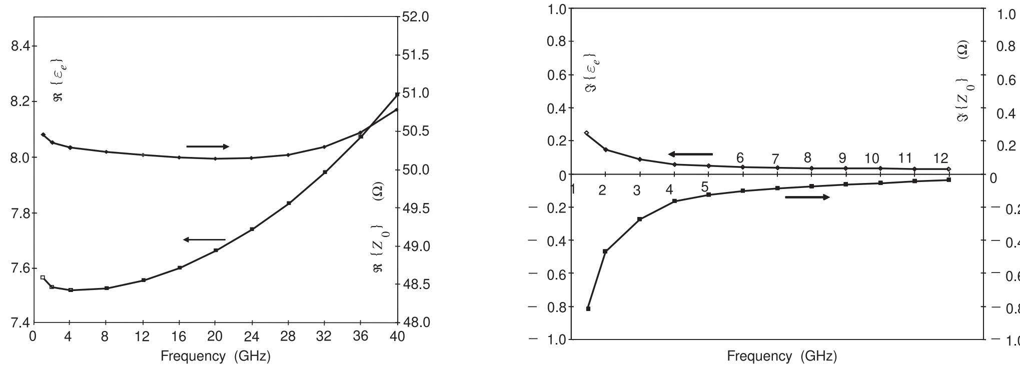

(a) w = 240 μm, h = 500 μm

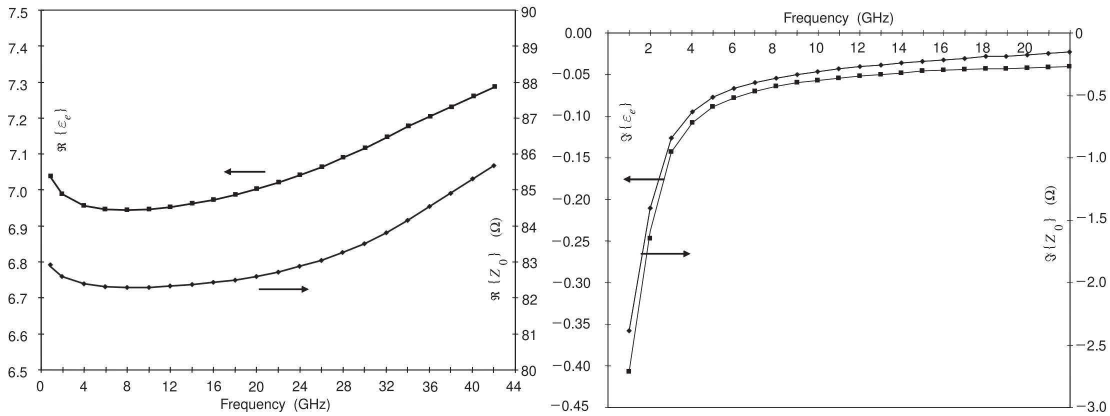

(b) w = 70 μm, and h = 635 μm

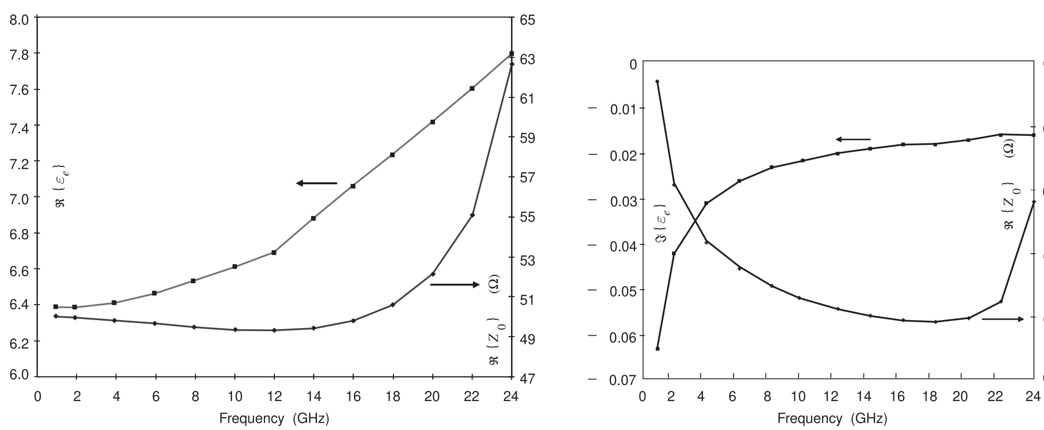

(c) $w = h$ = 635 μm

Figure 4-12: Frequency dependence of the real and imaginary parts of ε_e and Z_0 of a gold microstrip line on alumina with $\varepsilon_r(\mathrm{DC})$.

4.3.3 Summary

Today's microwave designer is indeed fortunate that in the 1980s considerable effort was put into developing frequency-dependent formulas for effective permittivity and characteristic impedance, Equations (4.6) and (4.12), and these can still be used. One effect that is not captured by these formulas is the increased transverse curl of the EM fields with increasing frequency and this tends to increase the characteristic impedance, e.g. see Section 4.3.2. But the frequency-dependence of effective relative permittivity is captured. To incorporate the geometric impact on frequency-dependent characteristic impedance it is necessary to optimize a design using EM field simulation following an initial design using the frequency-dependent formulas.

4.4 Multimoding on Transmission Lines

Multimoding is a phenomenon that affects the integrity of a signal as it travels on a transmission line. For transmission lines, multimoding occurs when there are two or more EM field configurations that can support a propagating wave. Different field configurations travel at different speeds so that the information traveling in two or modes modes would combine incoherently and, if the energy in the modes is comparable, it will be impossible to discern the intended information being sent. It is critical that the dimensions of transmission line structures be designed to avoid multimoding. The most common mode on a transmission line is when there is no, or the minimum possible, variation of the fields in the transverse direction (perpendicular to the direction of propagation).

The transmission structures of interest here are those that have conductors that establish boundary conditions to guide a wave along an intended path. For these lines the lowest-order mode with minimum transverse field variations is called the TEM mode. Higher-order modes occur when the fields can vary. From here the discussion necessarily invokes EM theory. If you need to do this, see Section 1.5, where EM theory is reviewed specifically with respect to multimoding. One of the important concepts is that electric and magnetic walls impose boundary conditions on the fields. Electric walls are conductors, whereas a magnetic wall is formed approximately at the interface of two regions having different permittivity.

It is the property of EM fields that spatial variations of the fields cannot occur too quickly. This comes directly from Maxwell's equations that relate the spatial derivative (the derivative with respect to distance) of the electric field to the time derivative of the magnetic field. The same is true for spatial variation of the magnetic field and time variation of the electric field. How fast a field varies with time depends on frequency. How fast an EM field changes spatially, its curl, depends on wavelength relative to geometry and on boundary conditions. Without electric and magnetic walls establishing boundary conditions, as in free space, a full wavelength is required to obtain the lowest-order variation of the fields. With electric or magnetic walls where the fields can terminate, a smaller distance is sufficient. Between two electric walls one-half wavelength of distance is required. The same is true for magnetic walls. With one electric wall and one magnetic wall, a quarter-wavelength separation of the walls will support a higher-order mode. A

	E field	H field
Electric wall	Normal	Parallel
Magnetic wall	Parallel	Normal

Table 4-1: Properties of the EM fields at electric and magnetic walls.

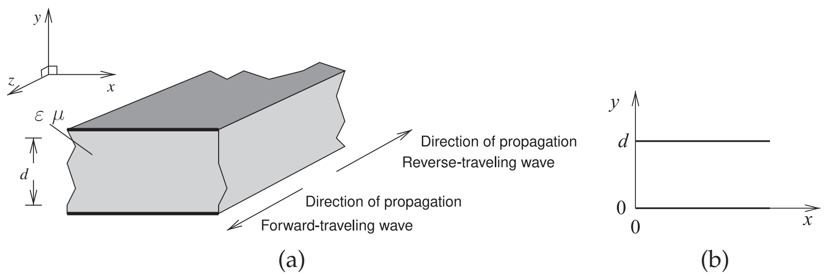

Figure 4-13: Parallel-plate waveguide: (a) three-dimensional view; and (b) cross-sectional (transverse) view.

general rule for avoiding multimoding is that critical transverse geometries must be kept to under a fraction of a wavelength (say, $< \lambda/2$ or $< \lambda/4$).

One type of multimoding has already been described. In the previous chapter it was seen that the signals on a regular transmission line have two simple solutions that are interpreted as the forward-traveling and backward-traveling modes. Each mode is a possible solution of the differential equations describing the signals. THese are not the modes being referred to by the term multimoding. The boundary conditions in the longitudinal direction are established by the source and load impedances, and so the variation can be any fraction of a wavelength. This section is concerned with other solutions to the equations describing the fields on a transmission line structure. In general, the other solutions arise when the transverse dimensions, such as the distance between the two conductors of a two-conductor transmission line, permits a variation of the fields.

The boundary conditions established at electric and magnetic walls were derived in Section 1.8 and are summarized in Table 4-1. Circuit structures such as transmission lines, substrate thicknesses, and related geometries are nearly always chosen so that only one solution of Maxwell's equations is possible. In particular, if the cross-sectional dimensions of a transmission line are much less than a wavelength then it will be impossible for the fields to curl up on themselves and so perhaps there will be only one or, in some cases, no solutions to Maxwell's equations.

4.5 Parallel-Plate Waveguide

The parallel-plate waveguide shown in Figure 4-13 is the closest regular structure to planar transmission lines such as a microstrip line. The aim here is to develop design guidelines that will enable transmission line structures to be designed to avoid multimoding.

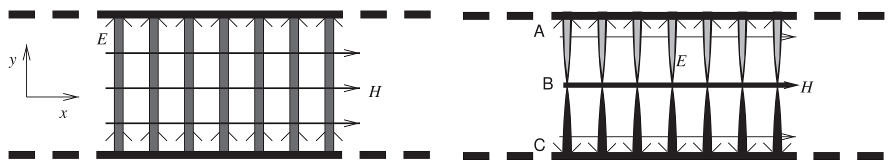

(a) TEM mode. (b) TE mode.

Figure 4-14: Parallel-plate waveguide showing electric, E, and magnetic, H, field lines. The electric (E) and magnetic (H) field lines are shown with the line thickness indicating field strength. The shading of the E field lines indicates polarity ($+$ or $-$) and the arrows indicate direction (and also polarity). The z direction is into the page.

4.5.1 Electromagnetic Derivation

The development of the wave equations begins with **Maxwell's equations** (Equations (1.1)–(1.4)). A simplification to the equations is to assume a linear, isotropic, and homogeneous medium, a uniform dielectric, so that ε and μ are independent of signal level and are independent of the field direction and position. Thus (in the time domain)

$$\nabla \times \bar{\mathcal{E}} = \frac{\partial \bar{\mathcal{B}}}{\partial t} \qquad \nabla \times \bar{\mathcal{H}} = \bar{\mathcal{J}} + \frac{\partial \bar{\mathcal{D}}}{\partial t} \tag{4.17}$$

$$\nabla \cdot \bar{\mathcal{D}} = \rho_V \qquad \nabla \cdot \bar{\mathcal{B}} = 0, \tag{4.18}$$

where ρ_V is the volume charge density and $\bar{\mathcal{J}}$ is the current density. $\bar{\mathcal{J}}$ and ρ_V will be zero except at an electric wall. The above equations do not include magnetic charge or magnetic current density. These do not actually exist and so a modified form of Maxwell's equations incorporating these is not necessary to solve the fields on a structure.

In the lateral direction, the x direction, the parallel-plate waveguide in Figure 4-13 extends indefinitely. For this regular structure, and with a few assumptions, the form of Maxwell's equations with multidimensional spatial derivatives can be simplified. One approach to solving differential equations is to assume a form of the solution and then test to see if it is a valid solution. The first solution to be considered is called the TEM mode and corresponds to the minimum possible variation of the fields. Also, it is assumed that the variation in the z direction is described by the traveling-wave equations. So the only fields of interest here are E and H in the transverse plane; all that is seen in Figure 4-13(b). If all the fields are in the xy plane, then it is sufficient to apply just the boundary conditions that come from the top and bottom ground planes. At first it appears that there are many possible solutions to the differential equations. This is simplified by assuming certain variational properties of the E_x, E_y, H_x, and H_y fields and then seeing if these solutions can be supported. The simplest solution is when there is no variation in the fields and then the only possible outcome is that $E_x = 0 = H_y$. This is the TEM mode indicated in Figure 4-14(a). At the boundaries, the top and bottom metal planes, there is a divergence of the electric field, as immediately inside the (ideal) conductor there is no electric field and immediately outside there is. This divergence is supported by the surface charge on the ground planes (see Equation (1.2)).

In Figure 4-14(a), the thickness of the lines indicates relative field strength and there is no variation in field strength in either the electric or magnetic fields shown. The coefficients of the field components are determined by the boundary conditions. The trial solution used here has $E_x = 0 = H_y$ and $E_z = 0 = H_z$; that is, the trial solution has the electric field in the y direction and the magnetic field is in the x direction. Maxwell's equations (Equations (4.17) and (4.18)) become (note that $\bar{\mathcal{E}} = \bar{\mathcal{E}}_x\hat{\mathbf{x}} + \bar{\mathcal{E}}_y\hat{\mathbf{y}} + \bar{\mathcal{E}}_z\hat{\mathbf{z}}$)

$$\nabla \times \bar{\mathcal{E}}_y\hat{\mathbf{y}} = -\frac{\partial \bar{\mathcal{B}}_x\hat{\mathbf{x}}}{\partial t} \qquad \nabla \times \bar{\mathcal{H}}_x\hat{\mathbf{x}} = \frac{\partial \bar{\mathcal{D}}_y\hat{\mathbf{x}}}{\partial t} + \bar{\mathcal{J}} \tag{4.19}$$

$$\nabla \cdot \bar{\mathcal{D}}_y\hat{\mathbf{y}} = \rho \qquad \nabla \cdot \bar{\mathcal{B}}_x\hat{\mathbf{x}} = 0. \tag{4.20}$$

Expanding the curl, $\nabla\times$, and div, $\nabla\cdot$, operators using Equations (1.21) and (1.22) these become (with $D = \varepsilon E$ and $B = \mu H$)

$$\hat{x}\frac{\partial \bar{\mathcal{E}}_y}{\partial z} = \frac{\partial \bar{\mathcal{B}}_x\hat{\mathbf{x}}}{\partial t} = \frac{\partial \mu\bar{\mathcal{H}}_x\hat{\mathbf{x}}}{\partial t} \tag{4.21}$$

$$\hat{\mathbf{y}}\frac{\partial \bar{\mathcal{H}}_x}{\partial z} = \frac{\partial \bar{\mathcal{D}}_y\hat{\mathbf{y}}}{\partial t} + \bar{\mathcal{J}} = \frac{\partial \varepsilon\bar{\mathcal{E}}_y\hat{\mathbf{y}}}{\partial t} + \bar{\mathcal{J}} \tag{4.22}$$

$$\frac{\partial \bar{\mathcal{D}}_y}{\partial y} = \frac{\partial \varepsilon\bar{\mathcal{E}}_y}{\partial y} = \rho \tag{4.23}$$

$$\frac{\partial \bar{\mathcal{B}}_x}{\partial x} = \frac{\partial \mu\bar{\mathcal{H}}_x}{\partial x} = 0. \tag{4.24}$$

These equations describe what happens at each point in space.

Equation (4.21) indicates that if there is a time-varying component of the x-directed B field then there must be a z-varying component of the E_y field component. This is just part of the wave equation describing a field propagating in the z direction. Equation (4.22) indicates the same thing, but now the roles of the electric and magnetic fields are reversed. Equation (4.21) shows that the y component of the electric field can be constant between the plates, but at the plates there must be a charge on the surface of the conductors (see Equation (4.23)), to terminate the electric field (as indicated by Equation (4.23)), as there is no electric field inside the conductors. Equation (4.24) indicates that the x component of the magnetic field cannot vary in the x direction (i.e., B_x and H_x are constant). Thus the assumption behind the trial solution about the form of this mode is correct. The electric and magnetic field are uniform in the transverse plane, the xy plane, and the only variation is in the direction of propagation, the z direction (but there is no z-directed component of the fields). Thus the test solution satisfies Maxwell's equations. This is the TEM mode, as all field components are in the x and y directions and none are in the z direction. The TEM mode can be supported at all frequencies in the parallel-plate waveguide.

In exploring the existence of higher-order modes, Maxwell's equations need to be simplified further. Putting Equations (4.21)–(4.24) in phasor form, and considering the source free region between the plates (so $J = 0$ and $\rho = 0$), these become (note that E_x is the phasor of $\mathcal{E}_x$)

$$\frac{\partial E_y}{\partial z} = \jmath\omega\mu H_x \qquad \frac{\partial H_x}{\partial z} = \jmath\omega\varepsilon E_y \tag{4.25}$$

$$\frac{\partial E_y}{\partial y} = 0 \qquad \frac{\partial H_x}{\partial x} = 0 \tag{4.26}$$

and the solution becomes

$$\frac{\partial^2 E_y}{\partial z^2} = \gamma^2 E_y \quad \text{and} \quad \frac{\partial^2 H_x}{\partial z^2} = \gamma^2 H_x, \tag{4.27}$$

where $\gamma = \jmath\omega\sqrt{\mu\varepsilon}$ and there is no variation of the E_y component of the electric field in the y direction and no variation of the H_x component of the magnetic field in the x direction.

Another possible set of modes occurs when the electric field is only in the y direction, but then there must be a variation of the field strength, as shown in Figure 4-14(b). The simplest variation is when there is a half-sinusoidal spatial variation of the E_y field component. Applying the methodology described above, it is found that there must be a component of the magnetic field in the z direction to support this mode. Hence these modes are called **transverse electric** (TE) modes. (Interchanging the roles of the electric and magnetic fields yields the **transverse magnetic** (TM) modes where there is an electric field component in the z direction.) The half-sinusoidal variation still enables the charge to support the existence of an E_y electric field.

A key result from our previous discussion is that there must be enough distance for the field to curl and this is related to wavelength, λ. This transverse electric mode can only exist when $h \geq \lambda/2$. When h is smaller than one-half wavelength, this mode cannot be supported, and is said to be cut off. Only the TEM mode can be supported all the way down to DC, so modes other than TEM have a cutoff frequency, f_c, and a cutoff wavelength, λ_c. The concept of wavenumber $k(= 2\pi/\lambda = \omega\sqrt{\mu\varepsilon})$ is also used. The cutoff wavelength, λ_c, and the cutoff wavenumber, k_c, are both related to the dimension below which a mode cannot "curl" sufficiently to be self-supporting. For the lowest TE mode, $k_c = 2\pi/\lambda_c$ with $\lambda_c = 2h$. In general, for TE modes, there can be n variations of the electric field, and n indicates the nth TE mode, denoted as TE$_n$, for which $k_{c,n} = n\pi/h$ and $\lambda_c = 2h/n$. The propagation constant of any mode in a uniform lossless medium (not just in a parallel-plate waveguide mode) is

$$\beta = \sqrt{k^2 - k_c^2}. \tag{4.28}$$

For the TEM mode, $k_c = 0$. High-order modes are described by their own k_c.

TM modes are similarly described, and again $k_c = n\pi/h$ for the TM$_n$ mode. A mode can be supported at any frequency above the cutoff frequency of the mode, it just cannot be supported at frequencies below the cutoff frequency as it is not possible for the fields to vary (or curl) below cutoff.

4.5.2 Multimoding and Electric and Magnetic Walls

In the above discussion, the parallel-plate waveguide had two electric walls—the top and bottom metal walls. Here results will be presented when magnetic walls are introduced. A magnetic wall can only be approximated, as magnetic conductors do not exist (since magnetic charges do not exist). Whereas an electric wall appears as a short circuit, a magnetic wall is an open circuit. Maxwell's equations and the electric and magnetic walls establish the following requirements on the fields:

Electric wall	Perpendicular electric field Tangential magnetic field
Magnetic wall	Perpendicular magnetic field Tangential electric field

Table 4-2: Requirements imposed on fields by electric and magnetic walls.

The lowest-order modes that can be supported by combinations of electric and magnetic walls are shown in Figure 4-15. With two electric or two magnetic walls, a TEM mode (having no field variations in the transverse plane) can be supported. Of course, there will be variations in the field components in the direction of propagation. The modes with the simplest geometric variations in the plane transverse to the direction of propagation establish the critical wavelength. In Figure 4-15 the distance between the walls is d. For the case of two like walls (Figures 4-15(a and c)), $\lambda_c = 2h$, as one-half sinusoidal variation is required. With unlike walls (see Figure 4-15(b)), the varying modes are supported with just one-quarter sinusoidal variation, and so $\lambda_c = 4h$.

EXAMPLE 4.2 Modes and Electric and Magnetic Walls

A magnetic wall and an electric wall are 1 cm apart and are separated by a lossless material having $\varepsilon_r = 9$. What is the cut-off frequency of the lowest-order mode in this system?

Solution:

The EM field established by the electric and magnetic walls is described in Figure 4-15(b). There is no solution to the Maxwell's equations that has no variation of the EM fields since it is not possible to have a spatially uniform electric field which is perpendicular to an electric wall while also being perpendicular to a parallel magnetic wall. The other solutions of Maxwell's equations require that the fields vary spatially, i.e. curl. Without electric and magnetic walls the minimum distance over which the EM fields will fold back on to themselves is a wavelength. With parallel electric and magnetic wall separated by h the minimum distance for a solution of Maxwell's equations is a quarter wavelength, λ, of the walls as shown on the right in Figure 4-15(b). That is

$$h = \lambda/4 \quad \text{or} \quad \lambda = 4h = 4\ \text{cm} = \lambda_0/(\sqrt{\varepsilon_t \mu_r}). \tag{4.29}$$

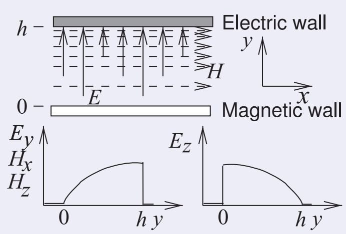

Since the relative permeability has not been specified assume that $\mu_r = 1$ so

$$\lambda_0 = \lambda\sqrt{9} = 12\ \text{cm} = c/f$$

The cut-off frequency is

$$\begin{aligned} f &= (2.998 \times 10^8\ \text{m/s})/(0.12\ \text{m}) \\ &= 2.498\ \text{GHz} \end{aligned} \tag{4.30}$$

4.6 Microstrip Operating Frequency Limitations

Different types of higher-order modes can exist with microstrip and the two maximum operating frequencies of microstrip lines are (a) the lowest-order TM mode and (b) the lowest-order transverse microstrip resonance mode. In practice, **multimoding** is a problem when two conditions are met. First it must be possible for higher-order field variations to exist, and second, that energy can be effectively coupled into the higher-order mode. Generally this

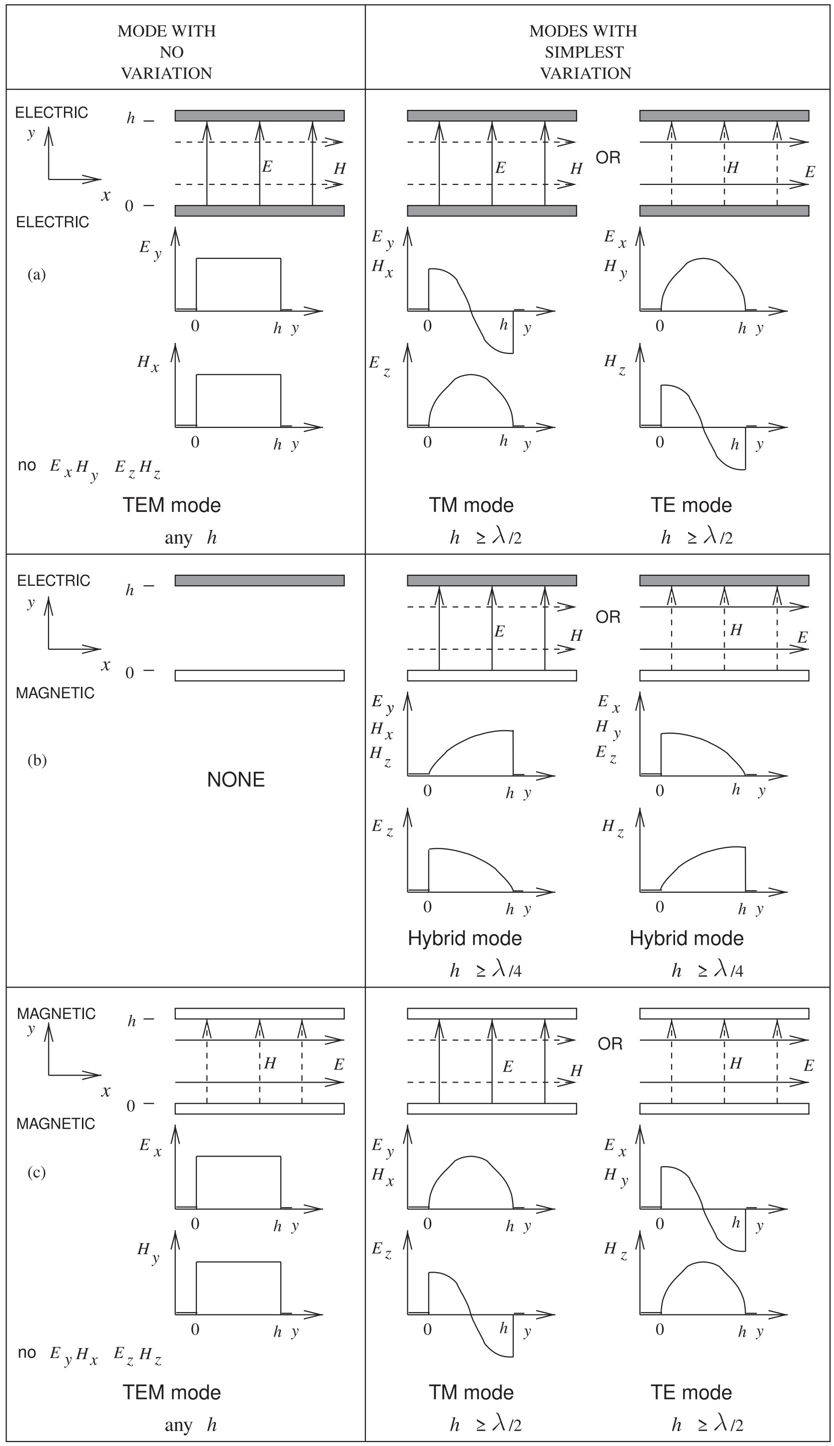

Figure 4-15: Lowest-order modes supported by combinations of electric and magnetic walls.

requires significant discontinuity on the line or that the phase velocities of two modes approximately coincide. An early discussion said that the phase velocities of two modes would be different and this is when the dielectric is uniform. However, with a nonhomogeneous line like microstrip, there can be frequencies where the phase velocities of two modes can coincide.

Since discontinuities are inevitable it is always a good idea to use only the first consideration. As was noted previously, the modal analysis that was possible with the parallel-plate waveguide cannot be repeated easily for the microstrip line because of the irregular cross section, but the phenomena is very similar. Instead of a TEM mode, there is a quasi-TEM mode and there are TE and TM modes.

4.6.1 Microstrip Dielectric Mode (Slab Mode)

A dielectric on a ground plane with an air region (of a wavelength or more above it) can support a TM mode, generally called a microstrip dielectric mode, **substrate mode**, **microstrip TM mode**, or slab mode. The microstrip dielectric mode is a problem for narrow microstrip lines. Whether this mode exists in a microstrip environment depends on whether energy can be coupled from the quasi-TEM mode (which is always generated) of the microstrip line into the TM dielectric mode. The critical frequency at which the TM mode becomes important is when there is significant coupling. Coupling is a problem with a microstrip line having a narrow strip, as the field orientations of the quasi-TEM mode and the dielectric mode align. Also, coupling occurs when the phase velocities of the two modes coincide. A detailed analysis reported in Chapter 11 of [12] and in [13] shows that this occurs at the first critical frequency,

$$f_{c1} = \frac{c \tan^{-1}(\varepsilon_r)}{\sqrt{2}\pi h \sqrt{\varepsilon_r - 1}}. \tag{4.31}$$

At f_{c1} the dielectric mode will be generated even if there is not a discontinuity. If there is a discontinuity, say a split of one microstrip line into two microstrip lines, multimoding will occur when the dielectric mode can exist. From Figure 4-15(b), the dielectric slab mode can be supported when $h > \lambda_g/4$, where λ_g is the wavelength in the dielectric. Now $\lambda_g = \lambda_0/\sqrt{\varepsilon_r} = c/(f\sqrt{\varepsilon_r})$, so the second critical frequency is

$$f_{c2} = \frac{c}{4h\sqrt{\varepsilon_r}}. \tag{4.32}$$

This development assumes that the interface between the dielectric and air forms a good magnetic wall. With a dielectric having a permittivity of 10, typical for microwave circuits, the effective value of h would be increased by up to 10%. However, it is difficult to place an exact value on this.

In summary, f_{c2} is the lowest frequency at which the dielectric mode will exist if there is a discontinuity, and f_{c1} is the lowest frequency at which the dielectric mode will exist if there is not a discontinuity.

EXAMPLE 4.3 Dielectric Mode

The strip of a microstrip has a width of 1 mm and is fabricated on a lossless substrate that is 2.5 mm thick and has a relative permittivity of 9. At what frequency does the substrate (or slab) mode first occur?

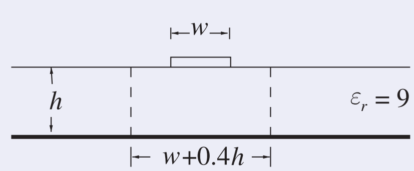

Solution:

Two frequencies must be considered. One that comes from the dimensions of the dielectric slab and the other from considerations of matching phase velocities. From phase velocity consideration used in developing Equation (4.31), the first critical frequency is

$$f_{c1} = \frac{c \tan^{-1}(\varepsilon_r)}{\sqrt{2}\pi h \sqrt{\varepsilon_r - 1}} = 13.9 \text{ GHz}.$$

The other critical frequency is when a variation of the magnetic or electric field can be supported between the ground plane and the approximate magnetic wall supported by the dielectric/free-space interface. This is when $h = \frac{1}{4}\lambda = \lambda_0/(4\sqrt{9}) = 2.5 \text{ mm} \Rightarrow \lambda_0 = 3 \text{ cm}$. Thus the second slab mode critical frequency is

$$f_{c2} = 10 \text{ GHz}.$$

Since discontinuities cannot be avoided, f_{c2} is the critical frequency to use.

4.6.2 Higher-Order Microstrip Mode

If the cross-sectional dimensions of a microstrip line are smaller than a fraction of a wavelength, then the electric and magnetic field lines will be as shown in Figure 3-2. These field lines have the minimum possible spatial variation and the fields are almost entirely confined to the transverse plane; this mode is called the quasi-TEM microstrip mode. However, as the frequency of the signal on the line increases it is possible for these fields to have one-quarter or one-half sinusoidal variations. Deriving the frequency at which a higher-order microstrip mode is supported is involved.

The following is a summary of a more complete discussion on operating frequency limitations in Section 7.8 of [12]. Some variations of the fields or modes do not look anything like the field orientations shown in Figure 3-2. However, the variations that are closest to the quasi-TEM mode are called higher-order microstrip modes and the one that occurs at the lowest frequency corresponds to a half-sinusoidal variation of the electric field between the edge of the strip and the ground plane. This path is a little longer than the path directly from the strip to the ground plane. However, for a wide strip, most of the EM energy is between the strip and the ground plane (both of which are electric walls) with approximate magnetic walls on the side of the strip. The modes are then similar to the parallel-plate waveguide modes described in Section 1.5. The next highest microstrip mode (or parallel-plate TE mode) occurs when there can be a half-sinusoidal variation of the electric field between the strip and the ground plane. This corresponds to Figure 4-15(a). However, for finite-width strips the first higher-order microstrip mode occurs at a lower frequency than implied by the parallel-plate waveguide model. This is because the microstrip fields are not solely confined to the dielectric region, and in fact the electric field lines do not follow the shortest distance between the strip and the ground plane. Thus the fields along the longer paths to the sides of the strip can vary at a lower frequency than on the direct path. With detailed EM modeling and with experimental support it has been established that the first higher-order microstrip mode can exist at frequencies greater than [12]

$$f_{\text{Higher-Microstrip}} = \frac{c}{4h\sqrt{\varepsilon_r - 1}}. \tag{4.33}$$

This is, however, only an approximate guide.

EXAMPLE 4.4 Higher-Order Microstrip Mode

The strip of a microstrip has a width of 1 mm and is fabricated on a lossless substrate that is 2.5 mm thick and has a relative permittivity of 9. At what frequency does the first higher microstrip mode first propagate?

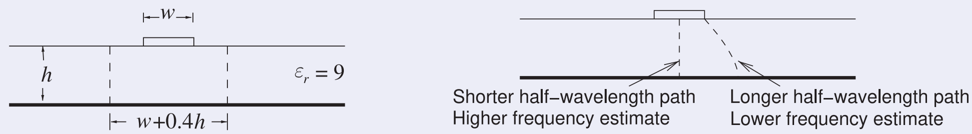

Solution:

The higher-order microstrip mode occurs when a half-wavelength variation of the electric field between the strip and the ground plane can be supported. When $h = \lambda/2 = \lambda_0/(3 \cdot 2) = 2.5$ mm; that is, the mode will occur when $\lambda_0 = 15$ mm. So

$$f_{\mathrm{Higher-Microstrip}} = 20 \text{ GHz}.$$

A better estimate of the frequency where the higher-order microstrip mode becomes a problem is given by Equation (4.33):

$$f_{\mathrm{Higher-Microstrip}} = c/(4h\sqrt{\varepsilon_r - 1}) = 10.6 \text{ GHz}.$$

So two estimates have been calculated for the frequency at which the first higher-order microstrip mode can first exist. The first estimate is approximate and is based on a half-wavelength variation of the electric field confined to the direct path between the strip and the ground plane. The second estimate is more accurate as it considers that on the edge of the strip the fields follow a longer path to the ground plane. It is the half-wavelength variation on this longer path that determines if the higher-order microstrip mode will exist. Thus the more precise determination yields a lower critical frequency.

4.6.3 Transverse Microstrip Resonance

For a wide microstrip line, a transverse resonance mode can exist. This is the mode that occurs when EM energy bounces between the edges of the strip with the discontinuity at the strip edges forming a weak boundary. This is illustrated in Figure 4-16, where the microstrip shown in cross section in Figure 4-16(a) is approximated as a rectangular waveguide in Figure 4-16(b) with magnetic walls on the sides and an extended electrical wall on the top surface of the dielectric. Figure 4-16(b) is called the microstrip waveguide model. The transverse resonance mode corresponds to the lowest-order H field variation between the magnetic walls. At the cutoff frequency for this transverse-resonant mode, the equivalent circuit is a resonant transmission line of length $w + 2d$, as shown in Figure 4-17, where $d = 0.2h$ accounts for the microstrip side fringing. A half-wavelength must be supported by the length $w + 2d$. Therefore the cutoff half-wavelength is

$$\frac{\lambda_c}{2} = w + 2d = w + 0.4h, \quad \text{that is,} \quad \frac{c}{2f_c\sqrt{\varepsilon_r}} = w + 0.4h. \tag{4.34}$$

Hence the critical frequency for transverse resonance is

$$f_{c,\mathrm{TRAN}} = \frac{c}{\sqrt{\varepsilon_r}\,(2w + 0.8h)}. \tag{4.35}$$

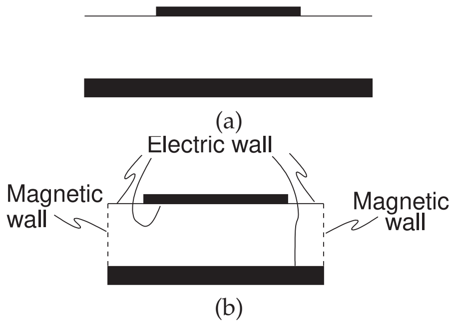

Figure 4-16: Approximation of a microstrip line as a waveguide: (a) cross section of microstrip; and (b) **microstrip waveguide model** having effective width $w + 0.4h$ with magnetic and electric walls.

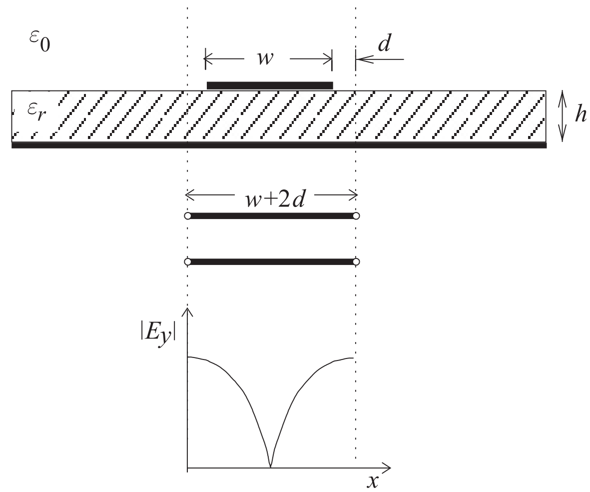

Figure 4-17: Transverse resonance: standing wave ($|E_y|$) and equivalent transmission line of length $w + 2d$, where $d = 0.2h$.

EXAMPLE 4.5 Transverse Resonance Mode

The strip of a microstrip has a width of 1 mm and is fabricated on a lossless substrate that is 2.5 mm thick and has a relative permittivity of 9.

(a) At what frequency does the transverse resonance first occur?

(b) What is the operating frequency range of the microstrip line?

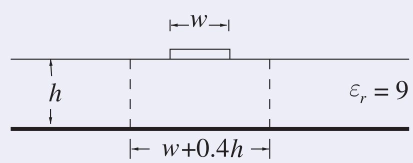

Solution:

h = 2.5 mm, $w = 1$ mm , $\lambda = \lambda_0/\sqrt{\varepsilon_r} = \lambda_0/3$

(a) The magnetic waveguide model of Figure 4-16 can be used in estimating the frequency at which this occurs. The frequency at which the first transverse resonance mode occurs is when there is a full half-wavelength variation of the magnetic field between the magnetic walls, that is, when $w + 0.4h = \lambda/2 = 2$ mm:

$$\frac{\lambda_0}{3 \cdot 2} = 2\text{ mm} \Rightarrow \lambda_0 = 12\text{ mm}, \qquad \text{and so} \qquad f_{c,\text{TRAN}} = 25\text{ GHz}. \tag{4.36}$$

(b) All of the critical multimoding frequencies must be considered here and the minimum taken: for the slab mode, f_{c1} (Equation (4.6.1)) and f_{c2} (Equation (4.6.1), see Example 4.3 for the calculation of these); for the higher-order microstrip mode, $f_{\text{High}-\text{Microstrip}}$ (Equation (4.33), see Example 4.4 for this calculation)); and for the transverse resonance mode (Equation (4.36), and calculated in this example). So the operating frequency range is DC to 10 GHz.

4.6.4 Summary

There are four principal higher-order modes that need to be considered with microstrip transmission lines:

Mode	Critical frequency
Dielectric (or substrate) mode with no discontinuity	Equation (4.31)
Dielectric (or substrate) mode with discontinuity	Equation (4.32)
Higher order microstrip mode	Equation (4.33)
Transverse resonance mode	Equation (4.35)

The lowest frequency determines the upper frequency of transmission line operation with a single mode.

4.7 High-Frequency Considerations for Coplanar Waveguide

The field orientation on CPW is little affected when frequency increases and as such the effective permittivity of CPW has little frequency dependence. (This is in marked contrast to microstrip.)Thus dielectric-related dispersion of CPW is minimal and this is one of the main advantages of using CPW over microstrip. CPW has the frequency-dependent line resistance

$$R(f) = \begin{cases} R(0) & f \text{ such that } t \leq 3\delta_s \\ R(0) + R_{\text{skin}}(f) & f \text{ such that } t > 3\delta_s, \end{cases} \tag{4.37}$$

where $R(0)$ $(= R_{\text{strip}}(0) + R_{\text{ground}}(0))$ is the resistance of the line at low frequencies. $R(f)$ describes the frequency-dependent line resistance, which is due to both the skin effect and current bunching. Approximately,

$$R_{\text{skin}}(f) = R(0)k\sqrt{f}, \tag{4.38}$$

where k is a constant. As with microstrip, EM simulations are recommended to determine line loss. This is necessary in any case to determine attenuation due to radiation, which can be ignored at low microwave frequencies.

The discussion of multimoding on CPW will consider the finite ground CPW structure (FGCPW) shown in Figure 4-18. Most of the considerations pertaining to multimoding on microstrip apply to FGCPW. However, with CPW the fields penetrate into the substrate a lesser distance and so it is less likely that the substrate mode or microstrip mode will be excited. To avoid the microstrip mode the FGCPW should be a sufficient distance from the bottom ground plane. Generally a substrate height three or more times both the gap and strip width is sufficient. A mode that can exist on FGCPW that does not have an equivalent with microstrip occurs when the ground strips on either side of the center strip acquire different voltages. The correct functioning of FGCPW requires these to be at the same potential. The solution is to connect the two side strips together using grounding straps as shown in Figure 4-19(a). The straps are realized using bond wires if FGCPW is used on a circuit board, or using air bridges if the line is on a monolithic integrated circuit. Placing the strips at approximately one-quarter wavelength distances is appropriate, although this can be relaxed if the line

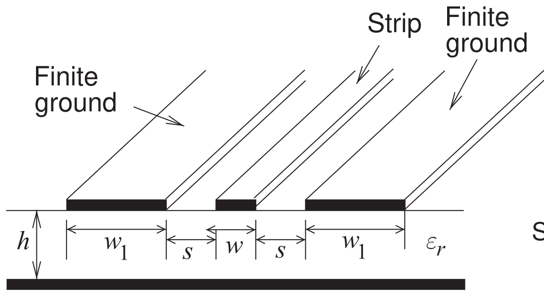

Figure 4-18: Finite ground CPW transmission line.

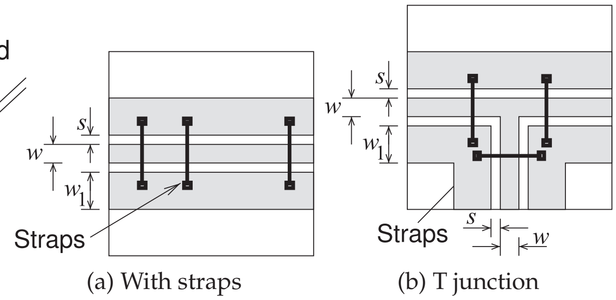

Figure 4-19: CPW structures with ground straps to suppress the parallel plate mode.

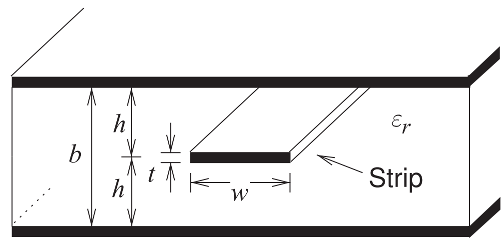

Figure 4-20: Stripline transmission line.

is fairly free of discontinuities. The straps should be placed randomly to avoid any filtering effect that could result from placing the straps at regular intervals. The straps should also be used whenever there is a discontinuity (see, e.g., the junction in Figure 4-19(b)).

4.8 High-Frequency Considerations for Stripline

A stripline transmission line is shown in Figure 4-20. Being a homogeneous line, stripline does not have a frequency-dependent permittivity until molecular effects become important at hundreds of gigahertz (depending on the substrate). Stripline has the frequency-dependent line resistance

$$R(f) = \begin{cases} R(0) & f \text{ such that } t \leq 3\delta_s \\ R(0) + R_{\text{skin}}(f) & f \text{ such that } t > 3\delta_s, \end{cases} \tag{4.39}$$

where $R(0) = R_{\text{strip}}(0) + R_{\text{ground}}(0)$ is the resistance of the line at low frequencies. $R(f)$ describes the frequency-dependent line resistance, which is due to both the skin effect and current bunching. Approximately,

$$R_{\text{skin}}(f) = R(0)k\sqrt{f}, \tag{4.40}$$

where k is a constant.

As with microstrip, EM simulations are recommended to determine line loss. However, provided that regular vias are used between the ground planes (and eliminating the TEM parallel plate mode), attenuation due to radiation loss is minimal.

The moding that is of most concern with stripline is the parallel plate waveguide mode that can be excited at stripline discontinuities. The simplest parallel plate waveguide mode has no variation of the fields in the transverse direction, so there is a uniform electric field from the top plate to the bottom plate. This mode can propagate down to DC. In normal operation a stripline has an E field directed from the strip to the top ground plane and an oppositely directed E field from the strip to the bottom ground plane. Thus excitation of the parallel plate waveguide mode can be suppressed by making sure that the two ground planes are at the same potential. This is done by periodically shorting the two ground planes together using through-substrate vias. Apart from this consideration, the multimoding considerations presented for the microstrip should also be considered.

4.9 Power Losses and Parasitic Effects

Four separate mechanisms lead to power losses in microstrip lines:

(a) Conductor losses.
(b) Dissipation in the dielectric of the substrate.
(c) Radiation losses.
(d) Surface-wave propagation.

The first two items are dissipative effects, whereas radiation losses and surface-wave propagation are essentially parasitic phenomena. The reader is directed to Chapter 8 of [12] for an extensive treatment. Here, summary results are presented.

Conductor losses greatly exceed dielectric losses for most microstrip lines fabricated on low-loss substrates. Lines fabricated on low-resistivity silicon wafers, however, can have high dielectric loss. These wafers are most commonly used for digital circuits, and the interconnect transverse dimensions are generally very small so that line resistance is very high, and again, resistive losses dominate.

Radiation from a microstrip line results from asymmetric structures. In particular, discontinuities such as abruptly open-circuited microstrip (i.e., open ends), steps, and bends will all radiate to a certain extent. Such discontinuities form essential features of microwave circuits and therefore radiation cannot be avoided. Efforts must be made to reduce such radiation and its undesirable effects. In most cases, radiation can be represented by a shunt admittance.

Surface waves, trapped just beneath the surface of the substrate dielectric, will propagate away from microstrip discontinuities as TE and TM modes. The effect of surface waves can be treated as a shunt conductance.

Various techniques can be used to suppress radiation and surface waves:

(a) Metallic shielding or "screening."
(b) The introduction of lossy (i.e., absorbent) material near any radiative discontinuity.
(c) The utilization of compact, planar, inherently enclosed circuits such as inverted microstrip and stripline.
(d) Reducing the current densities flowing in the outer edges of any metal sections and concentrate currents toward the center and in the middle of the microstrip.
(e) Possibly shaping the discontinuity in some way to reduce the radiative efficiency.

4.10 Lines on Semiconductor Substrates

Propagation on transmission line structures fabricated on semiconductor substrates can have peculiar behavior. The interest in such lines is in relation to RF integrated circuits (RFICs) and monolithic microwave integrated circuits (MMICs) using both silicon and compound semiconductor technologies. More specifically, interconnects on **metal-oxide-semiconductor** (**MOS**) or **metal-insulator-semiconductor** (**MIS**) systems, where an insulating layer, such as oxide, exists between the conductor and the semiconductor wafer (see Figure 4-21(a)), are of particular interest due to their ability to support a **slow-wave mode**. A slow-wave mode propagates much slower than would be expected. In the case of a semiconductor substrate with intermediate conductivity, the magnetic field penetrates into the substrate but the electric field does not. This separation of magnetic and electric fields slows the wave. Slow-wave structures find major use in distributed elements on-chip at RF. In particular, a silicon substrate can have a significant impact on microstrip propagation that derives from the charge layer formed at the silicon–silicon dioxide interface. The slow-wave effect is utilized in delay lines, couplers, and filters. With Schottky contact lines, the effect is used in variable-phase shifters, voltage-tunable filters, and various other applications.

Now, an intuitive explanation of the propagation characteristics of microstrip lines on layered substrates can be based on the parallel-plate structure shown in Figure 4-22. For an exact EM analysis of the slow-wave effect with silicon substrates, see [14]. As well as developing a very useful approximation for the important situation of transmission lines on an insulator such as silicon oxide on a semiconductor, the treatment below indicates the type of approach that can be used to analyze unusual structures. In this structure, assume a quasi-TEM mode of propagation. In other words, the wave propagation parameters α, β, and Z_0 can be deduced from electrostatic and magnetostatic solutions for the per unit length parameters C, G, L, and R.

The analysis begins with a treatment of the classic **Maxwell–Wagner capacitor**. Figure 4-23(a) shows the structure of such a capacitor where there are two different materials between the parallel plates of the capacitor with different permittivities and conductivities. The equivalent circuit is shown in

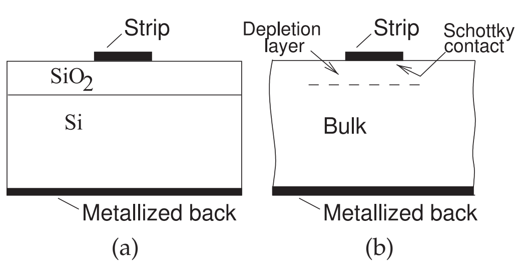

Figure 4-21: Transmission lines on silicon semiconductor: (a) silicon-silicon dioxide sandwich; and (b) bulk view.

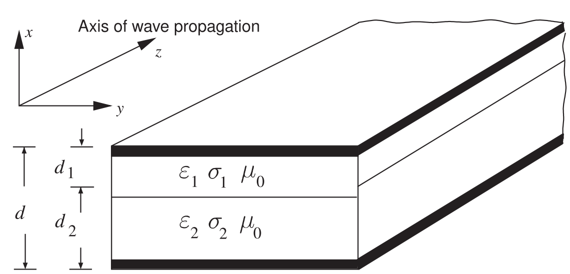

Figure 4-22: Parallel-plate transmission line structure.

Figure 4-23(b) with the elements given by (A is the plate area)

$$C_1 = \varepsilon_1 \frac{A}{d_1}, \ \ R_1 = \frac{1}{\sigma_1}\frac{d_1}{A}, \ \ C_2 = \varepsilon_2 \frac{A}{d_2}, \ \ R_2 = \frac{1}{\sigma_2}\frac{d_2}{A} \tag{4.41}$$

$$\tau_1 = R_1 C_1 = \frac{\varepsilon_1}{\sigma_1}, \ \ \tau_2 = R_2 C_2 = \frac{\varepsilon_2}{\sigma_2}. \tag{4.42}$$

The admittance of the entire structure at radian frequency ω is

$$Y(\omega) = \frac{1}{R_1 + R_2}\frac{(1 + \jmath\omega\tau_1)(1 + \jmath\omega\tau_2)}{1 + \jmath\omega\tau}, \tag{4.43}$$

where $$\tau = \frac{R_1\tau_2 + R_2\tau_1}{R_1 + R_2}. \tag{4.44}$$

Introducing $$Y(\omega) = \jmath\omega\left(\varepsilon_e \frac{A}{d}\right), \tag{4.45}$$

the effective complex permittivity, $\varepsilon_e = \varepsilon_e' - \jmath\varepsilon_e''$, can be defined in terms of Equation (4.43). Using Equations (4.43) and (4.45) yields

$$\varepsilon_e' = \frac{\tau_1 + \tau_2 - \tau + \tau\tau_1\tau_2\omega^2}{(R_1 + R_2)\left[1 + (\omega\tau)^2\right]}\frac{d}{A}. \tag{4.46}$$

Consider now the case when R_1 goes to infinity (i.e., Layer 1, the top layer, in Figure 4-23 is an insulator). For this case, Equation (4.46) becomes

$$\varepsilon_e' = \frac{1 + \left(1 + \frac{d_2}{d_1}\frac{\varepsilon_1}{\varepsilon_2}\right)\left(\frac{\omega\varepsilon_2}{\sigma_2}\right)^2}{1 + \left(1 + \frac{d_2}{d_1}\frac{\varepsilon_1}{\varepsilon_2}\right)^2\left(\frac{\omega\varepsilon_2}{\sigma_2}\right)^2}\left(\varepsilon_1 \frac{d}{d_1}\right). \tag{4.47}$$

It is clear from Equations (4.46) and (4.47) that the effective complex permittivity has a frequency-dependent component. Consider how this varies with a few cases of ω. For $\omega = 0$, the static value of the effective permittivity is

$$\varepsilon_{e,0}' = \varepsilon_1 \frac{d}{d_1}. \tag{4.48}$$

For the case where ω goes to infinity (the optical value), the real part of the effective permittivity is

$$\varepsilon_{e,\infty}' = \frac{\varepsilon_1\varepsilon_2(d_1 + d_2)}{\varepsilon_2 d_1 + \varepsilon_1 d_2}. \tag{4.49}$$

Note also that the value of $\varepsilon_{e,\infty}'$ can be approximately achieved for a large value of $\omega\varepsilon_2/\sigma_2$ (i.e., low-conductivity substrates can be used to ensure that the displacement currents dominate). In a similar way, it is clear that $\varepsilon_{e,0}'$ can be achieved by having a small value of $\omega\varepsilon_2/\sigma_2$. Also note that $\varepsilon_{e,0}'$ can be made very large by making d_1 much smaller than d.

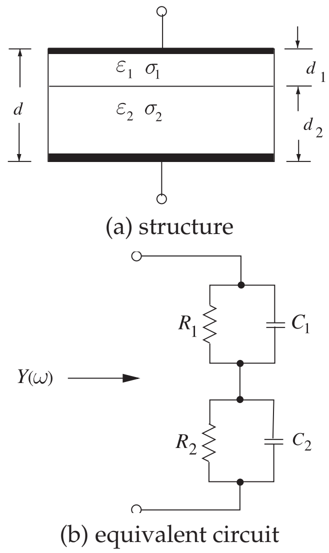

Figure 4-23: Maxwell–Wagner capacitor.

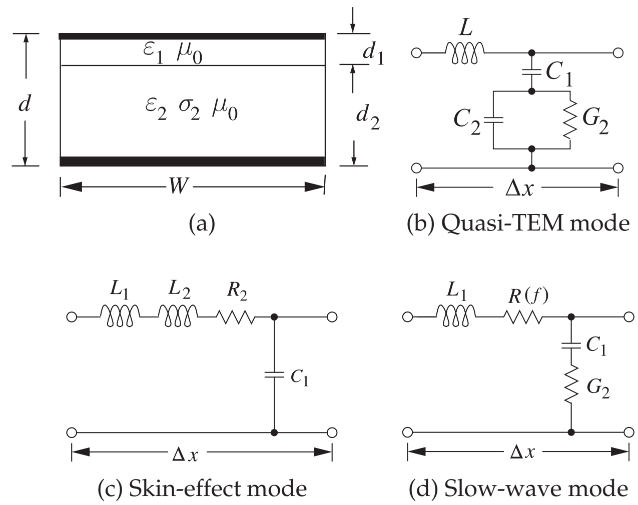

Figure 4-24: Modes on an MOS transmission line: (a) equivalent structure of the MOS line of Figure 4-21.

EXAMPLE 4.6 Two-Layer Substrate

Consider the structure in Figure 4-22. Determine the guide wavelength, λ_g, and the wavelength in the insulator, λ_1, at a frequency of 1 GHz. SiO_2 and Si are the dielectrics, with permittivities $\varepsilon_1 = 4\varepsilon_0$ and $\varepsilon_2 = 13\varepsilon_0$ (the conductivities are zero). The depths d_2 and d_1 of the two dielectrics are $d_2 = 250$ μm and $d_1 = 0.1$ μm.

Solution:

$$\lambda_1 = \frac{3\times 10^8}{10^9\sqrt{4}} = 0.15 \text{ m} = 15 \text{ cm},$$

$$\epsilon_e = \frac{\varepsilon_1\varepsilon_2(d_1+d_2)}{\varepsilon_1 d_2 + \varepsilon_2 d_1} = 12.99\varepsilon_0, \quad \lambda_g = \frac{3\times 10^8}{10^9\sqrt{12.99}} = 0.0832 \text{ m} = 8.32 \text{ cm}. \tag{4.50}$$

4.10.1 Modes on the MIS (MOS) Line

The previous description of the properties of a Maxwell–Wagner capacitor leads to a discussion of the possible modes on the MIS (MOS) line. To make the problem tractable, the transmission line shown in Figure 4-21(a) will be approximated as having the cross section shown in Figure 4-24(a).

Dielectric Quasi-TEM Mode

The first possible mode is the dielectric quasi-TEM mode, for which the sectional equivalent circuit model of Figure 4-24(b) is applicable. In this mode $\sigma_2 \ll \omega\varepsilon_2$. This implies from the earlier discussion that $\varepsilon'_e = \varepsilon'_{e,\infty}$ and $\mu'_e = \mu_0$. Thus the per unit length parameters are

$$L = \mu_0\frac{d_1}{W}, \quad C_1 = \varepsilon_1\frac{W}{d_1}, \quad C_2 = \varepsilon_2\frac{W}{d_2}, \quad G_2 = \sigma_2\frac{W}{d_2}. \tag{4.51}$$

These have the SI units H/m for L, F/m for C_1, F/m for C_2, and S/m for G_2.

Skin-Effect Mode

The second possible mode is the **skin-effect mode**, for which the sectional equivalent circuit model of Figure 4-24(c) is applicable. Here, $\sigma_2 \ll \omega\varepsilon_2$ is such that the skin depth $\delta_s = 1/\sqrt{\pi f \mu_0 \sigma_2}$ in the semiconductor is much smaller than d_2 and

$$\varepsilon'_e = \varepsilon'_{e,0}, \ \mu'_e = \frac{\mu_0}{d}\left(d_1 + \frac{\delta_s}{2}\right),$$

Thus

$$L_1 = \mu_0 \frac{d_1}{W}, \qquad C_1 = \varepsilon_1 \frac{W}{d_1} \tag{4.52}$$

$$L_2 = \mu_0 \frac{1}{W}\left(\frac{\delta_s}{2}\right), \qquad R_2 = 2\pi f \mu_0 \frac{1}{W}\left(\frac{\delta_s}{2}\right). \tag{4.53}$$

These have the SI units H/m for L_1 and L_2, F/m for C_1, and Ω/m for R_2.

Slow-Wave Mode

The third possible mode of propagation is the slow-wave mode [15, 16], for which the sectional equivalent circuit model of Figure 4-24(d) is applicable. This mode occurs when f is not so large and the resistivity is moderate so that the skin depth, δ_s, is larger than (or on the order of) d_2. Thus $\varepsilon'_e = \varepsilon'_{e,0}$, but $\mu'_e = \mu_0$. Therefore

$$v_p = \frac{1}{\sqrt{\varepsilon'_e \mu'_e}} = \frac{1}{\sqrt{\mu_0 \varepsilon_0}} \frac{1}{\sqrt{\varepsilon_1}} \sqrt{\frac{d_1}{d}} \tag{4.54}$$

(with SI units of m/s) and $\lambda_g = \lambda_1 \sqrt{d_1/d}$, where λ_1 is the wavelength in the insulator.

4.11 Summary

Design is an iterative process and initial RF design is based on frequency-independent characteristics. For a transmission line, quantities such as the characteristic impedance, effective permittivity, phase and group velocities, and the RLGC parameters are taken as fixed. The RLGC parameters are the basis of the simplest lumped-element circuit model of a transmission line. Each of the components of this model will vary with frequency. The resistance per unit length, R, increases with frequency as charges concentrate on the surface of conductors and charges bunch (i.e., become less spread out). Both of these effects are due to the finite time it takes to transmit the EM signal that rearranges charges to support an alternating wave.

An EM signal on a transmission line is described by Maxwell's equations and there can be many possible solutions depending on the boundary conditions. With transmission lines and other microwave structures such as resonators these are called modes. All transmission lines have at least two solutions, the forward- and backward-traveling waves. While strictly these are also modes, this classification is avoided by microwave engineers. Microwave engineers identify modes as different solutions to Maxwell's equations that, for transmission lines, are different orientations of the fields largely in the transverse direction to propagation. Each mode will, in general, have forward- and backward-traveling components. A two-conductor transmission line is designed to have dimensions that are small enough that there is only one mode, or else special precautions are taken to avoid a second mode being established. Sometimes multimoding is desirable. If these multimoded structures are used there are strict design criteria that enable the special functionality that is made available to be exploited. Multimoding sets the upper bound on the frequency of operation of most transmission line structures.

The most popular microwave transmission lines—microstrip, stripline and CPW—can all support multiple modes, but most are cut off by keeping transverse dimensions small with respect to a wavelength. When it is possible for a second (or higher-order) mode to exist, whether that mode is generated depends on the coupling mechanism between modes. This coupling mechanism is a discontinuity, which of course is common if circuit structures are to be incorporated. Stripline and CPW can support a second mode at quite low frequencies. With stripline the dominant second mode is the parallel-plate waveguide mode supported by the two ground planes of stripline.

A microwave designer must always be aware of frequency dependence and multimoding and choose dimensions to avoid their occurrence except when the use is intentional and controlled.

4.12 References

[1] C. Holloway and G. A. Hufford, "Internal inductance and conductor loss associated with the ground plane of a microstrip line," *IEEE Trans. on Electromagnetic Compatibility*, vol. 39, no. 2, pp. 73–78, May 1997.

[2] G. Ponchak and A. Downey, "Characterization of thin film microstrip lines on polyimide," *IEEE Trans. on Components, Packaging, and Manufacturing Technology, Part B: Advanced Packaging*, vol. 21, no. 2, pp. 171–176, May 1998.

[3] Hai-Young Lee and T. Itoh, "Phenomenological loss equivalence method for planar quasi-tem transmission lines with a thin normal conductor or superconductor," *IEEE Trans. on Microwave Theory and Techniques*, vol. 37, no. 12, pp. 1904–1909, Dec. 1989.

[4] W. Heinrich, "Quasi-tem description of MMIC coplanar lines including conductor-loss effects," *IEEE Trans. on Microwave Theory and Techniques*, vol. 41, no. 1, pp. 45–52, Jan. 1993.

[5] M. Born and E. Wolf, *Principles of Optics: Electromagnetic Theory of Propagation, Interference, and Diffraction of Light*, 7th ed. Cambridge University Press, 1999.

[6] K. Coperich, J. Morsey, V. Okhmatovski, A. Cangellaris, and A. Ruehli, "Systematic development of transmission-line models for interconnects with frequency-dependent losses," *IEEE Trans. on Microwave Theory and Techniques*, vol. 49, no. 10, pp. 1677–1685, Oct. 2001.

[7] W. Heinrich, "Full-wave analysis of conductor losses on MMIC transmission lines," *IEEE Trans. on Microwave Theory and Techniques*, vol. 38, no. 10, pp. 1468–1472, Oct. 1990.

[8] R. Faraji-Dana and Y. Chow, "The current distribution and ac resistance of a microstrip structure," *IEEE Trans. on Microwave Theory and Techniques*, vol. 38, no. 9, pp. 1268–1277, Sep. 1990.

[9] A. Djordjevic and T. Sarkar, "Closed-form formulas for frequency-dependent resistance and inductance per unit length of microstrip and strip transmission lines," *IEEE Trans. on Microwave Theory and Techniques*,, vol. 42, no. 2, pp. 241–248, Feb. 1994.

[10] B. Biswas, A. Glasser, S. Lipa, M. Steer, P. Franzon, D. Griffis, and P. Russell, "Experimental electrical characterization of on-chip interconnects," in *IEEE 6th Topical Meeting on Electrical Performance of Electronic Packaging*, 1997, pp. 57–59.

[11] A. Deutsch, R. Krabbenhoft, K. Melde, C. Surovic, G. Katopis, G. Kopcsay, Z. Zhou, Z. Chen, Y. Kwark, T.-M. Winkel, X. Gu, and T. Standaert, "Application of the short-pulse

propagation technique for broadband characterization of pcb and other interconnect technologies," *IEEE Trans. on Electromagnetic Compatibility*, vol. 52, no. 2, pp. 266–287, May 2010.

[12] T. Edwards and M. Steer, *Foundations for Microstrip Circuit Design*. John Wiley & Sons, 2016.

[13] G. Vendelin, "Limitations on stripline Q," *Microwave Journal*, pp. 63–69, 1970.

[14] H. Hasegawa, M. Furukawa, and H. Yanai, "Properties of microstrip line on si-sio2 system," *IEEE Trans. on Microwave Theory and Techniques*, vol. 19, no. 11, pp. 869–881, Nov. 1971.

[15] D. Jager, "Slow-wave propagation along variable schottky-contact microstrip line," *IEEE Trans. on Microwave Theory and Techniques*, vol. 24, no. 9, pp. 566–573, Sep. 1976.

[16] Y. K. et al, "Quasi-tem analysis of "slow-wave" mode propagation on coplanar microstructure mis transmission lines," *IEEE Trans. on Microwave Theory and Techniques*, vol. 35, no. 6, pp. 545–551, Jun. 1987.

4.13 Exercises

1. Current bunching and the skin effect result in transmission line loss increasing with frequency.
   (a) Show current bunching on a transverse diagram of the microstrip line.
   (b) Describe the skin effect on a transverse diagram of the microstrip line.
2. What is the skin depth on a copper microstrip line at 10 GHz? Assume that the conductivity of the deposited copper forming the strip is half that of bulk single-crystal copper. Use the data in the table on page 130.
3. What is the skin depth on a silver microstrip line at 1 GHz? Assume that the conductivity of the fabricated silver conductor is 75% that of bulk single-crystal silver. Use the data in the table on page 130.
4. What is the dominant source of dispersion on a microstrip transmission line?
5. Using Figure 4-12, determine the complex characteristic impedance and complex effective permittivity of a microstrip line at 12 GHz. The line is fabricated on alumina with $\varepsilon_r(0) = 9.9$, $w = 240$ μm, $h = 500$ μm.
6. A magnetic wall and an electric wall are 2 cm apart and are separated by a lossless material having a relative permittivity of 10 and a relative permeability of 23. What is the cut-off frequency of the lowest-order mode in this system?
7. Describe the transverse resonance mode on stripline. When can it occur?
8. The strip of a microstrip has a width of 600 μm and is fabricated on a lossless substrate that is 1 mm thick and has a relative permittivity of 10.
   (a) Draw the microstrip waveguide model of the microstrip line. Put dimensions on your drawing.
   (b) Sketch the electric field distribution of the first transverse resonance mode and calculate the frequency at which the transverse resonance mode occurs.
   (c) Sketch the electric field distribution of the first higher-order microstrip mode and calculate the frequency at which it occurs.
   (d) Sketch the electric field distribution of the slab mode and calculate the frequency at which it occurs.
9. A microstrip line has a width of 352 μm and is constructed on a substrate that is 500 μm thick with a relative permittivity of 5.6.
   (a) Determine the frequency at which transverse resonance would first occur.
   (b) When the dielectric is slightly less than one-quarter wavelength in thickness the dielectric slab mode can be supported. Some of the fields will appear in the air region as well as in the dielectric, extending the effective thickness of the dielectric. Ignoring the fields in the air (use a one-quarter wavelength criterion), at what frequency will the dielectric slab mode first occur?
10. The strip of a microstrip has a width of 600 μm and uses a lossless substrate that is 635 μm thick and has a relative permittivity of 4.1.
    (a) At what frequency will the first transverse resonance occur?
    (b) At what frequency will the first higher-order microstrip mode occur?
    (c) At what frequency will the slab mode occur?
    (d) Identify the useful operating frequency range of the microstrip.
11. The design space for transmission lines in microstrip designs is determined by the design project leader to be 20–100 Ω. The preferred substrate has a thickness of 500 μm and a relative permittivity of 8. What is the maximum operating frequency range of designs supported by this technology choice. Ignore frequency disper-

sion effects (i.e., frequency dependence of effective permittivity and losses). [Hint: First determine the dimensions of the strip that will provide the required impedance range and then determine the frequency at which lowest-order multimoding occurs.]

12. Consider the design of transmission lines in microstrip technology using a lossless substrate with a relative permittivity of 10 and thickness of 400 μm. You will want to use the formulas in Section 3.5.3.
    (a) What is the maximum characteristic impedance that can be achieved for a transmission line fabricated in this technology?
    (b) Plot the characteristic impedance versus strip width.
    (c) From manufacturing tolerance considerations, the minimum strip width that can be manufactured is 20 μm. What is the maximum characteristic impedance that can be achieved in practice?
    (d) If the operating frequency range is 1–10 GHz, determine the maximum width of the strip from higher-order mode considerations. You must consider the transverse resonance mode as well as higher-order microstrip modes.
    (e) Identify the electrical design space (i.e., the achievable characteristic impedance range).
    (f) Identify the physical design space (i.e., the range of acceptable strip widths).
    (g) If the electrical design space requires that transmission line impedances be achieved within $\pm 2\ \Omega$, what tolerance must be achieved in the manufacturing process if the substrate thickness can be achieved exactly? [Hint: First identify the critical physical process corner and thus the critical strip width that is most susceptible to width variations. Then determine the tolerance on the strip width to achieve the allowable characteristic impedance variation. That is, characteristic impedance is a function of strip width and height. If the substrate is perfect (no height variation), then how much can the strip width vary to keep the impedance within $\pm 2\ \Omega$ of the desired value? You can solve this graphically using a plot of Z_0 versus width or you can iteratively arrive at the answer by recalculating Z_0.]
    (h) If the electrical design space requires that transmission line impedances be achieved within $\pm 2\ \Omega$, what tolerance must be achieved in the manufacturing process if the substrate thickness tolerance is ± 2 μm? If the substrate is not perfect (the height variation is ± 2 μm), then how much can the strip width vary to keep the impedance within $\pm 2\ \Omega$ of the desired value? This problem is directly applicable to real-world process/design trade-offs.

13. The strip of a microstrip has a width of 500 μm and is fabricated on a lossless substrate that is 635 μm thick and has a relative permittivity of 12. [Parallels Examples 4.3, 4.4, and 4.5]
    (a) At what frequency does the transverse resonance first occur?
    (b) At what frequency does the first higher-order microstrip mode first propagate?
    (c) At what frequency does the substrate (or slab) mode first occur?

14. The strip of a microstrip has a width of 250 μm and uses a lossless substrate that is 300 μm thick and has a relative permittivity of 15.
    (a) At what frequency does the transverse resonance first occur?
    (b) At what frequency does the first higher-order microstrip mode propagate?
    (c) At what frequency does the substrate (or slab) mode first occur?
    (d) What is the highest operating frequency of the microstrip?

15. A microstrip line has a strip width of 100 μm and is fabricated on a substrate that is 150 μm thick and has a relative permittivity of 9.
    (a) Draw the microstrip waveguide model and indicate and calculate the dimensions of the model.
    (b) Based only on the microstrip waveguide model, determine the frequency at which the first transverse resonance occurs?
    (c) Based on the microstrip waveguide model, determine the frequency at which the first higher-order microstrip mode occurs?
    (d) At what frequency will the slab mode occur? For this you cannot use the microstrip waveguide model.

16. A microstrip line has a strip width of 100 μm and is fabricated on a substrate that is 150 μm thick and has a relative permittivity of 9.
    (a) Define the properties of a magnetic wall.
    (b) Identify two situations where a magnetic wall can be used in the analysis of a microstrip line; that is, give two situations where a magnetic wall approximation can be used.
    (c) Draw the microstrip waveguide model and indicate and calculate the dimensions of the model.

17. Consider the design of transmission lines in microstrip technology using a lossless substrate with relative permittivity of 20 and thickness of 200 μm.
    (a) Using qualitative arguments, show that the maximum characteristic impedance that can be achieved for a transmission line fabricated in this technology is 116 Ω. The maximum is not actually 116 Ω, but a simple argument will bring you to this conclusion.
    (b) Plot the characteristic impedance versus substrate width.
    (c) From manufacturing tolerance considerations, the minimum strip width that can be manufactured is 20 μm. What is the maximum characteristic impedance that can be achieved in practice?
    (d) If the operating frequency range is 2–18 GHz, determine the maximum width of the strip from higher-order mode considerations. You must consider the transverse resonance mode, the higher-order mode, and the slab mode.
    (e) Identify the electrical design space (i.e., the characteristic impedance range).
    (f) Identify the physical design space (i.e., the range of acceptable strip widths).
    (g) If the electrical design space requires that transmission line impedances be achieved within ± 2 Ω, what tolerance must be achieved in the manufacturing process if the substrate thickness can be achieved exactly? [Hint: First identify the critical physical process corner and thus the critical strip width that is most susceptible to width variations. Then determine the tolerance on the strip width to achieve the allowable characteristic impedance variation.]
    (h) If the electrical design space requires that transmission line impedances be achieved within ± 2 Ω, what tolerance must be achieved in the manufacturing process if the substrate thickness tolerance is ± 2 μm?
18. The strip of a microstrip line has a width of 0.5 mm, and the microstrip substrate is 1 mm thick and has a relative permittivity of 9 and relative permeability of 1.
    (a) Draw the microstrip waveguide model and calculate the dimensions of the model. Clearly show the electric and magnetic walls in the model.
    (b) Use the microstrip waveguide model to calculate the cut off frequency of the transverse resonance mode?
    (c) A substrate mode can also be excited but the cut off frequency of this mode cannot be calculated using the microstrip waveguide model. Provide a brief description of the substrate mode and calculate the lowest frequency at which it can exist.
19. A microstrip technology uses a substrate with a relative permittivity of 10 and thickness of 400 μm. If the operating frequency is 10 GHz, what is the maximum width of the strip from higher-order mode considerations.
20. A microstrip line operating at 18 GHz has a 200 μm thick substrate with a relative permittivity of 20.
    (a) Determine the maximum width of the strip from higher-order mode considerations. Consider the transverse resonance mode, the higher-order microstrip mode, and the slab mode.
    (b) Thus determine the minimum achievable characteristic impedance.
21. A microstrip line has a strip width of 100 μm and is fabricated on a 150 μm-thick lossless substrate with a relative permittivity of 9.
    (a) Define the properties of a magnetic wall.
    (b) Identify two situations where a magnetic wall can be used in determining multimoding on a microstrip line. That is, give two locations where a magnetic wall approximation can be used.
22. Two magnetic walls are separated by 1 mm in a lossless material having a relative permittivity of 9 and a relative permeability of 1.
    (a) What is the wavelength of a 10 GHz signal in this material?
    (b) Now consider a field variation, i.e. a mode and not constant, established by the magnetic walls. Describe this lowest order field variation. That is how does the H field vary or how does the E field vary (one is sufficient)?
    (c) What is the lowest frequency at which a field variation can be supported by those walls in the specified medium?
23. A microstrip line has a strip width of 250 μm and a 300 μm thick substrate with a relative permittivity of 15. At what frequency can the substrate mode first occur?
24. A microstrip line has a strip width of 250 μm and a 300 μm thick substrate with a relative permittivity of 15. At what frequency can a higher-order microstrip mode first propagate?
25. A microstrip line has a strip width of 200 μm and a substrate that is 400 μm thick and has a rela-

tive permittivity of 4. Use the microstrip waveguide model to determine the lowest frequency at which higher-order microstrip mode can occur.

26. A microstrip line has a strip width of 250 μm and a 300 μm thick substrate with a relative permittivity of 15. At what frequency can transverse resonance first occur?

27. The figure below is the cross section of a finite ground coplanar waveguide (FGCPW) transmission line over a ground plane. The FGCPW consists of the ground strips of width w_1 and the strip of width w. Now $w_1 = 2.5 \times s$, $w = 1.3 \times s$, and $h = 4 \times s$. The thickness is $t = 0.3 \times s$.

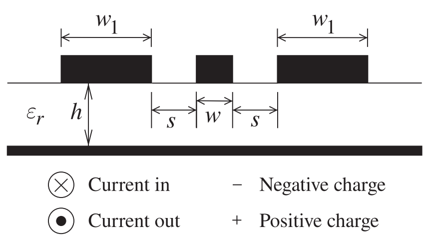

   (a) Ignore the bottom ground plane for now. Redraw the structure and indicate the charge and current distributions at microwave frequencies using the convention shown. On the strip the current flows in and the charge is positive.
   (b) Does this structure support a transverse EM mode?
   (c) Again ignoring the bottom ground plane, redraw the structure and indicate the region where the energy is concentrated.
   (d) Now consider the complete structure. If the guide wavelength is λ_g, and the wavelength in the dielectric is λ, indicate the criterion for the lowest frequency at which transverse resonance will become a problem.

28. Use a diagram to show the E and H fields of the microstrip mode on finite ground CPW.

29. Does finite ground CPW support a transverse resonance mode? Explain.

30. For a finite ground CPW line illustrate the following modes and the conditions under which they occur.
   (a) The microstrip mode.
   (b) The cross mode (the ground planes not at the same potential).
   (c) The transverse mode mode.

31. Consider a symmetrical stripline with the following parameters: total substrate thickness, d = 1.7 mm; strip width, w = 2.5 mm; relative permittivity of the substrate = 9; and operating frequency = 30 GHz.
   (a) What is the value of the effective permittivity?
   (b) What is the value of the free-space wavelength?
   (c) What is the value of the guide wavelength?

32. What is the dominant cause of dispersion on a stripline? That is, what is most likely to cause frequency dependence of the characteristic impedance and propagation constant of the line.

33. The strip of a microstrip line has a width of 200 μm and the substrate is 400 μm thick and has a relative permittivity of 4.
   (a) Draw the effective waveguide model of a microstrip line with magnetic walls and an effective strip width, w_{eff}.
   (b) What is the effective relative permittivity of the microstrip waveguide model?
   (c) What is w_{eff}?
   (d) Can the lowest frequency at which the transverse resonance mode first occurs be determined from the microstrip waveguide model?

34. The strip of a symmetrical stripline has a width of 200 μm and is embedded in a lossless medium that is 400 μm thick and has a relative permittivity of 13, thus the separation, h, from the strip to each of the ground planes is 200 μm.
   (a) Draw the waveguide model of a stripline with magnetic walls and an effective strip width, w_{eff}, which will be approximately the same as with a microstrip line.
   (b) What is the effective relative permittivity of the stripline waveguide model?
   (c) What is w_{eff}?
   (d) At what frequency will the first transverse resonance occur?
   (e) At what frequency will the first higher-order stripline mode occur?
   (f) At what frequency will the first parallel-plate waveguide mode occur? Do not consider the mode with no field variation, as this cannot be excited.
   (g) Identify the useful operating frequency range of the stripline.

35. Describe the parallel-plate mode on stripline.

36. Consider the structure in Figure 4-22. Determine the guide wavelength, λ_g, and the wavelength in the top insulator, λ_1, at a frequency of 20 GHz. The permittivities are $\varepsilon_1 = 3.9\varepsilon_0$ and $\varepsilon_2 = 13\varepsilon_0$. The depths of the dielectrics are $d_2 = 100$ μm and $d_1 = 1.0$ μm. [Parallels Example 4.6]

37. Consider a metal-oxide-semiconductor transmission medium as examined in Section 4.10.

The structure in the form of a Maxwell–Wagner capacitor is shown in Figure 4-23(a) with $d_1 = 100\ \mu\mathrm{m}$, $d_2 = 500\ \mu\mathrm{m}$, and relative permittivities $\varepsilon_{r1} = 3.9$ and $\varepsilon_{r2} = 13$. Ignore the finite conductivity. What is the capacitance model of this structure (see Figure 4-23(b)) and what are the values of the capacitances?

4.13.1 Exercises by Section

†challenging, ‡very challenging

§4.2	$1^\dagger, 2, 3$
§4.3	$4^\dagger$
§4.4	5
§4.5	$6, 7$
§4.6	$8^\dagger, 9^\dagger, 10^\dagger, 11^\ddagger, 12^\ddagger, 13^\dagger, 14^\dagger, 15^\dagger, 16^\dagger, 17^\ddagger, 18^\dagger, 19, 20, 21, 22, 23, 24, 25, 26$
§4.7	$27^\ddagger, 28, 29, 30$
§4.8	$31^\ddagger, 32^\dagger, 33^\dagger, 34^\ddagger, 35$
§4.10	$36, 37^\dagger$

4.13.2 Answers to Selected Exercises

3	$2.315\ \mu\mathrm{m}$
6	247 MHz
8(c)	25 GHz
9(c)	DC to 63.4 GHz
10(d)	DC $\leq f \leq 48.6$ GHz
14	104.6 GHz
17(a)	116 Ω
17(f)	$20\,\mu\mathrm{m} < w < 1.96\,\mathrm{mm}$
18(b)	55.6 GHz
34	207.9 GHz

CHAPTER 5

Coupled Lines and Applications

5.1 Introduction

This chapter describes what happens when two transmission lines are so close together that the fields produced by one line interfere with the other line. Then a portion of the signal energy on one line is transferred to the other resulting in coupling. For microstrip lines the coupling reduces as the lines separate and usually the coupling is small enough to be ignored if the separation is at least three times the height of the strips. Transmission line coupling may be undesirable in many situations, but the phenomenon is exploited to realize many novel RF and microwave elements such as filters. A coupled pair of transmissions lines also enables the forward- and backward-traveling waves on a line to be separately measured.

The chapter begins with a discussion of the physics of coupling which leads to the preferred description of propagation on a pair of **parallel coupled line**s (**PCL**s) as supporting an even mode and an odd mode, and forward- and backward-traveling versions of each. Many microwave circuit elements are based on PCL elements such as PCL filters. The separation of the fields into even and odd modes comes naturally from a consideration of the fields. This is leads to a low-frequency circuit model described in Section 5.4. Section 5.4.1 presents a high frequency model of a PCL with the L and C model of a single transmission line replaced by multiple inductances, capacitances, and mutual inductances and capacitances. As with single microstrip lines, formulas have been developed for the propagation characteristics of a pair of coupled microstrip lines, and these are presented in Section 5.6. The rest of the chapter builds up design concepts and presents some particular applications on the way.

Section 5.7 presents the analysis used to determine reflection coefficients of terminated coupled lines. The next section, Sections 5.8, describe two types of couplers that use a pair of coupled lines to selectively separate and tap off a portion of the power in either the forward-traveling wave, the backward-traveling wave, or both. A design technique for synthesizing them is presented and this is key to nearly all design using a pair of coupled lines as a circuit element. Section 5.9 presents the circuit models for various coupled line configurations and these models are essential to the synthesis of PCL-based microwave components. There are other ways to partition the modes on a pair of coupled lines and with RFICs the preferred description uses differential and common modes as described in Section 5.10. The difference between these modes and odd and even modes comes down to bookkeeping with a preference to use differential and common modes with circuits, and a preference to use odd and even modes when relating to fields. The final section, Section 5.11, describes another type of coupling, common impedance coupling. This is not always related to PCLs but this is the appropriate place to consider this phenomenon.

5.2 Physics of Coupling

If the fields of one transmission line intersect the region around another transmission line, then some of the energy propagating on the first line appears on the second. This coupling discriminates in terms of forward- and backward-traveling waves. In particular, consider the coupled microstrips shown in Figure 5-1. The direction of propagation comes from $\bar{\mathcal{E}} \times \bar{\mathcal{H}}$. Using the right-hand rule, the direction of propagation of the signal on the left-hand strip is out of the page. This is called the forward-traveling direction. Now consider the fields around the right-hand strip, the inactive line, and note the direction of the E field. The H field immediately to the left of the right-hand strip is stronger than on the right of the strip. So effectively there is a clockwise circulation of the H field around the right hand strip. By applying $\bar{\mathcal{E}} \times \bar{\mathcal{H}}$ to the signal induced on the right-hand strip, it is seen that the induced signal travels into the page, or in the backward-traveling direction. The coupling with parallel-coupled microstrip lines is called backward-wave coupling. This is, of course, a frequency-domain view of coupling. In practice, there is also a small component of forward coupling.

In digital systems the forward coupling is of most importance because of the way traveling waves are reinforced. To appreciate this, consider a voltage step traveling in the forward direction on one strip. The step edge couples across to the neighboring line, producing a large backward-traveling pulse and a smaller forward-traveling pulse (approximately the derivative of the original step signal). The coupled forward-traveling pulse travels at the same velocity as the step signal so that the coupled forward-traveling signal integrates over time, whereas the backward-traveling signal does not.

The discussion now returns to the frequency-domain view, as this is the

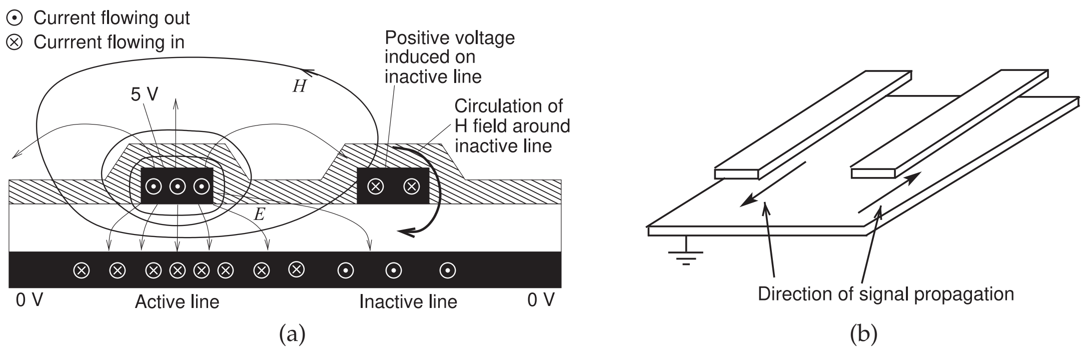

Figure 5-1: Edge-coupled microstrip lines with the left line driven with the forward-traveling field coming out of the page: (a) cross section of microstrip lines as found on a printed circuit board showing a conformal top passivation or solder resist layer; and (b) in perspective showing the direction of propagation of the driven line (left) and the direction of propagation of the main coupled signal on the victim line (right).

required orientation in designing narrowband systems (i.e., most RF and microwave circuits). Previously forward- and backward-traveling waves on an individual transmission line were introduced as separate modes; each mode is a self-sustaining and propagating field orientation on a transmission line. By analogy, in understanding coupled line behavior, and to facilitate design using transmission line coupling, it is a good idea to treat a pair of coupled lines as a single transmission structure. This structure supports two families of modes called the even mode and the odd mode, and both have forward- and backward-traveling components (see Figure 5-2).

In the even mode (Figures 5-2(a and b)), the amplitude and polarity of the voltages on the two signal conductors are the same. In the odd mode (Figures 5-2(c and d)), the voltages on the two signal conductors are equal but have opposite polarity. Any EM field orientation on the coupled lines can be represented as a weighted addition of the even-mode and odd-mode field configurations.

It is just as valid to consider the field orientations based on each of the lines (taken one at a time) and to consider the effect of the other line as a perturbation of the fields of the first line. However, the odd- and even-mode view of the fields assists in understanding and quantitatively describing coupling. This view facilitates the design of components that exploit coupling. The configuration of the fields supported by the coupled lines depends on how the lines are driven and terminated. The actual fields will be a superposition of the even and odd modes. Also, at any instant the voltages on the lines are composed of even and odd components.

The characteristic impedances of the even and odd modes will differ because of the different field orientations. These are termed the even-mode and odd-mode characteristic impedances, denoted by Z_{0e} and Z_{0o}, respectively. Here the e subscript identifies the even mode and the o subscript identifies the odd mode. With coupled microstrip lines, the phase velocities

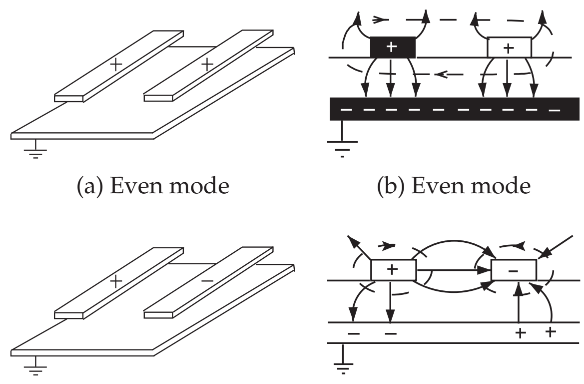

(a) Even mode (b) Even mode

(c) Odd mode (d) Odd mode

Figure 5-2: Modes on parallel-coupled microstrip lines. In (b) and (d) the electric fields are indicated as arrowed lines and the magnetic field lines are dashed.

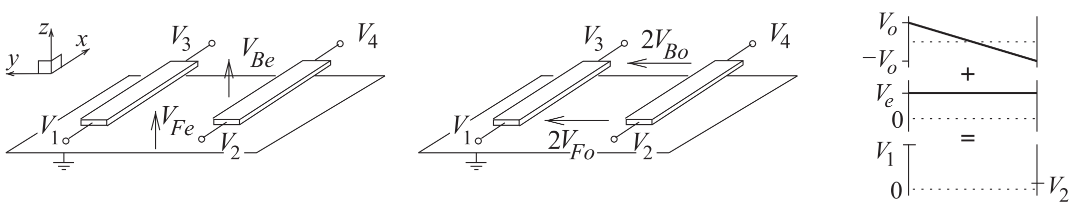

(a) Even mode (b) Odd mode (c)

Figure 5-3: Definitions of total voltages and even- and odd-mode voltage phasors on a pair of coupled microstrip lines: (a) even-mode voltage definition; (b) odd-mode voltage definition; (c) depiction of how even- and odd-mode voltages combine to yield the total voltages on individual lines. F indicates front and B indicates back.

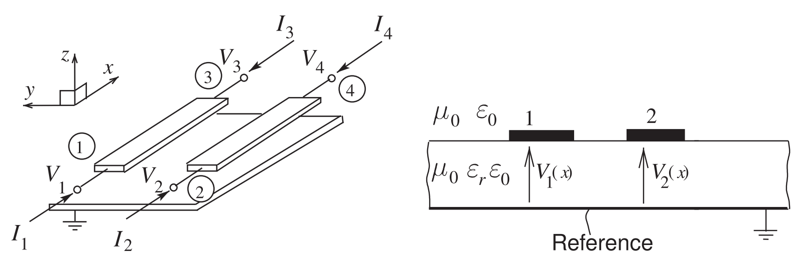

(a) (b)

Figure 5-4: Coupled microstrip lines: (a) with total voltage and current phasors at the four terminals; and (b) cross section.

of the two modes will differ since the two modes have different amounts of energy in the air and in the dielectric, resulting in different effective permittivities of the two modes.

Coupled lines are modeled by determining the propagation characteristics of the even and odd modes. Also, at the circuit level, coupling can be described by network parameters that relate total voltage and current. Using the definitions shown in Figures 5-3 and 5-4, the total voltage and current phasors on the original structure are a superposition of the even- and odd-mode solutions:

$$\left.\begin{array}{ll} V_1 = V_{Fe} + V_{Fo} & I_1 = I_{Fe} + I_{Fo} \\ V_2 = V_{Fe} - V_{Fo} & I_2 = I_{Fe} - I_{Fo} \\ V_3 = V_{Be} + V_{Bo} & I_3 = I_{Be} + I_{Bo} \\ V_4 = V_{Be} - V_{Bo} & I_4 = I_{Be} - I_{Bo} \end{array}\right\}, \tag{5.1}$$

with the subscripts F and B indicating the front and back, respectively, of the even- and odd-mode components. Also

$$\left.\begin{array}{ll} V_{Fe} = (V_1 + V_2)/2 & I_{Fe} = (I_1 + I_2)/2 \\ V_{Fo} = (V_1 - V_2)/2 & I_{Fo} = (I_1 - I_2)/2 \\ V_{Be} = (V_3 + V_4)/2 & I_{Be} = (I_3 + I_4)/2 \\ V_{Bo} = (V_3 - V_4)/2 & I_{Bo} = (I_3 - I_4)/2 \end{array}\right\}. \tag{5.2}$$

The forward-traveling components can be written as

$$\left.\begin{array}{ll} V_1^+ = V_{Fe}^+ + V_{Fo}^+ & I_1^+ = I_{Fe}^+ + I_{Fo}^- \\ V_2^+ = V_{Fe}^+ - V_{Fo}^+ & I_2^+ = I_{Fe}^+ - I_{Fo}^- \\ V_3^+ = V_{Be}^+ + V_{Bo}^+ & I_3^+ = I_{Be}^+ + I_{Bo}^- \\ V_4^+ = V_{Be}^+ - V_{Bo}^+ & I_4^+ = I_{Be}^+ - I_{Bo}^- \end{array}\right\}. \tag{5.3}$$

The backward-traveling components are written similarly so that the total front and back even- and odd-mode voltages are

$$\left.\begin{array}{ll} V_{Fe} = V_{Fe}^+ + V_{Fe}^- & V_{Be} = V_{Be}^+ + V_{Be}^- \\ V_{Fo} = V_{Fo}^+ + V_{Fo}^- & V_{Bo} = V_{Bo}^+ + V_{Bo}^- \end{array}\right\}. \tag{5.4}$$

With an ideal voltmeter the V_1, V_2, V_3, and V_4 voltages would be measured from a point on the strip to a point on the ground plane immediately below. The voltages $2V_{Fo}$ and $2V_{Bo}$ are the voltages that would be measured between the strips at the front and back of the lines, respectively (see Figure 5-2). It would not be possible to directly measure V_{Fe} and V_{Be}.

One set of network parameters describing a pair of coupled lines is the port-based admittance matrix equation relating the port voltages, V_1–V_4, to the port currents, I_1–I_4:

$$\begin{bmatrix} I_1 \\ I_2 \\ I_3 \\ I_4 \end{bmatrix} = \begin{bmatrix} y_{11} & y_{12} & y_{13} & y_{14} \\ y_{21} & y_{22} & y_{23} & y_{24} \\ y_{31} & y_{32} & y_{33} & y_{34} \\ y_{41} & y_{42} & y_{43} & y_{44} \end{bmatrix} \begin{bmatrix} V_1 \\ V_2 \\ V_3 \\ V_4 \end{bmatrix}. \tag{5.5}$$

These are port-based y parameters as the currents and voltages are defined for ports. Since microstrip lines are fabricated (most of the time) on non-magnetic dielectrics, then they are reciprocal so that $y_{ij} = y_{ji}$. Coupling from one line to another is described by the terms y_{12} (=y_{21}) and y_{34} (=y_{43}).

Summary

The important concept introduced in this section is that fields and the propagating waves on a pair of parallel coupled lines can be described as a combination of odd and even modes each of which has forward- and backward-wave versions.

5.3 Coupled Transmission Line Theory

In this section coupled transmission line theory is developed in terms of the quantities shown in Figure 5-4. The voltages and currents shown here are phasors that vary along the line and are functions of x.

The quasi-TEM mode of propagation is also assumed, and the transmission line system is completely lossless with perfect conductors and insulators. In phasor form, the generalized telegrapher's equations for a pair of coupled lines are[1]

$$\frac{dV_1(x)}{dx} = -\jmath\omega L_{11}I_1(x) - \jmath\omega L_{12}I_2(x) \tag{5.6}$$

$$\frac{dV_2(x)}{dx} = -\jmath\omega L_{21}I_1(x) - \jmath\omega L_{22}I_2(x) \tag{5.7}$$

$$\frac{dI_1(x)}{dx} = -\jmath\omega C_{11}V_1(x) - \jmath\omega C_{12}V_2(x) \tag{5.8}$$

$$\frac{dI_2(x)}{dx} = -\jmath\omega C_{21}V_1(x) - \jmath\omega C_{22}V_2(x). \tag{5.9}$$

These are generalizations of the telegrapher's equations of a single transmission line, and for reciprocity, $C_{12} = C_{21}$ and $L_{12} = L_{21}$. Compaction of the equations is obtained by introducing the per unit length inductance matrix, $\mathbf{L}$, and the per unit length capacitance matrix, $\mathbf{C}$, defined as

$$\mathbf{L} = \begin{bmatrix} L_{11} & L_{12} \\ L_{12} & L_{22} \end{bmatrix} \quad \text{and} \quad \mathbf{C} = \begin{bmatrix} C_{11} & C_{12} \\ C_{12} & C_{22} \end{bmatrix}. \tag{5.10}$$

The next step is to express the voltage on the pair of coupled transmission lines in vector form as

$$\mathbf{V}(x) = \begin{bmatrix} V_1(x) \\ V_2(x) \end{bmatrix} = [V_1(x)\ V_2(x)]^{\mathrm{T}}, \tag{5.11}$$

where T indicates transpose and converts the row vector into a column vector. Similarly the vector of currents on the coupled transmission lines is

$$\mathbf{I}(x) = [I_1(x)\ I_2(x)]^{\mathrm{T}}. \tag{5.12}$$

Using the above relations, the telegrapher's equation, from Equations (5.6)–(5.9), is represented in matrix form as

$$\frac{d}{dx}\mathbf{V}(\mathrm{x}) = -\jmath\omega\mathbf{L}\mathbf{I}(x) \quad (5.13) \qquad \text{and} \qquad \frac{d}{dx}\mathbf{I}(\mathrm{x}) = -\jmath\omega\mathbf{C}\mathbf{V}(x). \quad (5.14)$$

Rearranging Equations (5.13) and (5.14), taking derivatives, and after substitution, the final wave-equation form is obtained:

$$\frac{d^2}{dx}^2\mathbf{V}(x) + \omega^2\mathbf{LCV}(x) = 0 \quad (5.15) \qquad \text{and} \qquad \frac{d^2}{dx}^2\mathbf{I}(x) + \omega^2\mathbf{LCI}(x) = 0. \quad (5.16)$$

Solving these second-order differential equations yields descriptions of the

[1] In Figure 5-4(a) V_1 and V_2 are the voltages at terminals 1 and 2 of lines 1 and 2. They are also port voltages referenced to the ground immediately below the appropriate terminal. $V_1(x)$ and $V_2(x)$ are the total voltage anywhere on lines 1 and 2, respectively, as shown in Figure 5-4(b). Similar notation will be used for voltages and traveling-wave components.

propagation characteristics. With confidence, a solution in the form of propagating waves can be assumed:

$$\mathbf{V}(x) = \mathbf{V}_0\boldsymbol{\beta} = \mathbf{V}_0 \operatorname{diag}(\mathrm{e}^{-\jmath\beta_1 x}, \mathrm{e}^{-\jmath\beta_2 x}) = \mathbf{V}_0 \begin{bmatrix} \mathrm{e}^{-\jmath\beta_1 x} & 0 \\ 0 & \mathrm{e}^{-\jmath\beta_2 x} \end{bmatrix}. \quad (5.17)$$

Substituting this into Equation (5.15) yields

$$-\boldsymbol{\beta}^2\mathbf{V}_0 + \omega^2\,\mathbf{LCV}_0 = 0. \quad (5.18)$$

For a nontrivial solution of Equation (5.18), the determinant of the matrix equation should be zero:

$$\det\left(\mathbf{LC} - \frac{\boldsymbol{\beta}^2}{\omega^2}\mathbf{U}\right) = 0, \quad \text{where the unit matrix} \quad \mathbf{U} = \begin{bmatrix} 1 & 0 \\ 0 & 1 \end{bmatrix}. \quad (5.19)$$

Equation (5.19) is the characteristic equation that can be solved to determine the phase constant, β. There are many possible solutions, and weighted linear combinations of the solutions are also solutions.

If only the quasi-TEM modes are considered, then there are two possible sets of solutions for the phase constant, with one set of solutions being

$$\beta_1 = \pm\omega S_1 \quad (5.20) \qquad \text{and the other} \quad \beta_2 = \pm\omega S_2. \quad (5.21)$$

The different signs here are physically interpreted as referring to the forward- and backward-traveling waves. Thus the coupled pair of conductors supports two unique families of modes (each family comprising forward- and backward-traveling waves) with each family relating to a particular field configuration on the coupled line system.[2] That is, S_1 and S_2 are each single numbers and, just considering the forward-traveling waves, ωS_1 is the propagation constant of one mode and ωS_2 is the propagation constant of the second mode.

The circuit-level model of a coupled line pair is developed by considering the calculation of the **L** and **C** matrices. The elements of the capacitance matrix are obtained in two simulations in which the line charge is calculated. A variety of commercially available software packages exist for the extraction of the per unit length **L** and **C** matrices. The matrix **C** is calculated, in most packages, from the solutions of a two-dimensional electrostatic problem. The steps involve solving for the charges on the lines with voltages set on the conductors. With total voltages V_1 and V_2 on lines 1 and 2, the charges on lines Q_1 and Q_2 are

$$Q_1 = C_{11}V_1 + C_{12}V_2 \quad (5.22) \qquad \text{and} \quad Q_2 = C_{12}V_1 + C_{22}V_2. \quad (5.23)$$

Simulation 1: With $V_1 = 1$ and $V_2 = 0$, the charges are calculated with the result that

$$C_{11} = Q_1 > 0 \quad (5.24) \qquad \text{and} \quad C_{12} = Q_2 < 0. \quad (5.25)$$

(Note that $C_{ij}, i \neq j$, is negative.)

[2] Also it is up to the user to decide the form of the families to use. The most convenient family in microwave analysis is to use even and odd modes. In general, a system with N active conductors (and one reference conductor) will support $2 \times N$ (quasi-) TEM modes.

Simulation 2: With $V_1 = 0$ and $V_2 = 1$, the charges are recalculated, and now

$$C_{22} = Q_2 \quad \text{and} \quad C_{12} = Q_1. \tag{5.26}$$

The characterization of the lines is completed by determining the elements of the inductance matrix. This is done by calculating the capacitances with and without the dielectric. The principle effect of the dielectric is to alter the configuration and magnitude of the electric field. The dielectric has little effect on the magnitude and orientation of the magnetic field. With the same current on the coupled lines, the same magnetic energy is stored, and the inductances of the coupled line are unchanged by the dielectric. The other assumption is that with a TEM mode on the lines, and in the absence of a dielectric, the velocity of propagation is $c = 1/\sqrt{LC}$. Specifically, the assumption is that for a TEM mode and without a dielectric, the phase velocity is just c. This is a very good approximation and is exact if the conductors have infinite conductivity. (If the conductors have finite conductivity there would be field inside the conductors, and the wave slows down slightly.) Determining the capacitance matrix without the dielectric enables the inductance matrix to be calculated:

$$\mathbf{L} = \mathbf{L}_0 = \frac{1}{c^2}\mathbf{C}_0^{-1}, \tag{5.27}$$

where the subscript 0 indicates free space (but a subscript 0 on Z, e.g., Z_0, indicates characteristic impedance).

5.3.1 Summary

This section introduced the telegrapher's equations for a pair of coupled lines in a form that is an extension of the telegrapher's equations of a single line but with the L and C of a single line replaced by 2×2 L and C matrices. It is no longer necessary to deal with fields and a circuit model can be used.

5.4 Low-Frequency Capacitance Model of Coupled Lines

The low-frequency model of a pair of lossless coupled lines comprises only capacitances. A pair of coupled lines, as shown in Figure 5-5(a), has four terminals. At very low frequencies V_1 and V_3 are identical as are voltages V_2 and V_4. So the low-frequency model of the pair of coupled lines has just two terminals in addition to ground, as shown in Figure 5-5(b).

The capacitances in Figure 5-5(b) are the shunt capacitance C_1 and C_2 and the mutual capacitance C_g. In the even mode, the voltages at terminals 1 and 2 are the same so that C_g vanishes and the low-frequency capacitance model of the pair of coupled lines in the even mode comprises just the self-capacitances C_1 and C_2 (see Figure 5-5(c)). In the odd mode, the voltage at terminal 2 is the negative of the voltage at terminal 1. The result is that there is a virtual ground between the terminals. Now a better circuit model is that shown in Figure 5-5(d). This is where the restriction that the lines are of equal width is used. This assumption places the virtual ground between equal-value capacitances. The symmetrical case is the one of most interest. If asymmetrical coupled lines are to be analyzed, the analysis departs at this point and EM simulation is required.

To proceed, the capacitance model must be put in the form of per unit length capacitances and put in terms of the elements of a capacitance matrix.

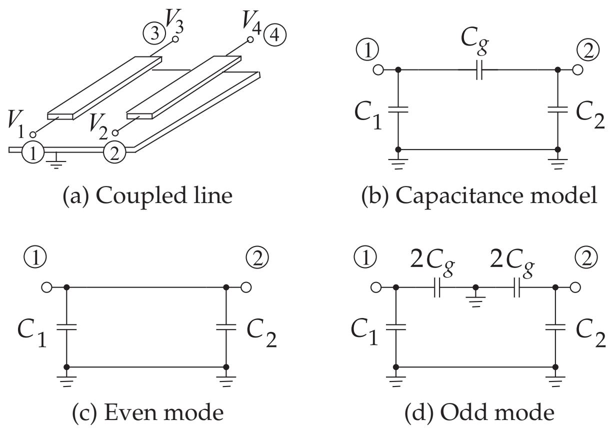

Figure 5-5: Very low frequency models of a pair of coupled lines.

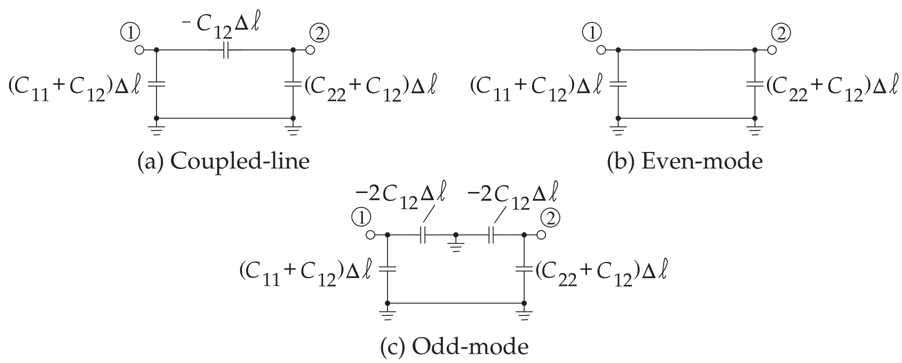

Figure 5-6: Low frequency capacitance models of a pair of coupled lines of length $\Delta\ell$.

The indefinite nodal admittance matrix of the low-frequency coupled-line model of Figure 5-5(b) is

$$\mathbf{Y} = \jmath\omega \begin{bmatrix} C_1 + C_g & -C_g \\ -C_g & C_2 - C_g \end{bmatrix} = \jmath\omega \mathbf{C}\Delta\ell, \tag{5.28}$$

where $\Delta\ell$ is the length of the coupled lines, and $\mathbf{C}$ is the per unit length capacitance matrix (see Equation (5.10)). Thus the low-frequency capacitance model of a pair of coupled lines of length $\Delta\ell$ and equal width is as shown in Figure 5-6(a). It is found in analysis that C_{12} is negative.

For symmetrical coupled lines (the strips having the same width) the per unit length even- and odd-mode capacitances, as defined in the definition of odd and even modes in Section 5.2, are

$$C_e = C_{11} + C_{12} \quad \text{and} \quad C_o = C_{11} - C_{12}. \tag{5.29}$$

That is, $$\mathbf{C} = \begin{bmatrix} C_{11} & C_{12} \\ C_{12} & C_{22} \end{bmatrix} = \begin{bmatrix} \frac{1}{2}(C_e + C_o) & \frac{1}{2}(C_e - C_o) \\ \frac{1}{2}(C_e - C_o) & \frac{1}{2}(C_e + C_o) \end{bmatrix}. \tag{5.30}$$

5.4.1 Capacitance Matrix Extraction

This section describes a general procedure for the extraction of the capacitance matrix of a number of coupled conductors [1]. Either measurements or measurement-like simulations can be used. This is done by evaluating one capacitance at a time for different connections of interconnects to each other.

Without loss of generality, consider the three-line structure shown in Figure 5-7, where there are four conductors, including ground. A 3×3 capacitance matrix is extracted from the capacitances of pairs of connected conductors. There are seven possible combinations, as shown on the left-hand side of Figure 5-8. However, because of reciprocity, $C_{ij} = C_{ji}$, there are only six capacitances $(C_{11}, C_{12}, C_{13}, C_{22}, C_{23}$, and $C_{33})$ to be determined, and only six sets of connections are required. The seventh set serves as a check. In an EM simulation, the connections are conveniently realized by holding the black group at one voltage (e.g., 1 V) and the white group at 0 V. The corresponding capacitance connections are shown on the right in the figure: the seven individual capacitance measurements are $C_A, C_B, C_C, C_D, C_E, C_F$, and C_G. Thus the elements of the capacitance matrix are

$$\left.\begin{array}{ll} C_{11} = C'_{11} + C'_{12} + C'_{13} & C_{12} = C_{21} = -C'_{12} \\ C_{22} = C'_{22} + C'_{12} + C'_{23} & C_{13} = C_{31} = -C'_{13} \\ C_{33} = C'_{33} + C'_{13} + C'_{23} & C_{23} = C_{32} = -C'_{23} \end{array}\right\}. \tag{5.31}$$

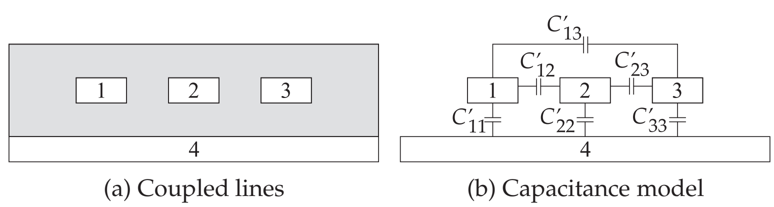

Figure 5-7: Three-line structure with four conductors labeled 1, 2, 3, and 4.

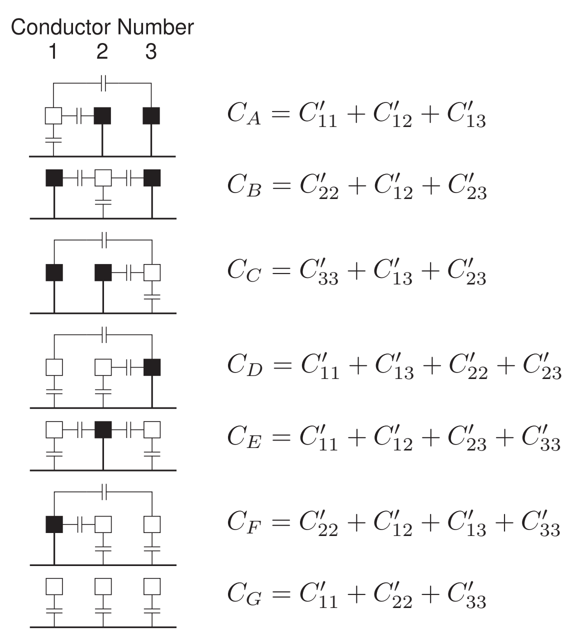

Figure 5-8: Combinations of conductors leading to various capacitance measurements. The capacitances $C_A, \ldots, C_G$ are measured between the conductor identified by the open square and the ground that is connected to the conductors, indicated by the closed squares.

Using the first six measurements in Figure 5-8,

$$\left.\begin{array}{ll} C_A = C_{11} & C_D = C_{11} + 2C_{12} + C_{22} \\ C_B = C_{22} & C_E = C_{11} + 2C_{13} + C_{33} \\ C_C = C_{33} & C_F = C_{22} + 2C_{23} + C_{33} \end{array}\right\}. \tag{5.32}$$

Thus

$$\left.\begin{array}{ll} C_{11} = C_A & C_{12} = C_{21} = \frac{1}{2}(C_D - C_A - C_B) \\ C_{22} = C_B & C_{13} = C_{31} = \frac{1}{2}(C_E - C_A - C_C) \\ C_{33} = C_C & C_{23} = C_{32} = \frac{1}{2}(C_F - C_B - C_C) \end{array}\right\}. \tag{5.33}$$

This extraction does not require the widths of the strips to be the same.

5.5 Symmetric Coupled Transmission Lines

In this section, even and odd modes are considered as defining independent transmission lines. The development is restricted to a symmetrical pair of coupled lines; that is, each transmission line of the pair is identical. Thus the strips have the same self-inductance, $L_s = L_{11} = L_{22}$, and self-capacitance, $C_s = C_{11} = C_{22}$, where the subscript s stands for "self." $L_m = L_{12} = L_{21}$ and $C_m = C_{12} = C_{21}$ are the mutual inductance and capacitance of the lines, and the subscript m stands for "mutual." Equations (5.6)–(5.9) can thus be written as

$$\frac{dV_1(x)}{dx} = -\jmath\omega L_s I_1(x) - \jmath\omega L_m I_2(x) \tag{5.34}$$

$$\frac{dV_2(x)}{dx} = -\jmath\omega L_m I_1(x) - \jmath\omega L_s I_2(x) \tag{5.35}$$

$$\frac{dI_1(x)}{dx} = -\jmath\omega C_s V_1(x) - \jmath\omega C_m V_2(x) \tag{5.36}$$

$$\frac{dI_2(x)}{dx} = -\jmath\omega C_m V_1(x) - \jmath\omega C_s V_2(x). \tag{5.37}$$

The even mode is defined as the mode corresponding to both conductors being at the same potential and carrying the same currents:[3]

$$V_1 = V_2 = V_e \quad \text{and} \quad I_1 = I_2 = I_e. \tag{5.38}$$

The odd mode is defined as the mode corresponding to the conductors being at opposite potentials relative to the reference conductor and carrying currents of equal amplitude but of opposite sign:[4]

$$V_1 = -V_2 = V_o \quad \text{and} \quad I_1 = -I_2 = I_o. \tag{5.39}$$

The characteristics of the two possible modes of the coupled transmission lines are now described. For the even mode, from Equations (5.34) and (5.35),

$$\frac{d}{dx}\left[V_1(x) + V_2(x)\right] = -\jmath\omega\left[L_m + L_s\right]\left[I_1(x) + I_2(x)\right], \tag{5.40}$$

which becomes

$$\frac{dV_e(x)}{dx} = -\jmath\omega\left(L_s + L_m\right) I_e(x). \tag{5.41}$$

---

[3] Here $I_e = (I_1 + I_2)/2$ and $V_e = (V_1 + V_2)/2$. The reason for the supposedly equally valid definition $I_e = I_1 + I_2$ not being used is that the adopted definition results in the desirable form of the even-mode characteristic impedance.

[4] Here $I_o = (I_1 - I_2)/2$ and $V_o = (V_1 - V_2)/2$.

Similarly, using Equations (5.36) and (5.37),

$$\frac{d}{dx}\left[I_1(x) + I_2(x)\right] = -\jmath\omega\left(C_s + C_m\right)\left[V_1(x) + V_2(x)\right], \tag{5.42}$$

which in turn becomes

$$\frac{dI_e(x)}{dx} = -\jmath\omega\left(C_s + C_m\right)V_e(x). \tag{5.43}$$

Defining the even-mode inductance and capacitance, L_e and C_e, respectively, as

$$L_e = L_s + L_m = L_{11} + L_{12} \quad \text{and} \quad C_e = C_s + C_m = C_{11} + C_{12} \tag{5.44}$$

leads to the **even-mode telegrapher's equations**:

$$\frac{dV_e(x)}{dx} = -\jmath\omega\, L_e I_e(x) \tag{5.45}$$ and $$\frac{dI_e(x)}{dx} = -\jmath\omega\, C_e V_e(x). \tag{5.46}$$

From these, the even-mode characteristic impedance can be found,

$$Z_{0e} = \sqrt{\frac{L_e}{C_e}} = \sqrt{\frac{L_s + L_m}{C_s + C_m}}, \tag{5.47}$$

and also the even-mode phase velocity,

$$v_{pe} = \frac{1}{\sqrt{L_e C_e}}. \tag{5.48}$$

The characteristics of the odd-mode operation of the coupled transmission line can be determined in a similar procedure to that used for the even mode. Using Equations (5.34)–(5.37), the **odd-mode telegrapher's equations** become

$$\frac{dV_o(x)}{dx} = -\jmath\omega\left(L_s - L_m\right)I_o(x) \tag{5.49}$$ and $$\frac{dI_o(x)}{dx} = -\jmath\omega\left(C_s - C_m\right)V_o(x). \tag{5.50}$$

Defining L_o and C_o for the odd mode such that

$$L_o = L_s - L_m = L_{11} - L_{12} \quad \text{and} \quad C_o = C_s - C_m = C_{11} - C_{12}, \tag{5.51}$$

then the odd-mode characteristic impedance is

$$Z_{0o} = \sqrt{\frac{L_o}{C_o}} = \sqrt{\frac{L_s - L_m}{C_s - C_m}} \tag{5.52}$$

and the odd-mode phase velocity is

$$v_{po} = \frac{1}{\sqrt{L_o C_o}}. \tag{5.53}$$

Now for a sanity check. If the individual strips are widely separated, L_m and C_m will become very small and Z_{0e} and Z_{0o} will be almost equal. As the strips become closer, L_m and C_m will become larger and Z_{0e} and Z_{0o} will diverge. This is as expected.

5.5.1 Odd-Mode and Even-Mode Capacitances

The previous section used the even- and odd-mode capacitances for two coupled microstrip lines with the strips having equal cross section so that each strip had the same self-capacitances. In this section this restriction is removed and the results apply to any pair of coupled lines in any technology and of any cross section. The results enable the capacitances of the capacitance matrix to be determined from calculations of the charges on the lines. Repeating Equations (5.22) and (5.23),

$$Q_1 = C_{11}V_1 + C_{12}V_2 \quad \text{and} \quad Q_2 = C_{21}V_1 + C_{22}V_2, \tag{5.54}$$

the capacitance matrix is

$$\mathbf{C} = \begin{bmatrix} C_{11} & C_{12} \\ C_{21} & C_{22} \end{bmatrix}. \tag{5.55}$$

In the even mode $V_1 = V_2 = V_e$ and so the even-mode charges on strip 1 and strip 2 are

$$Q_{1e} = (C_{11} + C_{12})\,V_e \quad \text{and} \quad Q_{2e} = (C_{21} + C_{22})\,V_e, \tag{5.56}$$

respectively. Defining the even-mode charge as

$$Q_e = (Q_{1e} + Q_{2e})\,/2, \tag{5.57}$$

then the even-mode charge becomes

$$Q_e = V_e(C_{11} + C_{22} + C_{12} + C_{21})/2. \tag{5.58}$$

This leads to the even-mode per unit length capacitance,

$$C_e = Q_e/V_e = (C_{11} + C_{22} + C_{12} + C_{21})/2. \tag{5.59}$$

Similarly, in the odd mode, $V_o = V_1 = -V_2$, and the odd-mode charges on strip 1 and strip 2 are

$$Q_{1o} = (C_{11} - C_{12})\,V_o \quad \text{and} \quad Q_{2o} = (C_{21} - C_{22})\,V_o, \tag{5.60}$$

respectively. The odd-mode charge is then

$$Q_o = (Q_{1o} - Q_{2o})\,/2 = (C_{11} + C_{22} - C_{12} - C_{21})\,V_o/2. \tag{5.61}$$

The odd-mode capacitance is

$$C_o = Q_o/V_o = (C_{11} + C_{22} - C_{12} - C_{21})/2. \tag{5.62}$$

EXAMPLE 5.1 Parallel Line Capacitance

EM software can be used to determine the even- and odd-mode parameters of a coupled line. This is usually done by setting the phasor voltages on the coupled line and evaluating the phasor charges. Consider a pair of coupled microstrip lines as in Figure 5-4. The voltage applied to the left strip is designated as V_1 and the voltage applied to the right strip is V_2. The phasor charge on the strips are Q_1 and Q_2, respectively. The analysis is repeated, but this time with the substrate removed, and so establishing the free-space situation. In this case the charges are denoted by Q_{01} and Q_{02}. The matrix of (computer-based) measurements is as follows:

Case	V_1 (V)	V_2 (V)	Q_1 (pC/m)	Q_2 (pC/m)	Q_{01} (pC/m)	Q_{02} (pC/m)
A	1	−1	70	−80	22.2	−24.7
B	1	1	30	40	2.82	5.32

(a) What is the two-port capacitance matrix?
(b) What is the even-mode capacitance?

(c) What is the odd-mode capacitance?
(d) What is the free-space (no dielectric) two-port capacitance matrix?
(e) What is the free-space even-mode capacitance?
(f) What is the free-space odd-mode capacitance?
(g) What is the even-mode effective relative permittivity?
(h) What is the odd-mode effective relative permittivity?
(i) Note that both the odd mode and even mode are TEM modes, so the phase velocity in the free-space situation is c. Determine the odd-mode and even-mode inductances per unit length in free space.
(j) Note that the inductances do not change when the dielectric is replaced. What is the even-mode impedance?
(k) What is the odd-mode impedance?
(l) What is the even-mode phase velocity?
(m) What is the odd-mode phase velocity?

Solution:

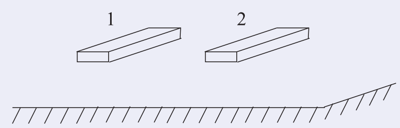

(a) Begin by considering the cross section of a coupled line shown to the right and use the basic equations relating the charges on the line to the voltages on them:

$$Q_1 = C_{11}V_1 + C_{12}V_2 \quad \text{and} \quad Q_2 = C_{21}V_1 + C_{22}V_2,$$

and consider two sets of voltage conditions.

Case A: This is the odd excitation, $V_1 = 1$ V and $V_2 = -1$ V and the charges are

$$Q_{1A} = C_{11} - C_{12} \quad (5.63) \qquad \text{and} \qquad Q_{2A} = C_{21} - C_{22}. \quad (5.64)$$

Case B: This is the even excitation, $V_1 = V_2 = 1$ V and the charges are

$$Q_{1B} = C_{11} + C_{12} \quad (5.65) \qquad \text{and} \qquad Q_{2B} = C_{21} + C_{22}. \quad (5.66)$$

Adding Equations (5.63) and (5.65) results in

$$Q_{1A} + Q_{1B} = 2C_{11}, \quad \text{thus} \quad C_{11} = \tfrac{1}{2}(Q_{1A} + Q_{1B}) = (70 + 30)/2 \text{ pF/m} = 50 \text{ pF}. \tag{5.67}$$

Subtracting Equation (5.63) from Equation (5.65) yields

$$Q_{1B} - Q_{1A} = 2C_{12}, \ \text{thus} \ C_{12} = \tfrac{1}{2}(Q_{1B} - Q_{1A}) = \tfrac{1}{2}(30 - 70) \text{ pF/m} = -20 \text{ pF/m}. \tag{5.68}$$

Because of reciprocity, $C_{21} = C_{12} = -20$ pF/m.
Subtracting Equation (5.64) from Equation (5.66) results in

$$Q_{2B} - Q_{2A} = 2C_{22}, \ \text{thus}\ C_{22} = \tfrac{1}{2}(Q_{2B} - Q_{2A}) = \tfrac{1}{2}(40 + 80) \text{ pF/m} = 60 \text{ pF/m}. \tag{5.69}$$

Thus the per unit length capacitance matrix of the coupled line is

$$\mathbf{C} = \begin{bmatrix} C_{11} & C_{21} \\ C_{12} & C_{22} \end{bmatrix} = \begin{bmatrix} 50 & -20 \\ -20 & 60 \end{bmatrix} \text{pF/m}. \tag{5.70}$$

(b) Even-mode capacitance, C_e:
The even mode has $V_1 = V_2$ and the even-mode voltage is $V_e = (V_1 + V_2)/2$.
The even-mode charge is $Q_e = (Q_1 + Q_2)/2 = (30 + 40)/2$ pC/m $= 35$ pC/m, so

$$C_e = Q_e/V_e = 35 \text{ pF/m}. \tag{5.71}$$

(c) Odd-mode capacitance, C_o:
The odd-mode voltage is $V_o = (V_1 - V_2)/2$ and the odd-mode charge is $Q_o = (Q_1 - Q_2)/2$. With $V_1 = +1V$ and $V_2 = -1V$, $V_0 = 1$,

$$Q_o = \tfrac{1}{2}\left[70 - (-80)\right]\ \mathrm{pC/m} = 75\ \mathrm{pC/m},\ \text{thus}\ C_o = Q_0/V_0 = 75\ \mathrm{pF/m}. \tag{5.72}$$

(d) Using a similar procedure to that in (a), but now using the free-space charge calculations, Q_{01} and Q_{02} results in the unit capacitance matrix:

$$\mathbf{C}_0 = \begin{bmatrix} 12.5 & -9.69 \\ -9.69 & 15.0 \end{bmatrix}\ \mathrm{pF/m}. \tag{5.73}$$

(e) $C_{e0} = 4.07\ \mathrm{pF/m}$.
(f) $C_{o0} = 23.5\ \mathrm{pF/m}$.
(g) $\varepsilon_{re} = C_e/C_{e0} = 35/4.07 = 8.6$.
(h) $\varepsilon_{ro} = C_o/C_{o0} = 75/23.5 = 3.2$.
(i) Phase velocity, $v_p = 1\big/\sqrt{LC}$. With no dielectric, the phase velocity is c:

$$v_p = c = 1\big/\sqrt{L_0 C_0} \rightarrow L_0 = 1/\left(c^2 C_0\right),$$

and the odd-mode free-space inductance is

$$L_{o0} = 1/\left(c^2 C_{o0}\right) = 1\Big/\left[\left(3\cdot 10^8\right)^2 23.5\cdot 10^{-12}\right]\ \mathrm{H/m} = 473\ \mathrm{nH/m}. \tag{5.74}$$

The free-space even-mode inductance is

$$L_{e0} = 1/\left(c^2 C_{e0}\right) = 1\Big/\left[\left(3\cdot 10^8\right)^2\cdot 4.07\cdot 10^{-12}\right]\ \mathrm{H/m} = 2.73\ \mathrm{\mu H/m}. \tag{5.75}$$

(j) $Z_0 = \sqrt{L_0/C_0}\,;\ L_o = L_{o0}\ \ Z_0 = \sqrt{473\cdot 10^{-9}/(75\cdot 10^{-12})}\ \Omega = 79.4\ \Omega.$
(k) $Z_e = \sqrt{L_e/C_e}\ \Rightarrow\ Z_e = \sqrt{2.73\cdot 10^{-6}/(35\cdot 10^{-12})}\ \Omega = 279\ \Omega.$
(l) $v_{pe} = 1\big/\sqrt{L_e C_e} = (2.73\cdot 10^{-6}\cdot 35\cdot 10^{-12})^{-\frac{1}{2}} = 1.023\cdot 10^8\ \mathrm{m/s}.$
(m) $v_{po} = 1\big/\sqrt{L_o C_o} = (473\cdot 10^{-9}\cdot 75\cdot 10^{-12})^{-\frac{1}{2}} = 1.68\cdot 10^8\ \mathrm{m/s}.$

5.6 Formulas for Characteristic Impedance of Coupled Microstrip Lines

Formulas for the characteristic impedance and effective permittivity of symmetric coupled microstrip lines, with the cross section shown in Figure 5-9, were developed by Hammerstad and Jensen [2] based on the concept of even and odd modes. The formulas are accurate to better than 1% for $0.1 \le u \le 10$ and $g > 0.01$, where u is the normalized width, and g is the normalized gap:

$$u = w/h, \qquad\qquad g = s/h. \tag{5.76}$$

In the following, Z_0 and ε_e refer to the characteristic impedance and effective permittivity of an individual microstrip line with a normalized width of u on a substrate with a relative dielectric constant of ε_r.

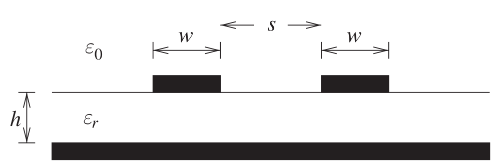

Figure 5-9: Cross section of symmetrically coupled microstrip lines.

5.6.1 Even-Mode Coupled-Line Parameters

The even-mode characteristic impedance is

$$Z_{0e}(u,g) = Z_{01e}(u,g)/\sqrt{\varepsilon_{ee}(u,g,\varepsilon_r)}, \tag{5.77}$$

where ε_{ee} is the effective relative permittivity of the even mode and Z_{01e} is the even-mode characteristic impedance with the dielectric replaced by free space:

$$Z_{01e}(u,g) = \frac{Z_0(u)}{1 - Z_0(u)\phi_e(u,g)/\eta_0}, \tag{5.78}$$

$$\text{where} \quad \phi_e(u,g) = \frac{\varphi(u)}{\psi(g)\left\{\alpha(g)u^{m(g)} + [1-\alpha(g)]\,u^{-m(g)}\right\}} \tag{5.79}$$

and $\eta_0 = 376.73\ \Omega \approx 377\ \Omega$ is the characteristic impedance of a TEM wave in a vacuum (i.e., free space). Now $Z_0(u)$ is the free-space characteristic impedance of an individual microstrip line and is given by Equation (3.21). In Equations (5.77) and (5.78), the effective permittivity of the even mode is

$$\varepsilon_{ee}(u,g,\varepsilon_r) = \frac{\varepsilon_r+1}{2} + \frac{\varepsilon_r-1}{2}F_e(u,g,\varepsilon_r), \tag{5.80}$$

where

$$F_e(u,g,\varepsilon_r) = \left[1 + \frac{10}{\mu(u,g)}\right]^{-a(u)b(\varepsilon_r)} \tag{5.81}$$

$$a(u) = 1 + \frac{1}{49}\ln\left[\frac{u^4 + \{u/52\}^2}{u^4 + 0.432}\right] + \frac{1}{18.7}\ln\left[1 + \left(\frac{u}{18.1}\right)^3\right] \tag{5.82}$$

$$b(\epsilon_r) = 0.564\left[\frac{\epsilon_r - 0.9}{\epsilon_r + 3}\right]^{0.053} \tag{5.83}$$

$$\varphi(u) = 0.8645u^{0.172} \tag{5.84}$$

$$\psi(g) = 1 + \frac{g}{1.45} + \frac{g^{2.09}}{3.95} \tag{5.85}$$

$$\alpha(g) = 0.5\exp(-g) \tag{5.86}$$

$$m(g) = 0.2175 + \left[4.113 + \left(\frac{20.36}{g}\right)^6\right]^{-0.251} + \frac{1}{323}\ln\left[\frac{g^{10}}{1 + (g/13.8)^{10}}\right] \tag{5.87}$$

$$\mu(u,g) = g\exp(-g) + \frac{u(20+g^2)}{10+g^2}. \tag{5.88}$$

5.6.2 Odd-Mode Coupled-Line Parameters

The odd-mode characteristic impedance is

$$Z_{0o}(u,g) = Z_{01o}(u,g)/\sqrt{\varepsilon_{eo}(u,g,\varepsilon_r)}, \tag{5.89}$$

where ε_{eo} is the effective relative permittivity of the odd mode and Z_{01o} is the odd-mode characteristic impedance with the dielectric replaced by free-space:

$$Z_{01o}(u,g) = \frac{Z_0(u)}{1 - Z_0(u)\phi_o(u,g)/\eta_0}. \tag{5.90}$$

$Z_0(u)$ is the free-space characteristic impedance of an individual microstrip line and is given by Equation (3.21). In Equations (5.89) and (5.90), the effective permittivity of the odd mode is

$$\varepsilon_{eo}(u, g, \varepsilon_r) = \frac{\varepsilon_r + 1}{2} + \frac{\varepsilon_r - 1}{2} F_o(u, g, \varepsilon_r), \tag{5.91}$$

where

$$F_o(u, g, \varepsilon_r) = f_o(u, g, \varepsilon_r)\,(1 + 10/u)^{-a(u)b(\varepsilon_r)} \tag{5.92}$$

$$\phi_o(u, g) = \phi_e(u, g) - \frac{\theta(g)}{\psi(g)} \exp\left[\beta(g) u^{n(g)} \ln(u)\right] \tag{5.93}$$

$$\theta(g) = 1.729 + 1.175 \ln\left(1 + \frac{0.627}{g + 0.327 g^{2.17}}\right) \tag{5.94}$$

$$\beta(g) = 0.2306 + \frac{1}{301.8} \ln\left[\frac{g^{10}}{1 + (g/3.73)^{10}}\right] + \frac{1}{5.3} \ln\left(1 + 0.646 g^{1.175}\right) \tag{5.95}$$

$$n(g) = \left\{\frac{1}{17.7} + \exp\left[-6.424 - 0.76 \ln(g) - (g/0.23)^5\right]\right\} \times \ln\left(\frac{10 + 68.3 g^2}{1 + 32.5 g^{3.093}}\right) \tag{5.96}$$

$$f_o(u, g, \varepsilon_r) = f_{o1}(g, \varepsilon_r) \exp\left[p(g) \ln(u) + q(g) \sin\left(\pi \frac{\ln u}{\ln 10}\right)\right] \tag{5.97}$$

$$p(g) = \exp\left(-0.745 g^{0.295}\right)/\cosh\left(g^{0.68}\right) \tag{5.98}$$

$$f_{o1}(g, \varepsilon_r) = 1 - \exp\left\{-0.179 g^{0.15} - \frac{0.328 g^{r(g,\varepsilon_r)}}{\ln\left[\exp(1) + (g/7)^{2.8}\right]}\right\} \tag{5.99}$$

$$r(g, \varepsilon_r) = 1 + 0.15\left\{1 - \frac{\exp\left[1 - (\varepsilon_r - 1)^2/8.2\right]}{1 + g^{-6}}\right\} \tag{5.100}$$

$$q(g) = \exp(-1.366 - g), \tag{5.101}$$

and $a(u)$, $b(\varepsilon_r)$, and $\psi(g)$ are the same as for the even mode (see Section 5.6.1).

5.6.3 System Impedance of Coupled Lines

The system impedance of a pair of coupled lines is

$$Z_{0S} = \sqrt{Z_{0e} Z_{0o}}. \tag{5.102}$$

This is derived in Section 5.7.1 where it is shown that there will be no odd-mode reflections, and even-mode reflections will be small, at the ports of a symmetrical coupled-line pair if each line of the directional coupler is terminated in an impedance Z_{0S}. That is, Z_{0S} is the impedance required for matching. Z_0 is the characteristic impedance of an individual line of the symmetrical coupled-line pair (when there is no coupling) and is only close to Z_{0S} when the separation, s, of the lines is large.

5.6.4 Discussion

Normalized even- and odd-mode characteristic impedances of a pair of coupled lines are plotted in Figure 5-10 for various normalized widths u

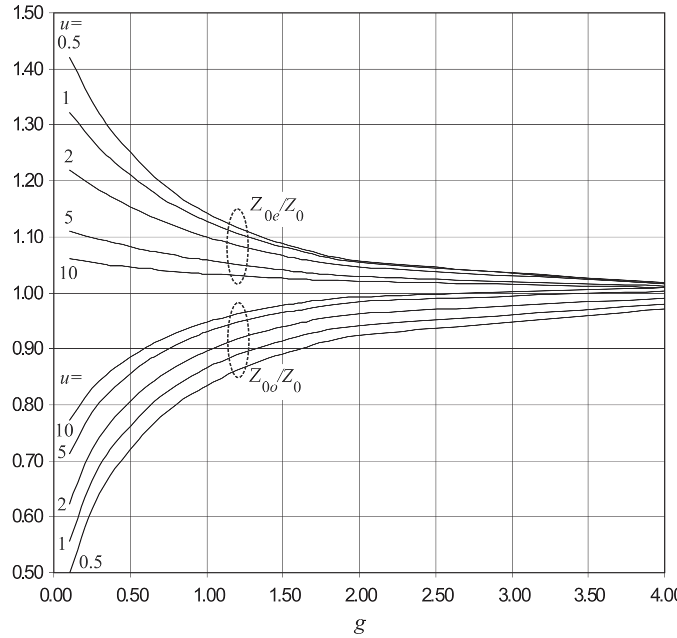

Figure 5-10: Normalized even-mode and odd-mode characteristic impedances of a pair of coupled microstrip lines ($\epsilon_r = 10$).

(= w/h) and as a function of normalized gap width g (= s/h). This plot illustrates the utility of using even- and odd-mode descriptions. In Figure 5-10, the even- and odd-mode impedances are normalized to the characteristic impedance of an individual line, Z_0. When the lines are far apart (i.e., g is large), the even- and odd-mode impedances converge to the characteristic impedance of a single line. As the lines get closer, the gap narrows, and the even- and odd-mode impedances diverge in opposite directions. To obtain the characteristic impedances of a coupled line the characteristic impedance of a single microstrip line must be found. This was given in Section 3.5.3 and the key result is repeated in Figure 5-11.

In the even mode, more of the field is in the dielectric than with the odd mode. It is therefore not surprising that the effective permittivities of the two modes differ. The normalized coupled-line effective permittivities are shown in Figure 5-12. The deviation of the even- and odd-mode permittivities as the gap between the lines narrows is not as large as the change in the characteristic impedance. Also, there is a difference in the phase velocities of the two modes along the line, and this has an appreciable effect on the performance of components such as filters that use coupled lines as a functional component. At the first reading of the plot (Figure 5-12) it would seem that there is nonmonotonic behavior at low g. This is an artifact of the normalization used, and the unnormalized permittivities are indeed monotonic with respect to both u and g.

Figure 5-13 plots, as a function of normalized separation, g, and for substrate permittivities ranging from 4 to 20, the even-mode and odd-mode characteristic impedances normalized to the characteristic impedance of a single strip for extremes of normalized widths (u = 0.5 and u = 5). The figure highlights that the split of the even- and odd-mode characteristic impedances is almost solely dependent on geometry (i.e., the separation of the strips) and not the permittivity of the substrate. In the figure appropriate normalization is used to highlight this fact. There are four families of curves,

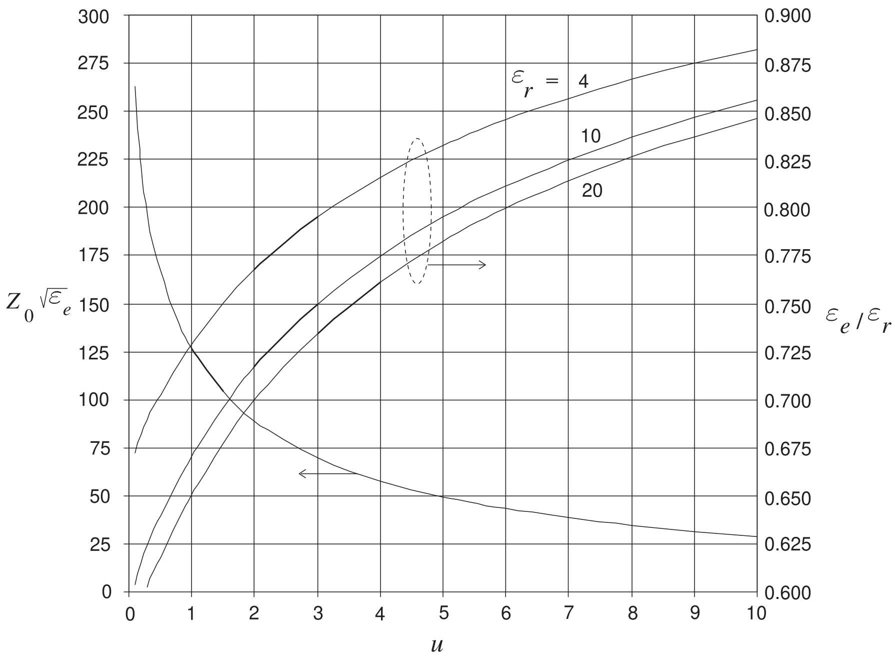

Figure 5-11: Normalized characteristic impedance and normalized effective permittivity of a microstrip line as a function of $u = w/h$. For example, if $u = 1$ and $\varepsilon_r = 10$, then from the figure, $Z_0\sqrt{\varepsilon_e} = 126\ \Omega$ and $\varepsilon_e/\varepsilon_r = 0.671$; thus $Z_0 = 48.6\ \Omega$ and $\varepsilon_e = 6.71$.

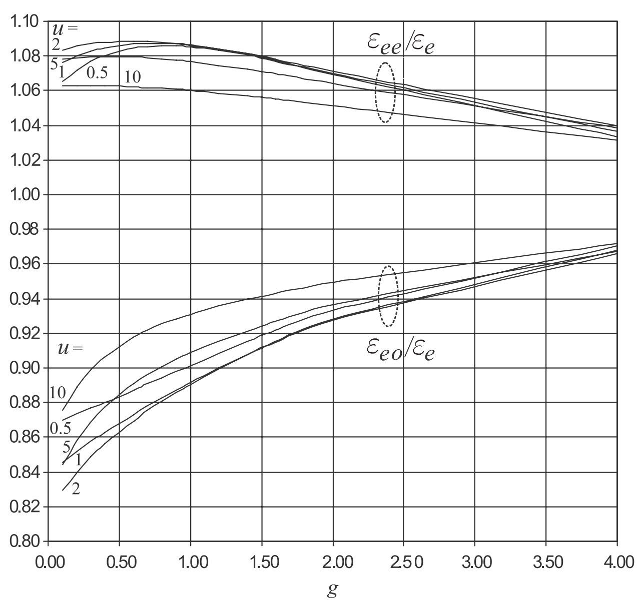

Figure 5-12: Normalized even-mode and odd-mode effective permittivity of a pair of coupled microstrip lines. The effective permittivity of an individual microstrip line with the same normalized width u is ε_e.

two for the even-mode characteristic impedances and two for the odd-mode characteristic impedances. Each family comprises the results for three widely different permittivities of the dielectric (specifically $\varepsilon_r = 4$, 10, and 20).

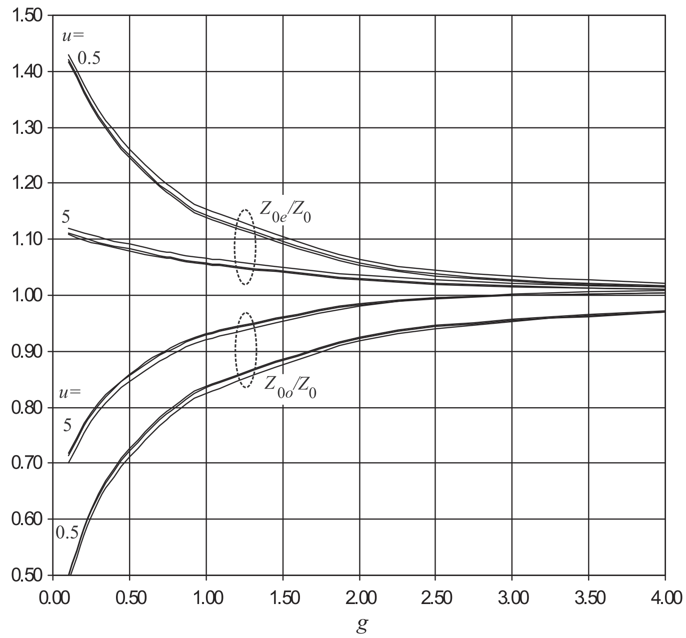

Figure 5-13: Normalized even-mode and odd-mode characteristic impedances of a pair of coupled microstrip lines for extremes of u. Each family of three curves is for $\varepsilon_r = 4$, 10, and 20. Z_0 is the characteristic impedance of an individual microstrip line with the same normalized width, $u = w/h$. The strips have equal width.

EXAMPLE 5.2 Even- and Odd-Mode Parameters

A coupled line is constructed on an alumina substrate of thickness 500 μm and relative permittivity $\varepsilon_r = 10$. The lines are 500 μm wide and the gap separation is 250 μm. What are the even- and odd-mode characteristic impedances and effective permittivities of the coupled line?

Solution:

The odd-mode characteristic impedance, Z_{0o}, and even-mode characteristic impedance, Z_{0e}, can be found using Figures 5-10 and 5-11. Now

$$u = w/h = (500\ \mu\text{m})/(500\ \mu\text{m}) = 1 \quad \text{and} \quad g = s/h = (250\ \mu\text{m})/(500\ \mu\text{m}) = 0.5.$$

From Figure 5-10,

$$Z_{0e}/Z_0 = 1.21 \quad \text{and} \quad Z_{0o}/Z_0 = 0.76, \tag{5.103}$$

where Z_0 is the characteristic impedance of an individual line. From Figure 5-11, and using the curve for $\varepsilon_r = 10$,

$$\varepsilon_e/\varepsilon_r = 0.671, \quad \text{and so} \quad \varepsilon_e = 10 \times 0.671 = 6.71. \tag{5.104}$$

Also from Figure 5-11,

$$Z_0\sqrt{\varepsilon_e} = 126, \quad \text{and so} \quad Z_0 = 126/\sqrt{6.71} = 48.6\ \Omega. \tag{5.105}$$

Consequently, combining Equations (5.103) and (5.105),

$$Z_{0o} = 37\ \Omega \quad \text{and} \quad Z_{0e} = 59\ \Omega. \tag{5.106}$$

The effective odd-mode and even-mode permittivities are obtained from Figure 5-12. The normalized even-mode effective permittivity is $\varepsilon_{ee}/\varepsilon_e = 1.086$ and the normalized odd-mode effective permittivity is $\varepsilon_{eo}/\varepsilon_e = 0.868$. Since $\varepsilon_e = 6.71$, the final result is

$$\varepsilon_{ee} = 7.28 \quad \text{and} \quad \varepsilon_{eo} = 5.82.$$

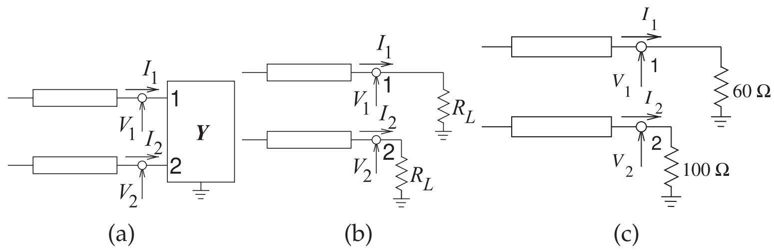

Figure 5-14: Terminated coupled lines: (a) with a load described by the y-parameter matrix $\boldsymbol{Y}$; (b) symmetrical loads; (c) loads considered in example.

5.6.5 Summary

This section presented formulas and graphs for determining the frequency-independent parameters of coupled lines given their dimensions. Frequency dependence of these electrical parameters are discussed in [3, 4]. The effect of finite metallization thickness is also discussed in [3]. Synthesis of coupled lines, i.e. determining their physical dimensions given their desired electrical parameters, is undertaken in the context of their use and is generally based on approximate, but reasonably accurate, models of a pair of coupled lines. This will be considered in Section 5.9.

5.7 Terminated Coupled Lines

A pair of coupled lines supports even and odd modes and these can be coupled by the terminations at the end of a line. Thus at a termination, such as that shown in Figure 5-14(a), where the termination is general and represented by a port-based admittance matrix $\boldsymbol{Y}$, the reflected even and odd modes will have contributions from both incident even and odd modes:

$$V_e^- = \Gamma_{Le} V_e^+ + C_{eo} V_o^+ \quad \text{and} \quad V_o^- = \Gamma_{Lo} V_o^+ + C_{oe} V_e^+ \tag{5.107}$$

where Γ_{Le} and Γ_{Lo} are even- and odd-mode reflection coefficients and C_{oe} and C_{eo} describe coupling first from the odd mode to the even mode and then from the even mode to the odd mode. The derivation of the reflection coefficients and coupling coefficients is left for an example at the end of this section. The summary results are

$$\Gamma_{Le} = \frac{2 + Z_{0o}Y_\Delta - Z_{0e}Y_\Sigma - 2Z_{0e}Z_{0o}Y_D}{2 + Z_{0o}Y_\Delta + Z_{0e}Y_\Sigma + 2Z_{0e}Z_{0o}Y_D} \tag{5.108}$$

$$C_{eo} = \frac{2Z_{0e}Y_E}{2 + Z_{0o}Y_\Delta + Z_{0e}Y_\Sigma + 2Z_{0e}Z_{0o}Y_D} = -C_{oe} \tag{5.109}$$

$$\Gamma_{Lo} = \frac{1 + Z_{0o}(y_{12} + y_{21}) - Z_{0e}Z_{0o}Y_D}{1 + Z_{0o}Y_\Delta + Z_{0e}Y_\Sigma + Z_{0e}Z_{0o}Y_D} \tag{5.110}$$

$$\left.\begin{aligned} \text{where } Y_\Sigma &= (y_{11} + y_{12} + y_{21} + y_{22}),\ Y_\Delta = (y_{11} - y_{12} - y_{21} + y_{22}) \\ Y_D &= (y_{11}y_{22} - y_{12}y_{21}) \quad \text{and } Y_E = (y_{11} - y_{12} + y_{21} - y_{22}). \end{aligned}\right\} \tag{5.111}$$

Controlling the coupling can be used in filter design based on parallel coupled lines.

5.7.1 Reflectionless Condition

In design of many coupled line sections it is important to minimize reflections of coupled lines. One quasi-reflectionless condition is to terminate individual lines of the coupled line in the system reference impedance

$Z_{0S} = \sqrt{Z_{0e}Z_{0o}}$. Then $y_{11} = 1/Z_{0S} = y_{22}$, and $y_{12} = 0 = y_{21}$ and referring to Equation (5.111), $Y_\Sigma = Y_\Delta = 2/Z_{0S} = 2/\sqrt{Z_{0e}Z_{0o}}$, $Y_E = 0$, and $Y_D = 1/Z_{0e}Z_{0o}$ and Equation (5.108) becomes

$$\Gamma_{Le} = \frac{2 + 2\sqrt{Z_{0o}Z_{0e}} - 2\sqrt{Z_{0e}Z_{0o}} - 2}{2 + 2\sqrt{Z_{0o}Z_{0e}} + 2\sqrt{Z_{0e}Z_{0o}} + 2} = \frac{\sqrt{Z_{0o}Z_{0e}} - 2\sqrt{Z_{0e}Z_{0o}}}{2 + \sqrt{Z_{0o}Z_{0e}} + \sqrt{Z_{0e}Z_{0o}}} \tag{5.112}$$

which is small and

$$\Gamma_{Lo} = \frac{1 + 0 - 1}{D} = 0. \tag{5.113}$$

Also note that the mode couplings C_{oe} and C_{oe} are both zero. So terminating the individual lines of a pair of coupled lines in Z_{0S} results in the odd-mode reflection coefficient Γ_{Lo} being zero and the odd-mode reflection coefficient Γ_{Lo} being small.

The even and odd-mode reflection coefficients can both be set to zero by simultaneously setting the numerators of Equations (5.108) and (5.108) to zero while maintaining symmetry, i.e. $y_{11} = y_{22}$, and because of reciprocity $y_{12} = y_{21}$ thus ensuring that $Y_E = 0$ and coupling is zero.

EXAMPLE 5.3 Reflection at the End of a Pair of Coupled Lines

A pair of coupled lines with even- and odd-mode characteristic impedances Z_{0e} and Z_{0o} respectively is loaded as shown in Figure 5-14(a) where the load has the two-port y-parameter matrix, $\mathbf{Y}$. Find the even and odd-mode reflections.

Solution:

The analysis begins by writing out the expressions relating the traveling-wave and total voltages and currents at the termination.

$$\begin{array}{llll}
V_e = \frac{1}{2}(V_1 + V_2) & V_o = \frac{1}{2}(V_1 - V_2) & I_e = \frac{1}{2}(I_1 + I_2) & I_o = \frac{1}{2}(I_1 - I_2) \\
V_1 = (V_1^+ + V_1^-) & V_2 = (V_2^+ + V_2^-) & I_1 = (I_1^+ + I_1^-) & I_2 = (I_2^+ + I_2^-) \\
V_1^+ = (V_e^+ + V_o^+) & V_2^+ = (V_e^+ - V_o^+) & I_1^+ = (I_e^+ + I_o^+) & I_2^+ = (I_e^- - I_o^+) \\
V_1^- = (V_e^- + V_o^-) & V_2^- = (V_e^- - V_o^-) & I_1^- = (I_e^- + I_o^-) & I_2^- = (I_e^- - I_o^-) \\
I_e^+ = V_e^+/Z_{0e} & I_e^- = -V_e^-/Z_{0e} & I_o^+ = V_o^+/Z_{0e} & I_o^- = -V_o^-/Z_{0o}
\end{array}$$

At the termination

$$\begin{bmatrix} I_1 \\ I_2 \end{bmatrix} = \begin{bmatrix} I_e^+ + I_o^+ + I_e^- + I_o^- \\ I_e^+ - I_o^+ + I_e^- - I_o^- \end{bmatrix} = \mathbf{Y} \begin{bmatrix} V_1 \\ V_2 \end{bmatrix} = \begin{bmatrix} y_{11} & y_{12} \\ y_{21} & y_{22} \end{bmatrix} \begin{bmatrix} V_1 \\ V_2 \end{bmatrix}$$

$$\begin{bmatrix} (V_e^+ - V_e^-)/Z_{0e} + (V_o^+ - V_o^-)/Z_{0o} \\ (V_e^+ - V_e^-)/Z_{0e} - (V_o^+ - V_o^-)/Z_{0o} \end{bmatrix} = \begin{bmatrix} y_{11} & y_{12} \\ y_{21} & y_{22} \end{bmatrix} \begin{bmatrix} V_e^+ + V_o^+ + V_e^- + V_o^- \\ V_e^+ - V_o^+ + V_e^- - V_o^- \end{bmatrix} \tag{5.114}$$

The reflected even and odd modes have contributions from incident even and odd modes:

$$V_e^- = \Gamma_{Le}V_e^+ + C_{eo}V_o^+ \quad \text{and} \quad V_o^- = \Gamma_{Lo}V_o^+ + C_{oe}V_e^+ \tag{5.115}$$

where Γ_{Le} and Γ_{Lo} are even- and odd-mode reflection coefficients, C_{oe} and C_{eo} describe coupling, and

$$\Gamma_{Le} = \left.\frac{V_e^-}{V_e^+}\right|_{V_o^+=0}, \Gamma_{Lo} = \left.\frac{V_o^-}{V_o^+}\right|_{V_e^+=0}, C_{eo} = \left.\frac{V_e^-}{V_o^+}\right|_{V_e^+=0} \text{ and } C_{oe} = \left.\frac{V_o^-}{V_e^+}\right|_{V_o^+=0}. \tag{5.116}$$

Γ_{Le} and C_{eo} are obtained by expanding Equation (5.114) with $V_o^+ = 0$:

$$(V_e^+ - V_e^-)/Z_{0e} - V_o^-/Z_{0o} = y_{11}\left(V_e^+ + V_e^- + V_o^-\right) + y_{12}\left(V_e^+ + V_e^- - V_o^-\right)$$

$$\text{i.e. } \frac{V_e^-}{Z_{0e}}(1 + y_{11}Z_{0e} + y_{12}Z_{0e}) = \frac{V_e^+}{Z_{0e}}(1 - y_{11}Z_{0e} - y_{12}Z_{0e}) - \frac{V_o^-}{Z_{0o}}(1 + y_{11}Z_{0o} - y_{12}Z_{0o}) \tag{5.117}$$

$$(V_e^+ - V_e^-)/Z_{0e} + V_o^-)/Z_{0o} = y_{21}\left(V_e^+ + V_e^- + V_o^-\right) + y_{22}\left(V_e^+ + V_e^- - V_o^-\right)$$

$$\text{i.e. } \frac{V_o^-}{Z_{0o}}(-1 + y_{21}Z_{0o} - y_{22}Z_{0o}) = \frac{V_e^+}{Z_{0e}}(1 - y_{21}Z_{0e} - y_{22}Z_{0e}) + \frac{V_e^-}{Z_{0e}}(-1 - y_{21}Z_{0e} - y_{22}Z_{0e}) \tag{5.118}$$

Γ_{Le} is obtained by eliminating V_o^- by multiplying Equation (5.118) by $(1 + y_{11}Z_{0o} - y_{12}Z_{0o})$ and subtracting it from Equation (5.117) multiplied by $(-1 + y_{21}Z_{0o} - y_{22}Z_{0o})$:

$$V_e^- \frac{a}{Z_{0e}} = V_e^+ \frac{b}{Z_{0e}}\bigg|_{V_o^+=0}. \quad \text{Thus} \quad \Gamma_{Le} = \frac{b}{a} \tag{5.119}$$

where

$$\begin{aligned} a &= (1 + y_{11}Z_{0e} + y_{12}Z_{0e})(-1 + y_{21}Z_{0o} - y_{22}Z_{0o}) - (1 + y_{21}Z_{0e} + y_{22}Z_{0e})(1 + y_{11}Z_{0o} - y_{12}Z_{0o}) \\ &= -2 - Z_{0o}Y_\Delta - Z_{0e}Y_\Sigma - 2Z_{0e}Z_{0o}Y_D \end{aligned} \tag{5.120}$$

$$\begin{aligned} b &= (1 - y_{11}Z_{0e} - y_{12}Z_{0e})(-1 + y_{21}Z_{0o} - y_{22}Z_{0o}) - (1 - y_{21}Z_{0e} - y_{22}Z_{0e})(1 + y_{11}Z_{0o} - y_{12}Z_{0o}) \\ &= -2 - Z_{0o}Y_\Delta + Z_{0e}Y_\Sigma + 2Z_{0e}Z_{0o}Y_D \end{aligned} \tag{5.121}$$

$$Y_\Sigma = (y_{11} + y_{12} + y_{21} + y_{22}), Y_\Delta = (y_{11} - y_{12} - y_{21} + y_{22}), \text{ and } Y_D = (y_{11}y_{22} - y_{12}y_{21}) \tag{5.122}$$

$$\Gamma_{Le} = \frac{b}{a} = \frac{2 + Z_{0o}Y_\Delta - Z_{0e}Y_\Sigma - 2Z_{0e}Z_{0o}Y_D}{2 + Z_{0o}Y_\Delta + Z_{0e}Y_\Sigma + 2Z_{0e}Z_{0o}Y_D} \tag{5.123}$$

As a sanity check, if the load is symmetrical $y_{11} = y_{22} = Y_L = 1/Z_L$, the differential load impedance is infinite $y_{12} = 0 = y_{21}$, if the lines are far apart $Z_{0e} = Z_{0o} = Z_0$, then $Y_\Sigma = 2Y_L$, $Y_\Delta = 2Y_L$, and $Y_D = Y_L^2$ and Equation (5.123) becomes

$$\begin{aligned} \Gamma_{Le} &= \frac{2 + 2Z_0Y_L - 2Z_0Y_L - 2Z_0^2Y_L^2}{2 + 2Z_0Y_L + 2Z_0Y_L + 2Z_0^2Y_L^2} = \frac{1 - Z_0^2Y_L^2}{1 + 2Z_0Y_L + Z_0^2Y_L^2} = \frac{(1 - Z_0Y_L)(1 + Z_0Y_L)}{(1 + Z_0Y_L)(1 + Z_0Y_L)} \\ &= \frac{1 - Z_0Y_L}{1 + Z_0Y_L} = \frac{Z_L - Z_0}{Z_L + Z_0}. \end{aligned} \tag{5.124}$$

This is the reflection coefficient of a transmission line of characteristic impedance Z_0 terminated in a load Z_L as expected.

Find C_{eo} by expanding Equation (5.114) with $V_e^+ = 0$:

$$-V_e^-/Z_{0e} + (V_o^+ - V_o^-)/Z_{0o} = y_{11}\left(V_o^+ + V_e^- + V_o^-\right) + y_{12}\left(-V_o^+ + V_e^- - V_o^-\right)$$

$$\text{i.e. } \frac{V_e^-}{Z_{0e}}(1 + y_{11}Z_{0e} + y_{12}Z_{0e}) = \frac{V_o^+}{Z_{0o}}(1 - y_{11}Z_{0o} + y_{12}Z_{0o}) - \frac{V_o^-}{Z_{0o}}(1 + y_{11}Z_{0o} - y_{12}Z_{0o}) \tag{5.125}$$

$$-V_e^-/Z_{0e} - (V_o^+ - V_o^-)/Z_{0o} = y_{21}\left(+V_o^+ + V_e^- + V_o^-\right) + y_{22}\left(-V_o^+ + V_e^- - V_o^-\right)$$

$$\text{i.e. } \frac{V_o^-}{Z_{0o}}(-1 + y_{21}Z_{0o} - y_{22}Z_{0o}) = -\frac{V_o^+}{Z_{0o}}(1 + y_{21}Z_{0o} - y_{22}Z_{0o}) - \frac{V_e^-}{Z_{0e}}(1 + y_{21}Z_{0e} + y_{22}Z_{0e}) \tag{5.126}$$

To eliminate V_o^- multiply Equation (5.126) by $(1 + y_{11}Z_{0o} - y_{12}Z_{0o})$ and subtract it from Equation (5.125) multiplied by $(-1 + y_{21}Z_{0o} - y_{22}Z_{0o})$:

$$\frac{V_e^-}{Z_{0e}}a = \frac{V_o^+}{Z_{0o}}c \quad \text{so that} \quad C_{eo} = \frac{c}{a}\frac{Z_{0e}}{Z_{0o}} \tag{5.127}$$

where a is as in Equation (5.120) and

$$c = (1 - y_{11}Z_{0o} + y_{12}Z_{0o})(-1 + y_{21}Z_{0o} - y_{22}Z_{0o}) + (1 + y_{21}Z_{0o} - y_{22}Z_{0o})(1 + y_{11}Z_{0o} - y_{12}Z_{0o})$$
$$= -2Z_{0o}Y_E \quad \text{where} \quad Y_E = (y_{11} - y_{12} + y_{21} - y_{22}). \tag{5.128}$$
$$C_{eo} = \frac{2Z_{0o}Y_E}{2 + Z_{0o}Y_\Delta + Z_{0e}Y_\Sigma + 2Z_{0e}Z_{0o}Y_D} \tag{5.129}$$

Now for a sanity check. If the load is symmetrical $y_{11} = y_{22}$ and $y_{12} = y_{21}$, then $Y_E = 0$ and $C_{eo} = 0$ indicating that a signal is not converted from odd mode to even mode with reflection from a symmetrical load, as expected.

The analysis is now repeated to find Γ_{Lo} and C_{oe}. Γ_{Lo} is found by eliminating V_e^- from Equations (5.125) and (5.126) by multiplying Equation (5.126) by $(1 + y_{11}Z_{0e} + y_{12}Z_{0e})$ and subtracting it from Equation (5.125) multiplied by $(1 + y_{21}Z_{0e} + y_{22}Z_{0e})$:

$$\frac{V_o^+}{Z_{0o}}d = \frac{V_o^-}{Z_{0o}}e\bigg|_{V_e^+=0} \quad \text{and} \quad \Gamma_{Lo} = \frac{V_o^-}{V_o^+}\bigg|_{V_e^+=0} = \frac{d}{e} \tag{5.130}$$
$$d = (1 - y_{11}Z_{0o} + y_{12}Z_{0o})(1 + y_{21}Z_{0e} + y_{22}Z_{0e}) + (1 + y_{21}Z_{0o} - y_{22}Z_{0o})(1 + y_{11}Z_{0e} + y_{12}Z_{0e})$$
$$= 2 + 2Z_{0o}(y_{12} + y_{21}) - 2Z_{0e}Z_{0o}Y_D \tag{5.131}$$
$$e = (1 + y_{11}Z_{0o} - y_{12}Z_{0o})(1 + y_{21}Z_{0e} + y_{22}Z_{0e}) - (-1 + y_{21}Z_{0o} - y_{22}Z_{0o})(1 + y_{11}Z_{0e} + y_{12}Z_{0e})$$
$$= 2 + 2Z_{0o}Y_\Delta + 2Z_{0e}Y_\Sigma + 2Z_{0e}Z_{0o}Y_D \tag{5.132}$$
$$\Gamma_{Lo} = \frac{1 + Z_{0o}(y_{12} + y_{21}) - Z_{0e}Z_{0o}Y_D}{1 + Z_{0o}Y_\Delta + Z_{0e}Y_\Sigma + Z_{0e}Z_{0o}Y_D}. \tag{5.133}$$

C_{oe} is found by eliminating V_e^- achieved by multiplying Equation (5.118) by $(1 + y_{11}Z_{0e} + y_{12}Z_{0e})$ and subtracting it from Equation (5.117) multiplied by $(1 + y_{21}Z_{0e} + y_{22}Z_{0e})$:

$$V_o^- \frac{f}{Z_{0o}} = V_e^+ \frac{g}{Z_{0e}}\bigg|_{V_o^+=0}. \quad \text{Thus} \quad C_{oe} = \frac{g}{f}\frac{Z_{0o}}{Z_{0e}} \quad \text{where} \tag{5.134}$$
$$g = -(1 - y_{11}Z_{0e} - y_{12}Z_{0e})(1 + y_{21}Z_{0e} + y_{22}Z_{0e}) + (1 - y_{21}Z_{0e} - y_{22}Z_{0e})(1 + y_{11}Z_{0e} + y_{12}Z_{0e})$$
$$= 2Z_{0e}(y_{11} + y_{12} - y_{21} - y_{22}) = 2Z_{0e}Y_E \tag{5.135}$$
$$f = -(1 + y_{11}Z_{0o} - y_{12}Z_{0o})(1 + y_{21}Z_{0e} + y_{22}Z_{0e}) + (-1 + y_{21}Z_{0e} - y_{22}Z_{0e})(1 + y_{11}Z_{0e} + y_{12}Z_{0e})$$
$$= -2 - Z_{0o}Y_\Delta - Z_{0e}Y_\Sigma - 2Z_{0e}Z0oY_D \tag{5.136}$$
$$C_{oe} = \frac{-2Z_{0o}Y_E}{2 + Z_{0o}Y_\Delta - Z_{0e}Y_\Sigma + 2Z_{0e}Z0oY_D} = -Ceo. \tag{5.137}$$

EXAMPLE 5.4 Even and Odd Mode Loads

A pair of coupled lines is loaded as shown in Figure 5-14(a). The even-mode characteristic impedance is $Z_{0e} = 90\ \Omega$ and the odd-mode characteristic impedance is $Z_{0o} = 45\ \Omega$.

(a) What is the even-mode reflection coefficient?

To simplify calculations let the forward-traveling even-mode voltage at the load $V_e+ = 1$ V, and there is no forward-traveling odd-mode voltage. V_e^- and V_o^- are the backward-traveling even- and odd-mode voltages and I_e+, I_e^- and I_o^- are the corresponding currents. At Port 1

$$I_1 = \tfrac{1}{60}V_1 = V_e^+ + V_o^+ + V_e^- + V_o^- = \tfrac{1}{60}(1 + 0 + V_e^- + V_o-)$$
$$I_1 = I_e^+ + I_o^+ + I_e^- + I_o^- = \frac{V_e^+}{Z_{0e}} + 0 - \frac{V_e^-}{Z_{0e}} - \frac{V_o^-}{Z_{0o}} = \frac{1}{90} - \frac{V_e^-}{90} - \frac{V_o^-}{45}$$

Equating these and multiplying by 180 $\quad 1 + 5V_e^- + 7V_o- = 0 \quad$ (5.138)

At Port 2

$$I_2 = \tfrac{1}{100}V_1 = \tfrac{1}{100}(V_e^- V_o^+ + V_e^- - V_o-) = \tfrac{1}{100}(1 + 0 + V_e^- - V_o-)$$

$$I_2 = I_e^+ - I_o^+ + I_e^- - I_o- = \frac{V_e^+}{Z_{0e}} + 0 - \frac{V_e^-}{Z_{0e}} + \frac{V_o^-}{Z_{0o}} = \frac{1}{90} - \frac{V_e^-}{90} + \frac{V_o^-}{45}$$

Equating these and multiplying by 900: $1 - 19V_e^- + 29V_o- = 0$ (5.139)

Multiplying Equation (5.139) by 7 and subtracting it from Equation (5.138) times 29:

$$(29 - 7) + (145 + 133)V_e^- + (203 - 203)V_o^- = 0 \;\Rightarrow\; V_e^- = -0.07914\,\text{V}$$

Thus $\Gamma_{Le} = V_e^-/V_e^+ = V_e^-/1 = -0.07914.$ (5.140)

Alternatively the general formula, Equation (5.108), can be used noting that $Z_{0e} = 90\ \Omega$, $Z_{0e} = 45\ \Omega$, $y_{11} = 1/60$, $y_{22} = 1/100$, and $y_{12} = 0 = y_{21}$. Then $y_\Delta = 0.026667\,\text{S}$, $y_\Sigma = 0.026667\,\text{S}$, $y_D = 0.00016667\,\text{S}$:

$$\Gamma_{Le} = \frac{2 + 45\cdot 0.026667 - 90\cdot 0.026667 - 2\cdot 45\cdot 90\cdot 0.00016667}{2 + 45\cdot 0.026667 + 90\cdot 0.026667 + 2\cdot 45\cdot 90\cdot 0.00016667} = -0.07914 \tag{5.141}$$

The two evaluations of Γ_{Le} are in agreement.

(b) What is the effective even-mode load resistance R_{Le}?
R_{Le} is the resistance that yields Γ_{Le} when referred to Z_{0e}. Thus

$$R_{Le} = Z_{0e}\frac{1 + \Gamma_{Le}}{1 - \Gamma_{Le}} = 90\frac{1 + (-0.07914)}{1 - (-0.07914)} = 76.80\ \Omega \tag{5.142}$$

(c) What is the odd-mode reflection coefficient?
Calculating this directly using Equation (5.110):

$$\Gamma_{Lo} = \frac{1 + 0 - 45\cdot 90\cdot 0.00016667}{1 + 45\cdot 0.026667 + 90\cdot 0.026667 + \cdot 45\cdot 90\cdot 0.00016667} = 0.06180 \tag{5.143}$$

(d) What is the effective odd-mode load resistance R_{Lo}?

$$R_{Lo} = Z_{0o}\frac{1 + \Gamma_{Lo}}{1 - \Gamma_{Lo}} = 45\frac{1 + 0.06180}{1 - 0.06180} = 50.92\ \Omega \tag{5.144}$$

5.8 Directional Coupler

Coupling can be exploited to realize a new type of element called a directional coupler. The schematic of a directional coupler is shown in Figure 5-15(a) and a microstrip realization is shown in Figure 5-15(b). The microstrip realization is typical of most directional couplers in that it comprises two parallel signal lines with the electric and magnetic fields of a signal on one line inducing currents and voltages on the other. A usable directional

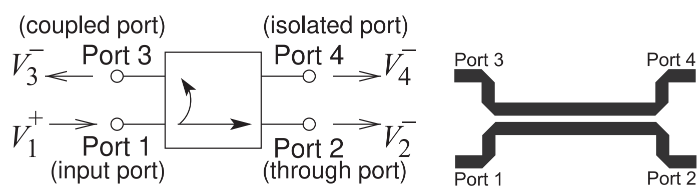

(a) (b)

Figure 5-15: Directional couplers: (a) schematic; and (b) backward-coupled microstrip coupler. (Note that not all couplers are backward-wave couplers as shown in (a).)

Table 5-1: Ideal and typical parameters of a directional coupler.

Parameter	Ideal	Ideal (dB)	Typical
Coupling, C	-	-	3–40 dB
Transmission, T	$\lvert\sqrt{1-1/C^2}\rvert$	$20\log\lvert\sqrt{1-1/C^2}\rvert$	-0.5 dB
Directivity, D	∞	∞	40 dB
Isolation, I	∞	∞	40 dB

coupler has a coupled line length of at least one-quarter wavelength, with longer lengths of line resulting in broader bandwidth operation. Directional couplers are used to sample a traveling wave on one line and to induce a usually much smaller image of the wave on another line. That is, the forward- and backward-traveling waves are separated. Here a prescribed amount of the incident power is coupled out of the system. Thus, for example, a 20 dB microstrip coupler is a pair of coupled microstrip lines in which $1/100$ of the power input is coupled from one microstrip line onto the another.

Referring to Figure 5-15, a coupler is specified in terms of the following parameters (always check the magnitude of the factors, as some papers and books on couplers use the inverse of the C used here):

- Coupling factor:
  $C = V_1^+/V_3^-$ = inverse of the voltage fraction "transferred" (coupled) across to the opposite arm ($C > 1$).
- Transmission factor (inverse of insertion loss):
  $T = V_2^-/V_1^+$ = transmission directly through the "primary" arm of the structure ($T < 1$).
- Directivity factor:
  $D = V_3^-/V_4^-$ = measure of the undesired coupling from Port 1 to Port 4 relative to the signal level at Port 3 ($D > 1$).
- Isolation factor:
  $I = V_1^+/V_4^-$ = isolation between Port 4 and Port 1 ($I > 1$).

It is usual to quote these quantities in decibels. For example, the coupling factor in decibels is $C|_{\text{dB}} = 20\log C$. So 20 dB coupling indicates that the coupling factor is 10. An ideal quarter-wave coupler has $D = \infty$ (i.e., infinite directivity) and

$$C = \frac{Z_{0e} + Z_{0o}}{Z_{0e} - Z_{0o}}. \tag{5.145}$$

This result comes from a detailed derivation for the case when the coupled-line section is one-quarter wavelength long—the length when the coupling is maximum. The derivation is given in Section 11.4 of [5]. In decibels the coupling is

$$C|_{\text{dB}} = 20\log\left(\frac{Z_{0e} + Z_{0o}}{Z_{0e} - Z_{0o}}\right). \tag{5.146}$$

Typical and ideal parameters of a directional coupler are given in Table 5-1. Since an ideal coupler does not dissipate power, the magnitude of the transmission coefficient is

$$|T| = |\sqrt{1 - 1/C^2}|. \tag{5.147}$$

There are many types of directional couplers, and the phases of the traveling waves at the ports will not necessarily coincide. The microstrip coupler shown in Figure 5-15(b) has maximum coupling when the lines are one-quarter wavelength long.[5] At the frequency where they are one-quarter wavelength long, the phase difference between traveling waves entering at Port 1 and leaving at Port 2 will then be $90°$.

EXAMPLE 5.5 Directional Coupler Isolation

A lossless directional coupler has coupling C = 20 dB, transmission factor 0.8, and directivity 20 dB. What is the isolation? Express your answer in decibels.

Solution:

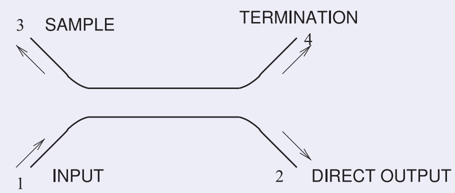

Coupling factor: $C = V_1^+/V_3^-$
Transmission factor: $T = V_2^-/V_1^+$
Directivity factor: $D = V_3^-/V_4^-$
Isolation factor: $I = V_1^+/V_4^-$

$$D = 20 \text{ dB} = 10 \quad \text{and} \quad C = 20 \text{ dB} = 10,$$

so the isolation is

$$I = \frac{V_1^+}{V_4^-} = \frac{V_3^-}{V_4^-} \cdot \frac{V_1^+}{V_3^-} = D \cdot C = 10 \cdot 10 = 100 = 40 \text{ dB}.$$

5.8.1 Design Equations for a Directional Coupler

In the previous section the coupling factor was expressed in terms of the even- and odd-mode impedances. However, design starts with the specification of the coupling level, and from this the required physical dimensions are derived. A one-quarter wavelength long coupler will be considered, as this is the optimum coupling length. From Equation (5.145), the desired coupling factor is

$$C = \frac{Z_{0e} + Z_{0o}}{Z_{0e} - Z_{0o}}, \tag{5.148}$$

where the coupling factor is an absolute voltage-referenced quantity and usually must be derived from the coupling factor in decibels; let this be $C|_{\text{dB}}$:

$$C = 10^{C|_{\text{dB}}/20}. \tag{5.149}$$

The system impedance comes from

$$Z_{0S}^2 \approx Z_{0e} Z_{0o}. \tag{5.150}$$

Z_{0S} is introduced here because Z_0 is used for the characteristic impedance of the individual lines of the coupler; note that Z_0 is not equal to Z_{0S}. Z_{0S} should match the characteristic impedance of the transmission lines connected to the coupler. From these expressions, the even- and odd-mode impedances required are

$$Z_{0e} \approx Z_{0S}\sqrt{\frac{C+1}{C-1}} \tag{5.151}$$

$$Z_{0o} \approx Z_{0S}\sqrt{\frac{C-1}{C+1}}, \tag{5.152}$$

and the ratio of impedances is

$$Z_{0e}/Z_{0o} \approx \frac{C+1}{C-1}. \tag{5.153}$$

[5] This is shown in a detailed derivation provided in Section 11.4 of [5].

EXAMPLE 5.6 Directional Coupler Electrical Design

Develop the electrical design of a 15 dB directional coupler in a 50 Ω system.

Solution:

The electrical design of a directional coupler comes down to determining the even- and odd-mode characteristic impedances required. Now the coupling factor, C, is $(Z_{0e} + Z_{0o}) / (Z_{0e} - Z_{0o})$ and

$$Z_{0e} = Z_{0S}\sqrt{\frac{C+1}{C-1}}.$$

For a 15 dB directional coupler, $C = 15\ \text{dB} = 5.618$ and, since $Z_{0S} = 50\ \Omega$,

$$Z_{0e} = 50\sqrt{\frac{5.618+1}{5.618-1}} = 59.9\ \Omega \quad \text{and} \quad Z_{0o} = Z_{0S}^2/Z_{0e} = 50^2/59.9 = 41.7\ \Omega.$$

The above are the required electrical design parameters.

5.8.2 Directional Coupler With Lumped Capacitors

Directional couplers using only coupled transmission lines can be large at low frequencies, as the minimum length is approximately one-quarter of a wavelength. This can be a problem at RF and low microwave frequencies, say, below 3 GHz. The length of the line can be reduced by incorporating lumped elements, as shown in Figure 5-16(a). The equivalence is established using $ABCD$ parameters. Figure 5-16(b) shows a hybrid directional coupler using a ferrite core, forming a magnetic transformer, to provide enhanced coupling of the coupled lines at low frequencies with a frequency range of 1–700 MHz. At high frequencies the ferrite core is a magnetic open circuit and the line coupling dominates.

5.8.3 Physical Design of a Pair of Coupled Lines

Equations (5.151)–(5.153) are the basic design expressions, as Z_{0e} and Z_{0o} can be related to physical dimensions. When the two strips of a microstrip directional coupler are close, the orientation of the field lines and hence the characteristic impedances of the individual lines change. That is, the characteristic impedance of each line on its own, Z_0, will differ from the system impedance, Z_{0S}. For a normalized line width of $u = (w/h)$, this effect is shown in Figure 5-17. Here Z_{0S} is the geometric mean of the even- and odd-mode impedances.

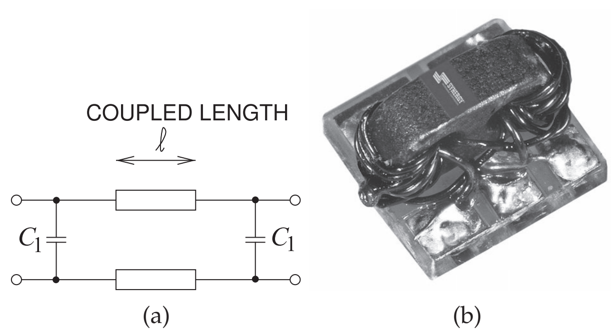

Figure 5-16: Parallel coupled lines with lumped capacitors bridging the ends to provide compensation: (a) schematic illustration; and (b) using a hybrid transformer to provide enhanced coupling of the coupled lines at low frequencies (Model GC6-2, copyright Synergy Microwave Corporation, used with permission [6]).

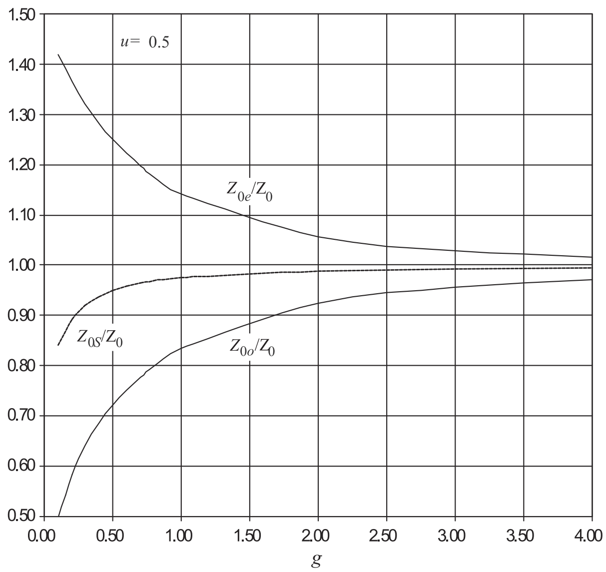

Figure 5-17: Normalized even- and odd-mode cvharacteristic impedances of coupled microstrip lines with normalized width, $u = 0.5$, versus normalized gap spacing, g.

Microstrip coupler design proceeds as follows. The first step is to examine the specifications and determine the substrate permittivity, ε_r, coupling factor, C, and the system characteristic impedance, Z_{0S}. From C find Z_{0e}/Z_0; the data in Tables 5-2 and 5-3 enable some of the physical parameters to be determined, including the normalized gap coupling parameter, g, and the normalized strip width, u. The next step is to design the dimensions of the individual microstrip lines connecting the directional coupler using Table 3-3. At this stage the widths and spacings of the microstrip circuit are normalized. Using the substrate height, these are unnormalized to obtain the actual physical dimensions. Finally, the coupler is one-quarter wavelength long, as this was the basis for the formula relating the even- and odd-mode impedances to the coupling factor in Equation (5.145). The even and odd modes have different effective permittivities and the $\lambda_g/4$ length should apply to both the even and odd modes. Clearly both cannot be satisfied. It is reasonable to use the average of the even- and odd-mode permittivities to establish the coupler length. The length is not a very sensitive parameter anyway. The connection of the individual lines to the coupler is not specifically part of the synthesis described, but if designed they should have the system characteristic impedance.

A comment on this design procedure is in order. The design procedure above yields a narrowband directional coupler. A broadband directional coupler, and indeed any component that is desired to have a broad bandwidth, should be designed using filter principles. Another comment is that the design flow is one of synthesis. An alternative procedure that is often used is to start with an approximate design and rely on optimization tools to obtain the desired characteristics. This works in many cases, but does lead to novel design. Having said that, the synthesis procedure does not yield a perfect design, as parasitic and dispersive effects are not taken into account. Optimization from the synthesized design usually requires only a small adjustment. In practice, the uncertainties of physical structures (e.g., variations in the effective permittivity of actual materials) require experimental iteration as well.

Table 5-2: Design parameters for coupled lines for $\varepsilon_r = 4$. The normalized gap, g, is chosen to obtain the desired coupled-line mode impedance ratio, Z_{0e}/Z_{0o}. Data are derived from the analysis in Section 5.6. Z_0 is the characteristic impedance of an individual microstrip line with a normalized width, u. For $Z_{0S} = 50\ \Omega$, $w/h = 2.056$, from Table 3-3.

$\varepsilon_r = 4$ (SiO$_2$ and FR4), $Z_{0S} = 50\ \Omega$							
g	Z_{0e}/Z_{0o}	u	Z_{0e} (Ω)	Z_{0o} (Ω)	ε_{ee}	ε_{eo}	Z_0 (Ω)
0.1	2.20	1.57	74.12	33.72	3.20	2.61	58.60
0.2	1.87	1.72	68.38	36.52	3.23	2.65	55.60
0.3	1.70	1.80	65.26	38.37	3.25	2.68	54.10
0.4	1.59	1.86	62.93	39.66	3.26	2.70	53.10
0.5	1.50	1.90	61.26	40.74	3.27	2.72	52.20
0.6	1.44	1.93	59.93	41.63	3.27	2.74	52.00
0.7	1.39	1.95	58.90	42.42	3.27	2.76	51.60
0.8	1.35	1.97	57.95	43.05	3.28	2.78	51.30
0.9	1.31	1.98	57.25	43.67	3.28	2.79	51.20
1.0	1.28	1.99	56.61	44.20	3.27	2.80	51.00
1.2	1.23	2.01	55.46	45.03	3.27	2.82	50.70
1.4	1.19	2.02	54.64	45.76	3.27	2.84	50.50
1.6	1.16	2.03	53.93	46.32	3.26	2.85	50.40
1.8	1.14	2.03	53.48	46.88	3.25	2.87	50.40
2.0	1.12	2.04	52.94	47.21	3.25	2.88	50.20
2.5	1.09	2.05	52.08	47.91	3.23	2.91	50.10
3	1.07	2.05	51.62	48.46	3.20	2.93	50.10
4	1.04	2.06	50.93	48.98	3.17	2.96	49.90
5	1.03	2.06	50.64	49.35	3.15	2.98	49.90
10	1.00	2.07	50.06	49.89	3.10	3.02	49.80

Table 5-3: Design parameters for a microstrip coupler on a substrate with ε_r of 10. Data are derived from the analysis in Section 5.6. Z_0 is the characteristic impedance of an individual microstrip line with a normalized width, u. For $Z_{0S} = 50\ \Omega$, $w/h = 0.954$, from Table 3-3.

$\varepsilon_r = 10$ (Alumina), $Z_{0S} = 50\ \Omega$							
g	Z_{0e}/Z_{0o}	u	Z_{0e} (Ω)	Z_{0o} (Ω)	ε_{ee}	ε_{eo}	Z_0 (Ω)
0.1	2.72	0.65	82.26	30.25	6.95	5.59	59.40
0.2	2.18	0.75	73.90	33.82	7.06	5.64	55.90
0.3	1.91	0.81	69.06	36.10	7.13	5.69	54.00
0.4	1.74	0.84	66.19	37.96	7.17	5.73	53.10
0.5	1.62	0.87	63.66	39.29	7.20	5.77	52.20
0.6	1.53	0.89	61.79	40.42	7.22	5.81	51.70
0.7	1.46	0.90	60.45	41.47	7.23	5.85	51.40
0.8	1.40	0.91	59.25	42.32	7.23	5.88	51.10
0.9	1.35	0.92	58.17	43.01	7.24	5.92	50.90
1.0	1.31	0.93	57.19	43.57	7.24	5.95	50.60
1.2	1.25	0.94	55.78	44.59	7.23	6.01	50.30
1.4	1.21	0.94	54.90	45.55	7.21	6.06	50.30
1.6	1.17	0.94	54.19	46.30	7.19	6.11	50.30
1.8	1.14	0.95	53.34	46.66	7.17	6.16	50.10
2.0	1.12	0.95	52.87	47.14	7.14	6.20	50.10
2.5	1.09	0.95	52.05	47.97	7.08	6.29	50.10
3	1.06	0.95	51.54	48.50	7.02	6.36	50.10
4	1.04	0.95	50.97	49.08	6.92	6.46	50.10
5	1.03	0.95	50.69	49.39	6.85	6.53	50.10
10	1.03	0.95	50.26	49.94	6.73	6.62	50.10

EXAMPLE 5.7 Physical Design of a 10 dB Microstrip Coupler

Design a microstrip directional coupler with the following specifications:

Transmission line technology	Microstrip	
Coupling coefficient	C	= 10 dB
Microstrip characteristic impedance	Z_0	= 50 Ω
Substrate permittivity	ε_r	= 10.0
Substrate thickness	h	= 1 mm
System center frequency (midband for the coupler)	f_0	= 5 GHz

The cross-sectional dimensions that must be determined are the strip width, w, and the strip separation, s, as shown in Figure 5-18. The procedure is to first determine the coupling factor:

$$C = 10^{(C|_{\text{dB}}/20)} = 10^{(10/20)} = 3.162. \tag{5.154}$$

The ratio of the even- and odd-mode impedances required to achieve the desired coupling is derived from Equation (5.153):

$$Z_{0e}/Z_{0o} = \frac{C+1}{C-1} = \frac{3.162+1}{3.162-1} = 1.925. \tag{5.155}$$

Solution:

The problem now is to determine the physical geometry (i.e., the line widths and spacing). The data in Table 5-3 apply here (as $\varepsilon_r = 10$), enabling the normalized gap, $g = s/h$, and normalized line width, $u = w/h$, to be determined for a specified impedance ratio, Z_{0e}/Z_{0o}. The table does not contain a line for $Z_{0e}/Z_{0o} = 1.925$ and so the table must be interpolated (e.g. using linear or bilinear interpolation as described in Appendix 1.A.12). The line for $Z_{0e}/Z_{0o} = 2.15$ has $g = 0.2$, and the line for $Z_{0e}/Z_{0o} = 1.90$ has $g = 0.3$. So for $Z_{0e}/Z_{0o} = 1.925$,

$$g = \left(\frac{0.3-0.2}{1.9-2.15}\right) \cdot (1.925 - 2.15) + 0.2 = 0.290, \tag{5.156}$$

thus $s = g \cdot h = 0.290 \text{ mm}.$ (5.157)

The value of u must also be interpolated from Table 5-3 and $u = 0.805$ is obtained; thus

$$w = u \cdot h = 0.805 \text{ mm}. \tag{5.158}$$

The coupler should be one-quarter wavelength long, so the effective relative permittivity of the even and odd modes is required. From Table 5-3, the interpolated values are

$$\varepsilon_{ee} = 7.124 \quad \text{and} \quad \varepsilon_{eo} = 5.686. \tag{5.159}$$

These effective permittivities are different, so determination of the optimum length of the coupler is not straightforward. The only choice is to use the average of the permittivities:

$$\varepsilon_{e,\text{avg}} = (\varepsilon_{ee} + \varepsilon_{eo})/2 = 6.405. \tag{5.160}$$

Thus the average wavelength is $\lambda_g = \dfrac{c}{f\sqrt{\varepsilon_{e,\text{avg}}}} = \dfrac{3 \cdot 10^8}{5 \cdot 10^9 \sqrt{6.405}} = 2.37 \text{ cm}$ (5.161)

and the length of the coupler is $L = \lambda_g/4 = 5.93 \text{ mm}.$ (5.162)

Finally, the widths of the feed lines must be determined. The system impedance is 50 Ω and, from Table 3-3, the width, w', is found to be 0.954 mm. The final layout of the coupler is shown in Figure 5-19. The realization of a microstrip directional coupler as a laboratory component is shown in Figure 5-20.

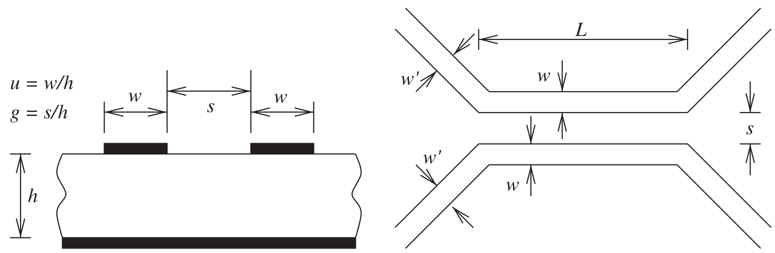

(a) Cross section (b) Layout

Figure 5-18: Dimensions to be determined in the physical design of a directional coupler.

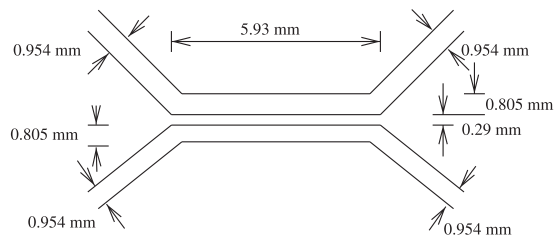

Figure 5-19: Final coupler layout for Example 5.7.

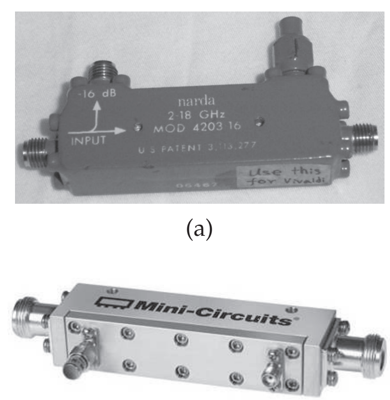

(a)

(b)

Figure 5-20: Connectorized directional couplers: (a) a microstrip directional coupler with SMA connectors connected to internal microstrip lines, the top right-hand connector has a 50 Ω termination; (b) a 250 W, 0.9–9 GHz coupler with N-type connectors on the through line and an SMA connector on the coupled port, insertion loss is less than 0.1 dB. Copyright 2012 Scientific Components Corporation d/b/a Mini-Circuits, used with permission [7].

EM analysis is often used to refine this synthesized coupler. There are two main uncertainties in the design. One is the uncertainty in the length of the coupler (due to the different even- and odd-mode effective permittivities). The other uncertainty is that the coupled-line equations come from low-frequency analysis—EM analysis will capture the frequency-dependent effects. However, only minor iteration would normally be required.

5.8.4 The Lange Coupler

A directional coupler comprised of two parallel microstrip lines cannot achieve a coupling of 3 dB, which corresponds to splitting the power of a traveling wave into two equal components. Lange [8] introduced a coupler, now known as the Lange coupler, in 1969. The Lange coupler (see Figure 5-21) has a coupling factor of around 3 dB. In this design, true quadrature coupling over an octave bandwidth is realized as a consequence of the interdigital coupling section, which also compensates for the differences of the even- and odd-mode phase velocities over the wide frequency range. Note the use of the center bond wires—this was the key invention. The bonding wires should look, electrically, as close as possible to a short-

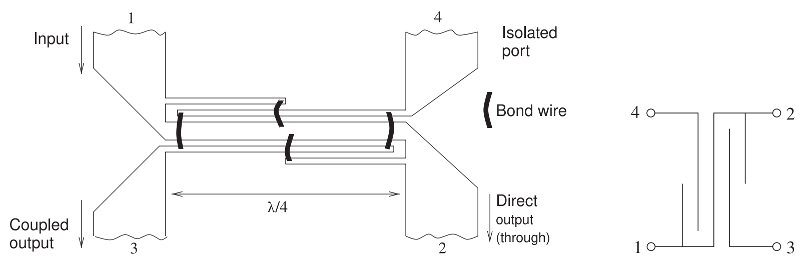

(a) Microstrip layout (b) Circuit symbol

Figure 5-21: A four-finger Lange coupler.

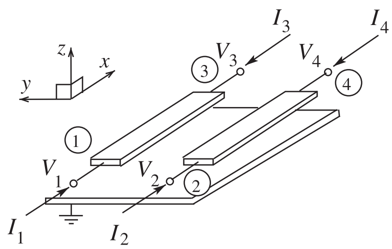

Figure 5-22: Coupled microstrip lines with total voltage and current phasors at the four terminals.

circuit. This means that their lengths, l_s, must be kept as short as possible: $l_s \ll \lambda_{gm}/4$, where λ_{gm} is the midband wavelength. In semiconductor technologies, these bond wires are replaced by air bridges, and in structures with two or more metal layers the wirebonds are replaced by vias to another metal layer and a short connection on the second metal layer. In some designs, six coupling fingers are used instead of the four shown in Figure 5-21. Note that the input-to-direct-output link meanders through the structure and this DC connection identifies the through connection.

The physical length of the coupler is approximately one-quarter wavelength long at the center frequency of the coupling band. As with many distributed components, this element was invented using intuition and empirical iterations. Since then, analytic design formulas have been developed to enable synthesis of the electrical parameters of the coupler (see [5]). The synthesis is based on even- and odd-mode impedances analogous to those developed in Section 5.8 for a coupler comprised of coupled microstrip lines. Synthesis leads to a design that is close to ideal, and subsequent modeling in an EM simulator can be used to obtain an optimized design accounting for frequency-dependent and parasitic effects.

5.9 Models of Parallel Coupled Lines

5.9.1 Chain Matrix Model of Coupled Lines

The chain matrix of a pair of coupled lines is the multiport version of the two-port $ABCD$ parameters and relates the input currents and voltages at one end of a pair of coupled lines to the voltages and currents at the other end. The chain matrix is derived here following the development in [9]. The terminal characteristics of the coupled lines shown in Figure 5-22 can be expressed in terms of the even and odd modes. For the even mode

$$\begin{bmatrix} \frac{1}{2}(V_1+V_2) \\ \frac{1}{2}(I_1+I_2) \end{bmatrix} = \begin{bmatrix} \cos\theta_e & \jmath X_{0e}\sin\theta_e \\ \jmath Y_{0e}\sin\theta_e & \cos\theta_e \end{bmatrix} \begin{bmatrix} \frac{1}{2}(V_3+V_4) \\ \frac{1}{2}(I_3+I_4) \end{bmatrix} \tag{5.163}$$

and for the odd mode

$$\begin{bmatrix} \frac{1}{2}(V_1 - V_2) \\ \frac{1}{2}(I_1 - I_2) \end{bmatrix} = \begin{bmatrix} \cos\theta_o & \jmath X_{0o}\sin\theta_0 \\ \jmath Y_{0o}\sin\theta_o & \cos\theta_o \end{bmatrix} \begin{bmatrix} \frac{1}{2}(V_3 - V_4) \\ -\frac{1}{2}(I_3 - I_4) \end{bmatrix}, \tag{5.164}$$

where $Y_{0e} = 1/Z_{0e}$ is the even-mode characteristic admittance and $Y_{0o} = 1/Z_{0o}$ is the characteristic admittance of the odd mode. Also, θ_e is the electrical length of the lines for the even mode, and θ_o is the odd-mode electrical length of the lines. Grouping Equations (5.163) and (5.164),

$$\begin{bmatrix} V_1 \\ V_2 \\ I_1 \\ I_2 \end{bmatrix} = \left[\begin{array}{cc|cc} a_{11} & a_{12} & b_{11} & b_{12} \\ a_{21} & a_{22} & b_{21} & b_{22} \\ \hline c_{11} & c_{12} & d_{11} & d_{12} \\ c_{21} & c_{22} & d_{21} & d_{22} \end{array}\right] \begin{bmatrix} V_3 \\ V_4 \\ -I_3 \\ -I_4 \end{bmatrix}, \tag{5.165}$$

where
$$a_{11} = a_{22} = d_{11} = d_{22} = \tfrac{1}{2}(\cos\theta_e + \cos\theta_o) \tag{5.166}$$
$$a_{12} = a_{21} = d_{12} = d_{21} = \tfrac{1}{2}(\cos\theta_e - \cos\theta_o) \tag{5.167}$$
$$b_{11} = b_{22} = \jmath\tfrac{1}{2}(Z_{0e}\sin\theta_e + Z_{0o}\sin\theta_o) \tag{5.168}$$
$$b_{12} = b_{21} = \jmath\tfrac{1}{2}(Z_{0e}\sin\theta_e - Z_{0o}\sin\theta_o) \tag{5.169}$$
$$c_{11} = c_{22} = \jmath\tfrac{1}{2}(Y_{0e}\sin\theta_e + Y_{0o}\sin\theta_o) \tag{5.170}$$
$$c_{12} = c_{21} = \jmath\tfrac{1}{2}(Y_{0e}\sin\theta_e - Y_{0o}\sin\theta_o). \tag{5.171}$$

Similarly the admittance equation for a pair of coupled lines is derived as

$$\begin{bmatrix} V_1 \\ V_2 \\ V_3 \\ V_4 \end{bmatrix} = \begin{bmatrix} y_{11} & y_{12} & y_{13} & y_{14} \\ y_{21} & y_{22} & y_{23} & y_{24} \\ y_{31} & y_{32} & y_{33} & y_{34} \\ y_{41} & y_{42} & y_{43} & y_{44} \end{bmatrix} \begin{bmatrix} I_1 \\ I_2 \\ I_3 \\ I_4 \end{bmatrix}, \tag{5.172}$$

where
$$y_{11} = y_{22} = y_{33} = y_{44} = -\jmath\tfrac{1}{2}(Y_{0e}\cot\theta_e + Y_{0o}\cot\theta_o) \tag{5.173}$$
$$y_{12} = y_{21} = y_{34} = y_{43} = -\jmath\tfrac{1}{2}(Y_{0e}\cot\theta_e - Y_{0o}\cot\theta_o) \tag{5.174}$$
$$y_{13} = y_{31} = y_{24} = y_{42} = \jmath\tfrac{1}{2}(Y_{0e}\csc\theta_e + Y_{0o}\csc\theta_o) \tag{5.175}$$
$$y_{14} = y_{41} = y_{23} = y_{32} = \jmath\tfrac{1}{2}(Y_{0e}\csc\theta_e - Y_{0o}\csc\theta_o). \tag{5.176}$$

5.9.2 $ABCD$ Parameters of Coupled-Line Sections

The chain matrix of a pair of coupled lines, Equation (5.165), can be used to develop the $ABCD$ parameters of two-port coupled line networks [9]. Several networks that are commonly used in realizing filters and other microwave circuits are shown in Table 5-4 with

$$\begin{bmatrix} V_1 \\ I_1 \end{bmatrix} = \begin{bmatrix} A & B \\ C & D \end{bmatrix} \begin{bmatrix} V_2 \\ -I_2 \end{bmatrix}. \tag{5.177}$$

One approach to developing the physical layout of microwave circuits from the electrical design equates the $ABCD$ parameters of the coupled-line networks to the $ABCD$ of the synthesized lumped-element circuit.

5.9.3 Synthesis of Specific Coupled-Line Connections

The equivalence of $ABCD$ parameters can be used in microwave network synthesis to transform uncoupled transmission line structures into a

Table 5-4: $ABCD$ parameters of coupled-line sections. Usage described in [10–13].

(a) Open-circuited interdigital coupled-line section (bandpass/bandstop networks) 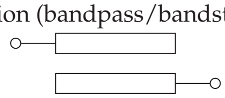 $A = D = (Z_{0e} \cot\theta_e + Z_{0o} \cot\theta_o)/\Delta$ $B = \frac{\jmath}{2\Delta}\left[Z_{0e}^2 + Z_{0o}^2 - 2Z_{0e}Z_{0o}\left(\cot\theta_e \cot\theta_o + \csc\theta_e \csc\theta_o\right)\right]$ $C = 2\jmath/\Delta$ $\Delta = Z_{0e}\csc\theta_e - Z_{0o}\csc\theta_o$ (5.178)	(b) Short-circuited interdigital coupled-line section (bandpass/bandstop networks) 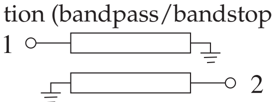 $A = D = (Y_{0e} \cot\theta_e + Y_{0o} \cot\theta_o)/\Delta$ $B = 2\jmath/\Delta$ $C = \frac{\jmath}{2\Delta}\left[Y_{0e}^2 + Y_{0o}^2 - 2Y_{0e}Y_{0o}\left(\cot\theta_e \cot\theta_o + \csc\theta_e \csc\theta_o\right)\right]$ $\Delta = Y_{0e}\csc\theta_e - Y_{0o}\csc\theta_o$ (5.179)
(c) Meander coupled-line section (lowpass networks) 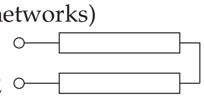 $A = D = (Z_{0e} \cot\theta_e - Z_{0o} \cot\theta_o)/\Delta$ $B = 2\jmath 2Z_{0e}Z_{0o}\cot\theta_e \tan\theta_o/\Delta$ $C = 2\jmath/\Delta$ $\Delta = Z_{0e}\cot\theta_e + Z_{0o}\tan\theta_o$ (5.180)	(d) Shorted symmetric coupled-line section (lowpass networks) 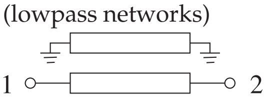 $A = D = (Y_{0e} \cot\theta_e + Y_{0o} \cot\theta_o)/\Delta$ $B = 2\jmath/\Delta$ $C = [\jmath/(2\Delta)]\left[Y_{0e}^2 + Y_{0o}^2 + 2Y_{0e}Y_{0o}\left(\csc\theta_e \csc\theta_o - \cot\theta_e \cot\theta_o\right)\right]$ $\Delta = Y_{0e}\csc\theta_e + Y_{0o}\csc\theta_o$ (5.181)
(e) Open-circuited combline coupled-line section (bandpass/bandstop networks) 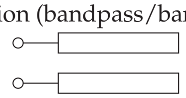 $A = D = (Z_{0e} \cot\theta_e + Z_{0o} \cot\theta_o)/\Delta$ $B = -\jmath 2Z_{0e}Z_{0o}\cot\theta_e \cot\theta_o/\Delta$ $C = 2\jmath/\Delta$ $\Delta = Z_{0e}\cot\theta_e - Z_{0o}\cot\theta_o$ (5.182)	(f) Short-circuited combline coupled-line section (bandpass/bandstop networks) 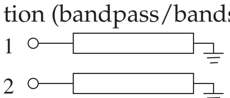 $A = D = (Y_{0o} \cot\theta_o + Y_{0e} \cot\theta_e)/\Delta$ $B = 2\jmath/\Delta$ $C = -\jmath 2Y_{0e}Y_{0o}\cot\theta_e \cot\theta_o/\Delta$ $\Delta = Y_{0o}\cot\theta_o - Y_{0e}\cot\theta_e$ (5.183)

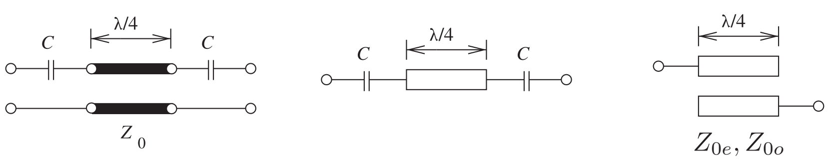

(a) (b) (c)

Figure 5-23: Coupled line equivalence: (a) a one-quarter wavelength long line with input and output series capacitance; (b) microstrip layout; and (c) equivalent coupled lines laid out in microstrip. The network in (a) is equivalent to the network in (c) if $Z_{0e} = (1/C + 2Z_0)$ and $Z_{0o} = Z_0$.

coupled-line section. As an example, consider the capacitively coupled one-quarter wavelength long line shown in both Figures 5-23(a) and 5-23(b). This configuration often occurs in filter design and an equivalent structure using coupled lines and not requiring discrete capacitors is shown in Figure 5-23(c). The equivalence is developed by equating the $ABCD$ parameters of the two

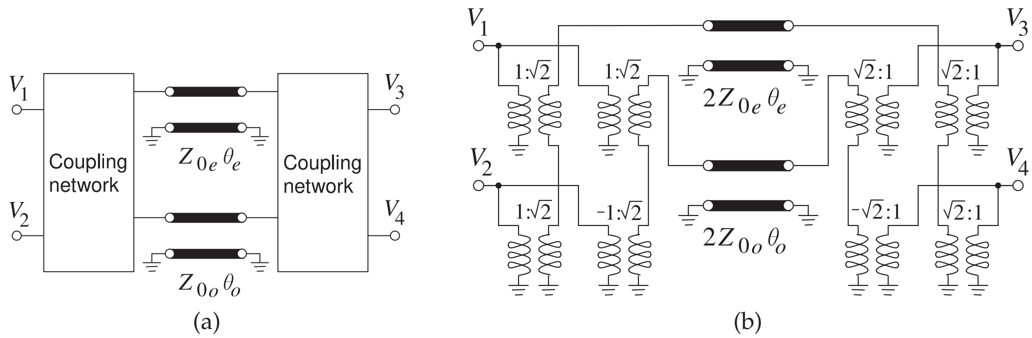

Figure 5-24: Models of a pair of coupled lines using even- and odd-mode lines: (a) with coupling network; and (b) with transformer-based coupling.

structures. The $ABCD$ matrix of the coupled-line network of Figure 5-23(c) is given in Table 5-4(a):

$$A = \frac{Z_{0e}\cot\theta_e + Z_{0o}\cot\theta_o}{Z_{0e}\csc\theta_e - Z_{0o}\csc\theta_o} = D \qquad C = \frac{2\jmath}{Z_{0e}\csc\theta_e - Z_{0o}\csc\theta_o}$$
$$B = \frac{\jmath}{2}\frac{Z_{0e}^2 + Z_{0o}^2 - 2Z_{0e}Z_{0o}\left(\cot\theta_e\cot\theta_o + \csc\theta_e\csc\theta_o\right)}{Z_{0e}\csc\theta_e - Z_{0o}\csc\theta_o}, \tag{5.184}$$

where Z_{0e} and Z_{0o} are the modal impedances, and θ_e and θ_o are the even- and odd-mode electrical lengths.

Developing the $ABCD$ parameters of the capacitively loaded one-quarter wavelength long line in Figure 5-23(a) and equating them with the $ABCD$ parameters in Equation (5.184) leads to an equivalence between the loaded line (Figure 5-23(b)) and the coupled line shown in Figure 5-23(c), where

$$Z_{0e} = (1/C + 2Z_0) \quad \text{and} \quad Z_{0o} = Z_0. \tag{5.185}$$

5.9.4 Model Using Even- and Odd-Mode Lines

The pair of coupled lines in Figure 5-22 can be modeled using even- and odd- mode transmission lines as shown in Figure 5-24(a). While the partitioning of the terminal voltages and currents of the coupled lines into even- and odd-mode components is simple to describe mathematically (e.g., the odd-mode voltage $V_o = \frac{1}{2}(V_1 - V_2)$), there is not a simple way to represent the partitioning in circuit form. Instead, in a circuit simulator the coupling network in Figure 5-24(a) is modeled using voltage-controlled current sources [14]. A circuit model that is more convenient to use in the analysis of a coupled line networks is shown in Figure 5-24(b). The equivalence of this network to a coupled line is demonstrated by showing that the chain matrix parameters of the circuit in Figure 5-24(b) are the same as those in Equations (5.165)–(5.171), see Example 5.8.

Coupled lines are an important element in many microwave circuits, including filters, matching networks, and biasing networks. Very often the circuit development leads to a particular topology that can be implemented using coupled-line networks. For example, the structure at the top in Figure 5-25(a) is known as an open-circuited interdigital section. The equivalent

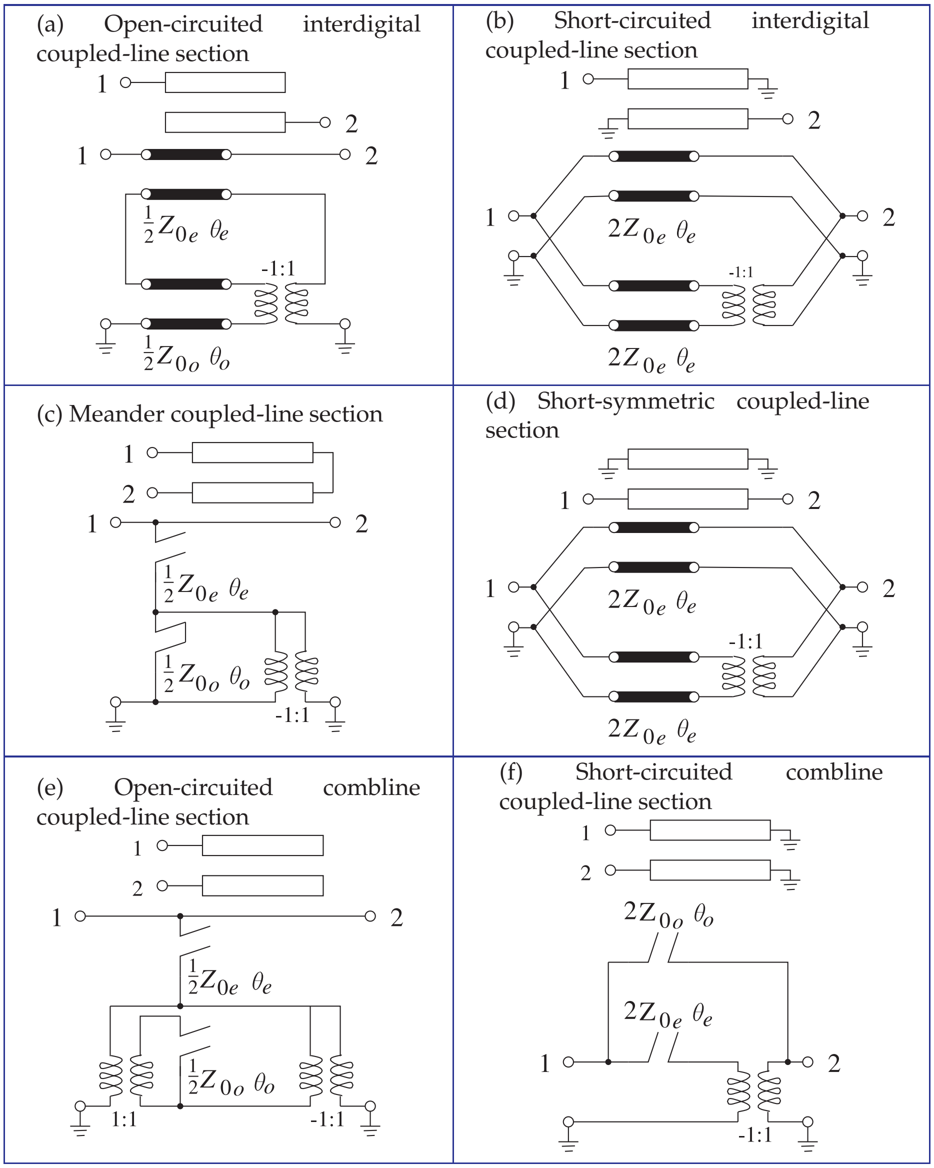

Figure 5-25: Coupled-line sections with models comprising individual transmission lines corresponsing to the even- and odd-modes.

circuit of this network, shown at the bottom in Figure 5-25(a), is derived from the coupled-line equivalent circuit shown in Figure 5-24(b).

EXAMPLE 5.8 Chain Matrix Parameters of Coupled Lines

Develop the chain matrix of the coupled-line model shown in Figure 5-24(b) and show that these are the chain matrix parameters of a coupled line.

Solution:

The coupled-line model is annotated with voltages and currents in Figure 5-26. Using Table 2-1 of [15], the even- and odd-mode lines have the following $ABCD$ parameters:

$$\begin{bmatrix} V_W \\ I_W \end{bmatrix} = \begin{bmatrix} \cos\theta_e & \jmath 2Z_e \sin\theta_e \\ \jmath\frac{1}{2}Y_e \sin\theta_e & \cos\theta_e \end{bmatrix} \begin{bmatrix} V_Y \\ I_Y \end{bmatrix} \tag{5.186}$$

and

$$\begin{bmatrix} V_X \\ I_X \end{bmatrix} = \begin{bmatrix} \cos\theta_o & \jmath 2Z_o \sin\theta_o \\ \jmath\frac{1}{2}Y_o \sin\theta_o & \cos\theta_o \end{bmatrix} \begin{bmatrix} V_Z \\ I_Z \end{bmatrix}. \tag{5.187}$$

While the $ABCD$ parameters of the transformers could be used, it is more convenient to write down the terminal characteristics of the transformers directly. First, the transformers on the right-hand side are described by

$$\begin{aligned} V_Y &= \tfrac{1}{\sqrt{2}}\,(V_3 + V_4)\,, \quad I_Y = \tfrac{1}{2\sqrt{2}}\,[(-I_3) + (-I_4)] \\ V_Z &= \tfrac{1}{\sqrt{2}}\,(V_3 - V_4)\,, \quad I_Z = \tfrac{1}{2\sqrt{2}}\,[(-I_3) - (-I_4)]\,. \end{aligned} \tag{5.188}$$

Combining Equations (5.186)–(5.188) yields

$$\begin{bmatrix} V_W \\ V_X \\ I_W \\ I_X \end{bmatrix} = \begin{bmatrix} \sqrt{2}\cos\theta_e & \sqrt{2}\cos\theta_e & \jmath\sqrt{2}Z_{0e}\sin\theta_e & \jmath\sqrt{2}Z_{0e}\sin\theta_e \\ \sqrt{2}\cos\theta_o & -\sqrt{2}\cos\theta_o & \jmath\sqrt{2}Z_{0o}\sin\theta_o & -\jmath\sqrt{2}Z_{0o}\sin\theta_o \\ \jmath\frac{1}{2\sqrt{2}}Y_{0e}\sin\theta_e & \jmath\frac{1}{2\sqrt{2}}Y_{0e}\sin\theta_e & \frac{1}{2\sqrt{2}}\cos\theta_e & \frac{1}{2\sqrt{2}}\cos\theta_e \\ \jmath\frac{1}{2\sqrt{2}}Y_{0o}\sin\theta_o & -\jmath\frac{1}{2\sqrt{2}}Y_{0o}\sin\theta_o & \frac{1}{2\sqrt{2}}\cos\theta_o & -\frac{1}{2\sqrt{2}}\cos\theta_o \end{bmatrix} \begin{bmatrix} V_3 \\ V_4 \\ -I_3 \\ -I_4 \end{bmatrix}. \tag{5.189}$$

The development is completed by using the voltage and current relations determined by the transformers on the left-hand side:

$$\begin{aligned} V_1 &= \tfrac{1}{2\sqrt{2}}\,(V_W + V_X)\,, \quad I_1 = \sqrt{2}\,(I_W + I_X) \\ V_2 &= \tfrac{1}{2\sqrt{2}}\,(V_W - V_X)\,, \quad I_2 = \sqrt{2}\,(I_W - I_X)\,. \end{aligned} \tag{5.190}$$

Combining Equations (5.189) and (5.190):

$$\begin{bmatrix} V_1 \\ V_2 \\ I_1 \\ I_2 \end{bmatrix} = \left[\begin{array}{cc|cc} a'_{11} & a'_{12} & b'_{11} & b'_{12} \\ a'_{21} & a'_{22} & b'_{21} & b'_{22} \\ \hline c'_{11} & c'_{12} & d'_{11} & d'_{12} \\ c'_{21} & c'_{22} & d'_{21} & d'_{22} \end{array}\right] \begin{bmatrix} V_3 \\ V_4 \\ -I_3 \\ -I_4 \end{bmatrix}, \tag{5.191}$$

where

$$\begin{aligned} &a'_{11} = a'_{22} = d'_{11} = d'_{22} = \tfrac{1}{2}(\cos\theta_e + \cos\theta_o) && a'_{12} = a'_{21} = d'_{12} = d'_{21} = \tfrac{1}{2}(\cos\theta_e - \cos\theta_o) \\ &b'_{11} = b'_{22} = \jmath\tfrac{1}{2}(Z_{0e}\sin\theta_e + Z_{0o}\sin\theta_o) && b'_{12} = b'_{21} = \jmath\tfrac{1}{2}(Z_{0e}\sin\theta_e - Z_{0o}\sin\theta_o) \\ &c'_{11} = c'_{22} = \jmath\tfrac{1}{2}(Y_{0e}\sin\theta_e + Y_{0o}\sin\theta_o) && c'_{12} = c'_{21} = \jmath\tfrac{1}{2}(Y_{0e}\sin\theta_e - Y_{0o}\sin\theta_o), \end{aligned}$$

which is identical to the chain matrix of the coupled transmission line, Equation (5.165). Thus Figure 5-24(b) is an accurate circuit model of a pair of coupled transmission lines.

5.9.5 Alternative Coupled-Line Model

The previous section developed a model of a pair of coupled lines and it was shown how the model related to various coupled-line sections. While $ABCD$ parameters can be used to equate two different implementations, it is useful to have a topology that can be visualized and used to guide synthesis.

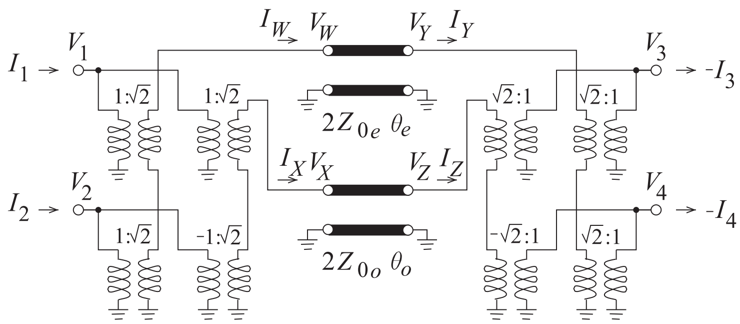

Figure 5-26: Annotated coupled-line model used in Example 5.4.

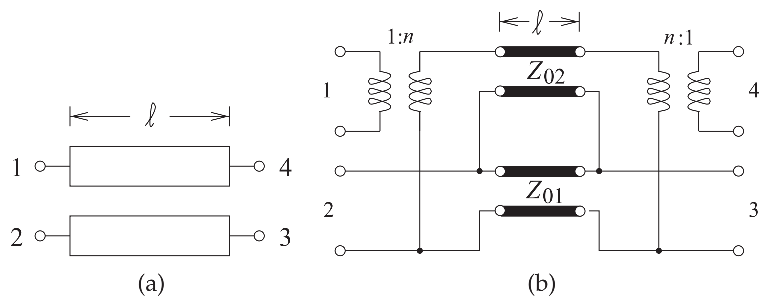

Figure 5-27: A pair of symmetrical coupled lines: (a) physical layout; and (b) its approximate equivalent circuit model in a form that appears in network synthesis. $n = (Z_{0e} + Z_{0o})/(Z_{0e} - Z_{0o})$.

The accurate form of the coupled-line model developed in the previous section does not often occur in network synthesis. (In synthesis, such as when designing a filter using coupled lines, a mathematical description can sometimes be converted into circuit form which includes transmission lines that are coupled.) An alternative but approximate model that has the same topology as many synthesized networks is shown in Figure 5-27(b).

A physical pair of coupled lines is shown in Figure 5-27(a) with even-mode characteristic impedance, Z_{0e}, and odd-mode impedance, Z_{0o}, with the coupling coefficient[6]

$$K = \frac{Z_{0e} - Z_{0o}}{Z_{0e} + Z_{0o}}. \tag{5.192}$$

The corresponding approximate equivalent network model of the coupled line in Figure 5-27(a) was developed by Malherbe [16] and is shown in Figure 5-27(b) with

$$Z_{01} = \frac{Z_{0S}}{\sqrt{1-K^2}} \tag{5.193}$$

$$Z_{02} = Z_{0S}\frac{\sqrt{1-K^2}}{K^2} \tag{5.194}$$

$$n = \frac{1}{K} = \frac{Z_{0e} + Z_{0o}}{Z_{0e} - Z_{0o}} \tag{5.195}$$

$$Z_{0S} = \sqrt{Z_{0e}Z_{0o}}. \tag{5.196}$$

The electrical length of the Z_{01} and Z_{02} lines is the electrical length of the coupled line. The reason this model is approximate is it assumes that the coupled lines are symmetrical (e.g., equal width for the microstrip lines) and uses a low-frequency capacitor-based development. Also a pair of coupled lines has two electrical lengths, the electrical length of the even mode and

[6] This is the inverse of the coupling factor, C used previously, see Equation (5.145). However using C introduces confusion since $ABCD$ parameters are often used in synthesis of coupled line networks. Note that here $K = 1/(\text{coupling factor})$, that is, $K = 1/C$.

the electrical length of the odd mode. So the best that can be done is to take the electrical lengths of the Z_{01} and Z_{02} lines as the average electrical lengths of the even and odd modes. Never-the-less this model is commonly used in developing the initial design of coupled-line networks that must then be followed by adjustment in a microwave circuit simulator.

5.9.6 Approximate Synthesis from the Coupled-Line Model

The electrical design of networks of coupled lines commonly leads to the parameters of the coupled-line model shown in Figure 5-27(b). From these the physical layout can be derived. That is, given $n = 1/K$, Z_{01}, and Z_{02}, the coupled-line parameters Z_{0S}, Z_{0e}, and Z_{0o} are found. Equations (5.193) and (5.194) lead to two equations for Z_{0S}:

$$Z_{0S,(5.197)} = Z_{01}\sqrt{1-K^2} \tag{5.197}$$

$$Z_{0S,(5.198)} = Z_{02}\frac{K^2}{\sqrt{1-K^2}}. \tag{5.198}$$

These could be different and this is a result of the model being approximate. If so, then the proper course forward is to use the geometric mean:

$$Z_{0S} = \sqrt{Z_{0S,(5.197)}Z_{0S,(5.198)}}. \tag{5.199}$$

Rearranging Equation (5.195),

$$\begin{aligned} 1+n = 1+\frac{Z_{0e}+Z_{0o}}{Z_{0e}-Z_{0o}} &= \frac{Z_{0e}-Z_{0o}+Z_{0e}+Z_{0o}}{Z_{0e}-Z_{0o}} = \frac{2Z_{0e}}{Z_{0e}-Z_{0o}} \\ 1-\frac{2}{n+1} = \frac{n-1}{n+1} = 1-\frac{Z_{0e}-Z_{0o}}{Z_{0e}} &= \frac{Z_{0o}-Z_{0e}+Z_{0e}}{Z_{0e}} = \frac{Z_{0o}}{Z_{0e}}. \end{aligned} \tag{5.200}$$

That is,

$$\frac{Z_{0e}}{Z_{0o}} = \frac{n+1}{n-1}. \tag{5.201}$$

Combining this with Equation (5.196),

$$Z_{0o} = Z_{0S}\sqrt{\frac{n-1}{n+1}} \quad \text{and} \quad Z_{0e} = \frac{Z_{0S}^2}{Z_{0o}}. \tag{5.202}$$

These equations can be used in physical synthesis. For example, if Z_{0S} is close to $50\ \Omega$ and the substrate is alumina, then the ratio Z_{0e}/Z_{0o} can be used to find the physical dimensions from Table 5-3. Otherwise the formulas described in Section 5.6 can be used iteratively.

The physical length of the coupled line is determined by using the geometric mean of the even- and odd-mode effective permittivities to convert from the electrical length (in degrees or wavelengths). This initial design is followed by adjustment in a microwave circuit simulator.

5.10 Differential and Common Modes

In working with RFICs it is convenient to use differential and common mode definitions, rather than odd and even mode definitions, as these directly relate to the differential circuits most commonly used in CMOS design. There are several reasons for this and one is that the most common type of amplifier with CMOS circuits is a differential amplifier where there are two input signal lines and two output signal lines and the actual signal is the differential signal which, in terms of voltage, is the difference of the two voltages on the lines. The situation is as shown in Figure 5-28(a) where there are two signal conductors and a ground plane (at 0 V). Here the differential voltage is $V_d = (V_1 - V_2)$. The common mode voltage is $V_c = \frac{1}{2}(V_1 + V_2)$ which will normally consist of a DC voltage and a usually small, and ideally zero, common mode signal which is the non-DC part of V_c. Most CMOS circuits are designed so that the DC component of $V_d = 0$. It is a quirk of history that microwave engineering and thus EM analysis used even- and odd-mode signals whose definitions differ by a factor of two from the definitions of common- and differential-mode signals. This section relates the two groups of signals and parameters for the common/differential mode group and the even/odd mode group.

The differential- and common-mode parameters of coupled lines can be derived from the odd- and even-mode parameters. The difference is in the definition of the voltage and currents in the modes as shown in Figure 5-28. The even mode is defined with $V_1 = V_2 = V_e$ and $I_1 = I_2 = I_e$, while for the common mode $V_1 = V_2 = V_c$ and $I_1 + I_2 = I_c$. Thus, in terms of the even-mode characteristic impedance, Z_{0e}, the common-mode characteristic impedance is

$$Z_{0c} = \tfrac{1}{2} Z_{0e}. \tag{5.203}$$

The odd mode is defined with $V_1 = -V_2 = V_o$ and $I_1 = -I_2 = I_o$, while for the differential mode $V_1 - V_2 = V_d$ and $I_1 = -I_2 = I_d$. Thus, in terms of the odd-mode characteristic impedance, Z_{0o}, the differential-mode characteristic impedance is

$$Z_{0d} = 2Z_{0o}. \tag{5.204}$$

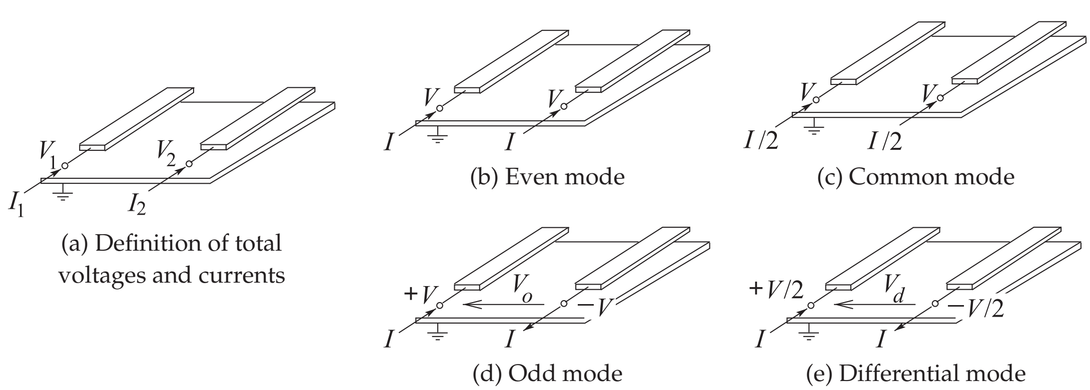

Figure 5-28: Definition of coupled-line modes.

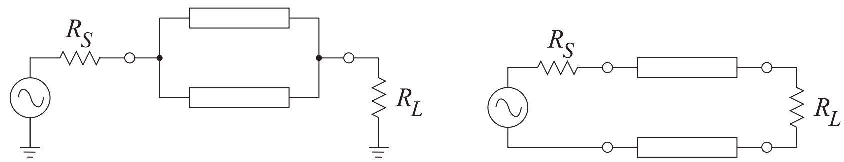

(a) Common mode (b) Differential mode

Figure 5-29: Driving configurations.

Other parameters remain unchanged. That is, the propagation constant, phase and group velocities, and wavelengths are the same for common and even modes, as they are for the differential and odd modes.

The driving and termination configurations for differential and common mode signals are shown in Figure 5-29. The reflectionless (i.e. matched) termination of coupled lines used in common mode is

$$R_L = Z_{0c} = \tfrac{1}{2} Z_{0e}, \tag{5.205}$$

as in Figure 5-29(a). The reflectionless termination of a differential line is

$$R_L = Z_{0d} = 2Z_{0o}, \tag{5.206}$$

as shown in Figure 5-29(b).

EXAMPLE 5.9 Common and Differential Mode Reflections at the End of Coupled Lines

A pair of coupled lines with common- and differential-mode characteristic impedances Z_{cC} and Z_{0d} respectively is loaded as shown in Figure 5-14(a) where the load has the two-port y-parameter matrix, $\boldsymbol{Y}$. Find the common and differential-mode reflections. This example parallels Example 5.3 where even and odd modes were considered.

Solution:

The analysis begins by writing out the expressions relating the traveling-wave and total voltages and currents at the termination.

$$\begin{array}{llll}
V_c = \frac{1}{2}(V_1 + V_2) & V_d = (V_1 - V_2) & I_c = (I_1 + I_2) & I_d = \frac{1}{2}(I_1 - I_2) \\
V_1 = (V_1^+ + V_1^-) & V_2 = (V_2^+ + V_2^-) & I_1 = (I_1^+ + I_1^-) & I_2 = (I_2^+ + I_2^-) \\
V_1^+ = (V_c^+ + \frac{1}{2}V_d^+) & V_2^+ = (V_c^+ - \frac{1}{2}V_d^+) & I_1^+ = (\frac{1}{2}I_c^+ + I_d^+) & I_2^+ = (\frac{1}{2}I_c^- - I_d^+) \\
V_1^- = (V_c^- + \frac{1}{2}V_d^-) & V_2^- = (V_c^- - \frac{1}{2}V_d^-) & I_1^- = (\frac{1}{2}I_c^- + I_d^-) & I_2^- = (\frac{1}{2}I_c^- - I_d^-) \\
I_c^+ = V_c^+/Z_{0c} & I_c^- = -V_c^-/Z_{0c} & I_d^+ = V_d^+/Z_{0c} & I_d^- = -V_d^-/Z_{0d}
\end{array}$$

At the termination

$$\begin{bmatrix} I_1 \\ I_2 \end{bmatrix} = \begin{bmatrix} \frac{1}{2}I_c^+ + I_d^+ + \frac{1}{2}I_c^- + I_d^- \\ \frac{1}{2}I_c^+ - I_d^+ + \frac{1}{2}I_c^- - I_d^- \end{bmatrix} = \boldsymbol{Y} \begin{bmatrix} V_1 \\ V_2 \end{bmatrix} = \begin{bmatrix} y_{11} & y_{12} \\ y_{21} & y_{22} \end{bmatrix} \begin{bmatrix} V_1 \\ V_2 \end{bmatrix}$$

$$\begin{bmatrix} \frac{1}{2}(V_c^+ - V_c^-)/Z_{0c} + (V_d^+ - V_d^-)/Z_{0d} \\ \frac{1}{2}(V_c^+ - V_c^-)/Z_{0c} - (V_d^+ - V_d^-)/Z_{0d} \end{bmatrix} = \begin{bmatrix} y_{11} & y_{12} \\ y_{21} & y_{22} \end{bmatrix} \begin{bmatrix} V_c^+ + \frac{1}{2}V_d^+ + V_c^- + \frac{1}{2}V_d^- \\ V_c^+ - \frac{1}{2}V_d^+ + V_c^- - \frac{1}{2}V_d^- \end{bmatrix} \tag{5.207}$$

The reflected even and odd modes have contributions from incident common and differential modes:

$$V_c^- = \Gamma_{Lc} V_e^+ + C_{cd} V_d^+ \quad \text{and} \quad V_d^- = \Gamma_{Ld} V_d^+ + C_{dc} V_c^+ \tag{5.208}$$

where Γ_{ce} and Γ_{Ld} are common- and differential-mode reflection coefficients, C_{dc} and C_{cd} describe coupling, and

$$\Gamma_{Lc} = \left.\frac{V_c^-}{V_c^+}\right|_{V_d^+=0}, \Gamma_{Ld} = \left.\frac{V_d^-}{V_d^+}\right|_{V_c^+=0}, C_{cd} = \left.\frac{V_c^-}{V_d^+}\right|_{V_c^+=0} \text{ and } C_{dc} = \left.\frac{V_d^-}{V_c^+}\right|_{V_d^+=0}. \tag{5.209}$$

Γ_{Lc} and C_{ed} are obtained by expanding Equation (5.207) with $V_d^+ = 0$

$$(V_c^+ - V_c^-)/Z_{0c} - 2V_d^-/Z_{0d} = y_{11}\left(2V_c^+ + 2V_c^- + V_d^-\right) + y_{12}\left(2V_c^+ + 2V_c^- - V_d^-\right)$$

$$\text{i.e. } \frac{V_c^-}{Z_{0c}}\left(1 + 2y_{11}Z_{0c} + 2y_{12}Z_{0c}\right) = \frac{V_c^+}{Z_{0c}}\left(1 - 2y_{11}Z_{0c} - 2y_{12}Z_{0c}\right) - \frac{V_d^-}{Z_{0d}}\left(2 + y_{11}Z_{0d} - y_{12}Z_{0d}\right) \tag{5.210}$$

$$(V_c^+ - V_c^-)/Z_{0c} + 2V_d^-)/Z_{0d} = y_{21}\left(2V_c^+ + 2V_c^- + V_d^-\right) + y_{22}\left(2V_c^+ + 2V_c^- - V_d^-\right)$$

$$\text{i.e. } \frac{V_d^-}{Z_{0d}}(-2 + y_{21}Z_{0d} - y_{22}Z_{0d}) = \frac{V_c^+}{Z_{0c}}(1 - 2y_{21}Z_{0c} - 2y_{22}Z_{0c}) + \frac{V_c^-}{Z_{0c}}(-1 - 2y_{21}Z_{0c} - 2y_{22}Z_{0c}) \tag{5.211}$$

Γ_{Lc} is obtained by eliminating V_d^- by multiplying Equation (5.211) by $(2 + y_{11}Z_{0d} - y_{12}Z_{0d})$ and subtracting it from Equation (5.210) multiplied by $(-2 + y_{21}Z_{0d} - y_{22}Z_{0d})$:

$$V_c^- \frac{a}{Z_{0d}} = V_c^+ \frac{b}{Z_{0c}}\bigg|_{V_d^+=0}. \quad \text{Thus} \quad \Gamma_{Le} = \frac{b}{a} \tag{5.212}$$

where

$$\begin{aligned} a &= (1 + 2y_{11}Z_{0c} + 2y_{12}Z_{0c})(-2 + y_{21}Z_{0d} - y_{22}Z_{0d}) - (1 + 2y_{21}Z_{0c} + 2y_{22}Z_{0c})(2 + y_{11}Z_{0d} - y_{12}Z_{0d}) \\ &= -2 - Z_{0d}Y_\Delta - 4Z_{0c}Y_\Sigma - 4Z_{0c}Z_{0d}Y_D \end{aligned} \tag{5.213}$$

$$\begin{aligned} b &= (1 - 2y_{11}Z_{0c} - 2y_{12}Z_{0c})(-2 + y_{21}Z_{0d} - y_{22}Z_{0d}) - (1 - 2y_{21}Z_{0c} - 2y_{22}Z_{0c})(2 + y_{11}Z_{0d} - y_{12}Z_{0d}) \\ &= -4 - Z_{0d}Y_\Delta + 4Z_{0c}Y_\Sigma + 4Z_{0c}Z_{0d}Y_D \end{aligned} \tag{5.214}$$

$$Y_\Sigma = (y_{11} + y_{12} + y_{21} + y_{22}), Y_\Delta = (y_{11} - y_{12} - y_{21} + y_{22}), \text{ and } Y_D = (y_{11}y_{22} - y_{12}y_{21}) \tag{5.215}$$

$$\Gamma_{Lc} = \frac{b}{a} = \frac{4 + Z_{0d}Y_\Delta - 4Z_{0c}Y_\Sigma - 4Z_{0c}Z_{0d}Y_D}{4 + Z_{0d}Y_\Delta + 4Z_{0c}Y_\Sigma + 4Z_{0c}Z_{0d}Y_D} \tag{5.216}$$

Compare this to the even-mode reflection coefficient, Γ_{Le}, found in Example 5.3. Substituting $Z_{0d} = 2Z_{0o}$ and $Z_{0c} = \frac{1}{2}Z_{0e}$ in Equation (5.216)

$$\Gamma_{Lc} = \frac{4 + 2Z_{0o}Y_\Delta - 2Z_{0e}Y_\Sigma - 4Z_{0c}Z_{0d}Y_D}{4 + 2Z_{0o}Y_\Delta + 4Z_{0c}Y_\Sigma + 4Z_{0c}Z_{0d}Y_D} = \Gamma_{Le}. \tag{5.217}$$

Find C_{cd} by expanding Equation (5.207) with $V_c^+ = 0$:

$$-V_c^-/Z_{0c} + (2V_d^+ - 2V_d^-)/Z_{0d} = y_{11}\left(V_d^+ + 2V_c^- + V_d^-\right) + y_{12}\left(-V_d^+ + 2V_c^- - V_d^-\right)$$

$$\text{i.e. } \frac{V_c^-}{Z_{0c}}\left(1 + 2y_{11}Z_{0c} + 2y_{12}Z_{0c}\right) = \frac{V_d^+}{Z_{0d}}\left(2 - y_{11}Z_{0d} + y_{12}Z_{0d}\right) - \frac{V_d^-}{Z_{0d}}\left(2 + y_{11}Z_{0d} - y_{12}Z_{0d}\right) \tag{5.218}$$

$$-V_c^-/Z_{0c} - (2V_d^+ - 2V_d^-)/Z_{0d} = y_{21}\left(+V_d^+ + 2V_c^- + V_d^-\right) + y_{22}\left(-V_d^+ + 2V_c^- - V_d^-\right)$$

$$\text{i.e. } \frac{V_d^-}{Z_{0d}}\left(-2 + y_{21}Z_{0d} - y_{22}Z_{0d}\right) = -\frac{V_d^+}{Z_{0d}}\left(2 + y_{21}Z_{0d} - y_{22}Z_{0d}\right) - \frac{V_c^-}{Z_{0c}}\left(1 + 2y_{21}Z_{0c} + 2y_{22}Z_{0c}\right) \tag{5.219}$$

To eliminate V_d^- multiply Equation (5.219) by $(2 + y_{11}Z_{0d} - y_{12}Z_{0d})$ and subtract it from Equation (5.218) multiplied by $(-2 + y_{21}Z_{0d} - y_{22}Z_{0d})$:

$$\frac{V_c^-}{Z_{0c}}a = \frac{V_d^+}{Z_{0d}}c \quad \text{so that} \quad C_{eo} = \frac{c}{a}\frac{Z_{0c}}{Z_{0d}} \tag{5.220}$$

where a is as in Equation (5.213) and

$$c = (2 - y_{11}Z_{0d} + y_{12}Z_{0d})(-2 + y_{21}Z_{0d} - y_{22}Z_{0d}) + (2 + y_{21}Z_{0d} - y_{22}Z_{0d})(2 + y_{11}Z_{0d} - y_{12}Z_{0d})$$
$$= -2Z_{0d}Y_E \quad \text{where} \quad Y_E = (y_{11} - y_{12} + y_{21} - y_{22}). \tag{5.221}$$

$$C_{cd} = \frac{4Z_{0c}Y_E}{4 + Z_{0d}Y_\Delta + 4Z_{0c}Y_\Sigma + 4Z_{0c}Z_{0d}Y_D} = C_{eo} \tag{5.222}$$

(which can be verified using the substitutions $Z_{0d} = 2Z_{0o}$ and $Z_{0c} = \frac{1}{2}Z_{0e}$).

Similarly,

$$\Gamma_{Ld} = \frac{2 + Z_{0d}(y_{12} + y_{21}) - 2Z_{0c}Z_{0d}Y_D}{2 + Z_{0d}Y_\Delta + 4Z_{0c}Y_\Sigma + 2Z_{0c}Z_{0d}Y_D} = \Gamma_{Lo} \tag{5.223}$$

$$\text{and} \quad C_{dc} = \frac{-4Z_{0c}Y_E}{4 + Z_{0d}Y_\Delta + 4Z_{0c}Y_\Sigma + 4Z_{0c}Z_{0d}Y_D} = C_{cd} = C_{oe}, \text{ and} \tag{5.224}$$

5.11 Common Impedance Coupling

So far coupling has been discussed in terms of the EM fields shared by two transmission lines. This is not the only way coupling of signals occurs. Sharing of a return path results in coupling, often called common impedance coupling, as there is a circuit element common to two or more transmission lines. The simplest situation is a shared impedance rather than a shared transmission line return, so that the return current attributed to one interconnect induces a voltage across the common impedance element. This signal then appears as though it is on the victim line. The common impedance could be the inductance or resistance of the ground conductor in the case of microstrip lines. In general, however, common impedance coupling will occur whenever the current return path is common.

5.12 Summary

Coupling from one transmission line to a nearby neighbor may often be undesirable. However, the coupling can be controlled and coupled lines have become an important circuit component in distributed microwave circuits. One example is a directional coupler, which is little more than a pair of coupled lines, and this device forms the special function of separating forward- and backward-traveling waves. Another example of the application of coupled lines is their use in microwave filters. Bandpass filters are essentially coupled resonators. In a filter that uses coupled lines, each individual line becomes a resonator and the coupling of the resonators is controlled by how far they are spaced.

The analysis and circuit model of a pair of coupled lines is based on describing the voltages and currents on the lines as the linear combination of an even mode and an odd mode. Each of these modes will have forward- and backward-traveling wave components. Separating the signals on a coupled-line pair into even and odd modes facilitates extraction of the coupled-line parameters from simulation and measurement. It also enables a model of the coupled line to be developed that consists of individual lines that are coupled by transformers.

With the differential circuits used with RFICs it is more convenient to consider the signals on a pair of coupled lines as comprising common and differential modes. These can be directly related to even and odd modes and the difference comes down to definitions of average voltage (i.e., the common- and even-mode voltages) and the definition of the difference voltage (i.e., the differential- and odd-mode voltages). There is a similar difference for the currents.

The suite of microwave elements that exploit distributed effects available to a microwave designer is surprisingly large. Coupled lines comprise a large proportion of these elements. This chapter concludes with an example of the broadband response of a pair of coupled microstrip lines.

EXAMPLE 5.10 Shorted Coupled Lines

AWR Design Environment Project File: RFDesign_Coupled_Shorted_Microstrip_Lines.emp

In this example a pair of shorted coupled microstrip lines are examined using EM analysis. The layout of the coupled lines is shown in Figure 5-30. The box used in simulation has electric side and top walls. The bottom of the box (below the strips) is an electric wall and forms the ground plane. The ground plane is specified as gold and the finite conductivity of gold is used for the strips and the ground plane. The coupled lines here are arranged as a two-port structure. Scattering (S) parameters are used to describe the characteristics of microwave structures. The transmission coefficient is S_{21}, and for a matched structure S_{11} is the reflection coefficient. The coupled-line structure is symmetrical, as the widths of the strips are the same so that $S_{11} = S_{22}$ and $S_{12} = S_{21}$. Each microstrip line on its own was designed to have a characteristic impedance of 50 Ω.

The calculated two-port S parameters are plotted in Figure 5-31. The loss of 0 dB corresponds to an S parameter absolute value of 1. Large S_{21} responses are centered at 1.5 GHz, 7.5 GHz, and 13 GHz and are shaped as bandpass filter responses. This suggests that coupled-line sections could be used as the basis of microwave bandpass filters. The passband frequencies are related to the lengths of the lines. The effective dielectric constant for one of the microstrip lines is 6.5 (from Table 3-2) and so at 1.5 GHz the 1 cm line length is $\lambda/8$ long, at 7.5 GHz it is $5\lambda/8$ long, and at 13 GHz it is $9\lambda/8$ long. The round-trip lengths are $\lambda/4$, $5\lambda/4$, and $9\lambda/4$ long at the respective frequencies. Thus the round-trip lengths are separated by λ and so the addition of half-wavelength sections of lossless line has no impact on the reflection and transmitted response amplitudes.

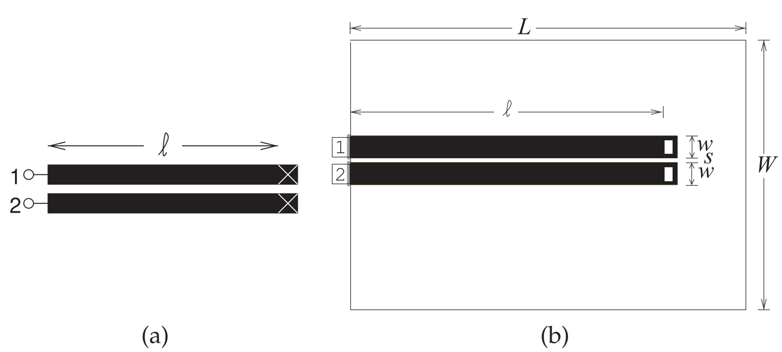

Figure 5-30: Coupled microstrip line layout: (a) schematic; and (b) layout in an EM field solver. Dimensions of the coupled lines are w = 500 μm, s = 100 μm, ℓ = 1 cm, W = 6 mm, L = 12 mm,. The metal is 6 μm thick gold (conductivity $\sigma = 42.6 \times 10^6$) and the alumina substrate height is 600 μm with relative permittivity ε_r = 9.8 and a loss tangent of 0.001.

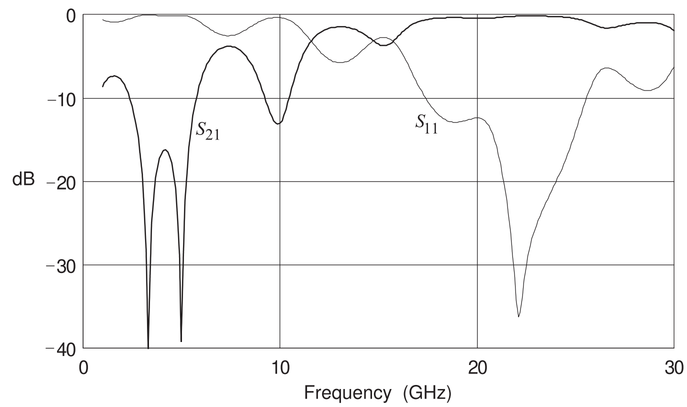

Figure 5-31: Insertion loss (S_{21}) and return loss (S_{11}) of the coupled line of Figure 5-30.

5.13 References

[1] B. Biswas, "Modeling and simulation of high speed interconnects," Master's thesis, North Carolina State University, 1998.

[2] E. Hammerstad and O. Jensen, "Accurate models for microstrip computer-aided design," in *1980 IEEE MTT-S Int. Microwave Symp. Digest*, May 1980, pp. 407–409.

[3] M. Kirschning and R. Jansen, "Accurate wide-range design equations for the frequency-dependent characteristic of parallel coupled microstrip lines," *IEEE Trans. on Microwave Theory and Techniques*, vol. 32, no. 1, pp. 83–90, Jan. 1984.

[4] ——, "Accurate wide-range design equations for the frequency-dependent characteristic of parallel coupled microstrip lines," *IEEE Trans. on Microwave Theory and Techniques*, vol. 32, no. 1, pp. 83–90, Jan. 1984.

[5] T. Edwards and M. Steer, *Foundations for Microstrip Circuit Design*. John Wiley & Sons, 2016.

[6] http://www.synergymwave.com.

[7] http://www.minicircuits.com.

[8] J. Lange, "Interdigitated strip-line quadrature hybrid," in *1969 G-MTT Int. Microwave Symp.*, May 1969, pp. 10–13.

[9] A. Johnson and G. Zysman, "Coupled transmission line networks in an inhomogeneous dielectric medium," in *1969 G-MTT Int. Microwave Symp.*, May 1969, pp. 329–337.

[10] R. Mongia, I. Bahl, and P. Bhartia, *RF and Microwave Coupled-line Circuits*. Artech House, 1999.

[11] J.-S. Hong and M. Lancaster, *Microstrip Filters for RF/Microwave Applications*. John Wiley & Sons, 2001.

[12] E. Jones, "Coupled-strip-transmission-line filters and directional couplers," *Microwave Theory and Techniques, IRE Trans. on*, vol. 4, no. 2, pp. 75–81, Apr. 1956.

[13] I. Hunter, *Theory and Design of Microwave Filters*. IEE Press, 2001.

[14] V. Tripathi and J. Rettig, "A spice model for multiple coupled microstrips and other transmission lines," *IEEE Trans. on Microwave Theory and Techniques*, vol. 33, no. 12, pp. 1513–1518, Dec. 1985.

[15] M. Steer, *Microwave and RF Design, Networks*, 3rd ed. North Carolina State University, 2019.

[16] J. Malherbe, *Microwave Transmission Line Filters*. Artech House, 1979.

5.14 Exercises

1. Consider the cross section of a coupled transmission line, as shown in Figure 5-1, with even and odd modes both traveling out of the page.
   (a) For an even mode on the coupled line, consider a phasor voltage of 1 V on each of the lines above the ground plane at 0 V. Sketch the directed electric field in the transverse plane, i.e. show the direction of the electric field.
   (b) For the even mode, sketch the directed magnetic fields in the transverse plane (the plane of the cross section).
   (c) For an odd mode on the coupled line, consider a phasor voltage of $+1$ V on the left line and a phasor voltage of -1 V on the right line. Sketch the directed electric fields in the transverse plane (the plane of the cross section).
   (d) For the odd mode, sketch the directed magnetic fields in the transverse plane (the plane of the cross section).

2. EM software can be used to determine the even- and odd-mode parameters of a coupled line. This is usually done by setting the phasor voltage on the coupled line and evaluating the phasor charge for each condition. The voltage applied to the left strip is V_1 and the voltage applied to the right strip is V_2. The phasor charges on the strips are Q_1 and Q_2, respectively. The analysis is repeated with the substrate replaced by free space. In this case, the charges are denoted by Q_{01} and Q_{02}. The (computer-based) measurements follow. [Parallels Example 5.1]

Charge	$V_1 = 1$ V; $V_2 = -1$ V	$V_1 = 1$ V; $V_2 = 1$ V
Q_1 (pC/m)	40	20
Q_2 (pC/m)	-50	30
Q_{01} (pC/m)	13.25	6
Q_{02} (pC/m)	-10	2.75

   (a) What is the two-port capacitance matrix?
   (b) What is the even-mode capacitance?
   (c) What is the odd-mode capacitance?
   (d) What is the free-space (no dielectric) two-port capacitance matrix?
   (e) What is the free-space even-mode capacitance?
   (f) What is the free-space odd-mode capacitance?
   (g) What is the even-mode effective relative permittivity?
   (h) What is the odd-mode effective relative permittivity?

3. Two 50 Ω microstrip lines are to be run parallel to each other on a 1 mm-thick printed circuit board with a relative permittivity $\varepsilon_r = 4$. The signal on the lines is 3 GHz. The effective permittivity of the lines is 3.1 and it is determined that the approximate distance over which the lines will be parallel is 1.42 cm. The coupling of the signals on the lines must be at least 30 dB down.
   (a) What is the free-space wavelength, λ_0, of the signal?
   (b) What is the guide wavelength, λ_g, of the signal?
   (c) How long is the parallel run of the microstrip lines in terms of λ_g?
   (d) What is the required maximum parallel-line coupling factor? Explain your reasoning.
   (e) What is the minimum separation of the lines? Explain your reasoning.

4. A pair of coupled lines has an even-mode effective permittivity, ε_{ee}, of 4.9 and an odd-mode effective permittivity of 5.2.
   (a) What is the even-mode phase velocity?
   (b) What is the odd-mode phase velocity?

5. A directional coupler using coupled lines is constructed on an alumina substrate of thickness 300 µm and $\varepsilon_r = 10$. The lines are 250 µm wide and the gap separation is 100 µm. What are (a) the characteristic impedances, (b) the effective permittivities, and (c) the phase velocities of the even and odd mode of the coupled line. (Hint: If you use a table you need to use interpolation as described in Section 1.A.12.)

6. An ideal directional coupler is lossless and there are no reflections at the ports. If the coupling factor is 10, what is the the magnitude of the transmission coefficient?

7. A directional coupler has the following characteristics: coupling factor C = 20, transmission factor 0.9, and directivity factor 25 dB. Also, the coupler is matched so that there is no reflection at any of the ports. What is the isolation in decibels?

8. A lossy 6 dB directional coupler is matched so that there is no reflection at any of the ports. The insertion loss (considering the through path) is 2 dB. If 1 mW is input to the directional coupler, what is the power in microwatts dissipated in the directional coupler? Ignore power leaving the isolated port.

9. A 1 GHz microstrip directional coupler has a coupling factor of 20 dB. The coupler must have a system impedance of 50 Ω.

(a) Draw the layout of the directional coupler.
(b) What is the even-mode impedance of the coupler?
(c) What is the odd-mode impedance of the coupler?
(d) What is the optimum electrical length of the directional coupler in degrees at the design center frequency?
(e) If, in addition, the isolation of the directional coupler is 40 dB, what is its directivity in decibels?

10. A directional coupler comprising a coupled pair of microstrip lines is to be designed in a $75\ \Omega$ system. The coupling factor is 10.
(a) What is the system impedance Z_{0S}?
(b) What is the odd-mode impedance of the coupler?
(c) What is the even-mode impedance of the coupler?

11. A matched directional coupler has a coupling factor C of 20, transmission factor 0.9, and directivity of 25 dB. What is the power dissipated in the directional coupler if the input power to Port 1 is 1 W.

12. Develop the design of a 10 dB directional coupler using coupled microstrip lines and a substrate with a permittivity of 10, a substrate thickness, h, of 600 µm, and a center frequency of 1 GHz. Develop the electrical design of the coupler (i.e., find the even- and odd-mode impedances required) and then develop the physical design (with widths and lengths) of the directional coupler. Use a system impedance of 50 Ω.

13. Design a microstrip directional coupler with the following specifications:

Transmission line technology: Microstrip
Coupling coefficient, C: 20 dB
Characteristic impedance, Z_{0S}: 50 Ω
Substrate permittivity, ε_r: 4.0
Substrate thickness, h: 635 µm
Center frequency, f_0: 10 GHz.

14. A directional coupler using coupled lines is constructed on an alumina substrate of thickness 300 µm. The lines are 250 µm wide and the gap separation is 100 µm. What are the characteristic impedances, effective permittivities, and phase velocities of the even- and odd-modes of the coupled line? Port 1 is the input, Port 2 is the through output, and Port 3 is the coupled output. (Hint: See Table 5-3.)
(a) Draw the schematic of the directional coupler and label the ports.
(b) What is the transmission coefficient of the coupler?
(c) Can the directivity of the coupler be determined? If so, what is the directivity, D, of the coupler?

15. Consider a pair of parallel microstrip lines separated by a spacing, s, of 100 µm.
(a) What happens to the coupling factor of the lines as s reduces?
(b) What happens to the system impedance as s reduces and no other dimensions change?
(c) In terms of wavelengths, what is the optimum length of the coupled lines for maximum coupling?

16. What is the coupling factor of a Lange coupler in decibels?

17. Consider the open-circuited interdigital coupled-line section in Table 5-4. If the coupled line is $\lambda/4$ long, write down the simplified $ABCD$ parameters. Assume that $\theta_o = \theta_e$.

18. Consider the shorted symmetric coupled-line section in Table 5-4. If the coupled line is $\lambda/4$ long, write down the simplified $ABCD$ parameters. Assume that $\theta_o = \theta_e$.

19. Consider the open-circuited combline coupled-line section in Table 5-4. If the coupled line is $\lambda/4$ long, write down the simplified $ABCD$ parameters. Assume that $\theta_o = \theta_e$.

20. Consider the short-circuited interdigital coupled-line section in Table 5-4. If the coupled line is $\lambda/4$ long, write down the simplified $ABCD$ parameters. Assume that $\theta_o = \theta_e$.

21. A coupled microstrip line has an odd-mode impedance of $30\ \Omega$ and an even-mode impedance of $65\ \Omega$.
(a) What is the differential characteristic impedance of the coupled lines?
(b) What is the common-mode characteristic impedance of the coupled lines?

22. A pair of coupled microstrip lines has odd- and even-mode characteristic impedances of $60\ \Omega$ and $70\ \Omega$ respectively. If a load resistance, R_L, is placed at the end of the lines from one strip to the other, what is the value of R_L for no reflection of the even mode?

23. The coupled lines below have odd- and even-mode characteristic impedances of $30\ \Omega$ and $60\ \Omega$ respectively.

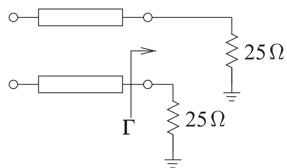

.

(a) What is the odd-mode reflection coefficient Γ?

(b) What is the common-mode characteristic impedance of the coupled lines?

24. The coupled lines below have odd- and even-mode characteristic impedances of 60 Ω and 100 Ω respectively. The coupled lines have a length ℓ and this is $\lambda/4$ long for the odd mode.

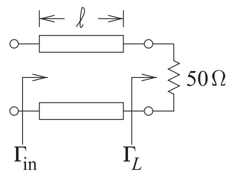

.

(a) What is the odd-mode reflection coefficient at the load, call this Γ_{Lo}?

(b) What is the odd-mode reflection coefficient at the input to the coupled lines?

25. The coupled microstrip lines below have an odd-mode characteristic impedance of 40 Ω and an even-mode characteristic impedance of 75 Ω.

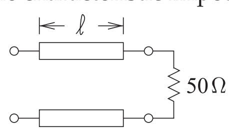

.

(a) What is the differential-mode characteristic impedance?

(b) What is the common-mode characteristic impedance?

26. The coupled lines below have odd- and even-mode characteristic impedances of 40 Ω and 75 Ω respectively.

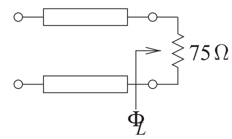

.

(a) What is the differential-mode characteristic impedance, Z_{0d}?

(b) What is the differential-mode load resistance, Z_{Ld}?

(c) What is the differential-mode reflection coefficient, Γ_{Ld}, at the load?

(d) What is the odd-mode reflection coefficient, Γ_{Ld}, at the load?

27. The coupled lines below have odd- and even-mode characteristic impedances of 60 Ω and 100 Ω respectively. The coupled lines have a length ℓ and this is $\lambda/4$ long for the odd mode.

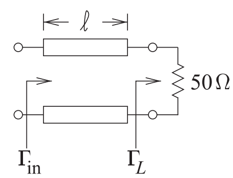

.

(a) What is the differential-mode reflection coefficient, Γ_d, at the load?

(b) What is Γ_d at the input of the lines?

5.14.1 Exercises by Section

†challenging, ‡very challenging

§5.2	$1^\dagger$	§5.8	$6, 7, 8, 9^\dagger, 10^\dagger, 11, 12^\dagger, 13^\dagger, 14^\dagger, 15^\dagger, 16$	§5.10	21, 22, 23, 24, 25, 26, 27
§5.5	$2^\dagger, 3^\ddagger$	§5.9	17, 18, 19, 20		
§5.6	4, 5,				

5.14.2 Answers to Selected Exercises

2(h)	3.87	9(e)	$D = 10$ dB	24	0.4118
5(c)	$v_{po} = 1.256 \cdot 10^8$ m/s	10	$Z_{0e} = 67.84\ \Omega$	26	-0.0323
6	0.9950	17	$C = 2\jmath/(Z_{0e} - Z_{0o})$		
7(b)	187 mW	21	32.5 Ω		

CHAPTER 6

Waveguides

6.1 Introduction

Rectangular waveguides are used to route millimeter-wave signals and high power microwave signals. The rectangular waveguide, often called just waveguide, shown in Figure 6-1 has metal walls forming a rectangular pipe. Charges and currents induced in the conductive walls guide propagating EM fields in the $+z$ and $-z$ directions. The rectangular waveguide has very little loss compared to a coaxial line because the EM field is away from the walls and there is little current in the walls, and what is there is spread out resulting in low current density. All of the waveguide loss, as with the loss of most transmission systems, is resistive loss so minimizing current density minimizes loss.

This chapter begins with Section 6.2 where symmetries and restricting

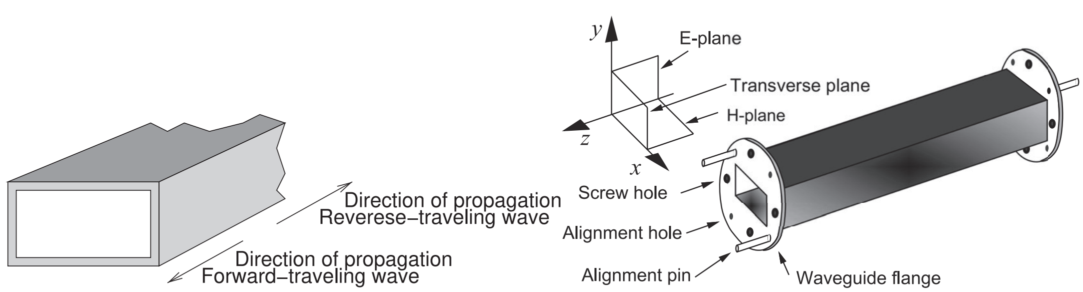

(a) Rectangular waveguide (b) Definition of planes

Figure 6-1: Rectangular waveguide.

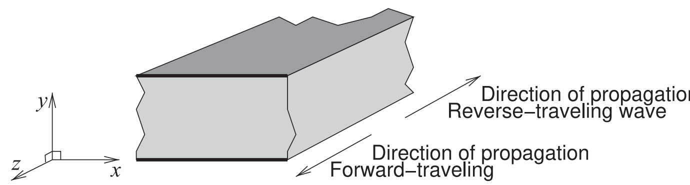

Figure 6-2: Parallel-plate waveguide.

propagation to only the $\pm z$ direction are applied to Maxwell's equations to yield the rectangular wave equation. These are then used in Section 6.3 to describe propagation between two metal planes forming what is called a parallel-plate waveguide, see Figure 6-2. Then the rectangular wave equations are applied to a rectangular waveguide in Section 6.4 to derive the field distribution inside a rectangular waveguide.

6.2 The Rectangular Wave Equation

Maxwell's equations will be put in a form that can be used in establishing the field descriptions in parallel-plate and rectangular waveguides. The EM fields in these structures vary sinusoidally with respect to both position and time so the first simplification of Maxwell's equations is to use phasors. Boundary conditions are established by the metal walls, and these walls match the Cartesian coordinate system. So Maxwell's equations are put in Cartesian coordinate form. Simplifications of the fields can be made that relate to the positions of the metal walls. Another simplification is made by assuming that there can only be propagation in the $\pm z$ direction. When the wave propagates in the $+z$ direction it is called the forward-traveling wave, and when it propagates in the $-z$ direction it is called the reverse-traveling wave.

The development begins with Maxwell's equations (Equations (1.1)–(1.4)) in a source-free region ($\rho = 0$ and $J = 0$). A simplification comes from assuming a linear, isotropic, and homogeneous medium so that ε and μ are independent of signal level and are independent of the field direction and of position, thus

$$\nabla\times\bar{\mathcal{E}} = -\frac{\partial\bar{\mathcal{B}}}{\partial t} = -\mu\frac{\partial\bar{\mathcal{H}}}{\partial t} \qquad (6.1) \qquad\qquad \nabla\times\bar{\mathcal{H}} = \frac{\partial\bar{\mathcal{D}}}{\partial t} = \varepsilon\frac{\partial\bar{\mathcal{E}}}{\partial t} \qquad (6.3)$$

$$\nabla\cdot\bar{\mathcal{D}} = 0 = \nabla\cdot\bar{\mathcal{E}} \qquad (6.2) \qquad\qquad \nabla\cdot\bar{\mathcal{B}} = 0 = \nabla\cdot\bar{\mathcal{H}}. \qquad (6.4)$$

Taking the curl of Equation (6.1) leads to

$$\nabla\times\nabla\times\bar{\mathcal{E}} = -\nabla\times\mu\frac{\partial\bar{\mathcal{H}}}{\partial t} = -\mu\frac{\partial(\nabla\times\bar{\mathcal{H}})}{\partial t}. \qquad (6.5)$$

Applying the identity $\nabla\times\nabla\times\bar{\mathcal{A}} = \nabla(\nabla\cdot\bar{\mathcal{A}}) - \nabla^2\bar{\mathcal{A}}$ to the left-hand side of Equation (6.5), and replacing $\nabla\times\bar{\mathcal{H}}$ with the right-hand side of Equation (6.3), the equation above becomes

$$-\nabla^2\bar{\mathcal{E}} + \nabla(\nabla\cdot\bar{\mathcal{E}}) = -\mu\frac{\partial}{\partial t}\left(\varepsilon\frac{\partial\bar{\mathcal{E}}}{\partial t}\right) = -\mu\varepsilon\frac{\partial^2\bar{\mathcal{E}}}{\partial t^2}. \qquad (6.6)$$

Using Equation (6.2) this reduces to

$$\nabla^2\bar{\mathcal{E}} = \mu\varepsilon\frac{\partial^2(\bar{\mathcal{E}})}{\partial t^2}, \qquad (6.7)$$

$$\text{where} \quad \nabla^2 \bar{\mathcal{E}} = \frac{\partial^2 \bar{\mathcal{E}}}{\partial x^2} + \frac{\partial^2 \bar{\mathcal{E}}}{\partial y^2} + \frac{\partial^2 \bar{\mathcal{E}}}{\partial z^2} = \nabla_t^2 \bar{\mathcal{E}} + \frac{\partial^2 \bar{\mathcal{E}}}{\partial z^2}. \tag{6.8}$$

$$\text{and} \quad \nabla_t^2 \bar{\mathcal{E}} = \frac{\partial^2 \bar{\mathcal{E}}}{\partial x^2} + \frac{\partial^2 \bar{\mathcal{E}}}{\partial y^2} \tag{6.9}$$

is used for fields propagating in the $\pm z$ direction and the subscript t indicates the transverse plane (the x–y plane here). Equation (6.9) can be put into the form of its components. Since

$$\bar{\mathcal{E}} = \mathcal{E}_x \hat{\mathbf{x}} + \mathcal{E}_y \hat{\mathbf{y}} + \mathcal{E}_z \hat{\mathbf{z}}, \tag{6.10}$$

$$\begin{aligned} \text{then} \quad \nabla^2 \bar{\mathcal{E}} &= \left(\frac{\partial^2 \mathcal{E}_x}{\partial x^2} \hat{\mathbf{x}} + \frac{\partial^2 \mathcal{E}_y}{\partial x^2} \hat{\mathbf{y}} + \frac{\partial^2 \mathcal{E}_z}{\partial x^2} \hat{\mathbf{z}} \right) + \left(\frac{\partial^2 E_x}{\partial y^2} \hat{\mathbf{x}} + \frac{\partial^2 \mathcal{E}_y}{\partial y^2} \hat{\mathbf{y}} + \frac{\partial^2 \mathcal{E}_z}{\partial y^2} \hat{\mathbf{z}} \right) \\ &\quad + \left(\frac{\partial^2 E_x}{\partial z^2} \hat{\mathbf{x}} + \frac{\partial^2 \mathcal{E}_y}{\partial z^2} \hat{\mathbf{y}} + \frac{\partial^2 \mathcal{E}_z}{\partial z^2} \hat{\mathbf{z}} \right) \qquad (6.11) \\ &= \left(\frac{\partial^2 E_x}{\partial x^2} + \frac{\partial^2 \mathcal{E}_x}{\partial y^2} + \frac{\partial^2 \mathcal{E}_x}{\partial z^2} \right) \hat{\mathbf{x}} + \left(\frac{\partial^2 E_y}{\partial x^2} + \frac{\partial^2 \mathcal{E}_y}{\partial y^2} + \frac{\partial^2 \mathcal{E}_y}{\partial z^2} \right) \hat{\mathbf{y}} \\ &\quad + \left(\frac{\partial^2 \mathcal{E}_z}{\partial x^2} + \frac{\partial^2 \mathcal{E}_z}{\partial y^2} + \frac{\partial^2 \mathcal{E}_z}{\partial z^2} \right) \hat{\mathbf{z}}, \qquad (6.12) \end{aligned}$$

$$\text{and} \quad \nabla_t^2 \bar{\mathcal{E}} = \left(\frac{\partial^2 \mathcal{E}_x}{\partial x^2} + \frac{\partial^2 \mathcal{E}_x}{\partial y^2} \right) \hat{\mathbf{x}} + \left(\frac{\partial^2 \mathcal{E}_y}{\partial x^2} + \frac{\partial^2 \mathcal{E}_y}{\partial y^2} \right) \hat{\mathbf{y}} + \left(\frac{\partial^2 \mathcal{E}_z}{\partial x^2} + \frac{\partial^2 \mathcal{E}_z}{\partial y^2} \right) \hat{\mathbf{z}}. \tag{6.13}$$

Invoking the phasor form, $\partial/\partial t$ is replaced by $\jmath\omega$, and with propagation only in the $\pm z$ direction there is an assumed $\mathrm{e}^{(\jmath\omega t - \gamma z)}$ dependence of the fields. Development is now simplified by introducing the phasor $\bar{E}$ defined so that

$$\bar{\mathcal{E}} = \bar{E} \mathrm{e}^{-\gamma z}. \tag{6.14}$$

Now Equation (6.7) further reduces to

$$\nabla^2 \bar{E} = \left(\nabla_t^2 \bar{E} + \frac{\partial^2 \bar{E}}{\partial z^2} \right) = \nabla_t^2 \bar{E} + \gamma^2 \bar{E} = (\jmath\omega)^2 \mu\varepsilon \bar{E} = -k^2 \bar{E}, \tag{6.15}$$

where $k = \omega\sqrt{\mu\varepsilon}$ is the **wavenumber** (with SI units of m^{-1}). Rearranging Equation (6.15) yields

$$\nabla_t^2 \bar{E} = -(\gamma^2 + k^2) \bar{E}. \tag{6.16}$$

A similar expression can be derived for the magnetic field:

$$\nabla_t^2 \bar{H} = -(\gamma^2 + k^2) \bar{H}. \tag{6.17}$$

Equations (6.16) and (6.17) are called wave equations, or Helmholtz equations, for phasor fields propagating in the z direction. Equations (6.16) and (6.17) are usually written as

$$\nabla_t^2 \bar{E} = -k_c^2 \bar{E} \qquad (6.18) \qquad\qquad \nabla_t^2 \bar{H} = -k_c^2 \bar{H}, \qquad (6.19)$$

where the **cutoff wavenumber** is

$$k_c^2 = \gamma^2 + k^2. \tag{6.20}$$

Equations (6.18) and (6.19) describe the transverse fields (the fields in the x–y plane) between the conducting plates of the parallel-plate as well as within the walls of the rectangular waveguide having a $\mathrm{e}^{(\jmath\omega t-\gamma z)}$ dependence. The general form of the solution of these equations is a sinusoidal wave moving in the z direction. For propagating waves in a lossless medium, $\gamma = \jmath\beta$, where β is the phase constant:

$$\beta = \pm\sqrt{k^2 - k_c^2}. \tag{6.21}$$

If β is not real, which occurs when $|k_c| < |k|$, then an EM wave cannot propagate and such modes are called evanescent modes. These are like fringing fields. If they are generated, say at a discontinuity, they will store reactive energy locally.

Boundary conditions, resulting from the charges and current on the plates, further constrain the solutions. Equation (6.1) with Equation (1.125) becomes

$$\nabla \times \bar{E} = \jmath\omega\mu\bar{H}. \tag{6.22}$$

In rectangular coordinates, $\bar{E} = E_x\hat{\mathbf{x}} + E_y\hat{\mathbf{y}} + E_z\hat{\mathbf{z}}$ and $\bar{H} = H_x\hat{\mathbf{x}} + H_y\hat{\mathbf{y}} + H_z\hat{\mathbf{z}}$, and Equation (6.22) becomes

$$\left.\begin{array}{l} \dfrac{\partial E_z}{\partial y} + \gamma E_y = -\jmath\omega\mu H_x, \quad -\dfrac{\partial E_z}{\partial x} - \gamma E_x = -\jmath\omega\mu H_y, \\ \dfrac{\partial E_y}{\partial x} - \dfrac{\partial E_x}{\partial y} = -\jmath\omega\mu H_z \end{array}\right\}. \tag{6.23}$$

Similarly for $\nabla \times \bar{H} = \jmath\omega\varepsilon\bar{E}$:

$$\left.\begin{array}{l} \dfrac{\partial H_z}{\partial y} + \gamma H_y = \jmath\omega\varepsilon E_x, \quad -\dfrac{\partial H_z}{\partial x} - \gamma H_x = \jmath\omega\varepsilon E_y, \\ \dfrac{\partial H_y}{\partial x} - \dfrac{\partial H_x}{\partial y} = \jmath\omega\varepsilon E_z \end{array}\right\}. \tag{6.24}$$

Solving Equations (6.23) and (6.24) yields the rectangular wave equations for $k_c \neq 0$ ($k_c^2 = k^2 + \gamma^2$ and if there is no loss $k_c^2 = \omega^2\mu\varepsilon - \beta^2$):

$$\left.\begin{array}{ll} E_x = \dfrac{-1}{k_c^2}\left(\gamma\dfrac{\partial E_z}{\partial x} + \jmath\omega\mu\dfrac{\partial H_z}{\partial y}\right) & E_y = \dfrac{1}{k_c^2}\left(-\gamma\dfrac{\partial E_z}{\partial y} + \jmath\omega\mu\dfrac{\partial H_z}{\partial x}\right) \\ H_x = \dfrac{1}{k_c^2}\left(-\gamma\dfrac{\partial H_z}{\partial x} + \jmath\omega\varepsilon\dfrac{\partial E_z}{\partial y}\right) & H_y = \dfrac{-1}{k_c^2}\left(\gamma\dfrac{\partial H_z}{\partial y} + \jmath\omega\varepsilon\dfrac{\partial E_z}{\partial x}\right) \\ E_z = \dfrac{-\jmath}{\omega\varepsilon}\left(\dfrac{\partial H_y}{\partial x} - \dfrac{\partial H_x}{\partial y}\right) & H_z = \dfrac{\jmath}{\omega\mu}\left(\dfrac{\partial E_y}{\partial x} - \dfrac{\partial E_x}{\partial y}\right). \end{array}\right\} \tag{6.25}$$

The solution for $k_c = 0$ is arrived at separately. Since $k_c = 0$ there is no loss. Also propagation at DC is a solution and the phasor fields at $\omega = 0$ will also be the field descriptions at any frequency. At $\omega = 0$, $\gamma = \jmath\beta = 0$ and $k = 0$. Equations (6.23)–(6.24) are now written as

$$\left.\begin{array}{ll} \dfrac{\partial E_z}{\partial y} + 0 \cdot E_y = 0 \cdot H_x = 0, & -\dfrac{\partial E_z}{\partial x} - 0 \cdot E_x = 0 \cdot H_y = 0, \\ \dfrac{\partial E_y}{\partial x} - \dfrac{\partial E_x}{\partial y} = -0 \cdot H_z = 0, & \dfrac{\partial H_z}{\partial y} + 0 \cdot H_y = 0 \cdot E_x = 0, \\ -\dfrac{\partial H_z}{\partial x} - 0 \cdot H_x = 0 \cdot E_y = 0, & \dfrac{\partial H_y}{\partial x} - \dfrac{\partial H_x}{\partial y} = 0 \cdot E_z = 0. \end{array}\right\}. \tag{6.26}$$

The only solutions to these with $\partial/\partial x = 0$ that also satisfies boundary conditions are that $E_z = 0 = H_z = E_x = H_y$, and H_y and E_x are constants.

Now that the fields are in the appropriate forms, classification of possible solutions (i.e. modes) can be developed for the parallel-plate and rectangular waveguides. At this stage the following simplifications have been made to Maxwell's equations to get them into the form of Equation (6.25)):

- Using phasors
- Restriction of propagation to the $+z$ and $-z$ directions
- Assuming that ε and μ are constants
- Putting the wave equations in rectangular form so that boundary conditions established by the metal walls can be easily applied.

6.3 Parallel-Plate Waveguide

This section derives the propagating EM fields for the parallel-plate waveguide shown in Figure 6-3. The parallel-plate waveguide shown in Figure 6-3(a) has conducting planes at the top and bottom that (as an approximation) extend infinitely in the x direction. Electromagnetic fields introduced between the plates, say by a sinusoidally varying voltage generator across the plates, will be guided by the charges and currents induced in the conductors.

The parallel-plate waveguide structure occurs in many planar circuits, such as between the ground and power planes of circuit boards. Understanding the EM propagation supported by parallel-plate waveguides enables design choices to be made that suppress unwanted propagation modes.

6.3.1 TEM Mode

In the transverse EM (TEM) mode, all of the E and H field components are in the plane transverse to the direction of propagation, that is, $E_z = 0 = H_z$. Thus Equation (6.26) requires that E_x, E_y, H_x, and H_y cannot vary with position in the transverse plane (i.e., with respect to x and y). Thus E_x, E_y, H_x, and H_y must be constant between the plates. Furthermore, boundary conditions require that $H_y = 0$ and $E_x = 0$ at the conductors. So in the TEM parallel-plate mode, only E_y and H_x exist, and they are constant. Equation

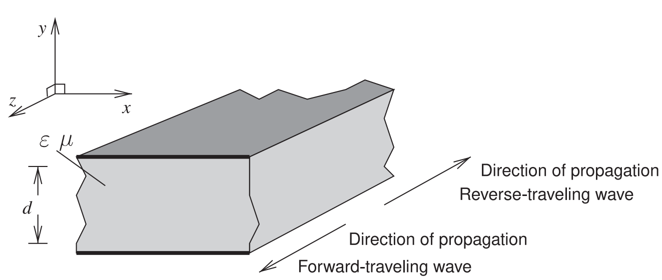

(a) Three-dimensional view

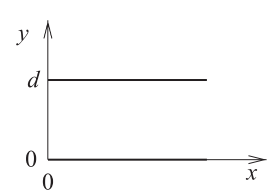

(b) Transverse view

Figure 6-3: Parallel-plate waveguide.

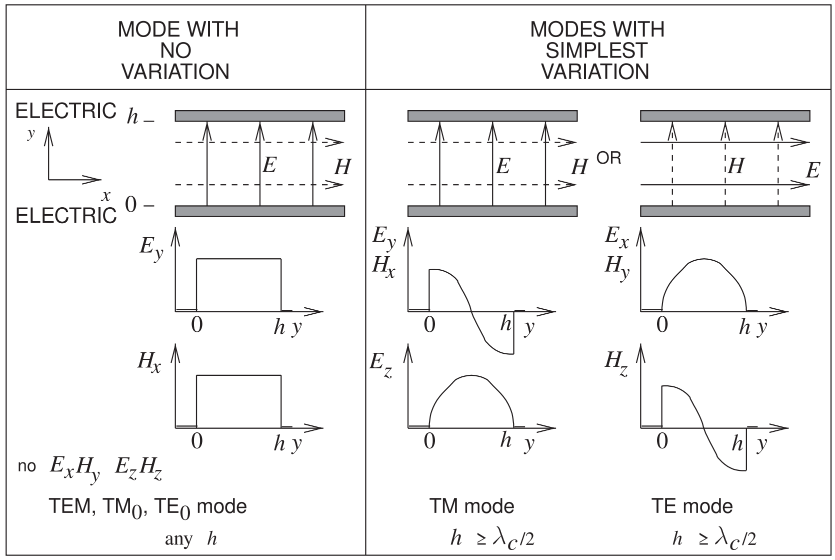

Figure 6-4: Lowest-order modes supported by combinations of electric and magnetic walls for the TEM (= TM_0 = TE_0), TM_1, and TE_1 modes.

(6.25) leads to

$$H_x = \frac{\gamma E_y}{\jmath\omega\mu} = \pm\frac{\jmath\omega\sqrt{\mu\varepsilon}}{\jmath\omega\mu}E_y = \pm\sqrt{\frac{\varepsilon}{\mu}}E_y = \pm\frac{1}{\eta}E_y, \tag{6.27}$$

where the plus sign describes forward-traveling fields (propagating in the $+z$ direction) and the minus sign describes backward-traveling fields (propagating in the $-z$ direction). The quantity $\eta = \sqrt{\mu/\varepsilon}$ is called the **wave impedance**, it is the **intrinsic impedance** of the medium between the parallel plates. This field variation is shown on the left in Figure 6-4(a). The TEM mode exists down to DC.

To determine the characteristic impedance of the parallel-plate waveguide first calculate the voltage of the top plate with respect to the bottom plate. This voltage is the integral of the electric field between the plates:

$$V = -\int_{y=0}^{d} E_y \mathrm{e}^{-\gamma z} dy = E_y d \mathrm{e}^{-\gamma z} \tag{6.28}$$

since E_y is a constant. The current on the top plate in the z direction is obtained by integrating the surface current density in the x direction. Assuming that the plates have a width W in the x direction then the current on the top plate is

$$I = -\int_{x=0}^{W} J_s \cdot \hat{z}\, dx = H_x W \mathrm{e}^{-\gamma z} \tag{6.29}$$

since E_y is a constant. In terms of voltage and current (and hence treating the parallel-plate waveguide as a transmission line) the characteristic impedance of the TEM mode is

$$Z_0 = \frac{V}{I} = \frac{E_y d}{H_x W} = \frac{\eta d}{W}. \tag{6.30}$$

Here η is the intrinsic impedance of a TEM mode in the medium. Since we are considering a TEM mode, the wave impedance of the TEM mode is just the intrinsic impedance, that is,

$$Z_{\text{TEM}} = E_y/H_x = Z_0|_{\text{free-space}} = \eta. \tag{6.31}$$

With $\eta_0 = \sqrt{\mu_0/\varepsilon_0}$ being the free-space impedance, the characteristic impedance can be written

$$Z_0 = \frac{\eta_0 d}{W}\sqrt{\frac{\mu_r}{\varepsilon_r}} \quad \text{and} \quad Z_{\text{TEM}} = \eta = \eta_0\sqrt{\frac{\mu_r}{\varepsilon_r}}. \tag{6.32}$$

The phase velocity ($= \omega/\beta$) is just the speed of light in the medium:

$$v_p = \frac{1}{\sqrt{\mu_0\varepsilon_0}} = \frac{c}{\sqrt{\mu_r\varepsilon_r}}. \tag{6.33}$$

Formulas for attenuation are developed in [1] and the conductor attenuation

$$\alpha_c = \frac{R_s}{\eta d} \quad \text{(with SI units of Np/m)} \tag{6.34}$$

where $R_s = 1/(\sigma\delta_s)$ is the surface resistance of the conductor, σ is the conductivity of the conductor, and δ_s is the skin depth in the conductor. The attenuation due to dielectric loss is

$$\alpha_d = \frac{k^2 \tan\delta}{2\beta} \quad \text{(with SI units of Np/m).} \tag{6.35}$$

6.3.2 TM Mode

The **Transverse Magnetic Mode** (**TM**) is characterized by $H_z = 0$. Another restriction that will be used here in developing the field equations is that there is no variation of the fields in the x direction. Examining Equation (6.25) the only components of the field that could exist are E_y, E_z, and H_x. Everywhere E_y is perpendicular, and H_y is parallel, to the electrical walls so boundary conditions are satisfied for E_y and H_x. E_z will be parallel to the electrical walls at the walls so boundary conditions need to be applied in deriving E_z.

The boundary conditions are that the E field parallel to the conducting walls is zero. Considering E_z only, Equation (6.18) becomes

$$\frac{d^2 E_z}{dy^2} = -k_c^2 E_z. \tag{6.36}$$

The solution to Equation (6.36) is

$$E_z = [E_0 \sin(k_c y) + E_1 \cos(k_c y)]\, \mathrm{e}^{-\gamma z}. \tag{6.37}$$

To find the coefficients E_0 and E_1 boundary conditions are applied so that E_z is zero at $y = 0$ and $y = d$ (since the E field parallel to the conductors must be zero), that is,

$$E_z|_{y=0} = 0 = E_1 \qquad \text{and} \qquad E_z|_{y=d} = 0 = E_0 \sin(k_c d). \tag{6.38}$$

This requires that $\sin(k_c d) = 0$, and thus requiring that there are discrete values of k_c:

$$k_c = m\pi/d \quad m = 1, 2, 3, \ldots\,. \tag{6.39}$$

(Note that $m = 0$ is also a solution but requires a separate derivation, see the summary for this section.) Each value of k_c identifies a different mode and m is the mode index. The mth mode is the TM_m mode and m indicates the number of half-sinusoidal variations of the fields in the y direction. The TM_m mode propagates if the wavelength of the signal is such that $\lambda \geq \lambda_c$, where λ_c is the critical wavelength of the mth mode.

Substituting the above results and assumptions (e.g., $\partial/\partial x = 0$) in Equation (6.25),

$$H_z = 0 \quad E_x = 0 \quad H_y = 0 \tag{6.40}$$

$$E_z = E_0 \sin(k_c y)\mathrm{e}^{-\gamma z} \tag{6.41}$$

$$E_y = -\frac{\gamma}{k_c^2}\frac{dE_z}{dy} = -\frac{\gamma}{k_c}E_0 \cos(k_c y)\mathrm{e}^{-\gamma z} \tag{6.42}$$

$$H_x = \frac{\jmath\omega\varepsilon}{k_c^2}\frac{dE_z}{dy} = \frac{\jmath\omega\varepsilon}{k_c}E_0 \cos(k_c y)\mathrm{e}^{-\gamma z}. \tag{6.43}$$

These are the complete field descriptions of the TM parallel-plate waveguide modes with zero variation in the x direction. Recall that the wavenumber $k = \omega\sqrt{\mu\varepsilon}$.

There are an infinite number of TM modes identified by the index m, which determines the cutoff wavenumber, k_c, of the particular mode. The propagation constant of the mth mode, i.e. the TM_m mode, is

$$\gamma = \sqrt{k_c^2 - k^2} = \sqrt{(m\pi/d)^2 - \omega^2\mu\varepsilon}. \tag{6.44}$$

Propagation is only possible if γ has an imaginary component. Thus in a lossless medium $\gamma = \jmath\beta$ and $\beta = \sqrt{k^2 - k_c^2}$. The cutoff frequency below which propagation is not possible is

$$f_c = \frac{1}{2\pi}\frac{k_c}{\sqrt{\mu\varepsilon}} = \frac{1}{2\pi}\frac{m\pi}{d\sqrt{\mu\varepsilon}} = \frac{m\nu}{2d}, \tag{6.45}$$

where $\nu = 1/\sqrt{\mu\varepsilon}$ is the velocity of a TEM mode in the medium. The cutoff wavelength can also be defined as

$$\lambda_c = \frac{\nu}{f_c} = \frac{2d}{m}. \tag{6.46}$$

where ν is the speed of light in the medium. The wavelength of the TM_m mode, at a particular frequency, is the guide wavelength

$$\lambda_g = \frac{2\pi}{\beta} = \frac{\lambda}{\sqrt{1 - (f_c/f)^2}}, \tag{6.47}$$

where λ is the wavelength of a TEM mode in the medium: $\lambda = \nu/f$ (so $\lambda_g = \lambda$ when $k_c = 0$). The phase velocity of the modes is dependent on the mode index m through the cutoff frequency:

$$v_p = \frac{\omega}{\beta} = \frac{\nu}{\sqrt{1 - (f_c/f)^2}}, \tag{6.48}$$

and the group velocity is

$$v_g = \frac{d\omega}{d\beta} = \nu\sqrt{1 - (f_c/f)^2}. \tag{6.49}$$

The phase velocity, v_p, of a TM mode is greater than ν while the group velocity, v_g, is slower than ν. The group velocity is the velocity at which energy is transmitted and thus can never be faster than the speed of light, c. The phase velocity, however, can be greater than c. The TM mode field variation is shown on the right in Figure 6-4.

The wave impedance of the TM_m mode is

$$Z_{\mathrm{TM}} = -E_y/H_x = \frac{\beta}{\omega\varepsilon} = \frac{\beta\eta}{k}. \tag{6.50}$$

Formulas for attenuation are developed in [1] and the conductor attenuation

$$\alpha_c = \frac{2kR_s}{\beta\eta d} \quad \text{(with SI units of Np/m)} \tag{6.51}$$

where $R_s = 1/(\sigma\delta_s)$ is the surface resistance of the conductor, σ is the conductivity of the conductor, and δ_s is the skin depth in the conductor. The attenuation due to dielectric loss is

$$\alpha_d = \frac{k^2 \tan\delta}{2\beta.} \quad \text{(with SI units of Np/m)} \tag{6.52}$$

6.3.3 TE Mode

The **transverse electric (TE) mode** is characterized by $E_z = 0$. Following the same development as for the TM modes, the TE_n mode fields with n variations of the H_z are

$$E_z = 0, \quad E_y = 0, \quad H_x = 0 \tag{6.53}$$

$$H_z = H_0 \cos(k_c y) \mathrm{e}^{-\gamma z} \tag{6.54}$$

$$E_x = \frac{\jmath\omega\mu}{k_c} H_0 \sin(k_c y) \mathrm{e}^{-\gamma z} \tag{6.55}$$

$$H_y = \frac{\gamma}{k_c} H_0 \sin(k_c y) \mathrm{e}^{-\gamma z}. \tag{6.56}$$

The equations for k_c, v_p, v_g, f_c, λ_c, and λ_g of the TE_n mode are the same as for the TM_m mode considered in the previous section with the replacement of the mode index m by n, $n = 1, 2, 3, \ldots$. (Note that $n = 0$ is also a solution but requires a separate derivation, see the summary for this section.) The TE mode field variation is shown on the right in Figure 6-4.

The wave impedance of the TE mode is

$$Z_{\mathrm{TE}} = \frac{k\eta}{\beta}. \tag{6.57}$$

Formulas for attenuation are developed in [1] and the conductor attenuation

$$\alpha_c = \frac{2k_c^2 R_s}{k\beta\eta d} \quad \text{(with SI units of Np/m)} \tag{6.58}$$

where $R_s = 1/(\sigma\delta_s)$ is the **surface resistance**, η, of the conductor, σ is the conductivity of the conductor, and δ_s is the skin depth pf the conductor. The attenuation due to dielectric loss is

$$\alpha_d = \frac{k^2 \tan\delta}{2\beta} \quad \text{(with SI units of Np/m).} \tag{6.59}$$

6.3.4 Summary

The TEM mode (where $k_c = 0$) is the same as the TM_0 mode and the TE_0 mode. Here derivations of the TE and TM modes began with from Equation (6.25) and were only solutions for $k_c \neq 0$. Development of the $0th$ order TE and TM modes requires derivation from Equation(6.26) but this was done for the TEM mode and so was not repeated for the TE_0 and TM_0 modes.

6.4 Rectangular Waveguide

A rectangular waveguide is shown in Figure 6-5(a). Rectangular waveguides guide EM energy between four connected electrical walls, and there is little current created on the walls. As a result, resistive losses are quite low, much lower than can be achieved using coaxial lines for example. One of the major uses of a rectangular waveguide is when losses must be kept to a minimum, so that a rectangular waveguide is used in very high-power situations such as radar, and at a few tens of gigahertz and above. At higher frequencies the loss of coaxial lines becomes very large, and it also becomes difficult to build small-diameter coaxial lines at 100 GHz and above. As a result, a rectangular waveguide is nearly always used above 100 GHz. There are many low- to medium-power legacy systems that use rectangular waveguides down to 1 GHz.

A rectangular waveguide supports many different modes, but it does not support the TEM mode. The modes are categorized as being either TM or TE, denoting whether all of the magnetic fields are perpendicular to the direction of propagation (these are the transverse magnetic fields) or whether all of the electric fields are perpendicular to the direction of propagation (these are the transverse electric fields). Dimensions of the waveguide can be chosen so that only one mode can propagate for a range of frequencies. With more than one mode propagating, the different components of a signal would travel at different speeds and thus combine at a load incoherently, since the ratio of the energy in the modes would vary (usually) randomly.

The TE and TM field descriptions are derived from the solution of differential equations—Maxwell's equations—subject to boundary conditions. The general solutions for rectangular systems are sinewaves and there are possibly many discrete solutions. The nomenclature that has developed over

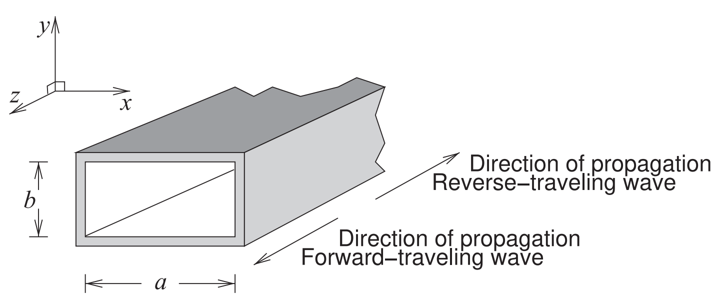

(a) Three-dimensional view

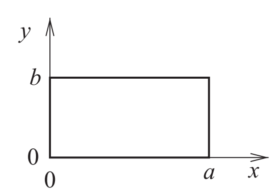

(b) Transverse cross section

Figure 6-5: Rectangular waveguide with internal dimensions of a and b.

the years to classify modes references the number of variations in the x direction, using the index m, and the number of variations in the y direction, using the index n. So there are TE_{mn} and TM_{mn} modes, and dimensions are usually selected so that only the TE_{10} mode can propagate.

6.4.1 TM Modes

The development of the field descriptions for the TM modes begins with the rectangular wave equations derived in Section 6.2. Transverse magnetic waves have zero H_z, but nonzero E_z. The differential equation governing E_z is, in rectangular coordinates (from Equations (6.13) and (6.16)),

$$\nabla_t^2 E_z = \frac{\partial^2 E_z}{\partial x^2} + \frac{\partial^2 E_z}{\partial y^2} = -k_c^2 E_z. \tag{6.60}$$

Using a separation of variables procedure, this equation has the solution

$$E_z = [A' \sin(k_x x) + B' \cos(k_x x)]\,[C' \sin(k_y y) + D' \cos(k_y y)]\,\mathrm{e}^{-\gamma z}, \tag{6.61}$$

where $$k_x^2 + k_y^2 = k_c^2. \tag{6.62}$$

The perfectly conducting boundary at $x = 0$ requires $B' = 0$ to produce $E_z = 0$ there. Similarly the ideal boundary at $y = 0$ requires $D' = 0$. Replacing $A'C'$ by a new constant A, then

$$E_z = A \sin(k_x x) \sin(k_y y) \mathrm{e}^{-\gamma z}. \tag{6.63}$$

The axial electric field, E_z, must also be zero at $x = a$ and $y = b$. This can only be so (except for the trivial solution $A = 0$) if $k_x a$ is an integral multiple of π so that $\sin(k_x a) = 0$:

$$k_x a = m\pi, \quad m = 1, 2, 3, \ldots . \tag{6.64}$$

Similarly, for E_z to be zero at $y = b$, $\sin(k_y b) = 0$ and $k_y b$ must also be a multiple of π:

$$k_y b = n\pi, \quad n = 1, 2, 3, \ldots . \tag{6.65}$$

So the cutoff frequency of the TM wave with m variations in x and with n variations in y (i.e., the TM_{mn} mode) is, from Equation (6.62),

$$f_{c_{m,n}} = \frac{k_{c_{m,n}}}{2\pi\sqrt{\mu\varepsilon}} = \frac{1}{2\pi\sqrt{\mu\varepsilon}}\left[\left(\frac{m\pi}{a}\right)^2 + \left(n\frac{\pi}{b}\right)^2\right]^{1/2}. \tag{6.66}$$

The remaining field components of the TM_{mn} wave are found with $H_z = 0$ and E_z from Equation (6.63) and Equation (6.25)):

$$E_x = -\frac{\gamma k_x}{k_{c_{m,n}}^2} A \cos(k_x x) \sin(k_y y) \mathrm{e}^{-\gamma z} \tag{6.67}$$

$$E_y = -\frac{\gamma k_y}{k_{c_{m,n}}^2} A \sin(k_x x) \cos(k_y y) \mathrm{e}^{-\gamma z} \tag{6.68}$$

$$H_x = \frac{\jmath\omega\varepsilon k_y}{k_{c_{m,n}}^2} A \sin(k_x x) \cos(k_y y) \mathrm{e}^{-\gamma z} \tag{6.69}$$

$$H_y = -\frac{\jmath\omega\varepsilon k_x}{k_{c_{m,n}}^2} A \cos(k_x x) \sin(k_y y) \mathrm{e}^{-\gamma z}. \tag{6.70}$$

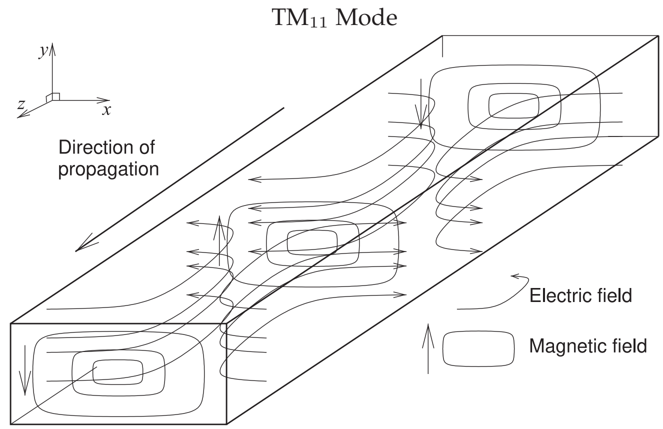

Figure 6-6: Electric and magnetic field distribution for the lowest-order TM mode, the TM_{11} mode.

The spatial field variations depend on the x and y cutoff wavenumbers, k_x and k_y, which in turn depend on the mode indexes and the cross-sectional dimensions of the waveguide. The cutoff wavenumber, k_c, is a function of the m and n indexes, and so $k_{c_{m,n}}$ is often used for the cutoff wavenumber with

$$k_{c_{m,n}}^2 = k_{x,m}^2 + k_{y,n}^2 = \left(\frac{m\pi}{a}\right)^2 + \left(\frac{n\pi}{b}\right)^2. \tag{6.71}$$

The lowest-order TM mode is the TM_{11} mode, with $m = 1$ and $n = 1$, and this has the minimum variation of the fields (of any TM mode); these are shown in Figure 6-6.

In summary, a mode can propagate only at frequencies above the cutoff frequency. Another quantity that defines when cutoff occurs is the cutoff wavelength, defined as

$$\lambda_c = \frac{\nu}{f_{c_{m,n}}}, \tag{6.72}$$

where $\nu = 1/\sqrt{\mu\varepsilon}$ is the velocity of a TEM mode in the medium (and of course this is not a rectangular waveguide mode). The cutoff wavelength is the wavelength in the medium (without the waveguide walls) at which cutoff occurs. Since k_c^2 is $k^2 - \beta^2$, the attenuation constant of a given mode for frequencies below the cutoff frequency is

$$\alpha = \sqrt{k_{c_{m,n}}^2 - k^2} = k_{c_{m,n}}\sqrt{1 - \left(\frac{f}{f_{c_{m,n}}}\right)^2}, \quad f < f_{c_{m,n}}. \tag{6.73}$$

The phase constant for frequencies above the cutoff frequency is

$$\beta = \sqrt{k^2 - k_{c_{m,n}}^2} = k\sqrt{1 - \left(\frac{f_{c_{m,n}}}{f}\right)^2}, \qquad f > f_{c_{m,n}}. \tag{6.74}$$

For a propagating mode (i.e., $f > f_{c_{m,n}}$) the wavelength of the mode, called the guide wavelength, is

$$\lambda_g = \frac{2\pi}{\beta} = \frac{\lambda}{\sqrt{1 - (f_c/f)^2}}, \tag{6.75}$$

where λ is the wavelength of a TEM mode in the medium (but of course not in the waveguide): $\lambda = \nu/f$. The phase velocity of the mode is also dependent on the mode indexes m and n through the cutoff frequency,

$$v_p = \frac{\omega}{\beta} = \frac{\nu}{\sqrt{1 - (f_{c_{m,n}}/f)^2}}, \tag{6.76}$$

and the group velocity is

$$v_g = \frac{d\omega}{d\beta} = \nu\sqrt{1 - (f_{c_{m,n}}/f)^2}. \tag{6.77}$$

6.4.2 TE Modes

Transverse electric waves have zero E_z and nonzero H_z so that, in rectangular coordinates,

$$\nabla_t^2 H_z = \frac{\partial^2 H_z}{\partial x^2} + \frac{\partial^2 H_z}{\partial y^2} = -k_c^2 H_z. \tag{6.78}$$

Solving using the separation of variables technique gives

$$H_z = [A'' \sin(k_x x) + B'' \cos(k_x x)]\,[C'' \sin(k_y y) + D'' \cos(k_y y)]\,\mathrm{e}^{-\gamma z}, \tag{6.79}$$

where $$k_x^2 + k_y^2 = k_c^2. \tag{6.80}$$

Imposition of a boundary condition in this case is a little less direct, but the electric field components are

$$\begin{aligned} E_x &= -\frac{\jmath\omega\mu}{k_c^2}\frac{\partial H_z}{\partial y} && (6.81)\\ &= -\frac{\jmath\omega\mu k_y}{k_c^2}\,[A'' \sin(k_x x) + B'' \cos(k_x x)]\,[C'' \cos(k_y y) - D'' \sin(k_y y)]\,\mathrm{e}^{-\gamma z} \\ E_y &= \frac{\jmath\omega\mu}{k_c^2}\frac{\partial H_z}{\partial x} && (6.82)\\ &= \frac{\jmath\omega\mu k_x}{k_c^2}\,[A'' \cos(k_x x) - B'' \sin(k_x x)]\,[C'' \sin(k_y y) + D'' \cos(k_y y)]\,\mathrm{e}^{-\gamma z}. \end{aligned}$$

For E_x to be zero at $y = 0$ for all x, $C'' = 0$; and for $E_y = 0$ at $x = 0$ for all y, $A'' = 0$. Defining $B''D'' = B$, then

$$H_z = B\cos(k_x x)\cos(k_y y) \tag{6.83}$$

$$E_x = \frac{\jmath\omega\mu k_y}{k_c^2} B\cos(k_x x)\sin(k_y y)\mathrm{e}^{-\gamma z} \tag{6.84}$$

$$E_y = -\frac{\jmath\omega\mu k_x}{k_c^2} B\sin(k_x x)\cos(k_y y)\mathrm{e}^{-\gamma z}. \tag{6.85}$$

E_y is zero at $x = a$, that is, $\sin(k_x a) = 0$, so that $k_x a$ must be a multiple of π:

$$k_x a = m\pi, \quad m = 1, 2, 3, \ldots\ . \tag{6.86}$$

Also, E_x is zero at $y = b$, that is, $\sin(k_y b) = 0$, so that $k_y b$ must be zero (so that E_x is always zero) or that it is a multiple of π. Therefore

$$k_y b = n\pi \quad n = 0, 1, 2, 3, \ldots\ . \tag{6.87}$$

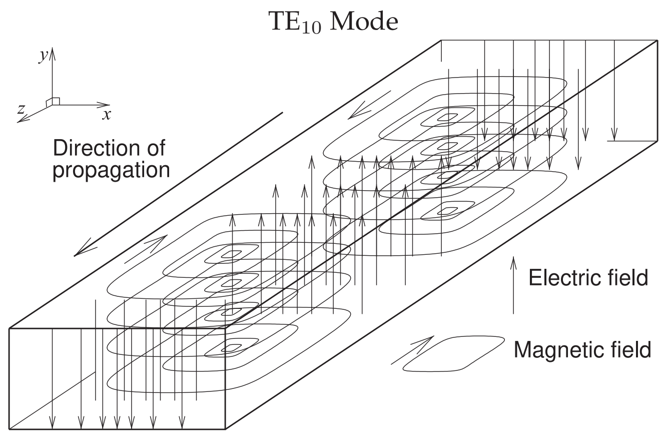

Figure 6-7: Electric and magnetic field distribution for the lowest-order TE mode.

The forms of the transverse electric field are then

$$E_x = \frac{\jmath\omega\mu k_y}{k^2_{c_{m,n}}} B\cos(k_x x)\sin(k_y y)\mathrm{e}^{-\gamma z} \tag{6.88}$$

$$E_y = -\frac{\jmath\omega\mu k_x}{k^2_{c_{m,n}}} B\sin(k_x x)\cos(k_y y)\mathrm{e}^{-\gamma z}, \tag{6.89}$$

and the corresponding transverse magnetic field components are

$$H_x = \frac{\gamma k_x}{k^2_{c_{m,n}}} B\sin(k_x x)\cos(k_y y)\mathrm{e}^{-\gamma z} \tag{6.90}$$

$$H_y = \frac{\gamma k_y}{k^2_{c_{m,n}}} B\cos(k_x x)\sin(k_y y)\mathrm{e}^{-\gamma z}. \tag{6.91}$$

Here the use of $k_{c_{m,n}}$ emphasizes that the cutoff wavenumber is a function of the m and n indexes:

$$k^2_{c_{m,n}} = k^2_{x,m} + k^2_{y,n} = \left(\frac{m\pi}{a}\right)^2 + \left(\frac{n\pi}{b}\right)^2. \tag{6.92}$$

The lowest-order TE mode is the TE_{10} mode (with $m = 1$ and $n = 0$) and this has the minimum variation of the fields; these are shown in Figure 6-7.

6.4.3 Practical Rectangular Waveguide

The dimensions and operating frequencies of a rectangular waveguide are chosen to support only one propagating mode. The operating frequency is between the cutoff frequency of the mode with the lowest cutoff frequency and the cutoff frequency of the mode with the next lowest cutoff frequency. Thus only one mode propagates.

Referring to Figure 6-5, if the dimensions are chosen so that b is greater than a, then the lowest-order TE mode (the TE$_{10}$ mode) has one variation of the fields in the x direction, while the lowest-order TM mode (the TM$_{11}$ mode) has one variation of the field in the x direction and one variation in the y direction. Thus the cutoff frequency of the TM$_{11}$ mode will be higher than the cutoff frequency of the TE$_{10}$ mode. Below the cutoff frequency the modes will not propagate (i.e., β (the imaginary part of the propagation constant) is zero). The propagation constants of the rectangular waveguide

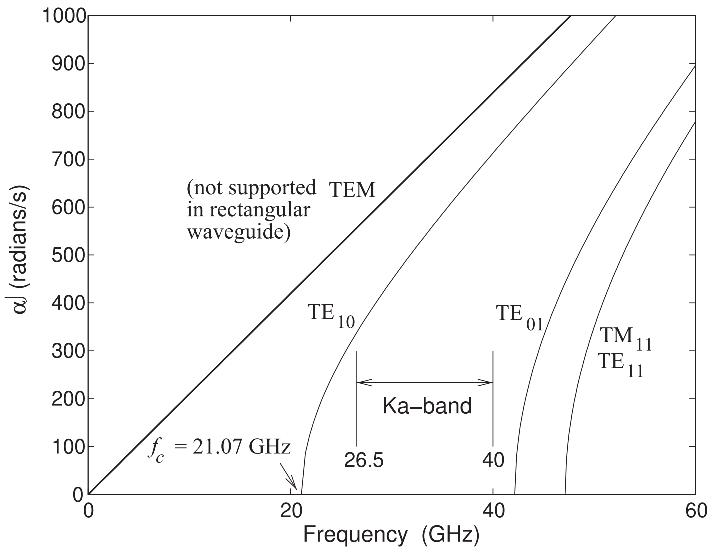

Figure 6-8: Dispersion diagram of waveguide modes in air-filled Ka-band rectangular waveguide with internal dimensions of 0.280×0.140 inches ($7.112\,\mathrm{mm} \times 3.556\,\mathrm{mm}$). Ka-band waveguide is used between 26.5 GHz and 40 GHz. Over this frequency range only the TE_{10} mode propagates.

Mode	Cut-off frequency (GHz)
TEM	not supported
TE_{10}	21.07 GHz
TE_{01}	42.15 GHz
TE_{11}	47.13 GHz
TM_{10}	not supported
TM_{01}	not supported
TM_{11}	47.13 GHz

Table 6-1: Cut-off frequencies of several modes in Ka-Band waveguide nominally used between 26.5 GHz and 40 GHz.

modes with the lowest cutoff frequencies are shown in Figure 6-8 for a Ka-band waveguide having internal dimensions of $a = 0.280$ inches and $b = 0.140$ inches. This figure is known as a dispersion diagram and is sometimes plotted as β versus k. There are four modes supported below 60 GHz and the line corresponding to the TEM mode is provided for reference, as the TEM mode is not supported in a rectangular waveguide.

Not all possible low-order modes can be supported in rectangular waveguide as the boundary conditions cannot be satisfied (see Table 6-1). The cutoff frequency of the TE_{10} mode is 21.07 GHz and the next lowest cutoff mode, the TE_{01} mode, has a cutoff frequency of 42.15 GHz. The mode has a cutoff frequency which is the frequency when the wavelength (in the medium, or free-space wavelength if the guide is air-filled) is twice the a dimension of the waveguide (see Figure 6-5). The next higher-order mode appears when it is possible for a variation in the y direction. This occurs at a frequency corresponding to the b dimension being one-half wavelength in the medium. The TE_{11} mode and TM_{11} modes have the same cutoff frequency of 47.13 GHz. In determining the operating frequency range both the phase and group velocity variations are considered. These are shown in Figure 6-9 for the TE_{10} mode, where they are normalized to c as the waveguide is air-filled. The group velocity, v_g, varies substantially, especially near the cutoff frequency of the mode. As a result, the lower operating frequency of the mode is chosen to be substantially above the cutoff frequency. The upper limit of the operating frequency is chosen to be about 5% below the cutoff frequency of the second propagating mode. This

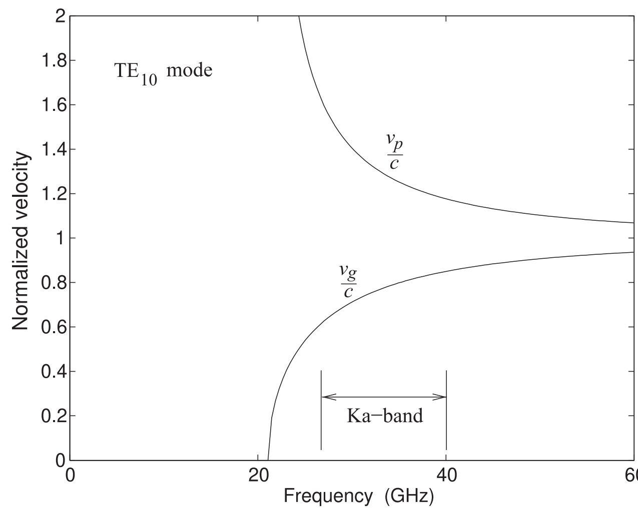

Figure 6-9: Normalized phase and group velocities of the TE_{10} mode in air-filled Ka-band waveguide.

is because small discontinuities can launch the higher-order mode. Thus the operating frequency of a Ka-band waveguide is 26.5 GHz–40 GHz, providing a margin of 5.4 GHz at the low end, and 2.2 GHz margin at the high end. So approximately one-half octave of bandwidth is supported by a rectangular waveguide if the wide dimension is twice the height of the waveguide. Since a rectangular waveguide is useful over a relatively narrow frequency range, standard dimensions have been developed, as listed in Table 6-2. A waveguide is referred to by its waveguide standard number (its WR designation), however, the old letter designations of bands are commonly used.

At times it is necessary to have a rectangular waveguide that can be used over more than one-half octave of bandwidth. This is achieved by reducing the height, b, of the waveguide, producing what is called a reduced-height waveguide. By reducing b to one-quarter of a, an octave of bandwidth can be obtained [2–4].

6.4.4 Rectangular Waveguide Components

Rectangular waveguide components require considerable machining, but the equivalents of many of the components that are available in microstrip can be realized. Invariably the lowest-order TE mode is used. This is the TE_{10} mode, with the field configuration shown in Figure 6-7. The characteristic of this mode is that the E-field is transverse to the direction of propagation. Many components have particular orientations to the planes of the E and H fields. Consider the rectangular waveguide bends shown in Figure 6-10. The bend in Figure 6-10(a) is called an H-plane bend, or H-bend, as the axis of the waveguide (which is in the direction of propagation) always remains parallel to the H field. With the E-plane bend, or E-bend, in Figure 6-10(b), the axis of the waveguide remains parallel to the E field. The flat sections at the end of the waveguide sections are called flanges. The pins in the flanges are alignment pins that insert into holes in the opposite flange.

In building circuits using rectangular waveguides, it is frequently necessary to rotate and twist the waveguide so that sections can be joined. Bends enable this, but **twists** (as shown in Figure 6-11) are also used.

Band	EIA waveguide band	Operating frequency (GHz)	Internal dimensions ($a \times b$, inches)	TE_{10} Cutoff (GHz)
	WR–2300	0.32–0.49	23.000×11.500	0.257
	WR–2100	0.35–0.53	21.000×10.500	0.281
	WR–1800	0.43–0.62	18.000×9.000	0.328
	WR–1500	0.49–0.74	15.000×7.500	0.393
	WR–1150	0.64–0.96	11.500×5.750	0.513
	WR–1000	0.75–1.1	9.975×4.875	0.592
	WR–770	0.96–1.5	7.700×3.385	0.766
	WR-650	1.12–1.70	6.500×3.250	0.908
R	WR-430	1.70–2.60	4.300×2.150	1.37
D	WR-340	2.20–3.30	3.400×1.700	1.74
S	WR-284	2.60–3.95	2.840×1.340	2.08
E	WR-229	3.30–4.90	2.290×1.150	2.58
G	WR-187	3.95–5.85	1.872×0.872	3.15
F	WR-159	4.90–7.05	1.590×0.795	3.71
C	WR-137	5.85–8.20	1.372×0.622	4.30
H	WR-112	7.05–10.00	1.122×0.497	5.26
X	WR-90	8.2–12.4	0.900×0.400	6.56
Ku	WR-62	12.4–18.0	0.622×0.311	9.49
K	WR-51	15.0–22.0	0.510×0.255	11.6
K	WR-42	18.0–26.5	0.420×0.170	14.1
Ka	WR-28	26.5–40.0	0.280×0.140	21.1
Q	WR-22	33–50	0.224×0.112	26.3
U	WR-19	40–60	0.188×0.094	31.4
V	WR-15	50–75	0.148×0.074	39.9
E	WR-12	60–90	0.122×0.061	48.4
W	WR-10	75–110	0.100×0.050	59.0
F	WR-8	90–140	0.080×0.040	73.8
D	WR-6	110–170	0.0650×0.0325	90.8
G	WR-5	140–220	0.0510×0.0255	116
	WR-4	170–260	0.0430×0.0215	137
	WR-3	220–325	0.0340×0.0170	174
Y	WR-2	325–500	0.0200×0.0100	295
	WR-1.5	500–750	0.0150×0.0075	393
	WR-1	750–1100	0.0100×0.0050	590

Table 6-2: Waveguide bands, operating frequencies, and internal dimensions. Waveguide dimensions specified in inches (use 25.4 mm/inch to convert to millimeters). The number in the WR designation is the long internal dimension of the waveguide in hundreds of an inch. The TE_{10} mode cutoff frequency is when the long dimension is one-half wavelength long (the free-space wavelength if vacuum- or air-filled, or modified by the square root of the permittivity if the waveguide is dielectric filled).

Waveguide **tees** are used to split and combine signals. There are both E-plane and H-plane versions, as there were for **bends** (see Figure 6-12).

There is a wide variety of waveguide components. The components are developed from EM field considerations and not derived from current and voltage circuits. For example, a **termination** in a rectangular waveguide is realized using a resistive wedge of material as shown in Figure 6-13(a). This provides a termination with a lower reactive component than would be obtained with a lumped resistor placed at the end of the line. The matched load absorbs all of the power in the traveling wave incident on it. The functional component is a lossy material, often shaped as a wedge or tall pyramid, that absorbs power over a distance corresponding, perhaps, to one-half wavelength or longer. So while the characteristic impedance of a wave in the rectangular waveguide varies with frequency, the termination is always matched to this impedance. A high-power waveguide matched load is shown in Figure 6-13(b). This component uses the structure illustrated in Figure 6-13(a) and has fins for the dissipation of heat. A **waveguide**

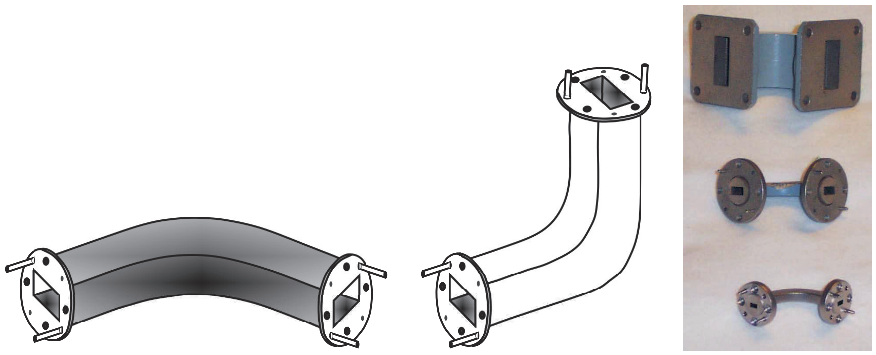

(a) H-plane bend (b) E-plane bend (c) Various bends

Figure 6-10: Rectangular waveguide bends. In (c), top is X-band (8–12 GHz), middle is Ku-band (12–18 GHz), and bottom is Ka-band (26–40 GHz).

(a) Diagrammatic view (b) Photograph

Figure 6-11: Rectangular waveguide twist.

attenuator is realized by introducing resistive material, as shown in Figure 6-13(c). This introduces a section of line with a high attenuation coefficient. By controlling the depth of the resistive vane, as shown in Figure 6-13(d), a **variable attenuator** is obtained.

Discontinuities in the waveguide introduce inductive, capacitive, and resonant elements. Several discontinuities that are used to realize these elements are shown in Figure 6-14. These illustrate most clearly the use of E and H field disturbances to realize capacitive and inductive components. An E-plane discontinuity (Figure 6-14(a)) is modeled approximately by a frequency-dependent capacitor. H-plane discontinuities (Figure 6-14(b and c)) resemble inductors, as does the circular iris of Figure 6-14(d). The resonant waveguide iris of Figure 6-14(e) disturbs the E and H fields and is modeled by a parallel LC resonant circuit near the frequency of resonance. Posts in the waveguide are used as reactive elements (Figure 6-14(f)) and to mount active devices (Figure 6-14(g)). The equivalent circuits of waveguide discontinuities are modeled by capacitive elements if the E field is interrupted and by inductive elements if the H field (or current) is disturbed. Many papers (e.g., [5–8]) have been devoted to analytic field solutions that lead to equivalent lumped element representations of waveguide discontinuities that can then be used in synthesis.

A rectangular waveguide circulator is shown in Figure 6-15. A **circulator** uses a special property of magnetized ferrites that provides a preferred direction of EM propagation.

It is sometimes necessary to interface between waveguide series, and one component to do this is the tapered waveguide section shown in Figure 6-16(a). Alternatively the one-quarter wavelength long impedance transformer

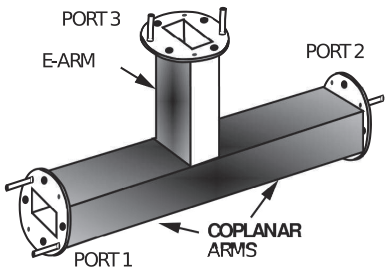

(a) E-plane tee

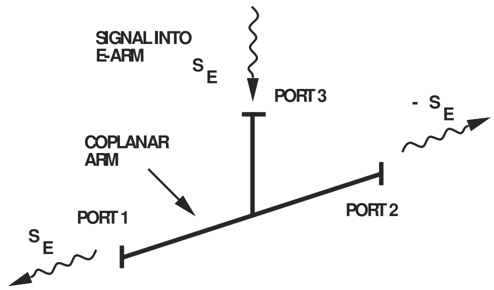

(b) Signal flow in an E-plane tee

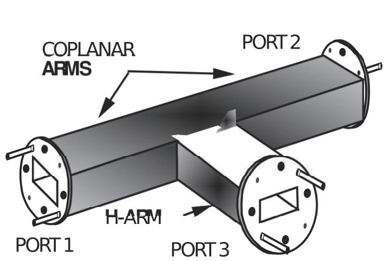

(c) H-plane tee

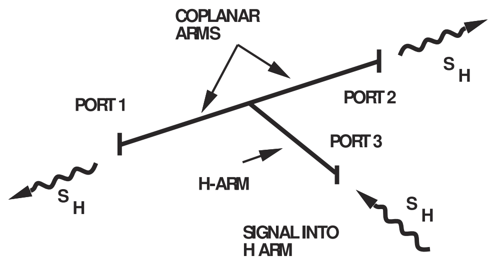

(d) Signal flow in an H-plane tee

(e) E-plane tee

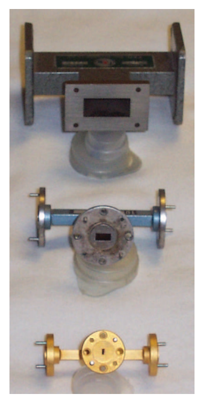

(f) Various tees

Figure 6-12: Rectangular waveguide tees: (a) three-dimensional representation of an E-plane tee; (b) description of the signal flow in an E-plane tee; (c) three-dimensional representation of an H-plane tee; (d) description of the signal flow in an H-plane tee; (e) photograph of an E-plane tee; and (f) photograph of waveguide tees for different waveguide bands (top, X-band H-plane tee; middle, Ku-band H-plane tee; bottom, Ka-band E-plane tee).

shown in Figure 6-16(b) could be used. This section can be shorter than the tapered waveguide section, which, however, has higher bandwidth.

Other components commonly encountered are the waveguide switch (see Figure 6-16(c)), the **coaxial-to-waveguide adaptor** (see Figure 6-17), and the waveguide horn antenna (see Figure 6-16(d)).

Distributed directional couplers are realized by two coupled transmission lines. A **rectangular waveguide directional coupler** is shown in Figure 6-18.

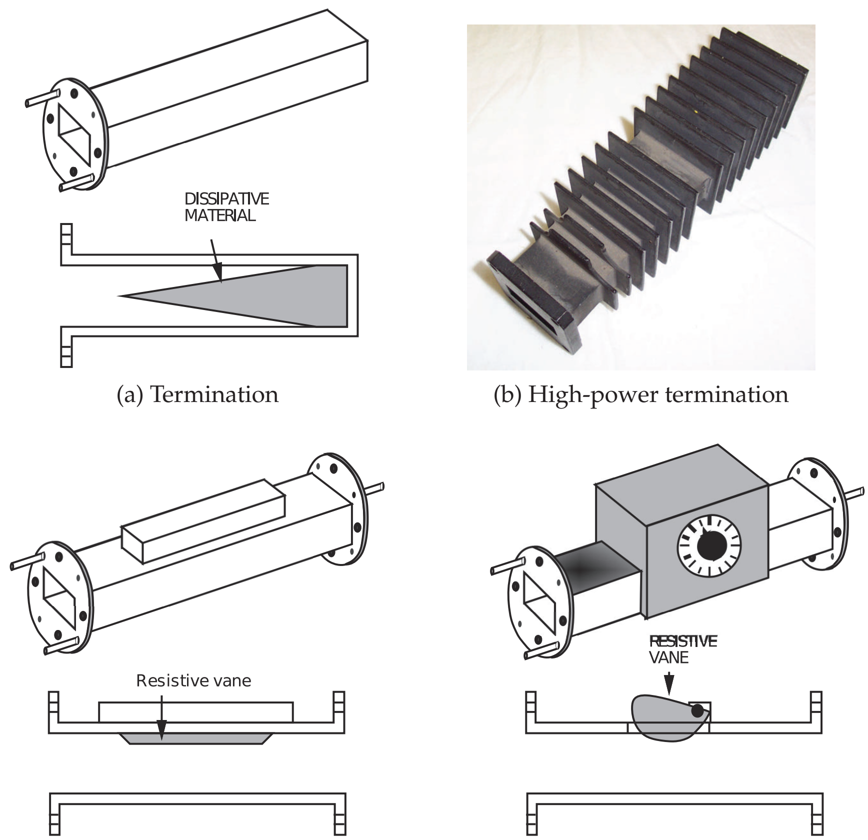

(a) Termination

(b) High-power termination

(c) Attenuator

(d) Variable attenuator

Figure 6-13: Terminations and attenuators in a rectangular waveguide.

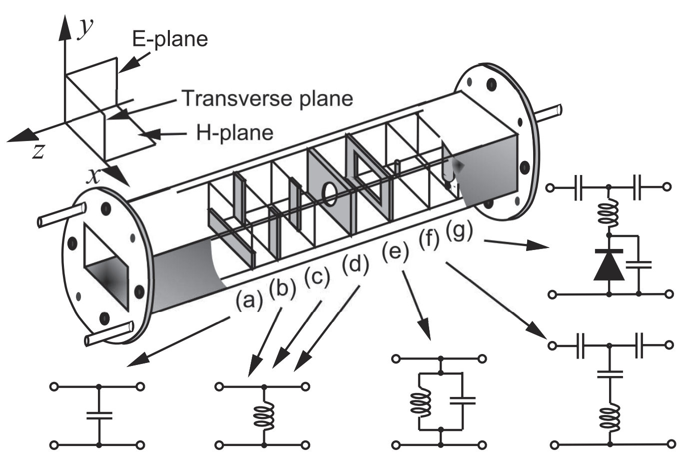

Figure 6-14: Rectangular waveguide discontinuities and their lumped equivalent circuits: (a) capacitive E-plane discontinuity; (b) inductive H-plane discontinuity; (c) symmetrical inductive H-plane discontinuity; (d) inductive post discontinuity; (e) resonant window discontinuity; (f) capacitive post discontinuity; and (g) diode post mount.

Here the two transmission lines, the rectangular waveguides, are coupled by slots in the common wall of the guides. In Figure 6-18(b) the EM wave from the bottom waveguide leaks into the top waveguide through the coupling slots. A quick check on phasing indicates that the coupled wave in the reverse direction is canceled. Meanwhile, in the forward-traveling direction there is constructive interference of the coupled EM wave.

Variable elements available in a rectangular waveguide include the micrometer **tuner**, shown in Figure 6-19. The tuner shown in Figure 6-19(a)

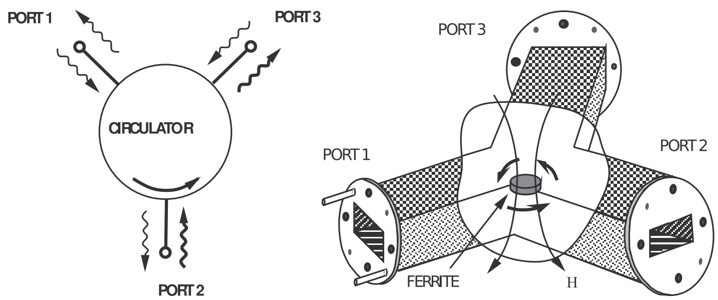

(a) (b)

Figure 6-15: Waveguide circulator: (a) schematic; and (b) three-dimensional representation showing H field lines magnetizing a ferrite disk.

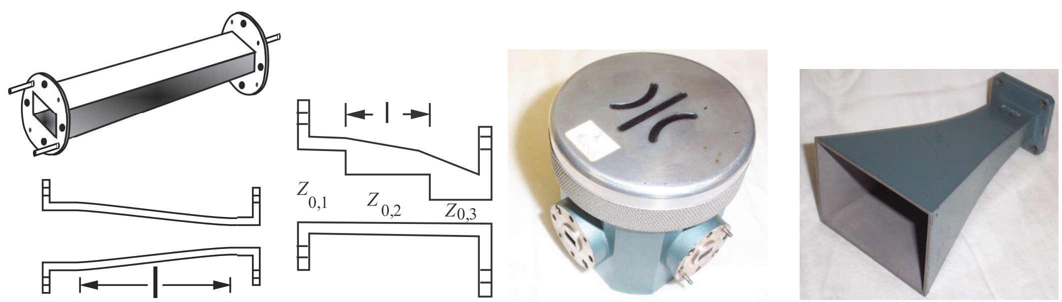

(a) Waveguide taper (b) $\lambda/4$ transformer (c) Waveguide switch (d) Waveguide horn

Figure 6-16: Waveguide components: (a) waveguide switch; (b) rectangular waveguide quarter-wavelength impedance transformer; (c) rectangular waveguide taper connecting one waveguide series to another; and (d) waveguide horn antenna.

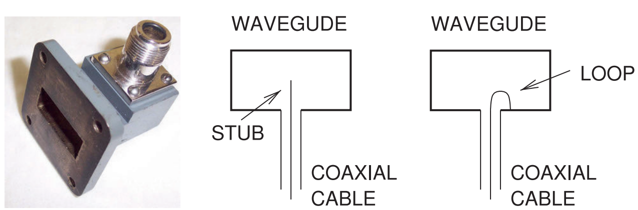

(a) (b) (c)

Figure 6-17: Coaxial transmission line to rectangular waveguide adaptor: (a) photograph; (b) adaptor using a coupling stub; and (c) adaptor using a coupling loop.

typically moves a reactive element along the waveguide. One example is the movable short circuit shown in Figure 6-19(b). Another variable element used in tuning is the waveguide slide tuner, shown in Figure 6-19(c). Here a slot is cut in the wide wall of the waveguide and a metal probe is inserted. The slot is in a region where the currents in the waveguide wall are minimum, so little discontinuity is introduced. The probe introduces a reactive discontinuity, and the reactance can be varied by changing the depth of penetration of the probe using the knob seen on top. The probe can move up-and-down along the slot to further increase the impedance range that can be presented.

Hybrids in waveguides (Figure 6-20) do not look anything like their microstrip equivalents.

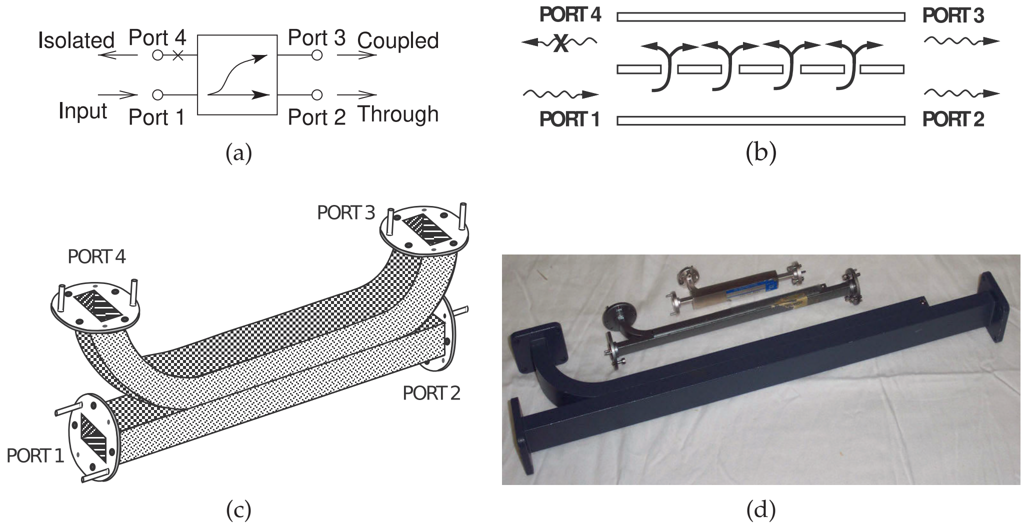

Figure 6-18: Rectangular waveguide directional couplers: (a) schematic; (b) and (c) waveguide directional coupler showing coupling slots; and (d) three directional couplers with the fourth port terminated in an integral matched load. In (d), from top to bottom: W-band, 10 cm long; Ka-band, 15 cm long, and X-band, 35 cm long.

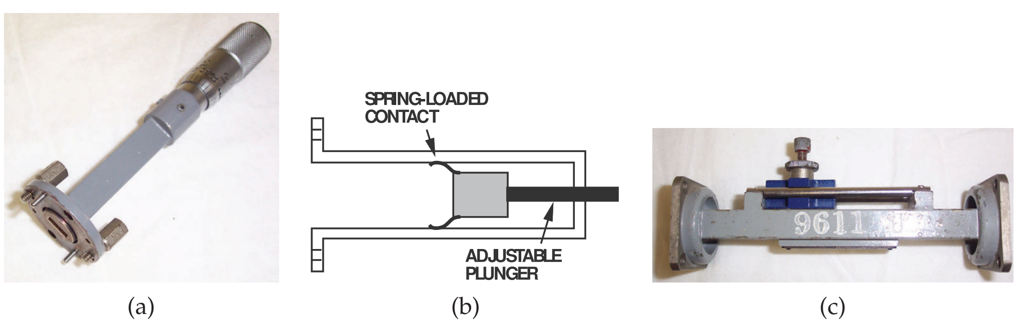

Figure 6-19: Waveguide tuners: (a) micrometer-driven variable short circuit; (b) internal details of a variable short circuit; and (c) waveguide slide tuner.

6.5 Summary

Rectangular waveguides guide EM fields in a rectangular pipe. Parallel plate waveguides are unintentional but are approximated by the planar conductors found in printed circuit boards. Rectangular wave equations describe propagation in these structures and are derived from Maxwell's equations by applying multiple simplifications such as using phasors, restricting propagation to just one direction, and applying symmetries. Important concepts that flow from the rectangular wave equations are that rectangular and parallel-plate waveguides support multiple modes, i.e. variations of the EM field, with all but the TEM mode having a finite cut-off frequency below which a particular mode cannot propagate. The rectangular waveguide does not support a TEM mode, a mode with no variations of the field between boundaries, so the rectangular waveguide cannot support a propagating mode below the lowest cut-off frequency. A mode with more variations of the field will have a higher cut-off frequency. A separate physical result is that if two modes can propagate the EM energy will be equally partitioned between them. Thus if two or more modes can propagate the information will become garbled since different modes travel at different speeds. This is observed in practice so for example, with rectangular waveguide the useful frequency range of operation is between the cut-off frequency of the mode with the simplest field variation, and hence the lowest cut-off frequency, and the cut-off frequency of the next higher-order mode.

6.6 References

[1] R. E. Collin, *Foundations for Microwave Engineering*. John Wiley & Sons, 2007.

[2] H.-S. Oh and K.-W. Yeom, "A full ku-band reduced-height waveguide-to-microstrip transition with a short transition length," *IEEE Trans. on Microwave Theory and Techniques*, vol. 58, no. 9, pp. 2456–2462, Sep. 2010.

[3] A. Tribak, J. Cano, A. Mediavilla, and M. Boussouis, "Octave bandwidth compact turnstile-based orthomode transducer," *IEEE Microwave and Wireless Components Letters*, vol. 20, no. 10, pp. 539–541, Oct. 2010.

[4] N. Erickson, "High efficiency submillimeter frequency multipliers," in *1990 IEEE MTT-S Int. Microwave Symp. Dig.*, May 1990, pp. 1301–1304.

[5] R. Eisenhart and P. Khan, "Theoretical and experimental analysis of a waveguide mounting structure," *IEEE Trans. on Microwave Theory and Techniques*, vol. 19, no. 8, pp. 706–719, Aug. 1971.

[6] J. Bornemann and R. Vahldieck, "Characterization of a class of waveguide discontinuities using a modified te$^{x}_{mn}$ mode approach," *IEEE Trans. on Microwave Theory and Techniques*, vol. 38, no. 12, pp. 1816–1822, Dec. 1990.

[7] T. Rozzi and W. Mecklenbrauker, "Wideband network modeling of interacting inductive irises and steps," *IEEE Trans. on Microwave Theory and Techniques*, vol. 23, no. 2, pp. 235–245, Feb. 1975.

[8] P. Khan and M. Steer, "Analysis of bias-pin resonator diode mounts for millimeter-wave oscillators," *Proc. IEEE*, vol. 67, no. 11, pp. 1556–1557, Nov. 1979.

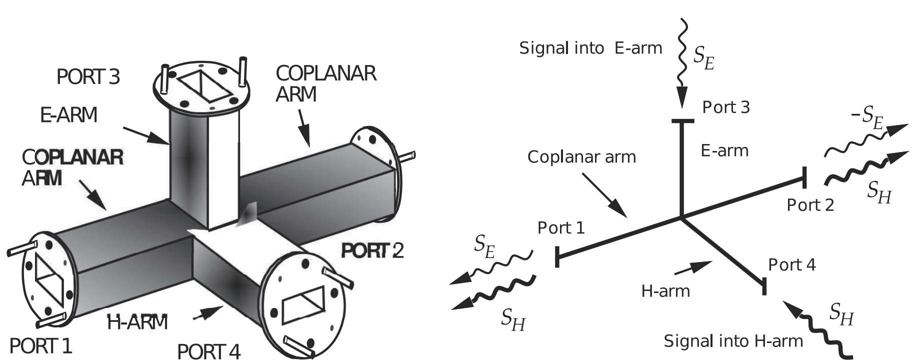

(a) Three-dimensional representation (b) Description of signal flow

Figure 6-20: Rectangular waveguide hybrid.

6.7 Exercises

1. A four-layer circuit board has four levels of metalization with the two inner layers being supply and ground planes are RF grounds. The top layer has a very dense concentration of signal lines and for the purposes of understanding the fields in the dielectric between the top two layers of metalization both layers of metalization can be considered to be solid. The situation now reduces to a parallel plate waveguide which allows signals to travel in the dielectric from one region of the circuit board to another. The dielectric has a relative permittivity of 4 and the thickness of the dielectric between the metal layers is 1 mm.
   (a) What is the mode that propagates at the lowest frequency and what is the cut-off wavenumber and cut-off frequency of this mode?
   (b) What is the wave impedance of this mode at 1 GHz?
   (c) What is the phase velocity of this mode at 1 GHz?
2. A multi-layer circuit board forms a parallel plate waveguide between the metal planes (even if they are broken up a little). Thus EM energy propagates around the circuit board and not all of the energy is confined by the circuit board lines.
   (a) What is the EM mode that is mostly to propagates?
   (b) Draw the E and H fields of the mode in cross section.
   (c) If the distance between the plates is 1 mm, what is the lowest frequency at which this lowest order mode can propagate.
3. Two adjacent layers of a circuit board are continuous ground planes separated by a 0.5 mm-thick dielectric having a relative permittivity of 4.
   (a) What is the lowest frequency at which the TEM mode propagates.
   (b) What is the wave impedance of the TEM mode at 10 GHz.
4. Two adjacent layers of a circuit board are continuous ground planes separated by a 0.5 mm-thick dielectric having a relative permittivity of 4. What is the lowest frequency at which the TM_1 mode propagates.
5. Two adjacent layers of a circuit board are continuous ground planes separated by a 0.5 mm-thick dielectric having a relative permittivity of 4. What is the lowest frequency at which the TE_1 mode propagates.
6. An air-filled W-band waveguide has a 75–100 GHz operating frequency, extends in the z direction and has internal dimensions of $\Delta x = 0.100$ in. by $\Delta y = 0.050$ in. f_c is the cut-off frequency, and k_c is the cutoff wavenumber.
   (a) Does the waveguide support a transverse electromagnetic (TEM) mode provide your reasons?
   (b) What is the distinguishing feature of the TE waveguide modes?
   (c) What is the distinguishing feature of the TM waveguide modes?
   (d) What modes other than TEM, TE, and TM modes propagate in rectangular waveguide?
   (e) Are TE_{00} and TM_{00} modes supported in the waveguide and why?
   (f) What is k_c of the TE_{10} mode?
   (g) What is k_c of the TE_{01} mode?
   (h) What is k_c of the TE_{11} mode?
   (i) What is f_c of the TE_{10} mode?
   (j) What is f_c of the TE_{01} mode?
   (k) What is the wavenumber of the TE_{01} mode at 90 GHz, discuss if your answer is not real?
   (l) What is the wavenumber of the TE_{10} mode at 90 GHz, discuss if your answer is not real?
   (m) What is f_c of the TE_{11} mode?
   (n) What is k_c of the TM_{10} mode?
   (o) What is k_c of the TM_{01} mode?
   (p) What is k_c of the TM_{11} mode?
   (q) What is k_c of the TM_{10} mode?
   (r) What is f_c of the TM_{01} mode?
   (s) What is f_c of the TM_{11} mode?
   (t) What can you say about the relative cut-off frequency of the TE_{mn} and TM_{mn}, $m + n \geq 2$, modes relative to the cutoff frequencies of the TE_{mn} and TM_{mn}, $m + n = 1$, modes?
   (u) Sketch and label the dispersion curves for the TE_{mn} and TM_{mn}, $m, n = 0, 1$, modes, i.e. β versus frequency over the frequency range 0 to 200 GHz.
   (v) What is the frequency range over which only one mode can propagate?
   (w) Why is it desirable that only one mode propagate?
   (x) Why is the operating frequency range specified for this waveguide less than the frequency range over which only one mode can exist.
7. An air-filled E-band waveguide has a 60–90 GHz operating frequency and has internal dimensions of 0.122 in by 0.061 in.
   (a) What is the phase velocity of the TE_{10} mode

at 60 GHz.
(b) What is the phase velocity of the TE_{10} mode at 90 GHz.
(c) What is the wave impedance of the TE_{10} mode at 60 GHz.
(d) What is the wave impedance of the TE_{10} mode at 90 GHz.
(e) What is the difference between characteristic impedance and wave impedance for the waveguide?

8. An X-band waveguide has the dimensions 0.9 in $\times$ 0.4 in. Calculate the cut-off frequencies for the TE_{10}, TE_{01}, and TM_{11}, modes.
9. An X-band waveguide has the dimensions 0.9 in $\times$ 0.4 in. Calculate the cut-off frequencies for the TE_{10}, TE_{01}, and TM_{11}, modes.
10. A W-band waveguide has the dimensions 0.1 in $\times$ 0.05 in and the cut-off frequency of the TE_{10} mode is 59.0 GHz. Verify this.
    (a) What is the cut-off frequencies of the TE_{01} mode?
    (b) What is the cut-off frequencies of the TM_{11} mode?
    (c) What is the the operating frequency range over which only one mode can exist?
11. An E-band waveguide has the dimensions 0.122 in $\times$ 0.061 in and the cut-off frequency of the TE_{10} mode is 48.4 GHz. Verify this.
    (a) What is the cut-off frequency of the TE_{01} mode?
    (b) What is the cut-off frequency of the TM_{11} mode?
    (c) What is the the frequency range over which only one mode can exist?
12. A W-band waveguide has the dimensions 0.1 in $\times$ 0.05 in. At 100 GHz only the TE_{10} mode can propagate. At 100 GHz and for the TE_{10} mode
    (a) what is the wave impedance?
    (b) what is the phase velocity?
    (c) what is the group velocity?
13. An E-band waveguide has the dimensions 0.1 in $\times$ 0.05 in. At 38 GHz only the TE_{10} mode can propagate. At 38 GHz and for the TE_{10} mode
    (a) what is the wave impedance?
    (b) what is the phase velocity?
    (c) what is the group velocity?
14. A communication system at 60 GHz has a bandwidth of 4 GHz so that the operating frequency range is 58 GHz to 62 GHz. Waveguide is to be used to route the millimeter-wave signal to an antenna. What waveguide should be used to justify your answer.
15. A communication system 15 GHz has a bandwidth of 1 GHz so that the operating frequency range is 14.5 GHz to 15.5 GHz. Waveguide is to be used to route the millimeter-wave signal to an antenna. What waveguide should be used to justify your answer.

6.7.1 Exercises by Section

§6.2 $1, 2, 3, 4, 5$

§6.4 $6, 7, 8, 9, 10, 11, 12, 13, 14, 15$

Index

MICROWAVE AND RF DESIGN: TRANSMISSION LINES

Third Edition

Microwave and RF Design: Transmission Lines builds on the concepts of forward- and backward-traveling waves. Many examples are included of advanced techniques for analyzing and designing transmission line networks with microstrip lines primarily used in design examples. Coupled-lines are an important functional element in microwave circuits, and circuit equivalents of coupled lines are introduced as fundamental building blocks in design. The text and examples introduce the often hidden design requirements of mitigating parasitic effects and eliminating unwanted modes of operation. This book is suitable as both an undergraduate and graduate textbook, as well as a career-long reference book.

KEY FEATURES

- The second volume of a comprehensive series on microwave and RF design
- Open access ebook editions are hosted by NC State University Libraries at: https://repository.lib.ncsu.edu/handle/1840.20/36776
- 56 worked examples
- An average of 31 exercises per chapter
- Answers to selected exercises
- Focus on planar lines including microstrip
- A companion book, *Fundamentals of Microwave and RF Design*, is suitable as a comprehensive undergraduate textbook on microwave engineering

ABOUT THE AUTHOR

Michael Steer is the Lampe Distinguished Professor of Electrical and Computer Engineering at North Carolina State University. He received his B.E. and Ph.D. degrees in Electrical Engineering from the University of Queensland. He is a Fellow of the IEEE and is a former editor-in-chief of *IEEE Transactions on Microwave Theory and Techniques*. He has authored more than 500 publications including twelve books. In 2009 he received a US Army Medal, “The Commander’s Award for Public Service.” He received the 2010 Microwave Prize and the 2011 Distinguished Educator Award, both from the IEEE Microwave Theory and Techniques Society.

OTHER VOLUMES

Microwave and RF Design
Radio Systems
Volume 1
ISBN 978-1-4696-5690-8

Microwave and RF Design
Networks
Volume 3
ISBN 978-1-4696-5694-6

Microwave and RF Design
Modules
Volume 4
ISBN 978-1-4696-5696-0

Microwave and RF Design
Amplfiers and Oscillators
Volume 5
ISBN 978-1-4696-5698-4

ALSO BY THE AUTHOR

Fundamentals of Microwave and RF Design
ISBN 978-1-4696-5688-5

Published by NC State University

Distributed by UNC Press

NC STATE UNIVERSITY